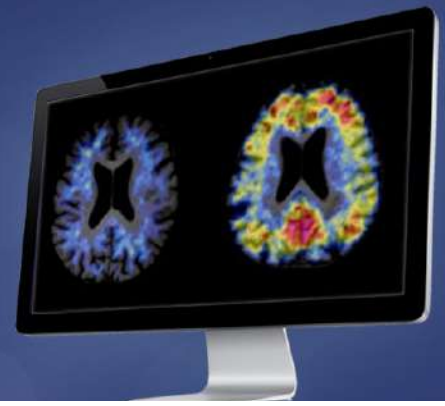


9th Human Amyloid Imaging

January 14-16, 2015
Miami, Florida



Co-Organizers:

Keith A. Johnson, MD • William J. Jagust, MD • William E. Klunk, MD, PhD • Chester A. Mathis, PhD

Conference Program and Abstracts

www.worldeventsforum.com/hai

TABLE OF CONTENTS

TABLE OF CONTENTS	1
PRESENTER INDEX.....	8
KEYWORD INDEX	9
HAI2015 – Program Overview	11

SESSION 1: Vascular14

Vascular Risk Factors Impact Cognition Independent of PIB PET and MRI Measures of AD and Vascular Brain Injury14

Charles DeCarli¹, Dan Mungas¹, Owen Carmichael², Sylvia Villeneuve³, Evan Fletcher¹, Baljeet Singh¹, William Jagust³, Bruce Reed¹

Presented by: DeCarli, Charles

Associations between β -amyloid, Memory and Longitudinal Brain Change across the Spectrum of Cognitive Functioning15

Evan Fletcher^{1,5}, Sylvia Villeneuve², Bruce Reed⁵, William Jagust⁴, Danielle Harvey³, Charles DeCarli^{1,5}

Presented by: Fletcher, Evan

Amyloid, Cerebrovascular Disease and Cognitive Decline in MCI patients: A Prospective

Longitudinal Study16

Hee Jin Kim¹, Yearn Seong Choe², Kyung-Han Lee², Sung Tae Kim³, Duk L. Na¹, Sang Won Seo¹

Presented by: Kim, Hee Jin

Interactions of Amyloid & Vascular Pathology in MCI.....17

William Klunk, Lisa Weissfeld, Julie Price, Chester Mathis, Howard Aizenstein, Beth Snitz, Ann Cohen, Milos Ikonovic, Oscar Lopez

Presented by: Klunk, William

SESSION 2: Amyloid-associated Phenomena ...18

Lower Body-Mass Index is Associated with Higher Cortical Amyloid Burden in Clinically Normal Elderly.....18

David Hsu, Alexander Dagley, Aaron Schultz, Rebecca Amariglio, Elizabeth Mormino, Nancy Donovan, Dorene Rentz, Keith Johnson, Reisa Sperling, Gad Marshall

Presented by: Hsu, David C

Regional Cerebral Iron Concentrations as Indicated by Magnetic Susceptibilities Measured with Quantitative Susceptibility Mapping at 7 Tesla Correlate with Brain A β plaque Density as Measured by 11-C-Pittsburgh Compound B Positron-Emission-Tomography (PiB-PET) in Elderly Subjects at Risk for AD19

Jiri van Bergen^{1,2}, Xu Li², Michael Wyss³, Simon Schreiner¹, Stefanie Steininger¹, Anton Gietl¹, Valerie Treyer⁴, Sandra Leh¹, Fred Buck⁴, Jun Hua², Roger Nitsch¹, Klaas Pruessmann³, Peter van Zijl², Christoph Hock¹, Paul Unschuld¹

Presented by: Unschuld, Paul

The Cognition-Mobility Interface (COMBINE) is Associated with Cerebral Amyloid Deposition and Glucose Metabolism in Older Adults without Cognitive or Mobility Impairment 20

Neelesh Nadkarni¹, Stephanie Studenski⁵, Oscar Lopez^{2,3}, Beth Snitz², Subashan Perera¹, Ann Cohen³, Chester Mathis⁴, Robert Nebes³, William Klunk^{2,3,4}

Presented by: Nadkarni, Neelesh K.

Multivariate AD Biomarker Profiles: Relation to Clinical and Cognitive Progression..... 22

Andrew Saykin¹, Shannon Risacher², Paul Crane³, William Jagust⁴, Clifford Jack⁵, Leslie Shaw⁶, John Trojanowski⁶, Laurel Beckett⁷, Sujuan Gao⁸, Paul Aisen⁹, Ronald Petersen¹⁰, Michael Weiner¹¹

Presented by: Saykin, Andrew J

KEYNOTE LECTURE 124

The Spectrum of Age-Associated Tauopathies 24

Dennis W. Dickson

Presented by: Dickson, Dennis

SESSION 3: Pathology25

Clinicopathologic and [11C]-PiB-PET Implications of Thal Amyloid Phase across the Spectrum of Alzheimer's Disease Pathology..... 25

Melissa Murray¹, Val Lowe², Neill Graff-Radford³, Amanda Liesinger¹, Ashley Cannon¹, Scott Przybelski⁵, Bhupendra Rawal⁴, Joseph Parisi⁶, Ronald Petersen⁷, Kejal Kantarci², Owen Ross¹, Ranjan Duara⁸, David Knopman⁷, Clifford Jack, Jr.², Dennis Dickson¹

Presented by: Murray, Melissa E

PiB PET and Postmortem Neuropathology Correlations in the Precuneus: A Role for Diffuse A β Plaques..... 26

Julie Price¹, Eric Abrahamson², Lan Shao², Carl Becker¹, Manik Debnath³, Lisa Weissfeld⁴, Chester Mathis¹, Oscar Lopez², William Klunk^{2,3}, Milos Ikonovic^{2,3}

Presented by: Price, Julie

Towards the Validation of Novel PET tracer T807 on Postmortem Human Brain Tissue Samples 27

Marta Marquie^{1,2}, Marc Normandin², Charles Vanderburg^{1,2}, Isabel Costantino^{1,2}, Bradford Dickerson², Matthew Frosch^{1,2}, Bradley Hyman^{1,2}, Keith Johnson², Teresa Gomez-Isla^{1,2}

Presented by: Marquie, Marta

AV-1451 Autoradiographic Evaluation in Subjects with TDP-43- versus Tau-immunoreactive Lesions 28

Val Lowe¹, Geoffry Curran¹, Keith Josephs¹, Joseph Parisi¹, David Knopman¹, Bradley Boeve¹, Kejal Kantarci¹, Leonard Petrucelli², Clifford Jack¹, Dennis Dickson², Ronald Petersen¹, Melissa Murray²

Presented by: Lowe, Val J

POSTER SESSION (Odd Numbers).....29

Amyloid Biomarkers in Cognitively Normal Older Adults: Comparison of ¹⁸F-flutemetamol to ¹¹C-PIB and CSF A β 4229

Katarzyna Adamczuk^{1,2}, Jolien Schaevebeke^{1,2}, Rose Bruffaerts^{1,2,3}, Natalie Nelissen^{1,2}, Veerle Neyens^{1,2}, Patrick Dupont^{1,2}, Karolien Goffin⁴, Mathieu Vandenbulcke^{2,5}, Koen Van Laere^{2,4}, Jos Tournoy⁶, Koen Poesen^{7,8}, Rik Vandenberghe^{1,2,3}

P1 Presented by: Adamczuk, Katarzyna

A Selective Impact of Regional PET 11C-PIB on Cognitive Functions in Healthy Controls and Patients with MCI and Alzheimer's Disease30

Ove Almkvist, Katharina Bruggen, Agneta Nordberg

P3 Presented by: Almkvist, Ove

Analysis Strategies for Quantitation of the PET Tau Radiotracer [¹⁸F]AV145131

Olivier Barret, David Alagille, Danna Jennings, David Russell, Kenneth Marek, John Seibyl, Gilles Tamagnan

P5 Presented by: Barret, Olivier

Differential Patterns of Cortical Thickness in Individuals with Elevated Beta-amyloid across the Adult Lifespan.....32

Gerard Bischof¹, Kristen Kennedy¹, Ian McDonough¹, Karen Rodrigue¹, Jenny Rieck¹, Michael Devous², Denise Park¹

P7 Presented by: Bischof, Gerard N

Prediction of Conversion to Preclinical Alzheimer's Disease Using Penalized Regression 33

Matthew Brier¹, Tammie Benzinger^{2,3}, Yi Su², Karl Friedrichsen², John Morris^{1,3}, Beau Ances^{1,2,3}, Andrei Vlassenko^{2,3}

P9 Presented by: Brier, Matthew R

The Relationship Between Cortical Thickness and Tau Pathology Measured with [¹⁸F]-(S)-THK5117-PET34

Konstantinos Chiotis¹, Laure Saint-Aubert¹, Anders Wall², My Jonasson², Mark Lubberink², Jonas Eriksson³, Gunnar Antoni², Nobuyuki Okamura⁴, Agneta Nordberg^{1,5}

P11 Presented by: Chiotis, Konstantinos

Amyloid- β Deposition in Normal Aging of Non-demented Adults with Down Syndrome35

Patrick Lao¹, Tobey Bethausen¹, Ansel Hillmer¹, Julie Price², William Klunk², Iulia Mihaila¹, Andrew Higgins¹, Peter Bulova², Sigan Hartley¹, Regina Hardison², Sterling Johnson¹, Murali Dhanabalan¹, Chet Mathis², Annie Cohen², Benjamin Handen², Bradley Christian¹

P13 Presented by: Christian, Bradley T

[¹⁸F] T807 PET of Frontotemporal Lobar Degeneration36

Bradford Dickerson, Scott McGinnis, Stephen Gomperts, Christina Caso, Sara Makarets, Kathleen Kelly, Aaron Schultz, Neil Vasdev, Keith Johnson

P15 Presented by: Dickerson, Bradford C

Correlation of White Matter Disease and Amyloid Burden in Patients with Prodromal Alzheimer's Disease.....37

David Douglas, Guofan Xu, Greer Murphy, Andrew Quon

P17 Presented by: Douglas, David B

Should the Threshold for a Positive Amyloid PET Scan Be Adjusted for APOE Carrier Status, Age and Level of Cognitive and Functional Impairment? 39

Ranjan Duara¹, Warren Barker¹, David Loewenstein², Maria Greig¹, Rosemarie Rodriguez¹, Mohammed Goryawala³, Qi Zhou³, Malek Adjouadi³

P19 Presented by: Duara, Ranjan

Development of an Alpha-synuclein PET Tracer 41

Dale Mitchell¹, Kevin Nash¹, David Hardick¹, Paul Kotzbauer², Zhude Tu², Jinbin Xu², Robert Mach³, Jamie Eberling⁴, Edilio Borroni⁵, Luca Gobbi⁵, Michael Honer⁵, N. Mason⁶, William Klunk⁶, Chester Mathis⁶

P21 Presented by: Eberling, Jamie

The Importance of Frontal and Temporal Amyloid Deposition in Middle Adulthood: The Predictive Value of APOE ϵ 4 and Lifetime Cognitive Engagement..... 42

Michelle Farrell¹, Gérard Bischof¹, Kristen Kennedy¹, Karen Rodrigue¹, Michael Devous², Denise Park¹

P23 Presented by: Farrell, Michelle E

Differences in Florbetapir Deposition by Race, Age, Gender, and ApoE Status: The ARIC-PET Study 43

Rebecca Gottesman¹, Xueqi Chen¹, Andrew Crabb¹, Edward Green², Naresh Gupta⁴, David Knopman⁵, Akiva Mintz³, Arman Rahmim¹, A. Sharrett¹, Lynne Wagenknecht³, Dean Wong¹, Yun Zhou¹, Thomas Mosley²

P25 Presented by: Gottesman, Rebecca F

The Relative Importance of Imaging Markers for the Prediction of Alzheimer's Disease Dementia in Mild Cognitive Impairment – beyond Classical Regression 44

Michel Grothe¹, Martin Dyrba¹, Stefan Teipel^{1,2}

P27 Presented by: Grothe, Michel J.

Cerebral Amyloid Angiopathy in Asymptomatic Community-Dwelling Older Adults..... 45

M. Edip Gurol, Aaron Schultz, Trey Hedden, Panagiotis Fotiadis, Sergi Martinez-Ramirez, Anand Viswanathan, J. Alex Becker, Reisa Sperling, Steven Greenberg, Keith Johnson

P29 Presented by: Gurol, M. Edip

Stroke Risk Interacts with AD Biomarkers in Conferring Risk for Cognitive Decline..... 46

Timothy Hohman, Dandan Lui, Lauren Samuels, Katherine Gifford, Angela Jefferson

P31 Presented by: Hohman, Timothy J

Longitudinal Change of PiB Accumulation with A One Year Interval in Alzheimer's Disease, Mild Cognitive Impairment, and Cognitively Normal Subjects 48

Takashi Kato^{1,2}, Kaori Iwata², Ken Fujiwara², Naohiko Fukaya¹, Yoshitaka Inui¹, Kengo Ito^{1,2}, Akinori Nakamura², MULNIAD Study Group²

P33 Presented by: Kato, Takashi

Comparative Assessment of SUVR Methods in Amyloid Cross-Sectional and Longitudinal Studies

.....49
Gregory Klein, Davis Staewen, Mehul Sampat, David Scott, Joyce Suh

P35 Presented by: Klein, Gregory

Regional Distribution of 3H-THK5117 in

Confirmed Alzheimer's Disease Cases.....50

Laetitia Lemoine¹, Laure Saint-Aubert¹, Fredrik Engman¹, Amelia Marutle¹, Gunnar Antoni^{2,3}, Jonas Eriksson³, Sergio Estrada², Nobuyuki Okamura⁴, Inger Nennesmo⁵, Per-Göran Gillberg¹, Agneta Nordberg^{1,6}

P37 Presented by: Lemoine, Laetitia

[18F]T807 ([18F]AV-1451) and Fluorescent Analog T726 Detect PHF-Tau but Not TDP-43 in Alzheimer's and FTD Post-Mortem Brain Tissue Sections51

Yin-Guo Lin¹, Felipe Gomez¹, Qianwa Liang¹, Eileen Bigio², Thomas Beach³, Mark Mintun¹, Giorgio Attardo¹

P39 Presented by: Lin, Yin-Guo

Effects of Age and β -amyloid on Tau Deposition Measured Using [¹⁸F] AV-1451 in Normal Older People52

Samuel Lockhart¹, Jacob Vogel¹, Daniel Schonhaut^{1,2}, Suzanne Baker³, Henry Schwimmer^{1,3}, Michael Schöll¹, Rik Ossenkoppele^{1,2}, Gil Rabinovici^{1,2,3}, William Jagust^{1,2,3}

P41 Presented by: Lockhart, Samuel N.

Relationship of Age, APOE genotype, Amyloid Load and Hippocampal Volume to Amnestic and Non-amnestic Cognitive Function – A Path

Analytic Study54

David Loewenstein^{1,2}, Warren Barker², Mohammed Goryawala³, Rosemarie Rodriguez², Malek Adjoudai³, Ranjan Dua², Maria Greig², Qi Zhou³

P43 Presented by: Loewenstein, David

Pittsburgh Compound-B (PiB): Radiologic-pathologic Correlations in a Series of 18 Autopsied Cases56

Marta Marquie^{1,2}, Beatriz G. Perez-Nievas^{1,2}, Isabel Costantino^{1,2}, Rebecca Betensky³, Isabel Barroeta-Espar^{1,2}, Joseph Parisi⁴, Ronald Petersen⁴, Matthew Senjem⁴, Clifford Jack Jr.⁴, Matthew Frosch^{1,2}, Bradley Hyman^{1,2}, Keith Johnson², Val Lowe⁴, Teresa Gomez-Isla^{1,2}

P45 Presented by: Marquie, Marta

Amyloid at the Threshold - Relationships between CSF Biomarkers, Amyloid PET, Glucose Metabolism, and Atrophy, with Implications for Diagnosis and Clinical Trials.....57

Dawn Matthews¹, Randolph Andrews¹, Ana Lukic¹, Mark Schmidt², et al.

P47 Presented by: Matthews, Dawn C

CogState Trajectories over 30 Months and the Effect of Amyloid Status and APOE E4 genotype in Cognitively Normal Individuals: The Mayo Clinic Study of Aging58

Michelle Mielke, Teresa Christianson, Clint Hagen, Mary Machulda, Rosebud Roberts, Prashanthi

Vemuri, Val Lowe, David Knopman, Kejal Kantarci, Clifford Jack, Ronald Petersen

P49 Presented by: Mielke, Michelle M

Automated Voxel-based Quantitation of Amyloid PET in Prodromal AD: Validation Study with up to Eight Years of Follow-up..... 59

Arthur Mikhno^{1,2}, Janos Redei², John Mann^{1,3}, Ramin Parsey⁴

P51 Presented by: Mikhno, Arthur

Distinct [¹⁸F]AV1451 Retention Patterns in Clinical Variants of Alzheimer's Disease 60

Rik Ossenkoppele^{1,2}, Daniel Schonhaut^{1,2}, Suzan Baker³, Andreas Lazaris¹, Nagehan Ayakte^{1,2}, Averill Cantwell¹, Sam Lockhart², Jacob Vogel², Henry Schwimmer^{2,3}, Michael Schöll², James O'Neill³, Maria Gorno-Tempini¹, Bruce Miller¹, William Jagust^{2,3}, Gil Rabinovici^{1,2}

P55 Presented by: Ossenkoppele, Rik

Task-fMRI Hyperactivity Predicts Cognitive Decline over Four Years in Cognitively-normal Older Adults with or without Amyloid Burden... 62

Judy Pa¹, Jacob Vogel², William Jagust^{2,3}

P57 Presented by: Pa, Judy

Patterns of Amyloid Plaque Deposition on AV-45 Positron Emission Tomography/Computed Tomography (PET/CT) Scans..... 63

Amy McCann, David Creed, Jeff Burns, Eric Vidoni, Paul Welch, Mark Perry

P59 Presented by: Perry, Mark

Comparison of CSF and [18F]Florbetapir Amyloid Measures for Predicting Memory Decline 64

Shannon Risacher¹, William Jagust³, Leslie Shaw⁴, John Trojanowski⁴, Paul Crane⁵, Paul Aisen⁶, Ronald Petersen⁷, Michael Weiner⁸, Andrew Saykin²

P61 Presented by: Risacher, Shannon L

Improved Longitudinal [18F]-AV45 Amyloid PET by White Matter Reference and VOI-based Partial Volume Effect Correction..... 66

Axel Rominger¹, Matthias Brendel¹, Marcus Hoegenauer¹, Andreas Delker¹, Julia Sauerbeck¹, Peter Bartenstein¹, John Seibyl²

P63 Presented by: Rominger, Axel

Relationship between longitudinal amyloid accumulation and T807-TAU 67

Aaron Schultz^{1,4}, Jasmeer Chhatwal^{1,4}, Elizabeth Mormino^{1,4}, Molly LaPoint^{1,4}, Alex Dagley^{1,4}, Reisa Sperling^{3,4}, Keith Johnson^{2,4}

P65 Presented by: Schultz, Aaron P

Comparison of White Matter and Cerebellar Reference Tissue in Estimating Change in Amyloid SUVR in SUMMIT and ACCTION..... 68

John Seibyl¹, Olivier Barret¹, Nzeera Ketter², Gerald Novak², H Brashear², Enchi Liu², Jianing Di², Kenneth Marek¹

P67 Presented by: Seibyl, John

Regional Correlations Between PiB-PET and Post-Mortem Burden of Amyloid Species..... 69

Sang Won Seo^{1,2,3,4}, Nagehan Ayakta^{1,2,3}, Manja Lehmann¹, Bruce Miller¹, Lea Grinberg¹, William Seeley¹, William Jagust^{1,2,3}, Gil Rabinovici^{1,2,3}

P69 Presented by: Seo, Sang Won

Weighted Two-point Correlation Functions for Longitudinal Amyloid-beta PET Analysis.....70	Are Low Levels of β-amyloid Deposition Clinically Significant? 82
<i>Sepideh Shokouhi¹, Hakmook Kang², Baxter Rogers¹, Daniel Claassen³, William Riddle¹</i>	<i>Sylvia Villeneuve^{1,2}, Helaine St. Amant¹, Jacob Vogel¹, Shawn Marks¹, Miranka Wirth^{1,3}, William Jagust¹</i>
<i>P71 Presented by: Shokouhi, Sepideh</i>	<i>Presented by: Villeneuve, Sylvia</i>
Amyloid Deposition Is Not Associated with fMRI Activation during Digit Symbol Substitution Task in the Cognitively Normal Elderly71	Distinct Biomarker Topographies Predict Alzheimer's Disease Onset at Different Stages 83
<i>Dana Tudorascu, Beth Snitz, Helmet Karim, Robert Nebes, Ann Cohen, Julie Price, Chester Mathis, William Klunk, Howard Aizenstein</i>	<i>Mathew Brier¹, Beau Ances^{1,2,3}, Karl Friedrichsen², Russ Hornbeck², Yi Su², Randall Bateman^{1,3}, John Morris^{1,3}, Tammie Benzinger^{2,3}</i>
<i>P73 Presented by: Tudorascu, Dana L</i>	<i>Presented by: Brier, Mathew R</i>
Using Neurostat and Statistical Stereotactic Surface Projection Maps to Compare Early Phase 18F-Florbetapir and FDG-PET Images.....72	Variable Isocortical vs. Limbic Distributions of [18F]-AV-1451 Binding in Braak Stage V-VI Alzheimer's Disease Subjects 84
<i>Angela Wang¹, Richard King², Satoshi Minoshima³, Norman Foster¹</i>	<i>Adam Schwarz¹, Sergey Shcherbinin¹, Bradley Miller¹, James Dickson², Abhinay Joshi², Michael Navitsky², Michael Devous, Sr², Mark Mintun²</i>
<i>P75 Presented by: Wang, Angela Y</i>	<i>Presented by: Schwarz, Adam J</i>
The Value of Amyloid Imaging in Differentiating Patients with Major Depressive Disorder vs Alzheimer's Disease with Depressive Symptoms .73	SESSION 6: Tau PET.....85
<i>Guofan Xu, David Douglas, Murphy Greer, Andrew Quon</i>	First-in-Human PET Study of a Novel Tau Tracer [18F]THK-5351 85
<i>P77 Presented by: Xu, Guofan</i>	<i>Ryuichi Harada¹, Nobuyuki Okamura^{1,2}, Shozo Furumoto³, Tetsuro Tago³, Katsutoshi Furukawa⁴, Aiko Ishiki⁴, Ren Iwata³, Manabu Tashiro³, Kazuhiko Yanai^{2,3}, Hiroyuki Arai⁴, Yukitsuka Kudo¹</i>
Longitudinal Change of Neuroimaging and Clinical Markers in Autosomal Dominant Alzheimer's Disease: Exploring Across-Group and Within-Individual Trajectories75	<i>Presented by: Harada, Ryuichi</i>
<i>Wai-Ying Wendy Yau¹, Eric McDade², Howard Aizenstein¹, Oscar Lopez², Chester Mathis³, Julie Price³, Beth Snitz², Lisa Weissfeld⁴, William Klunk^{1,2}</i>	Potential for PET Imaging Tau Tracer 18F-AV-1451 (also known as 18F-T807) to Detect Neurodegenerative Progression in AD 86
<i>P79 Presented by: Yau, Wai-Ying Wendy</i>	<i>Mark Mintun¹, Michael Devous¹, Michael Pontecorvo¹, Abhinay Joshi¹, Andrew Siderow¹, Keith Johnson², Michael Navitsky¹, Ming Lu¹</i>
SESSION 4: Biomarkers (part 1)76	<i>Presented by: Mintun, Mark</i>
In-vivo Staging of Preclinical Amyloid Deposition76	Diagnostic Utility and Clinical Significance of Tau PET Imaging with [11C]PBB3 in Diverse Tauopathies..... 87
<i>Michel Grothe¹, Henryk Barthel², Osama Sabri², Stefan Teipel^{1,3}</i>	<i>Hitoshi Shimada¹, Hitoshi Shinotoh^{1,2}, Naruhiko Sahara¹, Shigeki Hirano^{1,3}, Shogo Furukawa^{1,3}, Keisuke Takahata¹, Yasuyuki Kimura¹, Makiko Yamada^{1,4}, Yasumasa Yoshiyama⁵, Ming-Rong Zhang⁶, Hiroshi Ito^{7,8}, Makoto Higuchi¹, Satoshi Kuwabara³, Tetsuya Suhara¹</i>
<i>Presented by: Grothe, Michel J.</i>	<i>Presented by: Shimada, Hitoshi</i>
APOE ϵ4 allele is Associated with an Earlier Onset of Amyloid Accumulation78	Entorhinal, Parahippocampal, and Inferior Temporal F18-T807 SUVR Correlates with CSF Total Tau and Tau T181P in Cognitively Normal Elderly 88
<i>Murat Bilgel^{1,2}, Yang An¹, Yun Zhou³, Dean Wong³, Jerry Prince^{2,3,4}, Susan Resnick¹</i>	<i>Jasmeer Chhatwal^{1,3,5}, Aaron Schultz^{1,3,5}, Gad Marshall^{1,3,4,5}, Brendon Boot⁷, Teresa Gomez-Isla^{1,5}, Julien Dumurgier^{1,5}, Clemens Scherzer^{4,5,6}, Adrian Ivinson^{5,6}, Allyson Roe¹, Bradley Hyman^{1,3,5,6}, Reisa Sperling^{1,3,4,5}, Keith Johnson^{1,2,3,4,5}</i>
<i>Presented by: Bilgel, Murat</i>	<i>Presented by: Chhatwal, Jasmeer P</i>
Longitudinal Assessment of Aβ Accumulation in Non-demented Individuals: a 18F-flutemetamol Study79	KEYNOTE LECTURE 289
<i>Christopher Rowe¹, Vincent Doré², Pierrick Bourgeat³, Lennart Thurfjell⁴, Lance Macaulay⁵, Robert Williams⁷, Olivier Salvado³, David Ames⁶, Colin Masters⁷, Victor Villemagne^{1,7}</i>	Chronic Traumatic Encephalopathy: the Last Seven Years 89
<i>Presented by: Rowe, Christopher C</i>	<i>Ann McKee</i>
SESSION 5: Technical.....80	<i>Presented by: McKee, Ann</i>
Kinetics of AV-1451 Binding in Aging and Dementia.....80	
<i>Suzanne Baker¹, Daniel Schonhaut³, Sameul Lockhart², Gil Rabinovic³, William Jagust^{1,2}</i>	
<i>Presented by: Baker, Suzanne L</i>	

SESSION 7: Cognition90

Amyloid Negativity in Clinically Diagnosed ADNI Alzheimer's Disease Patients90

Susan Landau^{1,2}, Allison Fero^{1,2}, William Jagust^{1,2}

Presented by: Landau, Susan M

T807 PET Measures of Tau Pathology Associated with Episodic Memory Performance among Clinically Normal Older Individuals92

Reisa Sperling, Elizabeth Mormino, Dorene Rentz, Aaron Schultz, J. Alex Becker, Julius Trey Hedden, Jorge Sepulcre, Jasmeer Chhatwal, Rebecca Amariglio, Katherine Papp, Gad Marshall, David Hsu, Neil Vasdev, Keith Johnson

Presented by: Sperling, Reisa A

Preliminary Experience with [18F]AV1451 PET in Non-AD Neurodegenerative Syndromes.....93

Gil Rabinovici^{1,2,3}, Daniel Schonhaut^{1,2}, Suzanne Baker³, Andreas Lazaris¹, Rik Ossenkoppele^{1,2}, Sam Lockhart², Henry Schwimmer², Jacob Vogel², Nagehan Ayakta², Howard Rosen¹, Bruce Miller¹, James O'Neil³, Adam Boxer¹, William Jagust^{1,2,3}

Presented by: Rabinovici, Gil D

Longitudinal Effects of Amyloid Accumulation on Cognition in a Healthy Adult Cohort Aged 30-89: Results from the Dallas Lifespan Brain Study95

Denise Park¹, Michelle Farrell¹, Karen Rodrigue¹, Kristen Kennedy¹, Gérard Bischoff¹, Michael Devous, Sr.²

Presented by: Park, Denise C

SPECIAL LECTURE97

What Makes Association Networks Vulnerable to Neurodegeneration? Randy Buckner

Presented by: Buckner, Randy

POSTER SESSION (Even Numbers)98

The Pattern of [11C]-Pittsburgh Compound-B Binding in the Brains of Adults with Down's Syndrome.....98

Tiina Annus¹, Liam Wilson¹, Julio Acosta-Cabronero², Young Hong³, Tim Fryer³, Arturo Cardenas-Blanco², Shahid Zaman¹, Anthony Holland¹, Peter Nestor², et al.

P2 Presented by: Annus, Tiina

Clinical Utility of Amyloid Imaging in a Complex Case of Corticobasal Syndrome Presenting with Psychiatric Symptoms99

Mohamed Réda Bensaïdane^{1,2,3}, Marie-Pierre Fortin^{1,2}, Geneviève Damasse^{1,2}, Marise Chénard^{2,4}, Christine Dionne^{2,5}, Mélanie Duclos^{2,6}, Rémi Bouchard^{1,2,7}, Robert Jr. Laforce^{1,2,3}

P4 Presented by: Bensaïdane, Mohamed Réda

Temporal Progression of Cerebral Amyloid Deposition as Measured by ¹¹C-PiB PET Imaging101

Murat Bilgel^{1,2}, Susan Resnick¹, Dean Wong³, Bruno Jedynak⁴, Jerry Prince^{2,3,5}

P6 Presented by: Bilgel, Murat

Effects of Asymptomatic B-amyloid Positivity on Regional Cerebral Metabolism and CSF-pTau Levels 102

Andrea Bozoki, Monica Gentchev, David Zhu

P8 Presented by: Bozoki, Andrea C

Amyloid Exerts Distributed Effect on Glucose Metabolism in Preclinical Alzheimer's Disease. 103

Matthew Brier¹, John McCarthy², Karl Friedrichsen³, Tammie Benzinger^{3,4}, Russ Hornbeck³, Yi Su³, Randall Bateman^{1,4}, John Morris^{1,4}, Beau Ances^{1,3,4}

P10 Presented by: Brier, Matthew R

Striatal Amyloid Burden Measured by Quantitative [¹⁸F]flutemetamol PET Imaging on End of Life Subjects 104

Tom Beach¹, Dietmar Thal², Johan Lilja³, Chris Buckley⁴, Adrian Smith⁴, Gill Farrar⁴, Michelle Zanette⁵, Paul Sherwin⁵

P12 Presented by: Buckley, Chris J

Detecting Treatment Effects in Clinical Trials with Florbetapir-PET: An Alternative Statistical Approach to SUVR..... 105

Funan Shi^{1,2}, Thomas Bengtsson¹, David Clayton¹, Peter Bickel²

P14 Presented by: Clayton, David

Effect of Cognitively Stimulating Activities on PiB-PET in Cognitively Normal Elderly..... 107

Ann Cohen¹, Beth Snitz², Eric McDade², Howard Aizenstein¹, Robert Nebes¹, Lisa Weissfeld³, Julie Price⁴, Chester Mathis⁴, Oscar Lopez², William Klunk^{1,2}

P16 Presented by: Cohen, Ann D

Methods for the Quantitation of AV-1451 Uptake 108

Michael Devous, Sr, Abhinay Joshi, Ian Kennedy, Michael Navitsky, Michael Pontecorvo, Mark Mintun

P18 Presented by: Devous, Sr, Michael D

[F18] T807 PET Imaging of Hyperphosphorylated Tau to Differentiate PSP from PD 110

Stephen Gomperts, Sara Makaretz, Aaron Shultz, Christina Caso, Scott McGinnis, John Growdon, Brad Dickerson, Keith Johnson

P20 Presented by: Gomperts, Stephen N.

Comparison of NIA-AA Staging with CSF and Neuroimaging Biomarkers 111

Brian Gordon^{1,2}, Stephanie Vos³, John Morris^{2,4}, David Holtzman^{2,4,5}, Anne Fagan^{2,4,5}, Tammie Benzinger^{1,2}

P22 Presented by: Gordon, Brian A

In vitro and In vivo Evaluation of RO6931643, RO6924963 and RO6958948 Candidate PET Tracers for Aggregated Tau..... 113

Michael Honer¹, Henner Knust¹, Luca Gobbi¹, Hiroto Kuwabara², Dieter Muri¹, Heather Valentine², Robert Comley¹, Susanne Ostrowitzki¹, Robert Dannals², Dean Wong², Edilio Borroni¹

P24 Presented by: Honer, Michael

Development of a CAA Selective Radioligand for PET Imaging: a Preclinical Study in PSAPP Mice 114

Milos Ikonovic, Eric Abrahamson, Manik Debnath, Lan Shao, Li Shao, Guo-Feng Huang, William

Paljug, James Ruszkiewicz, William Klunk, Chester Mathis
P26 Presented by: Ikonomic, Milos
Amyloid Negativity in Progressive Cognitive Decline: Is it a Safety or a Risk for Alzheimer's Disease?.....115
Kenji Ishii, Kenji Ishibashi, Muneyuki Sakata, Kei Wagatsuma, Jun Toyohara, Kiichi Ishiwata, Shigeo Murayama
P28 Presented by: Ishii, Kenji
In vivo Competition between [11C]PiB and NAV4694 in a Transgenic Rat Model of Amyloidosis116
Min Su Kang^{1,2}, Maxime Parent^{1,2}, Eduardo Zimmer^{1,2}, Monica Shin^{1,2}, Sonia Carmo⁵, Antonio Aliaga⁴, Cornelia Reininger⁶, Jean-Paul Soucy⁴, Serge Gauthier², A. Claudio Cuello⁵, Pedro Rosa-Neto^{1,2,3,4,5}
P30 Presented by: Kang, Min Su
Investigating the Utility of FDG and AV45 PET in both Two-classification and Multi-classification of Alzheimer's Disease and Its Prodromal Stages..117
Chunfei Li¹, Qi Zhou¹, Mohammed Goryawala², Mercedes Cabrerizo¹, David Loewenstein³, Warren Barker⁴, Ranjan Duara⁴, Malek Adjouadi¹
P32 Presented by: Li, Chunfei
Differential Cortical Ribbon Binding of Amyloid and Tau Tracers in Alzheimer's disease.....118
Yi Li¹, Wai Tsui¹, Henry Rusinek¹, Nobuyuki Okamura², Momy de Leon¹, et al.
P34 Presented by: Li, Yi
Increased PiB Accumulation Occurs in the White Matter of PiB Positive Subjects119
Val Lowe, Matthew Senjem, Scott Przybelski, Stephen Weigand, David Knopman, Bradley Boeve, Kejal Kantarci, Clifford Jack, Ronald Petersen
P36 Presented by: Lowe, Val J
Regional Dynamics of Local Amyloid Burden on Hypo-metabolism in 24-month Follow-up.....120
Sulantha Mathotaarachchi^{1,5}, Sara Mohades¹, Thomas Beaudry¹, Monica Shin^{1,5}, Seqian Wang^{1,5}, Andrea Benedet^{1,5}, Tharick Pascoal^{1,5}, Maxime Parent^{1,5}, Min Kang^{1,5}, Vladimir Fonov^{1,5}, Sarinporn Manitsirikul¹, Serge Gauthier⁶, Aurélie Labbe^{3,4}, Pedro Rosa Neto^{1,2}
P38 Presented by: Mathotaarachchi, Sulantha
Early Striatal Binding of PiB-PET Amyloid Distinguishes Down's Syndrome and Autosomal Dominant Alzheimer Dementia Mutation Carriers From Late Onset Deposition.....122
Eric McDade¹, Annie Cohen¹, Brad Christian², Julie Price¹, Chet Mathis¹, William Klunk¹, Ben Handen¹
P40 Presented by: McDade, Eric
Tau Imaging with 18F-(S)-THK-5117 in MCI and AD Patients Using a PET Multi-tracer Concept123
Agneta Nordberg^{1,5}, Konstantinos Chiotis¹, Laure Aubert¹, Anders Wall², My Jonasson², Mark Lubberink², Jonas Eriksson³, Ove Almkvist¹, Nobuyuki Okamura⁴, Gunnar Antoni²
P44 Presented by: Nordberg, Agneta

Beta-amyloid Deposition is Associated with Increased Brain Activity during Working Memory and Executive Control Tasks among Cognitively Normal Elderly 124
Hwamee Oh^{1,2}, Jason Steffener^{1,2}, Ray Razlighi^{1,2}, Christian Habeck^{1,2}, Dan Liu², Sarah Janicki², Yaakov Stern^{1,2}
P46 Presented by: Oh, Hwamee
Validation of Automated Analysis of Tracer Binding on THK Tau PET Images 126
Nobuyuki Okamura^{1,2}, Ryuichi Harada², Shozo Furumoto³, Katsutoshi Furukawa⁴, Aiko Ishiki⁴, Ren Iwata³, Manabu Tashiro³, Kazuhiko Yanai^{1,3}, Hiroyuki Arai⁴, Yukitsuka Kudo²
P48 Presented by: Okamura, Nobuyuki
Determining Total Amyloid Plaque Burden in AV-45 Positron Emission Tomography/Computed Tomography (PET/CT) Scans..... 127
David Creed, Amy McCann, Jeff Burns, Eric Vidoni, Paul Welch, Mark Perry
P50 Presented by: Perry, Mark
Relationships between Florbetapir PET Amyloid and 18F-AV-1451 (aka 18F-T807) PET Tau Binding in Cognitively Normal Subjects and Patients with Cognitive Impairments Suspected of Alzheimer's Disease..... 129
Michael Pontecorvo, Michael Devous, Abhinav Joshi, Ming Lu, Andrew Siderowf, Anupa Arora, Mark Mintun
P54 Presented by: Pontecorvo, Michael J
Brain Amyloid Load Is Associated with Impaired Executive Functioning in Elderly Individuals at-risk to Develop Dementia..... 131
Juha Rinne^{1,2}, Nina Kemppainen^{1,2}, Tiia Ngandu^{3,4}, Alina Solomon^{4,5,6}, Riitta Parkkola⁷, Jarkko Johansson¹, Jenni Lehtisalo³, Tuomo Hänninen⁸, Teemu Paajanen⁹, Tiina Laatikainen^{3,10}, Hilikka Soininen⁵, Miia Kivipelto^{3,4,5,6}
P56 Presented by: Rinne, Juha O
Association of Vitamin E Use and Two-Year Amyloid Accumulation in Healthy Older Adults and Early Mild Cognitive Impairment..... 132
Shannon Risacher¹, Karmen Yoder¹, William Jagust³, Paul A⁴, Ronald Petersen⁵, Michael Weiner⁶, Andrew S²
P58 Presented by: Risacher, Shannon L
Longitudinal Multitracer PET Imaging Studies in Familial and Sporadic Alzheimer's Disease..... 133
Elena Rodriguez-Vieitez¹, Stephen F. Carter^{1,2}, Laure Saint-Aubert¹, Ove Almkvist^{1,3,4}, Karim Farid¹, Michael Schöll^{1,5}, Konstantinos Chiotis¹, Steinunn Thordardottir^{4,6}, Anders Wall⁷, Caroline Graff^{4,6}, Bengt Långström⁸, Agneta Nordberg^{1,4}
P60 Presented by: Rodriguez-Vieitez, Elena
Semiquantitative Analyses and Visual Assessment of the Novel β -Amyloid Tracer [18F]NAV4694 . 134
Axel Rominger¹, Matthias Brendel¹, Franziska Scheiwein¹, Julia Sauerbeck¹, Andreas Delker¹, Peter Bartenstein¹, John Seibyl², Cornelia Reininger³
P62 Presented by: Rominger, Axel

Relationship between Post-mortem THK-5117 Binding and In-vivo PET Biomarkers Uptake in AD135
Laure Saint-Aubert¹, Laetitia Lemoine¹, Amelia Marulle¹, Gunnar Antoni^{2,3}, Jonas Eriksson³, Nobuyuki Okamura⁴, Inger Nennesmo⁵, Per-Göran Gillberg¹, Agneta Nordberg^{1,6}
P64 Presented by: Saint-Aubert, Laure

Partial Volume Effect Simulations to Assess Regional Gray and White Matter Content in Brain PET and its Impact on Measuring Longitudinal Changes in Amyloid Burden136
Sandra Sanabria Bohorquez, Farshid Faraji, David Clayton, Alex de Crespiigny
P66 Presented by: Sanabria Bohorquez, Sandra

In vivo Braak Staging Using [18F]-AV1451 Tau PET Imaging138
Michael Schöll^{1,2}, Daniel Schonhaut³, Jacob Vogel¹, Samuel Lockhart¹, Suzanne Baker⁴, Henry Schwimmer¹, Rik Ossenkoppele³, Gil Rabinovici³, William Jagust¹
P68 Presented by: Schöll, Michael

Early Experience with the High Contrast Novel B-Amyloid Tracer 18F NAV4694: Correlation of Visual Interpretation with Clinical and Quantitative Parameters140
John Seibyl¹, Phillip Kuo², Cornelia Reininger³
P70 Presented by: Seibyl, John

Tau and Amyloid Deposits Relate to Distinctive Cortical Atrophy Patterns in Cognitively Normal Elderly141
Jorge Sepulcre^{1,2}, Aaron Schultz², Alex Becker¹, Reisa Sperling^{2,3,4}, Keith Johnson^{1,3,4}
P72 Presented by: Sepulcre, Jorge

Parametric Binding Potential Maps of the Tau Imaging Tracer [18F]-AV-1451 (T807)142
Sergey Shcherbinin¹, Adam Schwarz¹, Michael Devous², Abhinay Joshi², Michael Navitsky², James Dickson², Mark Mintun²
P74 Presented by: Shcherbinin, Sergey

Understanding the Diagnostic Accuracy of [18F]Flutemetamol143
Adrian Smith¹, Chris Buckley¹, Paul Jones¹, Michelle Zanette², Sherwin Paul², Milos Ikonovic³, Gill Farrar¹
P76 Presented by: Smith, Adrian PL

Longitudinal Processing Speed, Working Memory and Inhibitory Control in Relation to Baseline Preclinical Amyloid Staging144
Beth Snitz¹, Dana Tudorascu¹, Robert Nebes¹, Ann Cohen¹, Howard Aizenstein¹, Julie Price¹, Chester Mathis¹, Lisa Weissfeld², William Klunk¹
P78 Presented by: Snitz, Beth E.

Age-dependent Effect of Cortical Amyloid-Beta Deposition on Hippocampal Activity in Cognitively Normal Adults145
Zhuang Song, Denise Park
P80 Presented by: Song, Zhuang

Chirality of [18F]THK-5105 Affects its Preclinical Characteristics as a PET Tau Imaging Probe ... 146
Tetsuro Tago^{1,2}, Shozo Furumoto^{1,3}, Nobuyuki Okamura⁴, Ryuichi Harada⁵, Hajime Adachi^{1,2}, Yoichi Ishikawa¹, Kazuhiko Yanai⁴, Ren Iwata¹, Yukitsuka Kudo⁵
P82 Presented by: Tago, Tetsuro

Amyloid-Beta Burden is Inversely Associated with Gray Matter Volume but not Semantic Memory Performance in Cognitively Normal First-Degree Relatives at Risk for Alzheimer's Disease 147
Christopher van Dyck, Shuo Wang, Nicole Barcelos, Beata Planeta-Wilson, Adam Mecca, Joel Gelernter, Peter Van Ness, Richard Carson
P84 Presented by: van Dyck, Christopher H

A 52-week Pilot Study Targeting Aβ with PBT2: Neuroimaging Results 148
Victor Villemagne^{1,2}, Christopher Rowe¹, Kevin Barnham², Robert Cherny², Michael Woodward³, Svetlana Pejoska¹, Gareth Jones¹, Rudy Tanzi⁴, Colin Masters²
P86 Presented by: Villemagne, Victor L

Case Report: Longitudinal Measures of Beta-amyloid Burden and Grey Matter Atrophy in an Adult with Down's Syndrome without Dementia 149
Liam Wilson¹, Tiina Annus¹, Young Hong², Julio Acost-Cabronero³, Tim Fryer³, Peter Nestor², Anthony Holland¹, Shahid Zaman¹, et al.
P88 Presented by: Wilson, Liam R

Between Cohort Transferability of Clinical Trial Enrichment with Amyloid Imaging and Hippocampal Volume 150
Robin Wolz^{1,2}, Katherine Gray^{1,2}, Derek Hill¹
P90 Presented by: Wolz, Robin

SESSION 8: Biomarkers (part 2)151

Optimizing PiB-PET SUVR Calculations by a Large-Scale Analysis of Longitudinal Reliability 151
Christopher Schwarz¹, Matthew Senjem², Jeffrey Gunter², Nirubol Tosakulwong³, Scott Przybelski³, Stephen Weigand³, Anthony Sychalla¹, Ronald Petersen⁴, Val Lowe¹, Clifford Jack¹
Presented by: Schwarz, Christopher G

Beta-amyloid Deposition in Non-amnestic Clinical Presentations 152
Keith Josephs, Jennifer Whitwell, Joseph Duffy, Edythe Strand, Mary Machulda, Daniel Drubach, Matthew Senjem, Clifford Jack Jr, Ronald Petersen, Val Lowe
Presented by: Josephs, Keith A

Between SNAP and a Hard Aβ Rock: Characterizing the Fate of Preclinical AD 153
Samantha Burnham¹, Pierrick Bourgeat², Vincent Doré³, Belinda Brown⁴, Olivier Salvado², Ralph Martins⁴, Lance Macaulay⁵, Colin Masters⁶, Christopher Rowe⁷, Victor Villemagne^{6,7}
Presented by: Villemagne, Victor L

PRESENTER INDEX

LECTURES

Presented by: Baker, Suzanne L.....	81
Presented by: Bilgel, Murat.....	78
Presented by: Brier, Matthew R.....	83
Presented by: Buckner, Randy.....	97
Presented by: Chhatwal, Jasmeer P.....	88
Presented by: DeCarli, Charles.....	14
Presented by: Dickson, Dennis.....	24
Presented by: Fletcher, Evan.....	15
Presented by: Grothe, Michel J.....	77
Presented by: Harada, Ryuichi.....	85
Presented by: Hsu, David C.....	18
Presented by: Josephs, Keith A.....	152
Presented by: Kim, Hee Jin.....	16
Presented by: Klunk, William.....	17
Presented by: Landau, Susan M.....	91
Presented by: Lowe, Val J.....	28
Presented by: Marquie, Marta.....	27
Presented by: Mintun, Mark.....	86
Presented by: McKee, Ann.....	89
Presented by: Murray, Melissa E.....	25
Presented by: Nadkarni, Neelesh K.....	21
Presented by: Park, Denise C.....	96
Presented by: Price, Julie.....	26
Presented by: Rabinovici, Gil D.....	94
Presented by: Rowe, Christopher C.....	79
Presented by: Saykin, Andrew J.....	23
Presented by: Schwarz, Adam J.....	84
Presented by: Schwarz, Christopher G.....	151
Presented by: Shimada, Hitoshi.....	87
Presented by: Sperling, Reisa A.....	92
Presented by: Unschuld, Paul.....	19
Presented by: Villemagne, Victor L.....	153
Presented by: Villeneuve, Sylvia.....	82

ODD-NUMBERED POSTERS

P1 Presented by: Adamczuk, Katarzyna.....	29
P3 Presented by: Almkvist, Ove.....	30
P5 Presented by: Barret, Olivier.....	31
P7 Presented by: Bischof, Gerard N.....	32
P9 Presented by: Brier, Matthew R.....	33
P11 Presented by: Chiotis, Konstantinos.....	34
P13 Presented by: Christian, Bradley T.....	35
P15 Presented by: Dickerson, Bradford C.....	36
P17 Presented by: Douglas, David B.....	38
P19 Presented by: Duara, Ranjan.....	40
P21 Presented by: Eberling, Jamie.....	41
P23 Presented by: Farrell, Michelle E.....	42
P25 Presented by: Gottesman, Rebecca F.....	43
P27 Presented by: Grothe, Michel J.....	44
P29 Presented by: Gurol, M. Edip.....	45
P31 Presented by: Hohman, Timothy J.....	47
P33 Presented by: Kato, Takashi.....	48
P35 Presented by: Klein, Gregory.....	49
P37 Presented by: Lemoine, Laetitia.....	50
P39 Presented by: Lin, Yin-Guo.....	51
P41 Presented by: Lockhart, Samuel N.....	53
P43 Presented by: Loewenstein, David.....	55
P45 Presented by: Marquie, Marta.....	56
P47 Presented by: Matthews, Dawn C.....	57
P49 Presented by: Mielke, Michelle M.....	58

P51 Presented by: Mikhno, Arthur.....	59
P55 Presented by: Ossenkoppele, Rik.....	61
P57 Presented by: Pa, Judy.....	62
P59 Presented by: Perry, Mark.....	63
P61 Presented by: Risacher, Shannon L.....	65
P63 Presented by: Rominger, Axel.....	66
P65 Presented by: Schultz, Aaron P.....	67
P67 Presented by: Seibyl, John.....	68
P69 Presented by: Seo, Sang Won.....	69
P71 Presented by: Shokouhi, Sepideh.....	70
P73 Presented by: Tudorascu, Dana L.....	71
P75 Presented by: Wang, Angela Y.....	72
P77 Presented by: Xu, Guofan.....	74
P79 Presented by: Yau, Wai-Ying Wendy.....	75

EVEN-NUMBERED POSTERS

P2 Presented by: Annus, Tiina.....	98
P4 Presented by: Bensaidane, Mohamed Réda.....	100
P6 Presented by: Bilgel, Murat.....	101
P8 Presented by: Bozoki, Andrea C.....	102
P10 Presented by: Brier, Matthew R.....	103
P12 Presented by: Buckley, Chris J.....	104
P14 Presented by: Clayton, David.....	106
P16 Presented by: Cohen, Ann D.....	107
P18 Presented by: Devous, Sr, Michael D.....	109
P20 Presented by: Gomperts, Stephen N.....	110
P22 Presented by: Gordon, Brian A.....	112
P24 Presented by: Honer, Michael.....	113
P26 Presented by: Ikonovic, Milos.....	114
P28 Presented by: Ishii, Kenji.....	115
P30 Presented by: Kang, Min Su.....	116
P32 Presented by: Li, Chunfei.....	117
P34 Presented by: Li, Yi.....	118
P36 Presented by: Lowe, Val J.....	119
P38 Presented by: Mathotaarachchi, Sulantha.....	121
P40 Presented by: McDade, Eric.....	122
P44 Presented by: Nordberg, Agneta.....	123
P46 Presented by: Oh, Hwamee.....	125
P48 Presented by: Okamura, Nobuyuki.....	126
P50 Presented by: Perry, Mark.....	128
P54 Presented by: Pontecorvo, Michael J.....	130
P56 Presented by: Rinne, Juha O.....	131
P58 Presented by: Risacher, Shannon L.....	132
P60 Presented by: Rodriguez-Vieitez, Elena.....	133
P62 Presented by: Rominger, Axel.....	134
P64 Presented by: Saint-Aubert, Laure.....	135
P66 Presented by: Sanabria Bohorquez, Sandra.....	137
P68 Presented by: Schöll, Michael.....	139
P70 Presented by: Seibyl, John.....	140
P72 Presented by: Sepulcre, Jorge.....	141
P74 Presented by: Shcherbinin, Sergey.....	142
P76 Presented by: Smith, Adrian PL.....	143
P78 Presented by: Snitz, Beth E.....	144
P80 Presented by: Song, Zhuang.....	145
P82 Presented by: Tago, Tetsuro.....	146
P84 Presented by: van Dyck, Christopher H.....	147
P86 Presented by: Villemagne, Victor L.....	148
P88 Presented by: Wilson, Liam R.....	149
P90 Presented by: Wolz, Robin.....	150

KEYWORD INDEX

- [11C]PBB3, 87
- [11C]PiB, 116
- [18F] AV-1451, 53
- [18F] AV45-PET, 66
- [18F]Florbetapir, 23, 65
- [18F]Florbetapir PET, 132
- [18F]Fluorodeoxyglucose, 23
- [18F]flutemetamol, 104, 143
- [18F]NAV4694, 116
- 11C-deuterium-L-deprenyl, 133
- 18F-(S)-THK5117, 123
- 18F-FDG, 123
- AD biomarker, 32
- age, 145
- aging, 62, 81, 141
- agnosia, 152
- alpha-synuclein, 41
- Alzheimer's disease, 23, 25, 30, 38, 66, 79, 84, 87, 98, 102, 112, 117, 121, 135, 146
- Alzheimer's Disease Neuroimaging Initiative, 23, 49, 55, 65, 132
- amyloid, 16, 17, 38, 42, 49, 55, 92, 110, 130, 131
- amyloid angiopathy, 56
- amyloid imaging, 14, 96, 137
- amyloid PET, 53, 100
- amyloid plaques, 118
- amyloid therapy, 68
- amyloid-beta. *See* A β
- amyloid-phase, 104
- aphasia, 152
- APOE, 42, 55, 78
- ApoE-e4, 19, 58
- Astrocytosis, 133
- atrophy, 149
- autopsy, 47
- autoradiography, 27
- autosomal dominant, 122, 133
- AV-1451, 31, 61, 84, 86, 109, 130, 139
- AV45, 72
- AV45 PET, 77, 117
- A β , 19, 79, 145, 148
- Beta-amyloid, 15, 32, 56, 125
- binding, 142
- biomarkers, 112
- body-mass index, 18
- borderline pathology, 143
- Braak, 139
- Braak tangle stage, 25
- cerebral amyloid angiopathy, 45
- cerebral microbleeds, 45
- cerebrovascular disease, 16
- cerebrovascular risk, 14
- chronic traumatic encephalopathy, 94
- classification, 117
- clinical trials, 150
- clinically normal, 18
- cognition, 16, 21, 30, 47, 96, 130
- cognitive aging, 14
- cognitive decline, 153
- cognitive impairment, 14
- cognitively normal aging, 53
- CogState, 58
- competitive binding, 116
- cortical thickness, 34
- cortical thinning, 32
- corticobasal syndrome, 100
- CSF, 23, 29, 57, 65, 87, 88, 112
- CSF Biomarkers, 47
- CSF-A β , 91
- dementia, 81, 131
- depression, 74
- diagnosis, 91
- diagnostic accuracy, 143
- diffuse plaques, 56
- Down's syndrome, 98, 122, 149
- dual-tasking, 21
- DVR, 101
- Early Mild Cognitive Impairment (EMCI), 57, 132
- enrichment, 150
- epidemiology, 43
- FDG, 57, 61, 72, 91
- FDG PET, 102, 117
- florbetapir, 43, 49, 59, 72, 77, 91
- florbetapir PET, 106
- Flutemetamol, 29, 79
- fMRI, 62, 145
- Freesurfer, 49
- fronto-parietal network, 125
- frontotemporal dementia, 36, 94
- frontotemporal lobar degeneration, 152
- glucose metabolism, 121
- Grey matter, 147
- Grey matter volume, 141
- hippocampal volume, 150
- hippocampus, 55, 145
- image processing, 31
- image reading, 143
- imaging, 126
- in vitro, 135
- in vivo PET, 116
- interface, 21
- intervention, 131
- iron, 19
- kinetics, 142

leukoaraiosis, 45
Lewy body dementia, 41
lifespan, 32, 96
lifetime cognitive engagement, 42
linear regression, 106
longitudinal, 48, 58, 67, 96, 137, 151
longitudinal amyloid beta-PET, 70
longitudinal amyloid imaging, 132
longitudinal change, 15
longitudinal progression, 101
MCI, 19, 55, 59, 87, 150
memory, 62, 65, 92
metabolism, 21
methodology, 106
middle age, 42
mobility, 21
modeling, 142
MRI, 14, 34, 44, 47, 98, 149
NAV4694, 100, 134, 140
negative predict value, 74
neuritic plaques, 69
neurodegeneration, 153
neurofibrillary tangles, 86, 109, 118
neuropathology, 25, 26, 84
NIA-AA, 112
non-AD tauopathies, 87
non-amnestic, 152
normal aging, 32, 125
older adults, 29
Parkinson's disease, 41, 110
Partial Volume Correction, 147
Partial Volume Effect, 137
partial volume effect correction, 66
pathology, 17, 69
PBT2, 148
PET, 23, 26, 27, 31, 34, 44, 53, 56, 59, 61, 62, 68, 72, 84, 86, 109, 112, 121, 126, 134, 135, 140, 146
PET imaging, 123, 133
PET PIB, 30
PiB, 25, 26, 29, 56, 61, 67, 69, 101, 131
PiB change point, 78
PiB-PET, 19, 45, 48, 98, 149
Pittsburgh compound B. *See* PiB
plaques, 104
Pons, 104
power analysis, 48
preclinical Alzheimer's disease, 29, 147
predementia, 44
pre-symptomatic, 77, 102
primary progressive aphasia, 36
prodromal, 44
prodromal AD, 59
progressive supranuclear palsy, 94
PSP, 110
PVC, 151
quantitation, 134
racial disparities, 43
reference region, 66
Reference-Region, 151
regional progression pattern, 77
risk factor, 131
semantic memory, 147
SNAP, 153
statistical descriptors, 70
striatum, 104, 122
stroke risk, 47
structural magnetic resonance imaging, 23
superficial siderosis, 45
SUV, 68
SUVR, 49, 106, 151
T807, 31, 67, 86, 88, 109, 110, 130
tangles, 27
tau, 27, 31, 34, 61, 67, 84, 86, 88, 92, 109, 110, 123, 126, 130, 135, 139, 142
Tau AV-1451, 81
tau imaging, 87, 146
Thal amyloid phase, 25
therapeutics, 148
THK5117, 34
threshold, 57
tracer, 142
two-point correlation functions, 70
vascular disease, 17
visual assessment, 134
Vitamin E, 132
voxel-based, 59
white matter, 38

Human Amyloid Imaging 2015 – Program Overview

All sessions will be held at the Miami Beach Resort; the overflow room will be set up in the Spanish Suite (mezzanine)

Wednesday, January 14

6:00-6:30p	Check-in (Grande Promenade Foyer, Ground Floor) Poster Installation (odd numbers)
6:30-8:30p	Welcome and Networking Reception (Oceanview Room/Poolside)

Thursday, January 15

7:00-8:00a	Check-in (Grande Promenade Foyer, Ground Floor) Breakfast (Starlight Room, 18 th Floor) Odd-numbered Poster Installation (Regency Ballroom)	
8:00-8:10	Welcome and Introductory Notes (Grande Promenade Ballroom, Ground Floor)	Keith Johnson, MD Massachusetts General Hospital
8:10-9:10	SESSION 1: VASCULAR	Chairs: William Klunk, MD, PhD University of Pittsburgh Vladimir Hachinski, MD, FRCP University of Western Ontario
8:10-8:25	Vascular Risk Factors Impact Cognition Independent of PIB PET and MRI Measures of AD and Vascular Brain Injury	Charles DeCarli, MD University of California, Davis
8:25-8:40	Associations between β -amyloid, Memory and Longitudinal Brain Change across the Spectrum of Cognitive Functioning	Evan Fletcher, PhD University of California, Davis
8:40-8:55	Amyloid, Cerebrovascular Disease and Cognitive Decline in MCI patients: A Prospective Longitudinal Study	Hee Jin Kim, MD Sungkyunkwan Univ. School of Med.
8:55-9:10	Interactions of Amyloid and Vascular Pathology in MCI	William Klunk, MD, PhD University of Pittsburgh
9:10-9:40	Session 1 Discussion	
9:40-10:00	Break	
10:00-11:00	SESSION 2: AMYLOID-ASSOCIATED PHENOMENA	Chairs: Agneta Nordberg, MD, PhD Karolinska Institute Christopher Rowe, MD Austin Health
10:00-10:15	Lower Body-Mass Index is Associated with Higher Cortical Amyloid Burden in Clinically Normal Elderly	David Hsu, MD Harvard Medical School
10:15-10:30	Regional Cerebral Iron Concentrations as Indicated by Magnetic Susceptibilities Measured with Quantitative Susceptibility Mapping at 7 Tesla Correlate with Brain A β Plaque Density as Measured by 11-C-Pittsburgh Compound B Positron-Emission-Tomography in Elderly Subjects at Risk for Alzheimer's Disease	Paul Unschuld, MD University of Zürich
10:30-10:45	The Cognition-Mobility Interface (COMBINE) is Associated with Cerebral Amyloid Deposition and Glucose Metabolism in Older Adults without Cognitive or Mobility Impairment	Neelesh Nadkarni, MD, PhD University of Pittsburgh
10:45-11:00	Multivariate AD Biomarker Profiles: Relation to Clinical and Cognitive Progression	Andrew Saykin, PhD Indiana University School of Medicine
11:00-11:30	Session 2 Discussion	
11:30-12:00p	KEYNOTE LECTURE: The Spectrum of Age-Associated Tauopathies	Dennis Dickson, MD Mayo Clinic
12:00-12:15	Keynote Discussion	
12:15-1:30	Lunch	
1:30-2:30	SESSION 3: PATHOLOGY	Chairs: Gil Rabinovici, MD University of California San Francisco Dennis Dickson, MD Mayo Clinic
1:30-1:45	Clinicopathologic and [11C]-PiB-PET Implications of Thal Amyloid Phase across the Spectrum of Alzheimer's Disease Pathology	Melissa Murray, PhD, Mayo Clinic
1:45-2:00	PiB PET and Postmortem Neuropathology Correlations in the Precuneus: A Role for Diffuse A β Plaques	Julie Price, PhD, University of Pittsburgh
2:00-2:15	Towards the Validation of Novel PET Tracer T807 on Postmortem Human Brain Tissue Samples	Marta Marquie, MD, Massachusetts General Hospital
2:15-2:30	AV-1451 Autoradiographic Evaluation in Subjects with TDP-43- versus Tau-immunoreactive Lesions	Val Lowe, MD, Mayo Clinic
2:30-3:00	Session 3 Discussion	

3:00-4:30 POSTER SESSION (ODD NUMBERS) and COFFEE (<i>Regency Ballroom and Conference Room</i>)		
4:30-5:15	SESSION 4: BIOMARKERS 1	Chairs: Clifford Jack, MD Mayo Clinic Victor Villemagne, PhD Austin Health
4:30-4:45	In-vivo Staging of Preclinical Amyloid Deposition	Michel Grothe, PhD German Ctr. for Neurodegen. Diseases
4:45-5:00	APOE ε4 Allele is Associated with an Earlier Onset of Amyloid Accumulation	Murat Bilgel, BS Johns Hopkins University
5:00-5:15	Longitudinal Assessment of Aβ Accumulation in Non-demented Individuals: a 18F-flutemetamol Study	Christopher Rowe, MD Austin Health
5:15-5:45	Session 4 Discussion	
5:45-6:15	<i>Odd-numbered poster removal (posters not removed by 6:15 pm will be discarded)</i>	
6:15-6:45	<i>Even-numbered poster installation (Regency Ballroom)</i>	
5:45-8:00	NETWORKING RECEPTION (<i>Starlight Room, 18th Floor</i>)	
Friday, January 16		
7:00-8:00a	<i>Check-in (Grande Promenade Foyer, Ground Floor)</i>	
	<i>Breakfast (Starlight Room, 18th Floor)</i>	
	<i>Even-numbered Poster Installation (Regency Ballroom)</i>	
8:00-9:00	SESSION 5: TECHNICAL	Chairs: Chester Mathis, PhD University of Pittsburgh Robert Koeppe, PhD University of Michigan
8:00-8:15	Kinetics of AV-1451 Binding in Aging and Dementia	Suzanne Baker, PhD Lawrence Berkeley National Lab
8:15-8:30	Are Low Levels of β-amyloid Deposition Clinically Significant?	Sylvia Villeneuve, PhD Northwestern University
8:30-8:45	Distinct Biomarker Topographies Predict Alzheimer's Disease Onset at Different Stages	Matthew Brier, BS Washington University
8:45-9:00	Variable Isocortical vs. Limbic Distributions of [18F]-AV-1451 Binding in Braak Stage V-VI Alzheimer's Disease Subjects	Adam Schwarz, PhD Eli Lilly & Co., Inc.
9:00-9:30	Session 5 Discussion	
9:30-9:50	Break	
9:50-10:50	SESSION 6: TAU PET	Chairs: Keith Johnson, MD Massachusetts General Hospital William Jagust, MD University of California Berkeley
9:50-10:05	First-in-human PET Study of a Novel Tau Tracer [18F]THK-5351	Ryuichi Harada, MD Tohoku University
10:05-10:20	Potential for PET Imaging Tau Tracer 18F-AV-1451 (also known as 18F-T807) to Detect Neurodegenerative Progression in Alzheimer's Disease	Mark Mintun, MD Avid Pharmaceuticals
10:20-10:35	Diagnostic Utility and Clinical Significance of Tau PET imaging with [11C]PBB3 in Diverse Tauopathies	Hitoshi Shimada, MD, PhD National Institute of Radiological Sci.
10:35-10:50	Entorhinal, Parahippocampal, and Inferior Temporal F18-T807 SUVR Correlates with CSF Total Tau and Tau T181P in Cognitively Normal Elderly	Jasmeer Chhatwal, MD, PhD Harvard Medical School/MGH
10:50-11:20	Session 6 Discussion	
11:20-11:45	KEYNOTE LECTURE 2: Chronic Traumatic Encephalopathy: The Last Seven Years	Ann McKee, MD Boston University
11:45-12:00p	Keynote Discussion	
12:00-1:10	Lunch	
1:10-2:10	SESSION 7: COGNITION	Chairs: Randy Buckner, PhD Harvard University/MGH Susan Resnick, PhD NIH/NIA
1:10-1:25	Amyloid Negativity in Clinically Diagnosed ADNI Alzheimer's Disease Patients	Susan Landau, PhD University of California, Berkeley
1:25-1:40	T807 PET Measures of Tau Pathology Associated with Episodic Memory Performance among Clinically Normal Older Individuals	Reisa Sperling, MD Brigham and Women's Hospital
1:40-1:55	Preliminary Experience with [18F]AV1451 PET in Non-AD Neurodegenerative Syndromes	Gil Rabinovici, MD University of California, San Francisco

1:55-2:10	Longitudinal Effects of Amyloid Accumulation on Cognition in a Healthy Adult Cohort Aged 30-89: Results from the Dallas Lifespan Brain Study	Denise Park, PhD University of Texas, Dallas
2:10-2:30	SPECIAL LECTURE: What Makes Association Networks Vulnerable to Neurodegeneration?	Randy Buckner, PhD Harvard University/MGH
2:30-3:00	Session 7 Discussion	
3:00-4:30	POSTER SESSION (EVEN NUMBERS) and COFFEE (<i>Regency Ballroom and Conference Room</i>)	
4:30-4:40	AWARDS CEREMONY	
4:40-5:25	SESSION 8: BIOMARKERS 2	CHAIRS: Andrew Saykin, PhD Indiana University School of Medicine Julie Price, PhD University of Pittsburgh
4:40-4:55	Optimizing PiB-PET SUVR Calculations by a Large-Scale Analysis of Longitudinal Reliability	Christopher Schwarz, PhD Mayo Clinic
4:55-5:10	Beta-amyloid Deposition in Non-Amnesic Clinical Presentations	Keith Josephs, MD Mayo Clinic
5:10-5:25	Between SNAP and a Hard A β rock: Characterizing the Fate of Preclinical Alzheimer's Disease	Victor Villemagne, MD Austin Health
5:25-5:55	Session 8 Discussion	
5:55-6:00	Closing Notes	
6:00-6:30	<i>Poster removal (posters not removed by 6:30 pm will be discarded)</i>	

Human Amyloid Imaging 2015 (HAI-2015)

Miami, Florida, January 14 - 16, 2015

Oral communication

SESSION 1: Vascular

CHAIRS: William Klunk, MD, PhD, *University of Pittsburgh*
Vladimir Hachinski, MD, DSc, FRCP, *University of Western Ontario*

Vascular Risk Factors Impact Cognition Independent of PIB PET and MRI Measures of AD and Vascular Brain Injury

Charles DeCarli¹, Dan Mungas¹, Owen Carmichael², Sylvia Villeneuve³, Evan Fletcher¹, Baljeet Singh¹, William Jagust³, Bruce Reed¹

¹ *University of California at Davis, Sacramento, CA, United States*

² *Pennington Biomedical Research Center, Louisiana State University, Baton Rouge, Louisiana, United States*

³ *University of California at Berkeley, Berkeley, California, United States*

Background: Alzheimer's (AD) and vascular disease commonly causes dementia. Amyloid imaging in combination with MRI allows for in vivo assessment of the combined influence of vascular and AD on cognitive decline. Previous evidence showed that vascular brain injury is significantly associated with cognitive ability independent of amyloid load. We extended this work by examining the impact of vascular risk factors, MRI measures and amyloid load on cognition in a cohort representative of the general population.

Method: 65 subjects aged 73.2 ± 7.2 years of age, 35% of whom were minority with mean educational achievement of 15.5 ± 3.3 years were studied; 57% were cognitively normal and followed for 5.2 years. Extent of vascular risk or cerebrovascular disease was assessed at baseline evaluation. All subjects underwent PiB PET imaging quantified using a distribution volume ratio with cerebellar reference region. Quantitative MRI measured volumes of cerebral gray matter, hippocampi, and white matter hyperintensities (WMH). Mixed effects regression models of individual trajectories of memory and executive functioning were estimated with random effects of baseline level and rate of change.

Results: Baseline diagnosis was significantly associated with both baseline level and rate of change in memory and executive function. Global amyloid burden, when added to this model, was significantly associated with baseline level and rate of change in one or both cognitive domains. Hippocampal volume also was a significant predictor of baseline level and rate of change in cognitive domains. Adding vascular risk factor burden to the final model significantly predicted baseline level of executive function.

Conclusion: Greater vascular risk factor exposure was significantly associated with baseline level of executive function in a model that included amyloid burden and MRI measures of vascular and neurodegenerative disease. We conclude that modifiable vascular risk factors are important to cognitive health even after adjusting for the concurrent effects of cerebral amyloid burden.

Keywords: *Cognitive Aging, Cognitive Impairment, MRI, amyloid imaging, cerebrovascular risk*

Presented by: DeCarli, Charles

Submission ID: 5

Associations between β -amyloid, Memory and Longitudinal Brain Change across the Spectrum of Cognitive Functioning

Evan Fletcher^{1, 5}, Sylvia Villeneuve², Bruce Reed⁵, William Jagust⁴, Danielle Harvey³, Charles DeCarli^{1, 5}

¹ *IDeA Laboratory, Alzheimer's Disease Center, UC Davis, Davis, CA, United States*

² *Cognitive Neurology and Alzheimer's Disease Center, Northwestern University, Evanston, Illinois, United States*

³ *Department of Public Health Sciences, UC Davis School of Medicine, Davis, CA, United States*

⁴ *School of Public Health and Helen Wills Neuroscience Institute, UC Berkeley, Berkeley, CA, United States*

⁵ *Department of Neurology, UC Davis School of Medicine, Davis, CA, United States*

Background: Well-known biomarker models of cognitive decline describe β -amyloid accumulation followed by tau and then macroscopic GM atrophy, all preceding cognitive impairment. However, recent studies have raised questions about the completeness of this model. Some point to WM decline in memory circuits that may precede observed GM loss. Others have found that neurodegeneration (in APOE4 mutation carriers) may predate or accompany β -amyloid deposition, raising questions about the sequencing implied in the amyloid hypothesis. In this project we examined the association of β -amyloid deposition with longitudinal changes in brain structures and with cognition, to test the hypothesis that β -amyloid deposition underlies cognitive decline and neurodegeneration in memory –associated structures.

Subjects and Results: We used a cohort of 57 elderly subjects: 31 normal, 9 MCI and 17 AD. The AD showed high-magnitude average losses (diffeomorphism log-jacobians) in temporal and parietal cortex and lower magnitudes in splenium and posterior cingulate. The whole cohort showed significant associations of PiB as a predictor of tissue loss in the fornix body, splenium, genu and corpus callosum (CC), retrosplenial cortex (RSC) and inferior and superior longitudinal fasciculi (ILF and SLF, parieto-temporal branch), but no association with changes in lobar gray or hippocampus. We found significant associations of episodic memory with losses in fornix, splenium, genu, CC as a whole, retrosplenial cortex, ILF and SLF-PT, and also significant association of PiB with episodic but not executive function.

Discussion: These results suggest that β -amyloid underlies some but not all of the neurodegenerative changes accompanying cognitive decline. It was strongly associated with changes in medial and longitudinal WM structures but not with gray matter changes, including in the hippocampus. It was also strongly associated with episodic memory; thus it may implement cognitive decline via losses of connection in the affected WM structures. Larger samples are needed to confirm.

Keywords: *Beta-amyloid, longitudinal change*

Presented by: Fletcher, Evan

Submission ID: 13

Amyloid, Cerebrovascular Disease and Cognitive Decline in MCI patients: A Prospective Longitudinal Study

Hee Jin Kim¹, Yearn Seong Choe², Kyung-Han Lee², Sung Tae Kim³, Duk L. Na¹, Sang Won Seo¹

¹ Department of Neurology, Samsung Medical Center, Sungkyunkwan University School of Medicine, Seoul, Seoul, Korea, Republic of (South)

² Department of Nuclear Medicine and, Samsung Medical Center, Sungkyunkwan University School of Medicine, Seoul, Seoul, Korea, Republic of (South)

³ Department of Radiology, Samsung Medical Center, Sungkyunkwan University School of Medicine, Seoul, Seoul, Korea, Republic of (South)

Introduction: Cerebrovascular disease (CVD) and Alzheimer's disease (AD) are significant causes of cognitive impairment in the elderly. However, few studies have longitudinally evaluated the relationship between CVD and amyloid burden in living human subjects, or their synergistic effects on cognition. We investigated the relation between amyloid and CVD changes and their effects on cognitive decline.

Methods: We prospectively recruited 117 MCI patients (45 amnesic MCI (aMCI) and 72 subcortical vascular MCI (svMCI)) with structured MRI and PiB-PET and annually followed up with neuropsychological test and MRI. 83 (70.9%) patients (33 aMCI and 50 svMCI) completed PiB PET follow up with 30.3 months interval. PiB SUVR were measured using cerebellar cortex as reference region and CVD was quantified as lacune number detected by MRI. Their relationships were examined using linear mixed effects model.

Results: The overall conversion rate was 29.1% (19.4 % for svMCI and 44.4% for aMCI). For 30.3 months, PiB retention increased from 1.62 ± 0.47 to 1.65 ± 0.59 , and lacune number increased from 4.48 ± 6.64 to 4.64 ± 7.10 . Baseline PiB retention, but not lacunes, predicted further increase in PiB retention ($p < 0.015$). Baseline lacunes, but not PiB retention, predicted further increase in lacunes ($p < 0.001$). Increased PiB changes predicted rapid decline in attention, visual/verbal memory, and general cognitive function (MMSE and CDR-SOB) while lacune number changes predicted rapid decline in attention, visual memory and frontal dysfunctions. There was an interactive effect between PiB and lacunes changes on visual memory.

Conclusions and Relevance: Our finding suggested that higher lacune number predict further increase in lacune and greater amyloid burden predict further increase in amyloid burden. In addition, increased amyloid burden and lacune number each independently predicts further decline in specific cognitive domains and have interactive effect on visual memory decline.

Keywords: *amyloid, cerebrovascular disease, cognition*

Presented by: Kim, Hee Jin

Submission ID: 79

Interactions of Amyloid and Vascular Pathology in MCI

William Klunk, Lisa Weissfeld, Julie Price, Chester Mathis, Howard Aizenstein, Beth Snitz, Ann Cohen, Milos Ikonovic, Oscar Lopez

University of Pittsburgh, Pittsburgh, PA, United States

Background: The deposition of amyloid-beta ($A\beta$) does not clearly explain associated markers of neurodegeneration or changes in cognition. Subclinical vascular pathology frequently accompanies $A\beta$ pathology. This study examines the interactions of vascular and $A\beta$ pathologies in individuals with Mild Cognitive Impairment (MCI) and compares the findings in a younger (yMCI) and very elderly (veMCI) group.

Methods: All participants met Petersen 2004 Criteria for MCI (76% amnesic) and fell into a yMCI (67 ± 10 yrs; $n=29$) or a veMCI (88 ± 4 yrs; $n=36$). All subjects underwent structural MRI, PiB and FDG PET (cerebellar reference). Subclinical systemic vascular disease was assessed by ECG, history of cardiovascular disease, ankle-brachial index and ultrasound of the internal carotid and expressed as a systemic vascular burden index (SVBI). A central vascular burden index (CVBI) was determined from infarct number and white matter hyperintensities. All subjects were clinically evaluated using a standard battery similar to that of the Pittsburgh Alzheimer's Disease Research Center.

Results: The yMCI were no more likely to be PiB(+) ($p=0.87$), have more PiB retention ($p=0.89$) or be amnesic ($p=0.14$) than the veMCI. The veMCI had more evidence of systemic vascular disease ($p<0.0001$). PiB-hippocampal volume, PiB-cerebral metabolism and PiB-MMSE relationships all were significant. These relationships became stronger with the addition of vascular pathology (i.e., SVBI or CVBI) to the models. PiB(+) subjects had more frequent progression to AD than PiB(-), but this was not significant.

Conclusions: The yMCIs were no more amyloid-driven than the veMCIs, but the veMCIs had more systemic vascular disease. The associations of PiB retention with hippocampal volume, cerebral metabolism and MMSE, respectively, were strongest when vascular burden was added to the models, suggesting that vascular variables could play an important role in determining the impact of $A\beta$ deposition on the brain.

Keywords: *vascular disease, amyloid, pathology*

Presented by: Klunk, William

Submission ID: 56

SESSION 2: Amyloid-associated Phenomena

Chairs: Agneta Nordberg, MD, PhD, *Karolinska Institute*
Christopher Rowe, MD *Austin Health*

Lower Body-Mass Index is Associated with Higher Cortical Amyloid Burden in Clinically Normal Elderly

David Hsu, Alexander Dagley, Aaron Schultz, Rebecca Amariglio, Elizabeth Mormino, Nancy Donovan, Dorene Rentz, Keith Johnson, Reisa Sperling, Gad Marshall

Harvard Medical School, Massachusetts General Hospital, Boston, MA, United States

Background: Late-life lower body-mass index (BMI) has been associated with an increased risk of dementia in the elderly, and weight loss has been associated with more rapid decline in Alzheimer disease (AD) dementia. Previous studies across the spectrum of impairment have suggested that lower BMI is associated with higher amyloid burden, but have not focused on relationship with biomarkers in the asymptomatic population. We hypothesized that in a clinically normal (CN) elderly cohort, lower BMI will be associated with greater cortical amyloid burden visualized by Pittsburgh compound B (PiB) positron emission tomography (PET).

Objective: To determine the association between BMI and cortical amyloid burden in CN elderly at risk for AD.

Methods: Cross-sectional analyses were completed using baseline data from the Harvard Aging Brain Study, consisting of 284 community-dwelling CN older adults aged 62-90. Assessments included medical histories, physical exam and vital signs, PiB PET, and apolipoprotein genotyping. A general linear regression model with backward elimination was used to evaluate the association between BMI (predictor of interest) and PiB retention (dependent variable). Covariates included age, sex, verbal intelligence quotient, race, and apolipoprotein ϵ 4 (APOE4) carrier status.

Results: BMI was normally distributed and ranged from 16 to 41 with a mean of 26.9 (standard deviation of 4.5). In unadjusted, univariate analyses, lower BMI was associated with greater PiB retention ($\rho = -0.14$, $p = 0.02$). In the multiple linear regression model, greater PiB retention was associated with lower BMI ($\beta = -0.16$, $p = 0.005$). Of the covariates, the presence of one or more APOE4 alleles ($\beta = 0.39$, $p < 0.001$) was retained in the model. The model as a whole was significant ($R^2 = 0.17$, $p < 0.001$).

Conclusion: This finding offers new insight into the role of BMI at the preclinical stage, wherein lower BMI is associated with greater cortical amyloid burden. Future studies may consider further elucidating the mechanism behind this association, and longitudinal assessments of BMI and PiB retention may also help.

Keywords: *body-mass index, Pittsburgh compound B, amyloid, clinically normal*

Presented by: Hsu, David C

Submission ID: 38

Regional Cerebral Iron Concentrations as Indicated by Magnetic Susceptibilities Measured with Quantitative Susceptibility Mapping at 7 Tesla Correlate with Brain A β plaque Density as Measured by 11-C-Pittsburgh Compound B Positron-Emission-Tomography (PiB-PET) in Elderly Subjects at Risk for Alzheimer's Disease

Jiri van Bergen^{1,2}, Xu Li², Michael Wyss³, Simon Schreiner¹, Stefanie Steininger¹, Anton Gietl¹, Valerie Treyer⁴, Sandra Leh¹, Fred Buck⁴, Jun Hua², Roger Nitsch¹, Klaas Pruessmann³, Peter van Zijl², Christoph Hock¹, Paul Unschuld¹

¹ Division of Psychiatry Research and Psychogeriatric Medicine, University of Zürich, Zürich, Switzerland

² F.M. Kirby center for Functional Brain Imaging at Kennedy Krieger Institute and Johns Hopkins School of Medicine, Zürich, Zürich, Switzerland

³ Institute for Biomedical Engineering, University of Zürich and ETH Zürich, Zürich, Switzerland

⁴ Division of Nuclear Medicine, University of Zürich, Zürich, Switzerland

Introduction: To investigate combinations of biomarkers for early detection of Alzheimer's disease (AD) we used QSM (Quantitative Susceptibility Mapping) to assess iron levels, positron emission tomography using 11-C Pittsburgh Compound-B (PiB-PET) to assess accumulation of Amyloid beta (A β) and presence of the e4 allele of the Apolipoprotein E (ApoE) gene. All of which are associated with AD, but do not offer sufficient specificity for valid inferences on the individual pathophysiology.

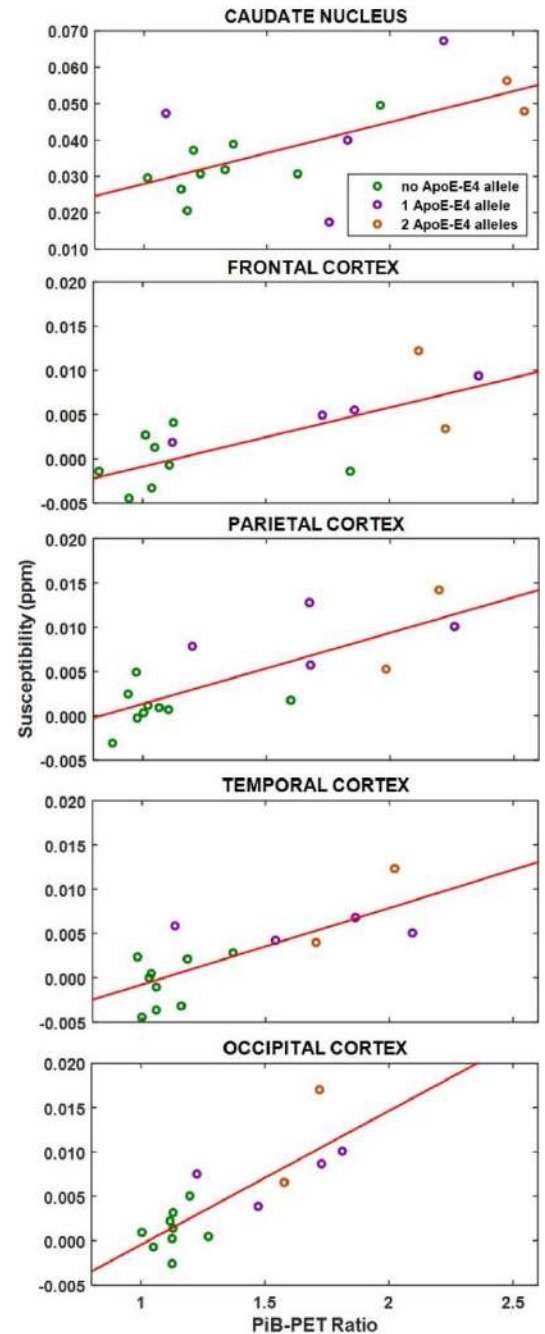
Methods: Eighteen subjects with MCI (11 male, 7 female) and twenty-two healthy elderly controls (14 male, 8 female) were studied using a 7T MR system. Isoforms of the ApoE gene were assessed in all subjects. High resolution 3D GRE scans were acquired and used to reconstruct the QSM images. Automated atlas based image segmentation was performed to select the regions of interest. Late-frame 3D PiB-PET images were acquired for each subject.

Results: In healthy controls none of the basal ganglia or cortical regions showed any correlation between iron and PiB-PET ratio. In subjects with MCI there were strong correlations ($p < 0.01$, $r > 0.65$) for the, frontal, temporal, parietal and occipital cortices and caudate nucleus. Among all the MCI subjects, carriers of the ApoE-e4 allele show stronger increases in iron and PiB-PET ratio. However, in the controls only the A β depositions increased with carriers of the ApoE-e4 allele, but not the iron levels.

Discussion and Conclusion: Our data indicate significant regional correlations between A β plaque density and iron load for the caudate nucleus, as well as frontal, temporal, parietal and occipital cortex in subjects with MCI. Relevance of our findings for AD pathology is further supported by the observation that ApoE-e4 carrier-status drives the correlation. Overall, our findings suggest that cerebral iron accumulation may reflect A β associated brain dysfunction in subjects at increased risk for late onset AD.

Keywords: iron, pib-pet, A β , ApoE-e4, MCI

Presented by: Unschuld, Paul



The Cognition-Mobility Interface (COMBINE) is Associated with Cerebral Amyloid Deposition and Glucose Metabolism in Older Adults without Cognitive or Mobility Impairment

Neelesh Nadkarni¹, Stephanie Studenski⁵, Oscar Lopez^{2,3}, Beth Snitz², Subashan Perera¹, Ann Cohen³, Chester Mathis⁴, Robert Nebes³, William Klunk^{2,3,4}

¹ Department of Medicine (Geriatric Medicine), University of Pittsburgh School of Medicine, Pittsburgh, PA, United States

² Department of Neurology, University of Pittsburgh School of Medicine, Pittsburgh, PA, United States

³ Department of Psychiatry, University of Pittsburgh School of Medicine, Pittsburgh, PA, United States

⁴ Department of Radiology, Pharmaceutical Sciences, Pharmacology, University of Pittsburgh, Pittsburgh, PA, United States



⁵ Longitudinal Studies Section, Intramural Research Program, National Institute on Aging, Bethesda, MD, United States

Background: Cognition and mobility rely on common brain areas prone to amyloidosis and neurodegeneration in older adults. The cognition-mobility interface (COMBINE), defined as the ability to simultaneously perform cognitive tasks while walking, can serve as “stress-tests” of the brain to detect impending functional decline and may relate to these aging-brain changes.

Aim: To explore the relationship between the COMBINE, cerebral amyloid deposition and synaptic function in clinically normal elders (CN, normal mobility and cognition).

Methods: Gait speed was measured on an automated walkway with and without multitasking (walking while performing motor-sequencing (Luria), response-inhibition (Go No-Go) and working-memory (2-back) functions and while dialing a phone). COMBINE was assessed by quantifying the decrement in gait speed while multitasking. Amyloid burden was quantified using Pittsburgh Compound-B (PiB) PET. Synaptic function was measured by glucose metabolism using fluoro-2-deoxy-glucose-PET (FDG-PET). Participants were grouped into high-amyloid (PiB(+)) and low-amyloid (PiB(-)) groups, using established cutoffs. PiB-group differences and atrophy-corrected global PiB-PET and FDG-PET correlates of the COMBINE tasks were explored.

Results: PiB(+) (n=16) and PiB(-) (n=12) groups were similar in age (75yrs), cognitive and physical function and gait speed (Table 1). However, the PiB(+) group demonstrated greater decrement in gait speed than the PiB(-) group on response-inhibition and motor-sequencing (both p=0.03) and the phone-dialing task (p=0.008, Figure 1). Greater global PiB-PET (r=0.39, p=0.04) and FDG-PET (r=0.44, p=0.02) correlated with greater magnitude of decline in gait speed on the phone-dialing task (Figure 2) while global PiB-PET alone correlated with the COMBINE measure on the motor-sequencing and response-inhibition task (both r=0.4, p=0.04). There were no significant correlations between regular gait speed and global PiB-PET or FDG-PET.

TABLE 1: SAMPLE CHARACTERISTICS	Whole group N=28	 PiB + N=16	 PiB - N=12	p-value for Aβ group differences
Age (yrs)	75.2±5.7	75.9 ± 5.01	74.8 ± 6.6	0.60
Women (n,%)	5 (50%)	75.9 ± 5.01	74.8 ± 6.6	0.60
Education (yrs)	14.7	15 ± 2.8	15.4 ± 2.6	0.74
MOCA	26.2±2.5	26.5 ± 2.5	25.9 ± 2.6	0.59
DSST	54±13	51.7 ± 12.2	59 ± 14	0.24
SPPB	11±1.5	10.2 ± 1.7	11.4 ± 1.1	0.08
Grip Strength (cm ²)	50.2±18	35.6 ± 18.4	37.4 ± 15.6	0.69
Regular gait speed (m/sec)	1.16 ± 0.16	1.14 ± 0.16	1.15 ± 0.25	0.95
UPDRS	2.6±2.4	3.7 ± 2.8	3.4 ± 2.1	0.70
PiB global SUVR	1.64±0.4	1.96 ± 0.36	1.35 ± 0.09	<0.0001

MOCA: Montreal Cognitive Assessment; DSST: Digit Symbol Substitution Test;
SPPB: Short Physical Performance Battery; UPDRS: Unified Parkinson's Disease Rating Scale

Conclusions: The COMBINE is related to dynamic changes in the aging brain in high-functioning older adults. The COMBINE appears to be adversely influenced by cerebral amyloidosis but the relationship with glucose metabolism remains unclear.

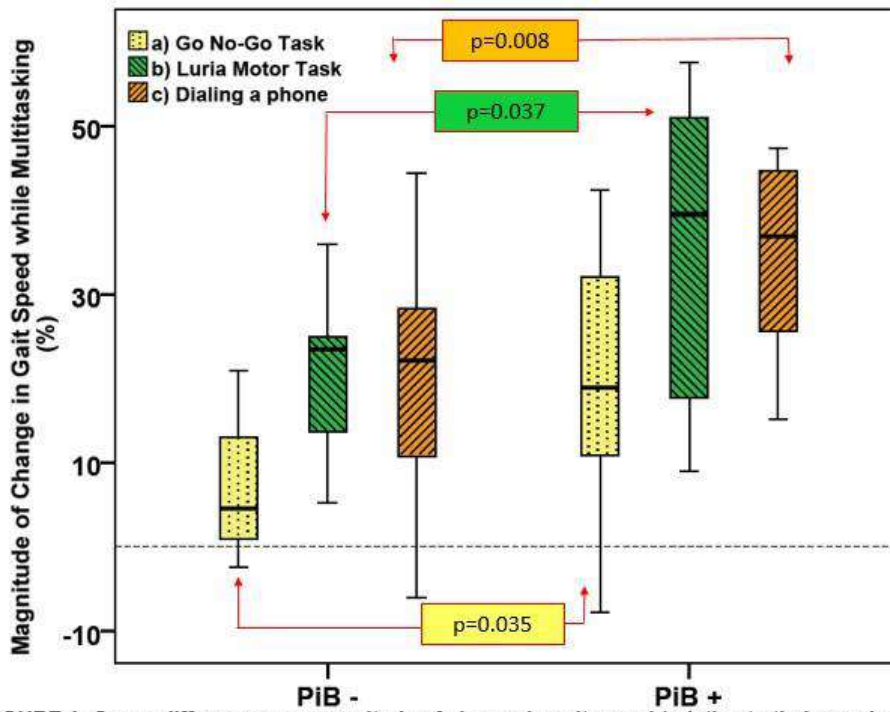


FIGURE 1: Group differences on magnitude of change in gait speed (relative to their regular gait speed) while performing: a) Go No-go task, b) Luria motor sequences and c) Dialing a phone.

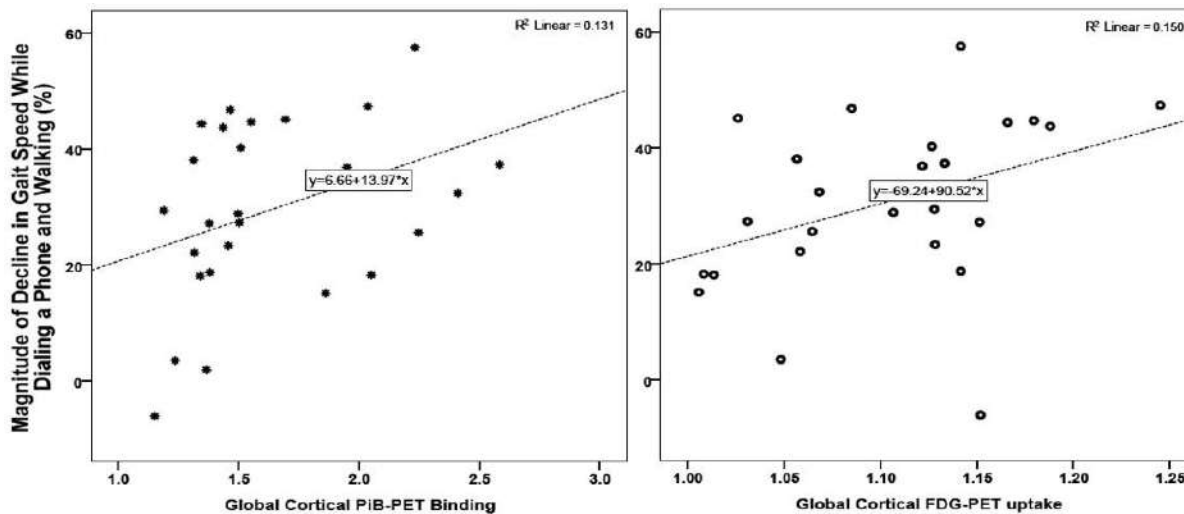


FIGURE 2: Correlation between magnitude of decline in gait speed and global PiB-PET (on left, closed asterisk) and global FDG-PET (on right, open circle) dialing a phone while walking.

Keywords: mobility, cognition, interface, dual-tasking, amyloid, metabolism.

Presented by: Nadkarni, Neelesh K.

Submission ID: 50

Multivariate AD Biomarker Profiles: Relation to Clinical and Cognitive Progression

Andrew Saykin¹, Shannon Risacher², Paul Crane³, William Jagust⁴, Clifford Jack⁵, Leslie Shaw⁶, John Trojanowski⁶, Laurel Beckett⁷, Sujuan Gao⁸, Paul Aisen⁹, Ronald Petersen¹⁰, Michael Weiner¹¹

¹ Department of Radiology and Imaging Sciences, Indiana Alzheimer Disease Center, Department of Medical and Molecular Genetics, Indiana University School of Medicine, Indianapolis, Indiana, United States

² Department of Radiology and Imaging Sciences, Indiana Alzheimer Disease Center, Indiana University School of Medicine, Indianapolis, Indiana, United States

³ Department of Medicine, University of Washington, Seattle, Washington, United States

⁴ Department of Neurology, University of California-Berkeley, Berkeley, California, United States

⁵ Department of Radiology, Mayo Clinic, Rochester, Minnesota, United States

⁶ Department of Pathology and Laboratory Medicine, University of Pennsylvania School of Medicine, Philadelphia, Pennsylvania, United States

⁷ Division of Biostatistics, Department of Public Health Sciences, University of California-Davis, Davis, California, United States

⁸ Department of Biostatistics, Indiana Alzheimer Disease Center, Indiana University School of Medicine, Indianapolis, Indiana, United States

⁹ Department of Neurology, University of California-San Diego, San Diego, California, United States

¹⁰ Department of Neurology, Mayo Clinic, Rochester, Minnesota, United States

¹¹ Departments of Radiology, Medicine and Psychiatry, University of California-San Francisco; Department of Veterans Affairs Medical Center, San Francisco, California, United States

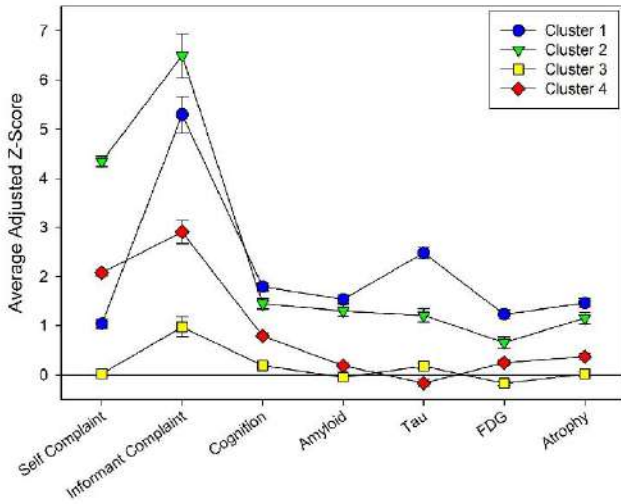
Introduction: The purpose of this study was to determine the relationship between baseline biomarker profile and one-year clinical and cognitive decline (progression) in early and late MCI patients from the Alzheimer's Disease Neuroimaging Initiative (ADNI).

Methods: 796 participants (158 HC, 86 SMC, 274 EMCI, 153 LMCI, 126 AD) were included. A priori domains representing AD pathologies/symptoms were created by combining z-scores from representative measures (standardized to HC; adjusted for age, gender, ICV; higher value = more pathology), including: subjective complaints (self ECog score in memory and executive function (EF) domains), informant complaints (ECog memory & EF; FAQ total), cognition (memory and EF performance), amyloid (CSF A β 1-42, cortical [18F]Florbetapir SUVR), tau (CSF tau, p-tau), glucose metabolism (cortical [18F]FDG SUVR), and atrophy (cortical and hippocampal volumes, lateral temporal cortical thickness). Profile composition was supported by multivariate dimension reduction. Cluster analysis was performed using hierarchical agglomerative and k-means clustering and profile domains were compared between clusters. The association between cluster assignment and one-year change (slope) in informant complaints and memory performance was evaluated.

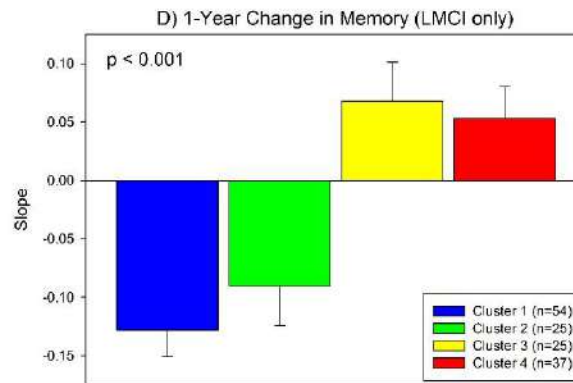
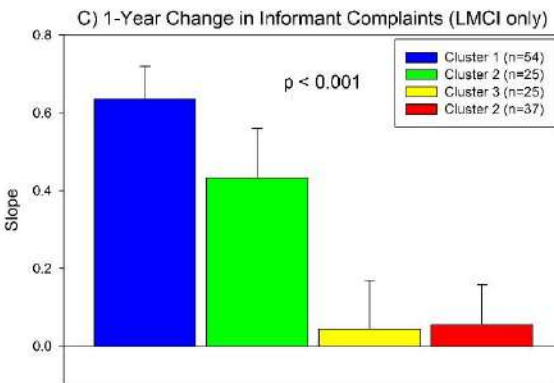
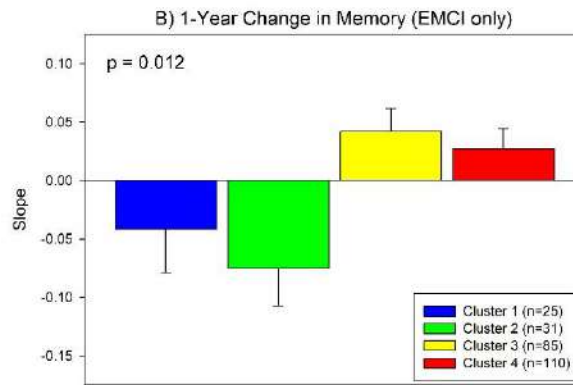
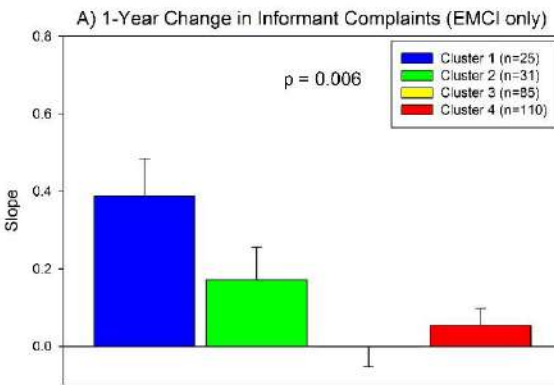
Results: Cluster analysis yielded a four cluster solution. Figure 1 shows the mean domain z-score by cluster and the number of participants assigned to each cluster by diagnosis. Clusters 1 and 2 had high informant complaints, lower cognitive performance, abnormal biomarkers, and variable subjective complaints (lower in 1, higher in 2). Cluster 3 showed minimal self or informant complaints, cognitive impairment, or biomarker pathology. Cluster 4 included relatively mild cognitive complaints but minimal impairment or biomarker pathology. EMCI and LMCI assigned to Clusters 1 or 2 showed increased informant complaints and memory decline over 1 year relative to those in Clusters 3 or 4 (Figure 2).

Discussion: Quantitative cognitive, imaging and biomarker phenotype profiles at baseline are predictive of one-year functional and memory progression. Biomarker profile analysis may reduce clinical heterogeneity and provide information regarding underlying pathophysiology.

Distribution of Clinical, Cognitive, and Biomarker Measures Across Clusters



	HC	SMC	EMCI	LMCI	AD
Cluster 1	3	1	29	56	75
Cluster 2	0	2	31	27	34
Cluster 3	133	50	92	28	3
Cluster 4	22	33	122	41	14



Keywords: *[18F]Florbetapir PET, cerebrospinal fluid (CSF), [18F]Fluorodeoxyglucose (FDG) PET, structural magnetic resonance imaging, Alzheimer's Disease Neuroimaging Initiative (ADNI)*

Presented by: Saykin, Andrew J

Submission ID: 92

KEYNOTE LECTURE 1

The Spectrum of Age-Associated Tauopathies

Dennis W. Dickson

Mayo Clinic, Jacksonville, FL, United States

Tau is a low molecular weight, heat-stable microtubule association protein (MAP) that in the healthy nervous system is neuron-specific and enriched in axons, while high molecular weight MAPs (*e.g.*, MAP2) are enriched in the somatodendritic domain. In certain pathological conditions and in the aging human brain, tau has an abnormal distribution within neurons and non-neuronal cells.

The most common neuronal tau pathology in aging is the neurofibrillary tangle (NFT), a fibrillar insoluble tau inclusion in the somatodendritic domain of neurons. Neurons vulnerable to this process undergo progressive changes in which non-fibrillar material accumulates first in dendrites and then cell soma (“pretangles”) followed by fully formed intracellular NFTs and after the neuron dies, extracellular NFTs. Similar tau protein aggregates accumulate in cell processes (“neuropil threads”) and in dystrophic neurites of senile plaques (“neuritic plaques”).

Progressive involvement of cerebral neurons that are selectively vulnerable to NFTs permit pathological staging, most often employing a scheme proposed originally by Heiko and Eva Braak (*Acta Neuropathol* 1991), and recently updated to include subcortical neuronal populations. The Braak staging scheme technically was developed to stage Alzheimer’s disease, but some elderly individuals do not have amyloid deposits, and this has led to the concept of “primary age-related tauopathy” (PART). While PART is meant to describe an age-associated neuronal tauopathy, it is increasingly recognized that aging is also associated with accumulation of tau within glia. In particular, subpial and perivascular fibrous astrocytes (“thorn-shaped astrocytes” (TSA)) at the base of the forebrain and the brainstem accumulate fibrillar tau in the elderly. The tau in TSA is enriched in 4-repeat tau (4R tau). TSA can also be detected in the elderly brain as patches in superficial subcortical white matter and in the subependymal region of the lateral ventricle. Similar lesions are detected in the convexity cortical gray matter in chronic traumatic encephalopathy (CTE). 4R tau accumulates in protoplasmic astrocytes in the medial temporal gray matter in argyrophilic grain disease (AGD), a 4R tauopathy that increases in frequency with age. Grains in AGD are tau aggregates in dendritic branch points of neurons. Oligodendroglia (“coiled bodies”) in temporal white matter accumulate 4R tau in AGD. Age-associated neuronal and glial tau pathology can sometimes resemble that seen in neurodegenerative tauopathies, such as progressive supranuclear palsy (PSP), corticobasal degeneration (CBD) or globular glial tauopathy (GGT), except it is not associated with neuronal loss and it can be seen in asymptomatic individuals. This has led to concepts such as preclinical PSP and preclinical CBD. Whether genetic (*e.g.*, *MAPT* haplotype) or environmental factors (*e.g.*, head trauma) contribute to age-associated neuronal and glial tauopathies is an area of current investigation.

SESSION 3: Pathology

Chairs: Gil Rabinovici, MD, *University of California San Francisco*
Dennis Dickson, MD, *Mayo Clinic*

Clinicopathologic and [11C]-PiB-PET Implications of Thal Amyloid Phase across the Spectrum of Alzheimer's Disease Pathology

Melissa Murray¹, Val Lowe², Neill Graff-Radford³, Amanda Liesinger¹, Ashley Cannon¹, Scott Przybelski⁵, Bhupendra Rawal⁴, Joseph Parisi⁶, Ronald Petersen⁷, Kejal Kantarci², Owen Ross¹, Ranjan Duara⁸, David Knopman⁷, Clifford Jack, Jr.², Dennis Dickson¹

¹ Mayo Clinic, Departments of Neuroscience, Jacksonville, FL, United States

² Mayo Clinic, Department of Radiology, Rochester, MN, United States

³ Mayo Clinic, Neurology, Jacksonville, FL, United States

⁴ Mayo Clinic, Biostatistics, Jacksonville, FL, United States

⁵ Mayo Clinic, Biostatistics, Rochester, MN, United States

⁶ Mayo Clinic, Pathology Laboratory Medicine, Rochester, MN, United States

⁷ Mayo Clinic, Neurology, Rochester, MN, United States

⁸ Mount Sinai Medical Center, Wien Center for Alzheimer's Disease and Memory Disorders, Department of Neurology, Miami Beach, FL, United States

⁹ University of Miami, Miller School of Medicine, Miami, FL, United States

Background: Thal amyloid phase, which describes the pattern of progressive amyloid- β (A β) plaque deposition in Alzheimer's disease (AD), has been incorporated into the latest NIA-AA neuropathologic assessment guidelines. Amyloid (PET and CSF) biomarkers have been included in clinical diagnostic guidelines for AD dementia, published by the NIA-AA and the International Work Group. The goals of this study were to evaluate the correspondence of Thal phase to 1) Braak neurofibrillary tangle stage, 2) antemortem clinical characteristics, and 3) antemortem PiB-PET imaging.

Methods: Cases (n=3618) from the Brain Bank for Neurodegenerative Disorders at Mayo Clinic Jacksonville were selected, regardless of antemortem clinical diagnosis and neuropathologic co-morbidities, and assigned Thal phase and Braak stage using thioflavin-S fluorescent microscopy. A subset of AD cases with Thal phase 3-to-5 were evaluated for clinicopathologic associations with regression modelling (n=1375). PiB-PET studies from Mayo Clinic Rochester were available for 35 participants scanned within two years of death. Cortical PiB-PET SUVR values were normalized to cerebellar grey/white matter.

Results: In the high-likelihood AD brain bank cohort (n=1375), cases with lower Thal phases were older at death, had a lower Braak stage, and were less frequently APOE- ϵ 4 positive. Regression modelling showed that Braak NFT stage, but not Thal phase predicted age at onset, disease duration, and final MMSE score. In the 35 cases with antemortem amyloid imaging, Thal phase, but not Braak stage, CERAD, or cerebral amyloid angiopathy predicted PiB-PET SUVR. A transition between Thal phases 1-to-2 seemed to correspond to PiB-PET SUVR of 1.4, the cutpoint used to denote amyloid positivity.

Conclusions: AD cases who were older and were APOE- ϵ 4 negative tended to have lower amyloid phases. Although Thal phase predicted clinical characteristics of AD patients, this was driven by Braak stage. This study also provides a rough correlation of PiB PET SUVR to Thal phase with an SUVR of 1.4 approximately equivalent to Thal phase of 1-to-2.

Keywords: *Alzheimer's disease, neuropathology, Thal amyloid phase, Pittsburgh compound B, Braak tangle stage*

Presented by: Murray, Melissa E

Submission ID: 53

PiB PET and Postmortem Neuropathology Correlations in the Precuneus: A Role for Diffuse A β Plaques

Julie Price¹, Eric Abrahamson², Lan Shao², Carl Becker¹, Manik Debnath³, Lisa Weissfeld⁴, Chester Mathis¹, Oscar Lopez², William Klunk^{2,3}, Milos Ikonovic^{2,3}

¹ Radiology, University of Pittsburgh, Pittsburgh, PA, United States

² Neurology, University of Pittsburgh, Pittsburgh, PA, United States

³ Psychiatry, University of Pittsburgh, Pittsburgh, PA, United States

⁴ Statistics Collaborative, Washington, DC, United States

Background: The relationship between in vivo imaging and postmortem measures of fibrillar amyloid-beta (A β) deposition is not fully understood. This study examined correspondence between in vivo [C-11]PiB PET retention and postmortem measures of A β -load, including both diffuse and cored A β plaques, in the precuneus.

Methods: [C-11]PiB PET (or PiB PET) was performed for 16 subjects representing a range of clinical states from cognitively normal to AD dementia. Subjects came to autopsy with an average imaging-to-death interval of 36 \pm 24 months. Postmortem A β plaque load was assessed using A β immunohistochemistry (IHC, antibody clone 4G8) and a highly fluorescent derivative of PiB (6-CN-PiB) applied to 12- μ m paraffin sections of the precuneus. A systematic anatomical match of the postmortem dissected precuneus region was identified on the antemortem MR and co-registered PiB PET images. PiB SUVR and histopathology correlations were assessed using Pearson correlations.

Results: In the precuneus from 16 PiB PET imaged autopsy cases, SUVR PET corresponded with 6-CN-PiB plaque load ($R^2=0.74$) and less strongly with A β IHC plaque load ($R^2=0.59$). In cases where total plaque load exceeded ~10% area by either A β IHC or 6-CN-PiB, SUVR values appeared to plateau at values greater than about 2.75. Surprisingly, the relationship between PiB SUVR and compact/cored plaque load (4G8) was nonlinear. However, several “mismatch” cases (high PiB SUVR values and low density of compact/cored plaques) had high diffuse plaque load.

Conclusions: These preliminary results suggest that in regions where A β load is high (>10% area) there is lower-than-expected PiB retention. This could result from saturation of the in vivo PiB PET signal with very high A β plaque load. Alternatively, semi-quantitative plaque load analyses may overestimate A β content in diffuse plaques. Nevertheless, diffuse A β plaques appear to make a significant contribution to regional PiB PET retention.

Keywords: PiB, Neuropathology, Positron Emission Tomography (PET)

Presented by: Price, Julie

Submission ID: 58

Towards the Validation of Novel PET tracer T807 on Postmortem Human Brain Tissue Samples

Marta Marquie^{1,2}, Marc Normandin², Charles Vanderburg^{1,2}, Isabel Costantino^{1,2}, Bradford Dickerson², Matthew Frosch^{1,2}, Bradley Hyman^{1,2}, Keith Johnson², Teresa Gomez-Isla^{1,2}

¹ *MassGeneral Institute for Neurodegenerative Disease, Charlestown, MA, United States*

² *Massachusetts General Hospital, Boston, MA, United States*

Introduction: The recent development of novel PHF-tau targeting PET tracers, such as T807, opens an exciting opportunity of using them as potential surrogate markers to measure tau pathology. A comprehensive approach to validate the sensitivity and specificity of T807 is critical to understand what T807 PET positivity means in terms of neuropathological substrate.

Objective: To examine region and substrate specific autoradiographic and fluorescent binding patterns of T807 in human postmortem tissue representing a diverse spectrum of neurodegenerative diseases to validate the site/s of T807 binding and determine whether there is off-target binding.

Methods: We studied the autoradiographic and fluorescent patterns of T807 using postmortem samples from multiple brain regions from patients with a pathological diagnosis of Alzheimer's disease (AD), frontotemporal lobar degeneration-tau (FTLD-tau), frontotemporal lobar degeneration-TDP43 (FTLD-TDP43), progressive supranuclear palsy (PSP), corticobasal degeneration (CBD), Parkinson's disease (PD), dementia with Lewy bodies (DLB), multiple system atrophy (MSA), cerebral amyloid angiopathy (CAA) and controls.

Results: Film autoradiography with [18F]T807 demonstrated that tangle containing areas in AD cases strongly bind ligand, while slides containing TDP43, LB or CAA pathology do not. Staining of adjacent sections with a fluorescent derivative of T807 and appropriate specific antibodies against PHF-1, A β , TDP43 and α -synuclein revealed a very strong fluorescent T807 labeling of tangles and PHF-1 containing dystrophic neurites in AD cases, Pick bodies in Pick's disease, and neuronal and glial tau containing lesions in PSP and CBD. T807 fluorescent labeling of TDP43 inclusions and of Lewy pathology was completely absent. Studies using slides dipped in photographic nuclear emulsion to obtain cellular resolution with [18F]T807 ligand binding are currently ongoing.

Conclusion: Our preliminary data on the postmortem validation of T807 are very encouraging and suggest that PHF-positive neuronal and glial cytoplasmic inclusions and neuritic elements likely account for the majority of tau related T807 ligand binding.

Keywords: *T807, PET, tau, tangles, autoradiography*

Presented by: Marquie, Marta

Submission ID: 89

AV-1451 Autoradiographic Evaluation in Subjects with TDP-43-versus Tau-immunoreactive Lesions

Val Lowe¹, Geoffry Curran¹, Keith Josephs¹, Joseph Parisi¹, David Knopman¹, Bradley Boeve¹, Kejal Kantarci¹, Leonard Petrucelli², Clifford Jack¹, Dennis Dickson², Ronald Petersen¹, Melissa Murray²

¹ Mayo Clinic, Rochester, MN, United States

² Mayo Clinic, Jacksonville, FL, United States

Background: Since tau protein imaging with PET is being evaluated in early clinical trials, it is essential to evaluate the specificity of AV-1451 PET to determine the appropriate applicability of this new tracer in dementia research. Recent data have suggested that AV-1451 may bind to TDP43 as well as tau. We therefore performed autoradiography on cases with and without TDP-43 pathology to evaluate the specificity of AV-1451 binding.

Methods: Cases from our research brain bank (n=8) were selected for evaluation of TDP-43- immunoreactive lesions (n=4) ranging from sparse to severe and with tau-immunoreactive lesions (without TDP-43) with and without beta-amyloid (CBD, AD, PSP, Picks; n=4). Serial sections of medial temporal lobe were stained with PHF-1 (tau) and phosphoserine 409/410 TDP-43 to compare adjacent sections with AV-1451 autoradiography. Visual comparison of the pattern of staining for tau and TDP-43 with the autoradiography results were performed on the amygdala, basal ganglia, white matter and any included cortical regions.

Results: No correlative uptake of AV-1451 and TDP-43 staining was identified in the cases we evaluated (see Figure 1). Uptake of AV-1451 mirrored most closely the staining pattern of PHF-1 suggesting tau uptake of AV-1451 (see Figure 2). Possible preferential association of AV-1451 with 4R tau (i.e., corticobasal degeneration and progressive supranuclear palsy) over 3R tau isoforms (i.e., Pick disease) was suggested in the primary tauopathy cases.

Conclusions: There was no significant uptake of AV-1451 in regions of TDP-43 pathology in cases evaluated. In contrast AV-1451 binding co-localized with tau pathology, with possible preferential AV-1451 association with 4R tau over 3R tau. Further comparisons of AV-1451 autoradiography with immunohistochemistry of affected subjects will be needed to further elucidate the specificity of AV-1451 PET.

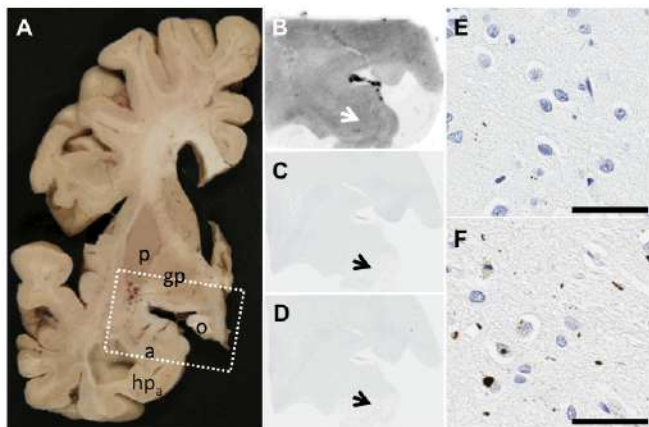


Figure 1: Neuropathologically-confirmed frontotemporal lobar degeneration case. A – Macroscopic autopsy photograph of coronally slabbed fixed tissue at the level of the amygdala. The tissue was sampled, paraffin embedded, and serial 5 μ m microscope sections were cut. B – Autoradiography using the AV-1451 radioligand did not reveal high signal. C & D – 1x magnification of both tau and TDP-43 immunohistochemical slides did not reveal visible staining. E – 20x magnification tau immunohistochemistry did not reveal significant pathology. F – 20x magnification of TDP-43 immunohistochemistry shows neuronal cytoplasmic inclusions and neuritic pathology. (Scale bar at 50 μ m) Acronyms: p=putamen; gp=globus pallidus; o=optic tract; a=amygdala; hp_a=anterior hippocampus

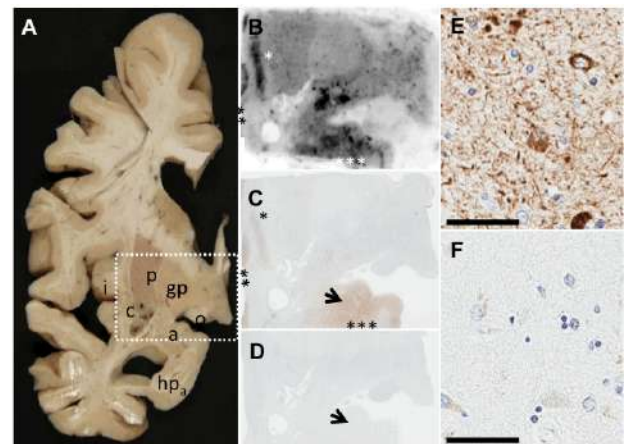


Figure 2: Neuropathologically-confirmed Alzheimer's disease case. (A) Macroscopic autopsy photograph of coronally slabbed fixed tissue at the level of the amygdala. The tissue was sampled, paraffin embedded, and serial 5 μ m microscope sections were cut. (B) Autoradiography using the AV-1451 radioligand revealed high signal in the insula (*), claustrum (**), and amygdala (***). (C) 1x magnification of tau staining revealed visible tau pathology in matching AV-1451-positive regions, but not (D) TDP-43-positive regions. (E) 20x magnification of tau immunohistochemistry revealed pretangle, mature tangle, and neuritic pathology. (F) 20x magnification did not reveal significant TDP-43 pathology. (Scale bar at 50 μ m) Acronyms: i=insula; c=claustrum; p=putamen; gp=globus pallidus; o=optic tract; a=amygdala; hp_a=anterior hippocampus

Presented by: Lowe, Val J

Submission ID: 46

POSTER SESSION (Odd Numbers)

Odd-numbered submissions organized by last name of author

P1 Amyloid Biomarkers in Cognitively Normal Older Adults: Comparison of ¹⁸F-flutemetamol to ¹¹C-PIB and CSF Aβ42

Katarzyna Adamczuk^{1,2}, Jolien Schaevebeke^{1,2}, Rose Bruffaerts^{1,2,3}, Natalie Nelissen^{1,2}, Veerle Neyens^{1,2}, Patrick Dupont^{1,2}, Karolien Goffin⁴, Mathieu Vandenbulcke^{2,5}, Koen Van Laere^{2,4}, Jos Tournoy⁶, Koen Poesen^{7,8}, Rik Vandenberghe^{1,2,3}

¹ Laboratory for Cognitive Neurology, KU Leuven, Leuven, Belgium

² Alzheimer Research Centre, Leuven Institute of Neuroscience and Disease, KU Leuven, Leuven, Belgium

³ Neurology Department, UZ Leuven, Leuven, Belgium

⁴ Nuclear Medicine and Molecular Imaging, KU Leuven and UZ Leuven, Leuven, Belgium

⁵ Old Age Psychiatry Department, UZ Leuven, Leuven, Belgium

⁶ Gerontology and Geriatrics, UZ Leuven, Leuven, Belgium

⁷ Laboratory for Molecular Neurobiomarker Research, KU Leuven, Leuven, Belgium

⁸ Laboratory medicine, UZ Leuven, Leuven, Belgium

Objectives: Biomarkers for amyloid play a central role in the NIA-AA research definition of preclinical AD. In a prospective community-recruited cohort of cognitively intact older adults, we compared three amyloid markers within-subjects: ¹⁸F-flutemetamol, ¹¹C-PIB and CSF Aβ42.

Methods: We recruited 44 cognitively normal older adults (mean age 72, range 65-80 years). Of these, 22 underwent all 3 investigations: ¹⁸F-flutemetamol, ¹¹C-PIB, and CSF Aβ42 measurement. An additional 22 subjects underwent either ¹⁸F-flutemetamol with ¹¹C-PIB (n=10), or ¹⁸F-flutemetamol with CSF Aβ42 (n=12). As our primary outcome measures, we evaluated the concordance of binary classification based on ¹⁸F-flutemetamol versus ¹¹C-PIB according to SUVRcomp cut-offs as determined in independent datasets, and separately, according to visual reads. As our secondary outcome measures, we determined the correlation between SUVRcomp values of the tracers, and between ¹⁸F-flutemetamol SUVRcomp and CSF Aβ42. In an ROC analysis, we also defined the CSF Aβ42 cut-off that yields optimal sensitivity and specificity with ¹⁸F-flutemetamol positivity as comparator.

Results: Binary classification based on SUVRcomp cut-offs was concordant between ¹¹C-PIB and ¹⁸F-flutemetamol in 94% of the cases (95% CI 85-102). Concordance of binary visual reads between tracers was 84% (95% CI 72-97). ¹⁸F-flutemetamol SUVRcomp was highly correlated with ¹¹C-PIB SUVRcomp ($\rho=0.84$, slope=0.98, $p<0.0001$) and also with CSF Aβ42 ($\rho=0.66$, $p<0.0001$). The area under the ROC curve for the accuracy of CSF Aβ42 to predict positive ¹⁸F-flutemetamol scan was 0.94 (95% CI 0.81-0.99). The Aβ42 cut-off that optimally separated flutemetamol-positive versus negative cases was 817 pg/ml.

Conclusions: For the definition of preclinical AD based on amyloid imaging, semiquantitative cut-offs tended to produce more consistent results than visual reads. The CSF Aβ42 cut-off that yields maximal concordance with a PET-based diagnosis of preclinical AD was substantially higher than what is commonly used in clinical practice to separate AD from non-AD causes of cognitive decline.

Keywords: *Flutemetamol, PIB, CSF, older adults, preclinical Alzheimer's disease*

P1 Presented by: Adamczuk, Katarzyna

Submission ID: 15

P3 A Selective Impact of Regional PET 11C-PIB on Cognitive Functions in Healthy Controls and Patients with MCI and Alzheimer's Disease

Ove Almkvist, Katharina Bruggen, Agneta Nordberg

Center for Alzheimer Research, Karolinska Institutet, Stockholm, Sweden

Background: Neocortical PET 11C-PIB is an indicator of in vivo beta-amyloid pathology in Alzheimer's Disease (AD). Less is known about the influence of regional PIB on clinical status and cognition. In the present study, the relationship between pathology in specific brain regions as measured by PET 11C-PIB and cognitive functions was investigated.

Methods: 186 individuals were examined with PET 11C-PIB in 13 brain regions of both hemispheres and with cognitive tests covering 8 domains. The participants were patients with AD (n=90) and Mild Cognitive Impairment (n=62) and healthy controls (n=34) recruited from a European Multicenter study (Nordberg et al. Eur J Nucl Med Mol Imaging. 2013, 40, 104-114). Multiple hierarchical regression analyses were performed on each cognitive test as dependent variable and demographic characteristics (age and years of education) entered simultaneously in the first block, neocortical PIB in the second block and PIB measures in 13 brain regions entered stepwise in the third block.

Results: Word list delayed recall and complex tracking (TMTB) were influenced by PIB in nucleus accumbens in addition to neocortical regions. Word list learning, simple tracking (TMTA) and semantic fluency (Animals) were influenced by neocortical PIB only. Design copying and Delayed reproduction of designs were influenced by occipital PIB. In addition, age was a significant factor for tracking (TMTA & TMTB) and Design copying, whereas education was a significant factor for episodic memory (word list learning and delayed recall), complex tracking (TMTB) and global cognition (MMSE). Considering ApoE status, did not change the pattern of results.

Conclusion: After control of demographics and neocortical PET PIB, PIB in specific brain regions were selectively associated with cognitively demanding test performance in a heterogeneous sample of individuals.

Keywords: *Alzheimer's disease, PET PIB, cognition*

P3 Presented by: Almkvist, Ove

Submission ID: 75

P5

Analysis Strategies for Quantitation of the PET Tau Radiotracer [18F]AV1451

Olivier Barret, David Alagille, Danna Jennings, David Russell, Kenneth Marek, John Seibyl, Gilles Tamagnan

Institute for Neurodegenerative Disorders, New Haven, CT, United States

Objective: Tau PET images in Alzheimer's disease (AD) demonstrates a pattern of localized, asymmetric cortical uptake roughly consistent with postmortem studies of the distribution of neurofibrillary tangles in AD brain. This heterogeneous abnormal uptake creates difficulties for volume of interest sampling which may result in a brain region which has distinct subregions with either abnormal or normal radiotracer uptake. The objective of this study is to explore strategies for optimal quantification of [18F]AV1451.

Methods: [18F]AV1451 PET images from 7 subjects (3 AD, 2 PD, 2 CTE) were co-registered with subject's MRI and both images spatially normalized into standard space. PET uptake was extracted in different brain regions for grey matter only. Voxel-wise SUV_r images were created by intensity normalization to cerebellar cortex. Regional SUV_r histograms were made and images quantified using both sampling of average SUV_r and threshold sampling of the area under the curve (AUC) and number of voxels (NVOX) representing the intensity and extent of the increased uptake, respectively.

Results: The SUV_r histogram distribution in the cerebellar cortex was similar for all subjects, ranging from about 0.6-1.4. For the AD subjects, a multi-modal distribution was observed in the cortical regions, one similar to that observed in the cerebellar cortex mixed with others corresponding to increased uptake, with maximum SUV_r up to 2.5-3.0, especially in the inferior and superior-lateral temporal cortex. Separation between populations was increased for the AUC and NVOX with increasing SUV_r threshold, but at the expense of distorting the within-cohort spread.

Conclusions: These preliminary data suggests that [18F]AV1451 quantification using standard average regional SUV_r is reliable. Other outcome measures would need further investigation to assess their reliability given the observed increased spread. Other reference regions may prove useful in improving the accuracy of these measurements at different SUV_r thresholds.

Keywords: *tau, AV1451, T807, PET, image processing*

P5 Presented by: Barret, Olivier

Submission ID: 71

P7

Differential Patterns of Cortical Thickness in Individuals with Elevated Beta-amyloid across the Adult Lifespan

Gerard Bischof¹, Kristen Kennedy¹, Ian McDonough¹, Karen Rodrigue¹, Jenny Rieck¹, Michael Devous², Denise Park¹

¹ Center for Vital Longevity, School of Behavioral and Brain Sciences, University of Texas at Dallas, Dallas, TX, United States

² Department of Neurology, UT Southwestern Medical Center & Center for Vital Longevity, School of Behavioral and Brain Sciences, University of Texas at Dallas, Dallas, TX, United States

Background: Gray matter atrophy and beta-amyloid deposition are fundamental characteristics of Alzheimer's disease (AD). Specifically, cortical thinning is indicative of AD status and progression from prodromal stages to the diagnosis of probable AD. However, compared to cortical thinning, beta-amyloid is an earlier biomarker and has been observed in vivo using Positron Emission Tomography (PET) in clinically normal adults. The direct or indirect effect of beta-amyloid burden on cortical brain aging is still under debate. In fact some research has shown both increases and decreases in thickness associated with beta-amyloid pathology in clinically normal older adults.

Methods: Here we investigated the impact of beta-amyloid on whole brain thickness from a healthy aging perspective using adults across the lifespan (N=142, Range: 30-89 years) who underwent structural and PET imaging (18F-Florbetapir). Cortical amyloid was computed by extracting counts across 8 cortical regions, normalized to cerebellar gray (SUVR). Participants were categorized into amyloid negative or positive group based on a median split on SUVR values (>1.14). Structural scans were processed using FreeSurfer to derive thickness values across the whole brain. Amyloid group and continuous age were entered in a general linear model, controlling for apolipoprotein-E status.

Results: We observed an age × amyloid group interaction in bilateral posterior regions and left lateralized frontal regions. These interactions were characterized by steeper age-related thinning patterns in amyloid positive individuals than amyloid negative individuals. Elevated beta-amyloid was associated with greater thickness in middle-aged adults, but less thickness in older adults.

Conclusions: These results make an important contribution to our understanding of the differential consequences of AD pathology across the lifespan. That is, in younger ages, high amyloid deposition may lead to a dynamic response (i.e., thickening) in the face of AD pathology, while in older ages, these mechanisms may not be sufficient enough to sustain the impending effect of amyloid deposition.

Keywords: *Beta-amyloid, normal aging, cortical thinning, AD biomarker, lifespan*

P7 Presented by: Bischof, Gerard N

Submission ID: 29

Prediction of Conversion to Preclinical Alzheimer's Disease Using Penalized Regression

Matthew Brier¹, Tammie Benzinger^{2,3}, Yi Su², Karl Friedrichsen², John Morris^{1,3}, Beau Ances^{1,2,3}, Andrei Vlassenko^{2,3}

¹ Department of Neurology, Washington University in St. Louis, St. Louis, MO, United States

² Department of Radiology, Washington University in St. Louis, St. Louis, MO, United States

³ Knight Alzheimer Disease Research Center, Washington University in St. Louis, St. Louis, MO, United States

In the longitudinal study of the natural course of Alzheimer's disease (AD) pathology in cognitively normal (CN) adults, A β deposition represents one of the earliest measurable biomarker changes indicating preclinical AD. Our aim was to identify an approach to predict transition to preclinical AD (PIB+) from PIB-negative (PIB-) stage. PIB deposition was estimated for cortical and subcortical regions of interest using the FreeSurfer software. and a cut-off for PIB+ was the mean cortical (MC) standard uptake value ratio (SUVR) of 1.42. Participants (n=131) were divided into two groups: 1) sixteen individuals who were PIB-negative at baseline but became PIB+ on the second scan (CNnp) and 2) one hundred fifteen individuals who remained PIB- at both PIB scans (CNnn). There was a substantial overlap between two groups in the distribution of baseline MC SUVR. The area under the ROC curve corresponding to conversion prediction using MC SUVR alone was 0.96. The present strategy was to fit a multivariate linear regression that predicts conversion from regional PIB values. To isolate a small number of regions, we imposed the L1 penalty on regression coefficients. This ensures that each model parameter provides significant additional predictive power. To quantify performance, we randomly set aside 51 datasets as a hold-out validation cohort; the remaining participants were used for training. Parameter tuning was performed by cross validation in the training set. Application of this classifier to the hold-out cohort yielded improved performance over MC SUVR alone (AUC=0.99). This classifier provided 11 regions to make its prediction including precuneus, rostral middle frontal, supramarginal, anterior and posterior cingulate, and entorhinal cortex and caudate nucleus. Thus, we suggested a new approach to predict conversion to preclinical AD in CN adults which may be used in the diagnosis and staging of AD.

P9 Presented by: Brier, Matthew R

Submission ID: 43

The Relationship Between Cortical Thickness and Tau Pathology Measured with [18F]-(S)-THK5117-PET

Konstantinos Chiotis¹, Laure Saint-Aubert¹, Anders Wall², My Jonasson², Mark Lubberink², Jonas Eriksson³, Gunnar Antoni², Nobuyuki Okamura⁴, Agneta Nordberg^{1,5}

¹ Karolinska Institutet, Dept NVS, Center for Alzheimer Research, Translational Alzheimer Neurobiology, Huddinge, -, Sweden

² PET center, Section of Nuclear Medicine & PET, Department of Radiology, Oncology and Radiation Sciences, Uppsala University, Uppsala, -, Sweden

³ Department of Medicinal Chemistry, Preclinical PET Platform, Uppsala University, Uppsala, -, Sweden

⁴ Department of Pharmacology, Tohoku University School of Medicine, Sendai, -, Japan

⁵ Department of Geriatric Medicine, Karolinska University Hospital Huddinge, Stockholm, -, Sweden

Objectives: The recent advances in PET imaging enabled the development of novel tau tracers that detect neurofibrillary tangles pathology. However, the in vivo regional progression of neurofibrillary tangles in relation to the other pathological hallmarks of Alzheimer's Disease (AD) pathology, neurodegeneration and amyloid plaques, remains largely unknown.

Methods: Patients with Mild Cognitive Impairment (MCI), dementia due to AD and Healthy Controls (HC) underwent a dynamic PET scan (0-90 minutes) with the novel tau tracer [18F]-(S)-THK5117. All participating individuals underwent high-resolution structural MRI (T1). Standard Uptake Value Ratio images were created for [18F]-(S)-THK5117 in respect to the grey matter of the cerebellum, and regional sampling was performed based on the Hammer's atlas. Cortical thickness measurements were performed.

Results: Comparisons were conducted between the [18F]-(S)-THK5117 retention in cortical and subcortical regions across diagnostic groups. Moreover, the distribution of [18F]-(S)-THK5117 retention was compared with the cortical thickness of the different regions examined.

Conclusions: This study provides further insight into imaging in vivo the regional distribution of tau deposition with the novel PET tau tracer [18F]-(S)-THK5117 at different stages of AD in relation to neurodegeneration.

Keywords: *PET, tau, THK5117, cortical thickness, MRI*

P11 Presented by: Chiotis, Konstantinos

Submission ID: 103

P13

Amyloid- β Deposition in Normal Aging of Non-demented Adults with Down Syndrome

Patrick Lao¹, Tobey Betthausen¹, Ansel Hillmer¹, Julie Price², William Klunk², Iulia Mihaila¹, Andrew Higgins¹, Peter Bulova², Sigan Hartley¹, Regina Hardison², Sterling Johnson¹, Murali Dhanabalan¹, Chet Mathis², Annie Cohen², Benjamin Handen², Bradley Christian¹

¹ University of Wisconsin-Madison, Madison, WI, United States

² University of Pittsburgh, Pittsburgh, PA, United States

Introduction: Adults with Down syndrome (DS) are at an extremely high risk for developing AD, with most individuals over age 40 evidencing amyloid deposits. The majority (95%) of DS cases result from a triplication of chromosome 21 and overproduction of the gene encoding for the amyloid precursor protein (APP). This is hypothesized to predispose young adults with DS to early expression of Alzheimer-like neuropathology. The goal of this work was to use [C-11]PiB imaging to examine the pattern of amyloid- β deposition in nondemented adults with DS to determine its relationship with normal aging.

Methods: A population of 68 nondemented individuals (30 - 53 yrs) with DS underwent [C-11]PiB PET scans. SUVR images were created using the cerebellum as the reference region. The relationship between SUVR and age was examined with multiple linear regression in a voxel-wise approach. ROI analysis was also performed using the anterior cingulate, frontal, parietal, precuneus and temporal cortices and the striatum defined in standardized space. Sparse k-means clustering was used for classifying PiB positivity using the ROIs.

Results: All regions contained clusters showing a slight but highly statistically significant positive correlation (corrected $p < 0.05$) of SUVR with age. The striatum showed the strongest correlation, followed by the precuneus, parietal, anterior cingulate, frontal and temporal cortex. From 68 subjects, 17 (25%) were classified as PiB positive with 16 of them being above the threshold in the striatum. Elevated cortical retention or PiB positivity did not appear in participants less than 35 years old.

Conclusions: There is a statistically significant positive correlation between PiB SUVR with natural aging in the DS population. As the amyloid burden increases and a pattern of elevated cortical retention emerges, the correlation with age loses significance. This finding suggests that factors, unrelated to aging, may drive a rapid increase in deposition during this stage.

P13 Presented by: Christian, Bradley T

Submission ID: 51

P15

[18F] T807 PET of Frontotemporal Lobar Degeneration

Bradford Dickerson, Scott McGinnis, Stephen Gomperts, Christina Caso, Sara Makaretz, Kathleen Kelly, Aaron Schultz, Neil Vasdev, Keith Johnson

Massachusetts General Hospital, Boston, MA, United States

Background: A critical unmet need for FTLD research, especially therapeutic trials, is the development of biomarkers to detect and monitor FTLD-tau and to distinguish it from FTLD-TDP.

Methods: We are using [18F] T807, a novel PET ligand, to scan a series of patients with FTLD, including symptomatic and asymptomatic MAPT mutation carriers, patients with sporadic Primary Progressive Aphasia, and patients along the PSP/CBD spectrum. We have compared them with cognitively intact controls as well as typical and atypical forms of Alzheimer's disease. We analyzed SUVR (cerebellum reference) data to localize and quantify [18F] T807 signal. We also co-registered analyzed [18F] T807 images to MRI images for visualization and calculation of % atrophy relative to controls.

Results: [18F] T807 signal is elevated in frontal, insular, and anterior temporal cortex in symptomatic MAPT mutation carriers, and colocalized with atrophy. One such patient has come to autopsy. In non-fluent aphasic patients, [18F] T807 signal was highest in dorsolateral prefrontal and insular cortex with marked asymmetry, most prominent in the dominant hemisphere, and highly co-localized with atrophy. In semantic aphasic patients, [18F] T807 signal was highest in anterior temporal cortex with marked asymmetry, most prominent in the dominant hemisphere, and highly co-localized with atrophy. PSP patients showed elevated brainstem, basal ganglia, thalamic/subthalamic, cerebellar, and frontal signal; one such patient has come to autopsy.

Conclusions: T807 is a promising new PET ligand for imaging tau pathology in vivo in patients with FTLD, but needs additional in vivo/post-mortem validation which is ongoing.

Keywords: *frontotemporal dementia, primary progressive aphasia*

P15 Presented by: Dickerson, Bradford C

Submission ID: 61

P17

Correlation of White Matter Disease and Amyloid Burden in Patients with Prodromal Alzheimer's Disease

David Douglas, Guofan Xu, Greer Murphy, Andrew Quon

Stanford University, Stanford, CA, United States

Abstract

Purpose: Both amyloid deposition and cerebral vascular disease have been suggested as risk factors in developing Alzheimer's dementia (AD). The aim in this study is to determine the relationship between the extent of white matter disease (WMD) and amyloid burden among a cohort of clinical population concerning for AD.

Methods: The study group is comprised of 26 consecutive patients underwent clinical Amyvid PET scans, including 18 prodromal AD and 8 non-demented patients including major depressive disorder. Amyvid imaging was interpreted visually and also analyzed quantitatively. WMD and basal ganglia (BG) changes were evaluated by visual interpretation using CT and MRI images with the Fazekas rating system. ANCOVA was performed to evaluate correlation between WMD, amyloid burden and their effect on AD.

Results: Significant correlation with age is found in both amyloid deposition and WMD among all the patients ($p < 0.05$). When adjusted for age, there is a significant difference in amyloid burden between the AD group and non-dementia group ($p < 0.05$). When adjusted for age, there is no significant difference between the WMD between the AD group and non-dementia group ($p = 0.81$).

Conclusion: Our data suggests that there is a correlation between age and amyloid deposition and WMD. When adjusted for age, we did not find a difference in WMD between the AD group and the non-dementia group. This suggests brain amyloid burden and vascular etiology are not co-associated pathologies. Among our clinical cohort of suspicious AD group, amyloid burden shows positive predictive value for AD diagnosis.

	No dementia (n = 8)	Dementia (n = 18)	Overall (n = 26)
Age (yrs)	mean: 71.3 standard dev: 5.6	mean: 73.1 standard dev: 7.9	mean: 72.5 standard dev: 7.2
White matter score	mean: 1.25 standard dev: 0.46	mean: 1.33 standard dev: 0.91	mean: 1.31 standard dev: 0.79
Basal ganglia score	mean: 0.38 standard dev: 0.74	mean: 0.39 standard dev: 0.61	mean: 0.38 standard dev: 0.64

Figure 1: Patient demographics.

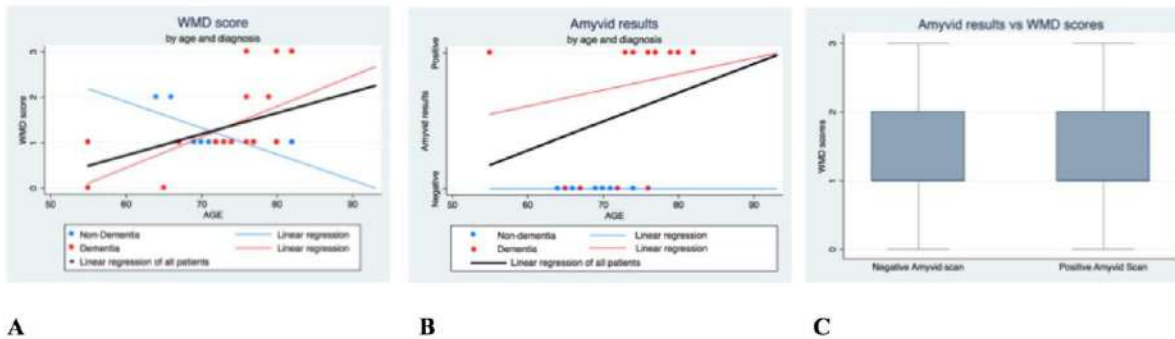


Figure 2: (A) WMD scores and (B) Amyvid results by age and diagnosis. (C) Relationship between WMD scores and Amyvid results.

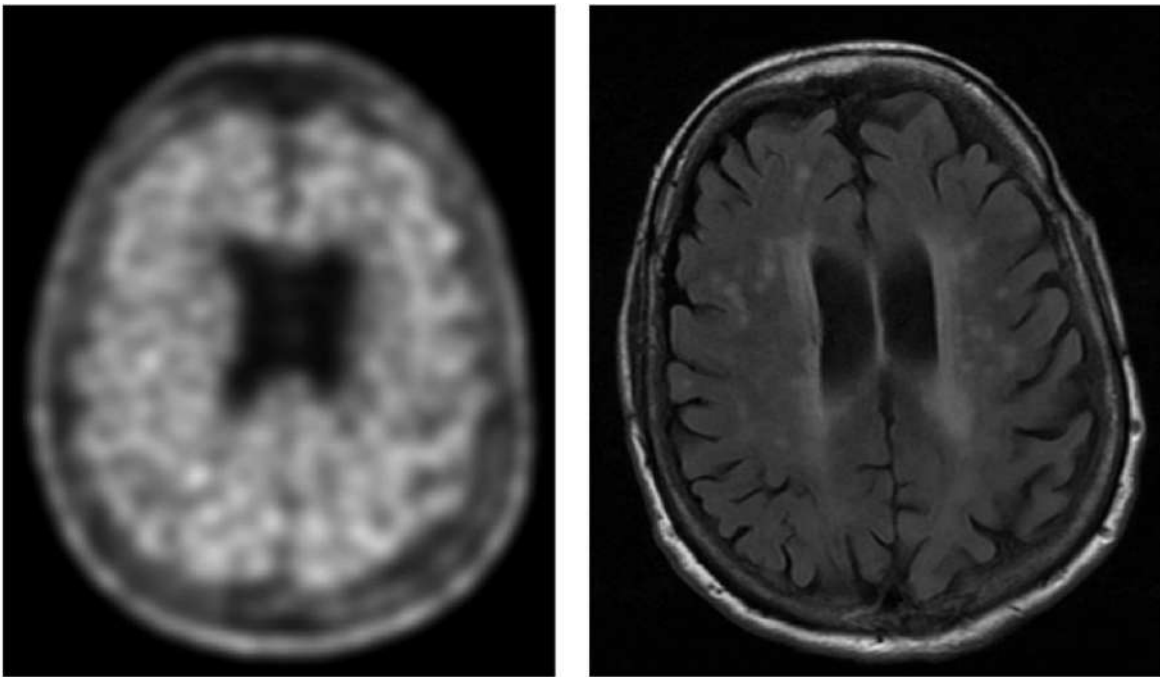


Figure 3: (A) Amyvid scan and (B) T2 FLAIR MRI of a patient with AD.

Keywords: *white matter, amyloid, Alzheimer's*

P17 Presented by: Douglas, David B

Submission ID: 87

P19

Should the Threshold for a Positive Amyloid PET Scan Be Adjusted for APOE Carrier Status, Age and Level of Cognitive and Functional Impairment?

Ranjan Duara¹, Warren Barker¹, David Loewenstein², Maria Greig¹, Rosemarie Rodriguez¹, Mohammed Goryawala³, Qi Zhou³, Malek Adjouadi³

¹ Wien Center for Alzheimer's Disease & Memory Disorders, Mount Sinai Medical Center, Miami Beach, Florida, United States

² Department of Psychiatry and Behavioral Sciences, University of Miami Miller School of Medicine, Miami, FL, Miami, Florida, United States

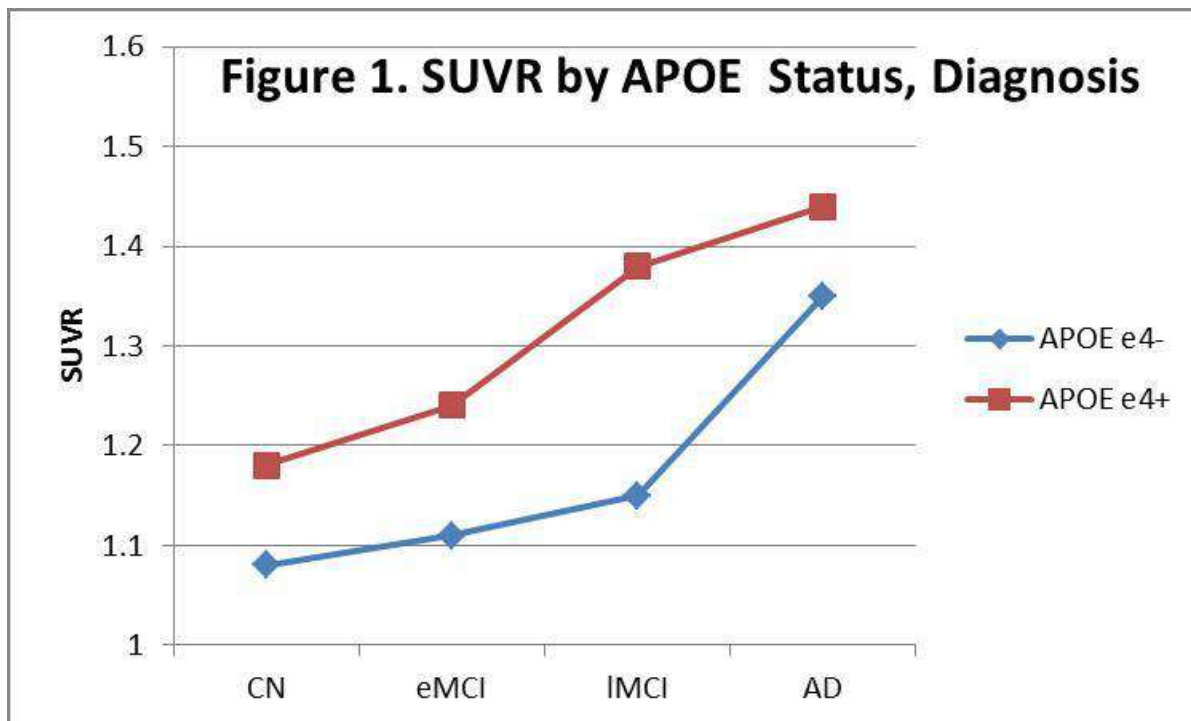
³ Center for Advanced Technology and Education, Florida International University, Miami, Florida, United States

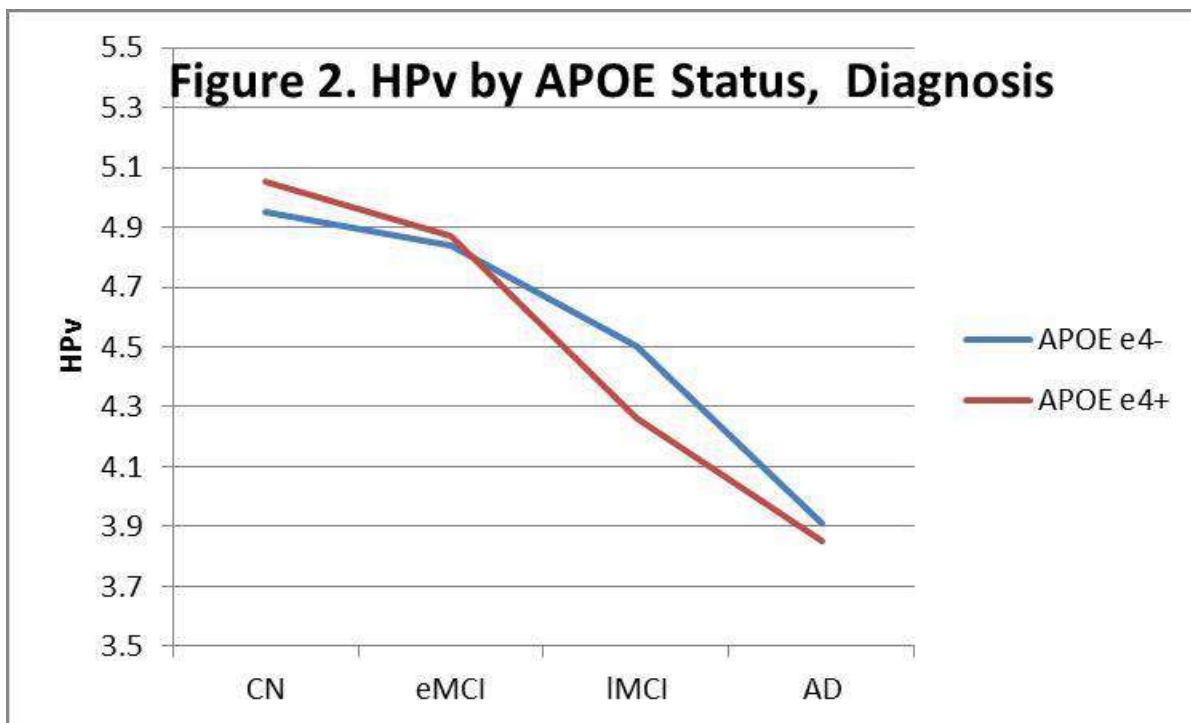
Objective: A high screen failure rate (50-70%) has been observed when a positive amyloid PET scan is required as an inclusion criterion in AD clinical trials. Consequently, we evaluated variables which could impact the threshold for amyloid positivity.

Methods: Subjects were 675 participants in the ADNI study, classified as cognitively normal (CN), early (EMCI) or late MCI (LMCI) or AD. Using multiple linear regression models we evaluated the influence of age, APOE $\epsilon 4$ carrier status, memory score (RAVLT score) and functional performance (CDRsb score) on amyloid load (AV45 SUVR) and normalized hippocampal volume (HPv), as outcome variables.

Results: Higher amyloid load and lower HPv were associated with increasing age and worsening disease stage (CN, EMCI, LMCI and AD) (Fig 1 and 2), RAVLT and CDRsb scores. Amyloid load was higher among $\epsilon 4+$, as compared to $\epsilon 4-$ subjects (Fig. 1) (interaction term significant at $p=.001$). In each stage of clinical impairment amyloid load was significantly greater among $\epsilon 4+$, as compared to $\epsilon 4-$ subjects. Because of the possibility that higher amyloid load among $\epsilon 4+$ subjects was related to a higher percentage of subjects who harbored genuine AD pathology, a corrected AV45 value (AV45 SUVRc) was calculated by subtracting from each subject's Z-transformed AV45 SUVR score their Z-transformed HPv score. Similar to findings for uncorrected AV45 SUVR values AV45 SUVRc scores were found to be higher, in each diagnostic group, among $\epsilon 4+$ as compared to $\epsilon 4-$ subjects (Table 1 and Fig 1), although AV45 SUVRc values did not show a monotonic increase from CN to AD

Conclusions: Amyloid load increases in relation to age, worsening clinical impairment and $\epsilon 4+$ carrier status (even when amyloid load is corrected for severity of neurodegeneration). Appropriately adjusted thresholds for amyloid positivity should provide a more accurate estimate of the presence of AD pathology.





Z transformed scores		CN	eMCI	LMCI	AD
AV45	$\epsilon 4-$	+0.17	-0.13	-0.31	-1.58
	$\epsilon 4+$	-0.38	-0.99	-1.86	-2.20
HPv	$\epsilon 4-$	-0.05	+0.12	-0.73	-1.62
	$\epsilon 4+$	0.12	-0.16	-1.09	-1.71
AV45 SUVRc*	$\epsilon 4-$	0.01	0.08	0.22	0.05
	$\epsilon 4+$	-0.66	-0.83	-0.84	-0.49

Z-score reference group is all CN subjects combined. Negative z-scores represent higher AV45 SUVR and lower HPv (compared to CN).

A negative AV45 SUVRc score represents higher amyloid load relative to hippocampal volume.

P19 Presented by: Duara, Ranjan

Submission ID: 99

P21 Development of an Alpha-synuclein PET Tracer

Dale Mitchell¹, Kevin Nash¹, David Hardick¹, Paul Kotzbauer², Zhude Tu², Jinbin Xu², Robert Mach³, Jamie Eberling⁴, Edilio Borroni⁵, Luca Gobbi⁵, Michael Honer⁵, N. Mason⁶, William Klunk⁶, Chester Mathis⁶

¹ BioFocus, Canterbury, Canterbury, United Kingdom

² Washington University, St. Louis, MO, United States

³ University of Pennsylvania, Philadelphia, PA, United States

⁴ Michael J. Fox Foundation, New York, NY, United States

⁵ Hoffman-La Roche, Basel, Basel, Switzerland

⁶ University of Pittsburgh, Pittsburgh, PA, United States

The Michael J Fox Foundation (MJFF) is supporting a consortium to develop novel positron emission tomography (PET) radiotracers for imaging alpha-synuclein in the brain. These agents could be useful biomarkers for the presence and progression of Parkinson's Disease, dementia with Lewy bodies, and other synucleinopathies, and as drug development tools.

As part of our screening approach to identify novel compounds with appropriate properties for potential PET ligands, two high throughput screens were developed targeting different binding sites on alpha-synuclein fibrils. A Thioflavin T fluorescence based assay and an antibody-based 384-well scintillation proximity assay (SPA) using the radioligand [3H]-Chrysamine G were developed for high throughput screening purposes using aggregated alpha-synuclein fibrils. 100,000 compounds selected from the BioFocus screening libraries based on chemical diversity and lead-like properties were screened for their ability to bind to alpha-synuclein fibrils in both assay formats. Initial hits were subjected to hit confirmation and assessed for binding selectivity to alpha-synuclein fibrils over amyloid-beta and tau fibrils. Compounds were prioritized based on selectivity and calculated properties for good CNS penetration.

Multiple chemical series have yielded tractable hits and medicinal chemistry programs are underway to optimise hits from both screens. Promising leads are radiolabeled with 11C, 18F, and/or 3H for additional binding assays in Parkinson's disease and Alzheimer's disease tissues. These studies have resulted in establishment of structure-activity relationships (SAR) for further lead optimization and permitted chemical incorporation of good PET-like properties into the leads. We hope to deliver a selective alpha-synuclein PET tracer for use by the research and drug development communities.

Keywords: *alpha-synuclein, Parkinson's, Lewy body dementia*

P21 Presented by: Eberling, Jamie

Submission ID: 47

P23

The Importance of Frontal and Temporal Amyloid Deposition in Middle Adulthood: The Predictive Value of APOE ϵ 4 and Lifetime Cognitive Engagement

Michelle Farrell¹, Gérard Bischof¹, Kristen Kennedy¹, Karen Rodrigue¹, Michael Devous², Denise Park¹

¹ University of Texas at Dallas, Dallas, TX, United States

² Avid Radiopharmaceutical, A Subsidiary of Eli Lilly, Philadelphia, PA, United States

Background: We examined whether low lifetime cognitive activity and APOE ϵ 4 would be predictors of amyloid accumulation in healthy middle aged adults, as previously demonstrated in older adults. We hypothesized that these predictors would affect amyloid deposition in frontal and temporal cortices, but not other regions, as Braak staging suggests amyloid begins to accumulate in frontal and temporal cortices during middle age before spreading throughout the neocortex.

Methods: 18F-florbetapir PET data were analyzed from a sample of 85 healthy adults, aged 30-59 from two cohorts of the Dallas Lifespan Brain Study. Eight bilateral ROIs (DLPFC, OFC, PCC, ACC, precuneus, temporal, parietal and occipital cortex) were normalized to whole cerebellum. Using GLM, lifetime cognitive activity and APOE ϵ 4 carrier status were used to predict SUVR in each region, as well as mean SUVR, while controlling for age, education, gender and cohort.

Results: A significant Lifetime Cognitive Activity x APOE interaction was detected in DLPFC, OFC and temporal ROIs but not other ROIs. In APOE ϵ 4 carriers (n=26), lower lifetime cognitive engagement predicted higher SUVR, while non-carriers did not show a significant relationship. When we used mean cortical SUVR, the effect of lifetime activities was more muted, but significant. Notably, SUVR in the DLPFC, OFC and temporal ROIs was higher than all other ROIs, with many subjects above a typical positivity threshold (SUVR=1.1).

Conclusion: Similar to previous findings in older adults, low lifetime cognitive engagement in APOE ϵ 4 carriers is associated with greater amyloid in middle age. However, in middle age this relationship is specific to frontal and temporal regions implicated as the earliest sites of amyloid deposition by autopsy data. More research is needed to assess whether frontal and temporal amyloid deposition in middle age may be a predictor of future cognitive decline related to healthy aging or preclinical AD.

Keywords: amyloid, middle age, lifetime cognitive engagement, APOE

P23 Presented by: Farrell, Michelle E

Submission ID: 91

P25**Differences in Florbetapir Deposition by Race, Age, Gender, and ApoE Status: The ARIC-PET Study**

Rebecca Gottesman¹, Xueqi Chen¹, Andrew Crabb¹, Edward Green², Naresh Gupta⁴, David Knopman⁵, Akiva Mintz³, Arman Rahmim¹, A. Sharrett¹, Lynne Wagenknecht³, Dean Wong¹, Yun Zhou¹, Thomas Mosley²

¹ Johns Hopkins University, Baltimore, MD, United States

² University of Mississippi Medical Center, Jackson, MS, United States

³ Wake Forest School of Medicine, Winston-Salem, NC, United States

⁴ Hagerstown Imaging, Hagerstown, MD, United States

⁵ Mayo Clinic, Rochester, MN, United States

Objective: The purpose of this study is to evaluate differences in florbetapir deposition among nondemented older adults in the Atherosclerosis Risk in Communities (ARIC)-PET study, to determine if deposition varies by age, race, gender, and apoE genotype.

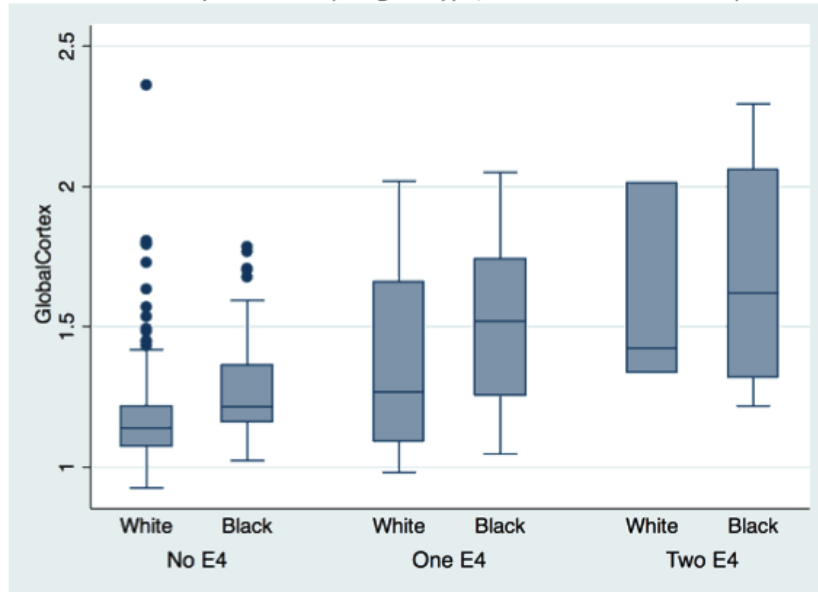
Methods: 302 ARIC-PET participants, ages 67-89, were imaged using florbetapir PET, at three sites (Washington County, MD; Forsyth County, NC; and Jackson, MS). Standardized Uptake Value Ratios (SUVR) were calculated using the cerebellum as reference region. Calculations were made in separate regions of interest (ROI's), with a global cortical SUVR calculated. Age, race, sex, and apoE genotype (number of $\epsilon 4$ alleles) were evaluated in a multivariable linear regression model.

Results: 111 of participants (36.8%) were African-American, and 164 (54%) were female. Only 2.4% of participants had a 4/4 apoE genotype, with 28.5% having a 2/4 or 3/4 genotype. Median global cortical SUVR was 1.2 (IQR 1.1-1.4). In multivariable models, increasing age was significantly associated with higher global cortical SUVR ($\beta=0.08$ per 10 yrs, 95% CI 0.03-0.13), as was African-American race ($\beta=0.10$, 95% CI 0.04-0.16), with no difference by gender. One $\epsilon 4$ allele was associated with 0.21 points higher global SUVR (95% CI 0.15, 0.28), with even higher SUVR observed with two $\epsilon 4$ alleles ($\beta=0.39$, 95% CI 0.21-0.58). Results were nearly identical for separate ROI's including the precuneus and posterior cingulate. Differences in SUVR by race and apoE genotype had an additive effect (Figure).

Conclusion: Florbetapir uptake increases with age and with more $\epsilon 4$ alleles, in this community-based nondemented cohort. Independent of age, gender, and number of apoE $\epsilon 4$ alleles, higher SUVR was associated with African-American race. The increase in SUVR in association with African-American race was equivalent to the amount of increase in SUVR associated with a 12-year increase in age. Reasons for and consequences of these substantial differences by race warrant further study.

Keywords: florbetapir, epidemiology, racial disparities

Figure. Boxplots of florbetapir SUVR for a composite global cortex measurement* by race and ApoE genotype; number of $\epsilon 4$ alleles is presented.



* Global cortex: weighted average (weighted by region of interest (ROI) size) of the following 9 ROIs: orbitofrontal cortex, prefrontal cortex, superior frontal cortex, lateral temporal lobe, parietal lobe, precuneus, occipital lobe, anterior cingulate, posterior cingulate.

P25 Presented by: Gottesman, Rebecca F

Submission ID: 77

P27

The Relative Importance of Imaging Markers for the Prediction of Alzheimer’s Disease Dementia in Mild Cognitive Impairment – beyond Classical Regression

Michel Grothe¹, Martin Dyrba¹, Stefan Teipel^{1,2}

¹ German Center for Neurodegenerative Diseases (DZNE) - Rostock, Rostock, Germany

² Department of Psychosomatic Medicine, University of Rostock, Rostock, Germany

Selecting a set of relevant imaging markers to predict conversion from mild cognitive impairment (MCI) to Alzheimer’s disease (AD) has become a challenging task given the wealth of regional pathologic information that can be extracted from multimodal imaging data.

Here, we used regularized regression approaches with an elastic net penalty for best subset selection of multiregional information from AV45-PET, FDG-PET and volumetric MRI data to predict conversion from MCI to AD. The study sample consisted of 127 MCI subjects from ADNI-2 who had a clinical follow-up between 6 and 31 months. Additional analyses assessed the effect of partial volume correction on predictive performance of AV45- and FDG-PET data.

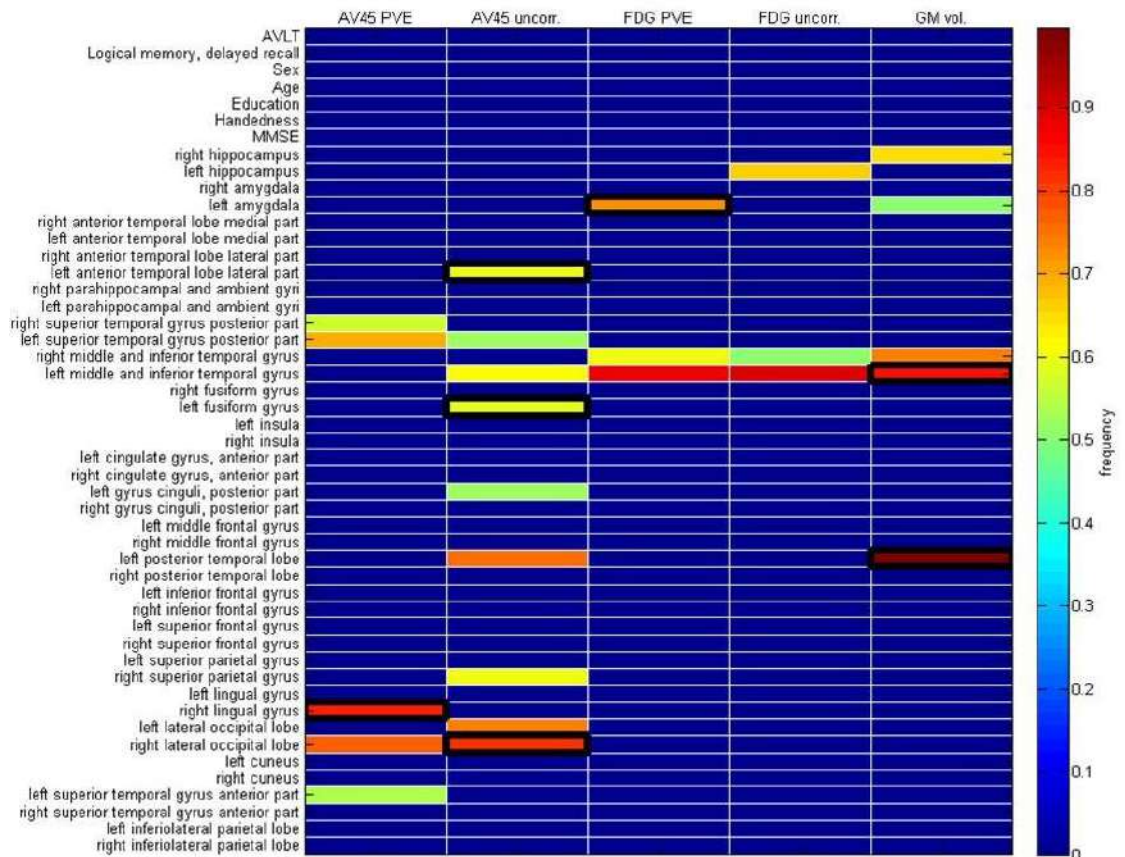
Predictor variables were highly collinear within and across imaging modalities. Penalized Cox regression yielded more parsimonious and neurobiologically plausible prediction models compared to unpenalized Cox regression. Within single modalities, time to conversion was best predicted by increased AV45 signal in posterior medial and lateral cortical regions, decreased FDG-PET signal in medial temporal and temporobasal regions, and reduced gray matter volume in medial, basal, and lateral temporal regions (Figure 1). In combined multimodal regression models, AV45-PET made the strongest contribution to the prediction model, followed by regional gray matter volumes, whereas FDG-PET had only a minor contribution. Logistic regression models reached up to 69% cross-validated accuracy for prediction of conversion status, which was comparable to cross-validated accuracy of non-linear support vector machine classification. Regularized regression outperformed unpenalized stepwise regression when number of parameters approached or exceeded the number of training cases. Partial volume correction had a negative effect on the predictive performance of AV45-PET, but slightly improved the predictive value of FDG-PET data.

Penalized regression yields more parsimonious models for the integration of multiregional and multimodal imaging information, and highlights the relative importance of amyloid-PET for prediction of conversion from MCI to AD.

Keywords: *predementia, prodromal, florbetapir, PET, MRI*

P27 Presented by: Grothe, Michel J.

Submission ID: 17



P29

Cerebral Amyloid Angiopathy in Asymptomatic Community-Dwelling Older Adults

M. Edip Gurol, Aaron Schultz, Trey Hedden, Panagiotis Fotiadis, Sergi Martinez-Ramirez, Anand Viswanathan, J. Alex Becker, Reisa Sperling, Steven Greenberg, Keith Johnson

Massachusetts General Hospital, Harvard Medical School, Boston, MA, United States

Background: Cerebral amyloid angiopathy (CAA), characterized by accumulation of β -amyloid in cortical vessels, is an established cause of hemorrhagic and ischemic brain damage. Although Boston criteria can accurately diagnose CAA in patients who had lobar intracerebral hemorrhage (ICH), its value in asymptomatic older adults is unknown.

Objective: We aimed to compare the amyloid load, structural MRI measures and risk factors between asymptomatic subjects who would qualify for a diagnosis of probable CAA based on lobar microbleeds (LMB) and superficial siderosis (SS) to subjects without these MRI findings.

Methods: Healthy older adults (n=181) prospectively enrolled in Harvard Aging Brain study had research MRIs and PiB-PET scans. Probable CAA was diagnosed based on presence of 2 or more LMBs or a combination of LMB/SS, similar to modified Boston criteria. Distribution volume ratio (DVR) of PiB-retention, white matter hyperintensity (WMH) and hippocampal volume (HV) were calculated. Demographics, APOE status, risk factors, and imaging markers were compared between subjects with and without probable CAA based on LMB/SS.

Results: Participants had mean age 74.5 ± 5.8 and 56% were female. Forty-six (25%) subjects had lobar MBs, 11(6%) had deep and 4(2%) cerebellar MBs. The 22 subjects diagnosed with probable CAA had higher occipital DVR (1.35 vs 1.28, $p=0.004$) and higher WMH (0.51 vs 0.16 percent of intracranial volume, $p=0.005$) when compared to persons without MB. These associations remained significant after adjustment for age and gender. Age, HV, APOE status and vascular risk factors were similar between probable CAA and no MB subjects (all $p>0.2$).

Conclusions: Probable CAA diagnosis based on presence of lobar MBs and SS on MRI of healthy elderly volunteers is associated with other radiologic markers of CAA (posterior amyloid load, WMH) but not with vascular risk factors or markers of Alzheimer's Disease (HV, APOE 4). Boston criteria and amyloid imaging thus may allow early diagnosis of CAA even in asymptomatic subjects without ICH or dementia.

Keywords: *cerebral amyloid angiopathy, cerebral microbleeds, superficial siderosis, PiB-PET, leukoaraiosis*

P29 Presented by: Gurol, M. Edip

Submission ID: 97

P31

Stroke Risk Interacts with AD Biomarkers in Conferring Risk for Cognitive Decline

Timothy Hohman, Dandan Lui, Lauren Samuels, Katherine Gifford, Angela Jefferson

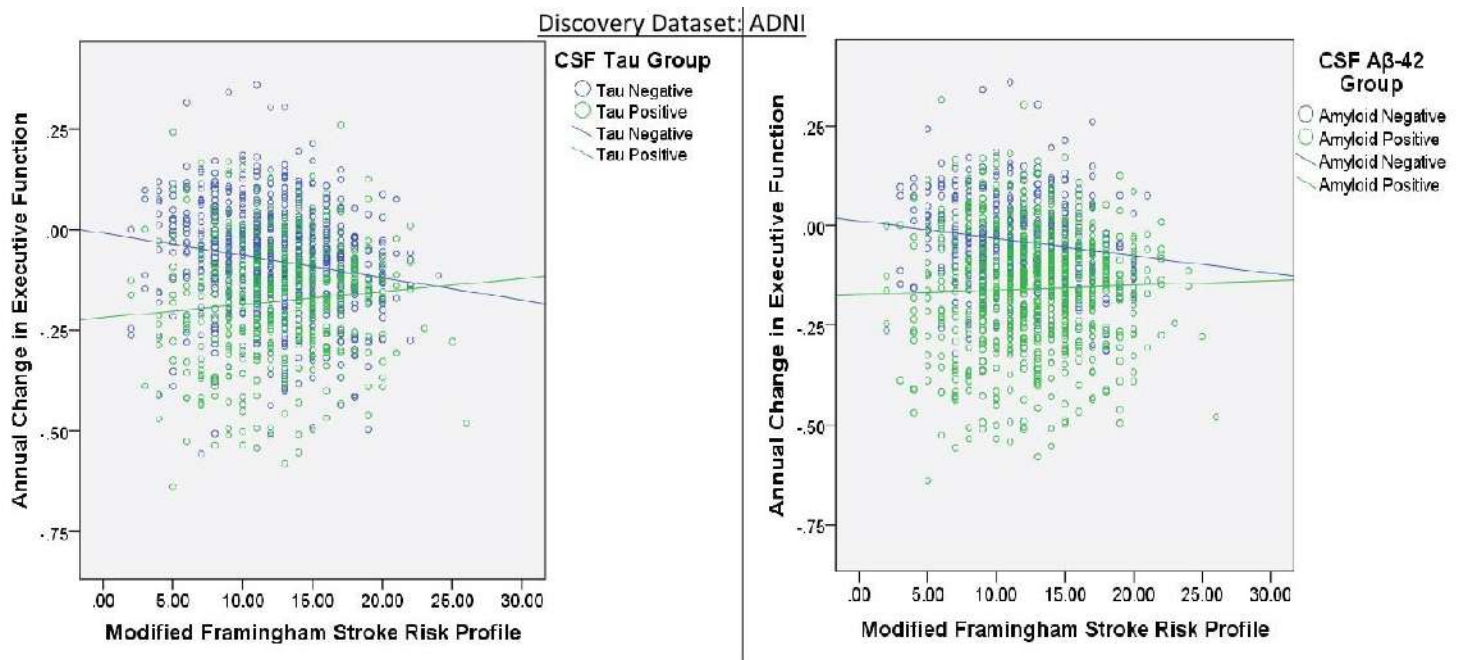
Vanderbilt Memory & Alzheimer's Center Vanderbilt University Medical Center, Nashville, TN, United States

Background: Stroke risk factors and Alzheimer's disease (AD) biomarkers are associated with cognitive decline. Recent work has demonstrated that the most common presentation of dementia is a mixed dementia with both vascular and AD pathologies contributing to cognitive impairment. Yet, no work to date has performed a comprehensive evaluation of the interaction between stroke risk factors and AD biomarkers in relation to brain aging outcomes. This project evaluated such an interaction in two large national databases to test whether the effect of stroke risk factors depends on the levels of AD biomarkers.

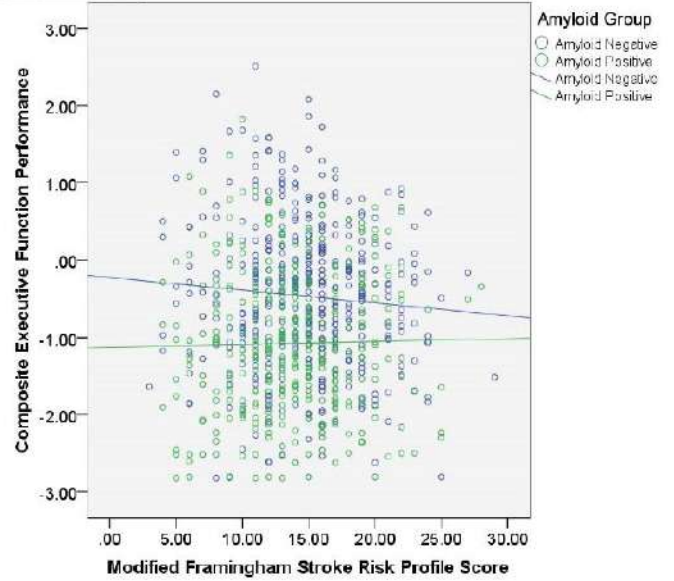
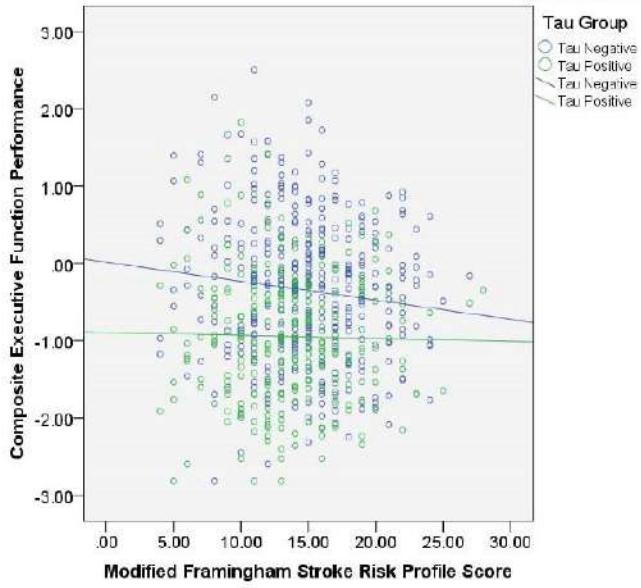
Methods: Participants were drawn from the Alzheimer's Disease Neuroimaging Initiative (ADNI; n=1202) and the National Alzheimer's Coordinating Center (NACC; n=983). Stroke risk was quantified using a Framingham Stroke Risk Profile (FSRP) and AD biomarkers were quantified as levels of relevant proteins (amyloid- β 42, total tau (t-tau), phosphorylated tau (p-tau)) in cerebrospinal fluid. The interaction between stroke risk and AD biomarkers was cross-sectionally related to brain aging outcomes (hippocampal volume, episodic memory performance, executive function performance) using a general linear model and longitudinally using mixed-effects regression.

Results: In baseline analyses, we observed an interaction between FSRP and A β -42 in relation to hippocampal volume (p=0.004) and memory (p=0.0004). In longitudinal analyses, we observed an interaction between FSRP and A β -42 in relation to executive function (p=0.020), FSRP and t-tau in relation to memory (p=0.017) and executive function (p=0.030), and between FSRP and p-tau in relation to memory (p=0.038). Interactions in relation to cognition were replicated in NACC using autopsy measures of pathology.

Conclusions: The effect of stroke risk and AD biomarkers appears strongest in the absence of the other risk factor. Targeted interventions aimed at reducing stroke risk factors in early and middle life may be particularly beneficial in those individuals who would otherwise be at low risk for cognitive impairment.



Replication Results: NACC Dataset



Keywords: Stroke Risk, CSF Biomarkers, Cognition, MRI, Autopsy

P31 Presented by: Hohman, Timothy J

Submission ID: 21

P33

Longitudinal Change of PiB Accumulation with A One Year Interval in Alzheimer's Disease, Mild Cognitive Impairment, and Cognitively Normal Subjects

Takashi Kato^{1,2}, Kaori Iwata², Ken Fujiwara², Naohiko Fukaya¹, Yoshitaka Inui¹, Kengo Ito^{1,2}, Akinori Nakamura², MULNIAD Study Group²

¹ Department of Radiology, National Center for Geriatrics and Gerontology, Obu, Aichi, Japan

² Department of Clinical and Experimental Neuroimaging, National Center for Geriatrics and Gerontology, Obu, Aichi, Japan

Background and purpose: PiB PET is an imaging biomarker of amyloid plaque that is a main target of disease modifying drugs for Alzheimer's disease (AD). Amyloid imaging PET is expected to evaluate the therapeutic effects. The purpose of this study was to investigate longitudinal PiB PET data in PiB-positive cognitively normal (CN) mild cognitive impairment (MCI), and AD in order to estimate the sample size to detect a significant change of PiB accumulation.

Subjects and method: Subjects selected from in-house studies were nine CN subjects (age: 73.4±3.9 y.o.), nine patients with MCI (age:75.6±4.9), and five patients with AD (age:75.8±4.2) whose PiB PET images were visually rated as positive scans. They underwent PiB PET and MRI with an interval of one year. The mean cortical standardized uptake value ratio (mcSUVR) was obtained from PET images of 50-70 min after the injection of PiB and 3D-T1 weighted MRI using DARTEL and the Automated Anatomical Labeling Atlas. One-year percent change of mcSUVR was calculated in each subject. The necessary sample sizes were calculated to detect 5% change of mcSUVR with a one-year assessment interval at 80% power and a significance level of two-tailed 5%

Results: The mcSUVR values at the baseline in CN, MCI, and AD were 1.42±0.15, 1.77±0.24, and 1.95±0.23, respectively. The mean and S.D. of percent change of mcSUVR with a one-year interval were 5.76±4.06 in CN, 5.40±6.59 in MCI, and 6.19±3.95 in AD. The estimated number of PiB positive subjects needed to detect 5% change of mcSUVR were 24 CN, 58 MCI, and 22 AD.

Conclusion: The results suggest that mcSUVR value of PiB PET obtained with the atlas-based ROIs have sufficient power to evaluate therapeutic effects of anti-amyloid drugs.

Keywords: *PiB PET, longitudinal, power analysis*

P33 Presented by: Kato, Takashi

Submission ID: 59

P35

Comparative Assessment of SUVR Methods in Amyloid Cross-Sectional and Longitudinal Studies

Gregory Klein, Davis Staewen, Mehul Sampat, David Scott, Joyce Suhy

BioClinica, Inc, Newark, CA, United States

Objectives: We compare results of standard uptake value ratio (SUVR) analyses in the Alzheimer's Disease population using a native space compared to SPM template methods. While an SPM approach has shown amyloid differences between normal and AD subjects, the smoothing and deformable registration used for alignment may sacrifice information otherwise retained in a native space approach.

Methods: Freesurfer was used to obtain an ROI parcellation on T1 MRI data from 458 subjects (175 Normal, 92 EMCI, 153 LMCI, 39AD). Florbetapir data from two time points approximately 24 months apart were registered to the MRI data in T1 native space, and SUVR's were computed for 110 subregions. Eight reference regions including whole cerebellum, brainstem and subcortical white matter were evaluated. SUVR's were also computed in template space using SPM and both grey matter-masked AAL regions and on regions described by Clark2011. Effect sizes between AD and Normal groups were evaluated using Cohen's d. Effect size of longitudinal change in SUVR was also compared.

Results: The native space approach showed largest differences between AD and normals in regions traditionally showing high A β load, including the precuneus, frontal, temporal and cingulate area (effect size = 1.92, 1.63 and 1.20 for the Freesurfer, Clark2011 and AAL approaches respectively). In the Freesurfer cross-sectional and longitudinal analysis, the putamen was also seen to have a high effect size. Effect size was largest using a composite reference region composed of an average of subcortical white matter, whole cerebellum and brainstem. In a longitudinal analysis, the native space approach also showed larger effect size than the template-based approach consistently across all patient groups.

Conclusions: A native space approach shows promise in providing improved regional differentiation between normal and AD groups, and possibly reduced sample size requirements in clinical trials.

[Clark2011] JAMA. 2011;305(3):275-283

Keywords: *SUVR, Freesurfer, Amyloid, florbetapir, ADNI*

P35 Presented by: Klein, Gregory

Submission ID: 57

P37**Regional Distribution of 3H-THK5117 in Confirmed Alzheimer's Disease Cases**

Laetitia Lemoine¹, Laure Saint-Aubert¹, Fredrik Engman¹, Amelia Marutle¹, Gunnar Antoni^{2,3}, Jonas Eriksson³, Sergio Estrada², Nobuyuki Okamura⁴, Inger Nennesmo⁵, Per-Göran Gillberg¹, Agneta Nordberg^{1,6}

¹ Center For Alzheimer Research, NVS department, Division of Translational Alzheimer Neurobiology, Karolinska Institutet, Stockholm, 14157, Sweden

² Preclinical PET Platform, Department of Medicinal Chemistry, Faculty of Pharmacy, Uppsala University, Uppsala, 75105, Sweden

³ PET Centre, Centre for Medical Imaging, Uppsala University Hospital, Uppsala, 75105, Sweden

⁴ Department of Pharmacology, Tohoku University School of Medicine, Sendai, 980-8575, Japan

⁵ Department of Pathology, Karolinska University Hospital, Stockholm, 14186, Sweden

⁶ Department of Geriatric Medicine, Karolinska University Hospital Huddinge, Stockholm, 14186, Sweden

Objectives: It is assumed that the accumulation of NFT, composed by aggregation of hyperphosphorylated TAU protein, precedes the early onset of clinical symptoms of AD and correlate with the progression of memory dysfunction. The non invasive imaging of Tau may facilitate the early diagnosis of AD. In this study we aim to characterize the in vitro distribution of 3H-THK5117 in AD Brain cases.

Methods: Binding assays studies including saturation and competition assay, were performed on brain homogenates of Tau rich known AD cases. The regional distribution of 3H-THK5117 was determined with single concentration assay in different Brain regions on AD and controls cases. Autoradiography have been performed on large tissue sections from frozen whole hemisphere of AD brain with 3H-THK5117.

Results: Competition binding studies with 3H-THK5117 versus cold THK5117 in AD temporal cortex brain homogenates showed multiple binding site for the 3H-THK5117. Saturation binding studies (1-200 nM) with 3H-THK5117 revealed 50-60 % specific binding and confirmed the high affinity site (Kd, 10 to 20 nM) measured in competition studies. The regional distribution is different between AD and control cases. The autoradiography show a pattern very similar for THK5117 in accordance with the literature.

Conclusions: THK5117 shows multiple binding sites with high specific binding in selective AD brain regions promising for present development of PET tau imaging.

P37 Presented by: Lemoine, Laetitia

Submission ID: 125

P39

[18F]T807 ([18F]AV-1451) and Fluorescent Analog T726 Detect PHF-Tau but Not TDP-43 in Alzheimer's and FTD Post-Mortem Brain Tissue Sections

Yin-Guo Lin¹, Felipe Gomez¹, Qianwa Liang¹, Eileen Bigio², Thomas Beach³, Mark Mintun¹, Giorgio Attardo¹

¹ Avid Radiopharmaceuticals, Philadelphia, PA, United States

² Northwestern ADC Neuropathology, Chicago, IL, United States

³ Banner Sun Health Research Institute, Sun City, AZ, United States

Background: We have previously shown that [18F]T807 ([18F]AV-1451) and its fluorescent analog T726 bind to PHF-Tau in brain sections from Alzheimer's (AD) and non-AD Tauopathies, such as PSP, Pick's disease and CTE. TDP-43 inclusions can occur in AD and Frontotemporal Dementia (FTD) therefore it would be useful to characterize the selectivity of [18F]T807 and T726 towards PHF-Tau versus TDP-43.

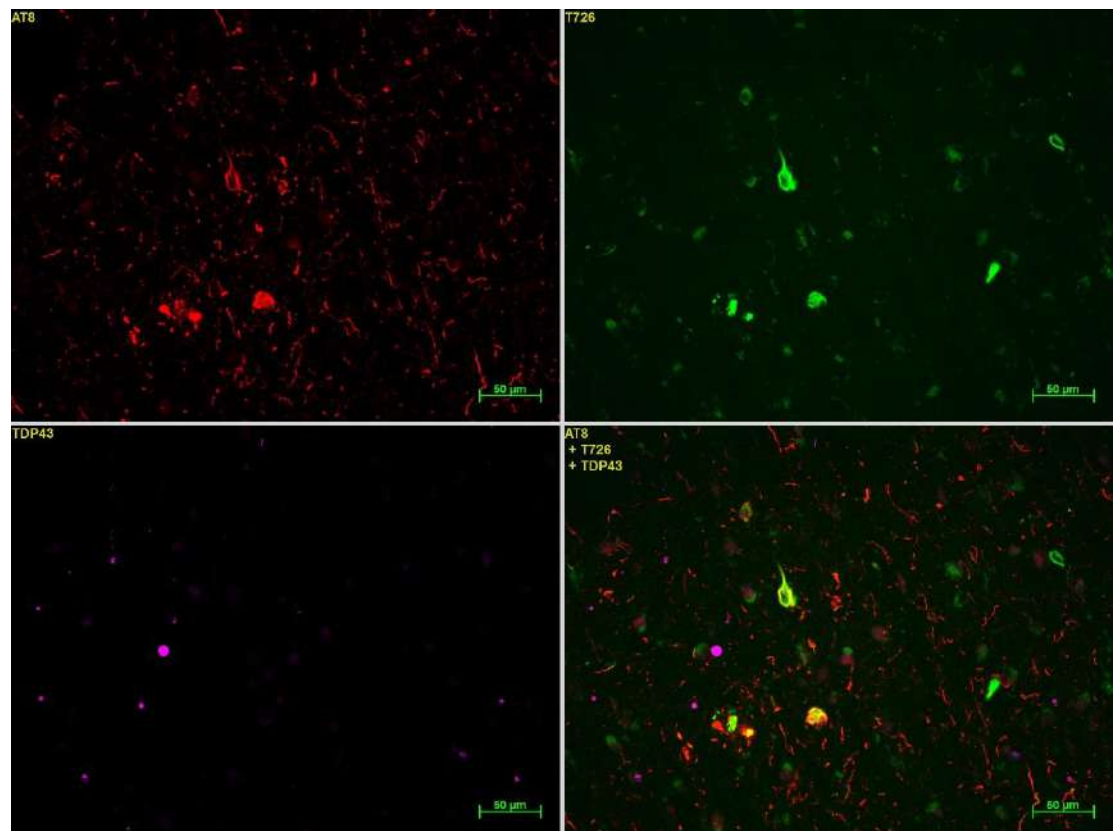
Objective: The objective of this study was to determine if [18F]T807 and its fluorescent analog T726 bind to TDP-43 in AD and FTD post-mortem human brain tissue.

Methods: 14 AD and 15 FTD cases as well as 1 normal control were selected for this study. Frontal, medial-temporal, parietal gyrus, amygdala, hippocampus, and entorhinal cortex were included for a total of over 50 brain slice sections analyzed. Fresh frozen brain sections were stained with phospho-Tau (AT8, AT100) and TDP-43 antibodies (TDP-43, and pTDP-43). Double or triple immunofluorescence staining using T726 was performed to investigate whether the observed signal from T726 co-localized with staining from PHF-Tau or TDP-43 antibodies. Additionally, autoradiography with [18F]T807 in the absence or presence of excess T807 was conducted to investigate the ability of [18F]T807 to label PHF-Tau or TDP-43 pathology in brain sections containing these aggregates.

Results: No co-localization of fluorescent signals occurred between T726 and TDP-43 antibodies in AD, FTD/PPA and FTLTDP cases. [18F]T807 produced intense and specific autoradiography signal in all tau-rich brain sections but not in TDP-43 positive/tau negative tissue.

Conclusion: Autoradiography experiments with [18F]T807 in AD and FTD as well as immunofluorescence studies with T726 suggest that no interference due to cross-reactivity with TDP-43 binding should occur when [18F]T807 is used to detect PHF-tau in human brain tissue.

Figure: Section of Cingulate Gyrus of FTD patient stain with the Anti PHF-Tau antibody AT8, the anti TDP-43 antibody TDP-43 and the fluorescent compound T726. Arrows indicate clear T726-Tau colocalization.



P39 Presented by: Lin, Yin-Guo

Submission ID: 63

P41**Effects of Age and β -amyloid on Tau Deposition Measured Using [^{18}F] AV-1451 in Normal Older People**

Samuel Lockhart¹, Jacob Vogel¹, Daniel Schonhaut^{1,2}, Suzanne Baker³, Henry Schwimmer^{1,3}, Michael Schöll¹, Rik Ossenkoppele^{1,2}, Gil Rabinovici^{1,2,3}, William Jagust^{1,2,3}

¹ Helen Wills Neuroscience Institute, University of California Berkeley, Berkeley, CA, United States

² Memory and Aging Center, University of California San Francisco, San Francisco, CA, United States

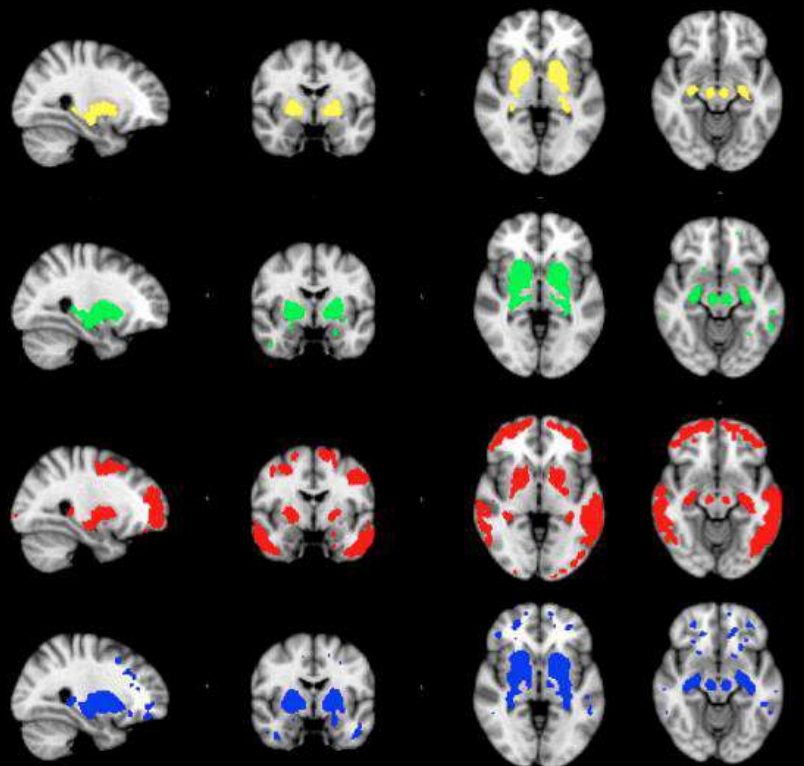
³ Life Sciences Division, Lawrence Berkeley National Laboratory, Berkeley, CA, United States

Objectives: To examine the effects of age and β -amyloid (A β) deposition on *in vivo* aggregation of the tau protein, measured using [^{18}F] AV-1451 PET.

Methods: 17 cognitively normal elders (78.6 ± 5.1 y) received [^{18}F] AV-1451 and [^{11}C] PiB PET. Elders were stratified by age (Old-old $n = 8$, Young-old $n = 9$) or PiB status ($n = 6$ PiB+ [DVR ≥ 1.08]). [^{18}F] AV-1451 SUVR images (80-100 min post-injection, cerebellar gray reference region) were transformed into a common space. Intensities of all subjects' supratentorial gray and white matter voxels were plotted, and a threshold at 90% (1.45) was selected to visualize spatial distributions (highest 10% of voxels), based on averaging subjects' SUVR images within age X PiB status levels (Figure 1). We then smoothed individual common-space AV-1451 SUVR images by a 4mm FWHM kernel and tested for clusters where greater age and A β were significantly associated (*t*-test, $p < 0.01$ uncorrected, $k = 50$, unthresholded supratentorial gray/white matter mask) with tau as measured by AV-1451 SUVR (Figure 2).

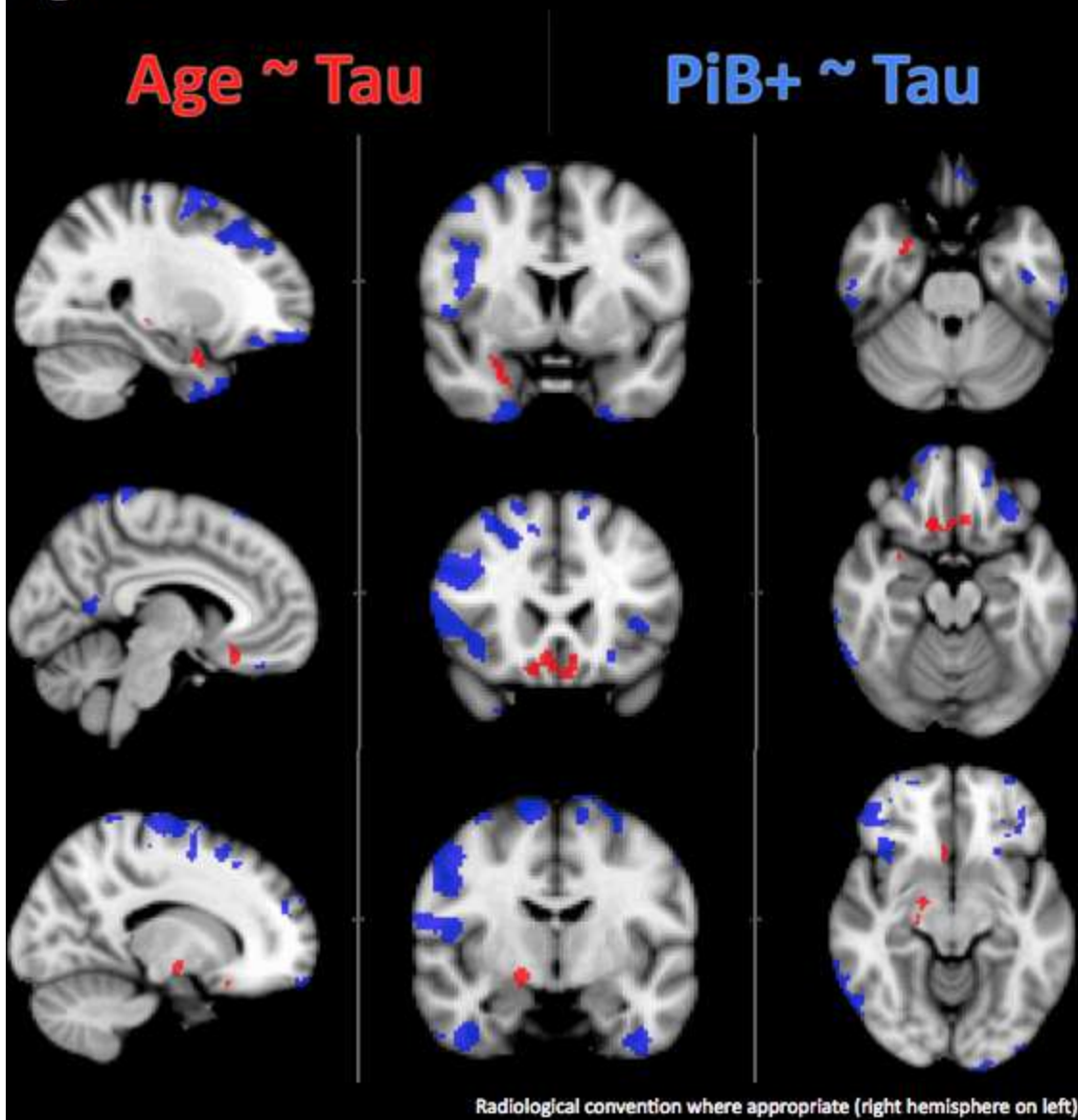
Results: AV-1451 spatial distributions based on age group and PiB status (Figure 1) demonstrate substantial accumulation in basal ganglia, midbrain, hippocampus, and fornix even in relatively younger, A β -free cognitively normal elders; accumulation extends with increasing age and A β to neocortex. Voxelwise nonparametric *t*-tests revealed significant positive relations (Figure 2) between age group and AV-1451 accumulation in regions including right entorhinal cortex and midline ventral frontal cortex, and between PiB status and AV-1451 in numerous regions in bilateral temporal, frontal, and parietal cortices.

Conclusions: Age and A β differentially predict AV-1451 accumulation patterns *in vivo*. In particular, advancing age predicts AV-1451 accumulation in medial temporal lobe (MTL) and ventral regions, while A β predicts accumulation outside MTL. Preclinical AD and aging processes may be inadvertently conflated in many studies investigating gradual late-life cognitive decline.

Figure 1**Young-Old, PiB- ($n=6$)****Old-Old, PiB- ($n=5$)****Young-Old, PiB+ ($n=3$)****Old-Old, PiB+ ($n=3$)**

Clusters represent voxels with mean SUVR > 1.45 (90% threshold of all gray/white voxels)
Radiological convention where appropriate (right hemisphere on left)

Figure 2



Keywords: [18F] AV-1451 PET, Cognitively normal aging, Amyloid PET

P41 Presented by: Lockhart, Samuel N.

Submission ID: 55

Relationship of Age, APOE genotype, Amyloid Load and Hippocampal Volume to Amnestic and Non-amnestic Cognitive Function – A Path Analytic Study

David Loewenstein^{1, 2}, Warren Barker², Mohammed Goryawala³, Rosemarie Rodriguez², Malek Adjoudai³, Ranjan Duara², Maria Greig², Qi Zhou³

¹ Department of Psychiatry and Behavioral Sciences, University of Miami, Miller School of Medicine, Miami FL, Miami, Florida, United States

² Wien Center For Alzheimer's Disease & Memory Disorders, Mount Sinai Medical Center, Miami Beach FL, Miami Beach, Florida, United States

³ Center for Advanced Technology and Education, Florida International University, Miami FL, Miami, Florida, United States

Objective: Structural path analyses were used to investigate inter-relationships between APOE genotype, age, amyloid load and hippocampal volume (HPv) to determine their direct and indirect influences on amnestic and non-amnestic cognition.

Methods: Data was obtained from ADNI for 333 MCI and 202 cognitively normal (CN) cases. The Rey Auditory Verbal Learning Test-30 min delayed (RAVLT-D) and Trails-B scores were indices of memory and executive function. Path analysis was done separately among CN and MCI subjects, using age and APOE4 genotype as independent measured variables, HPv and amyloid load as mediating variables and cognitive scores (RAVLT and Trails-B) as dependent variables.

Results - CN subjects:

- RAVLT-D scores were not predicted by any variable (Figure-1a)
- HPv was predicted by age (beta weight = -.36; $p < .001$) (Figure-1a&b)
- Amyloid load was predicted by APOE4 (beta weight = .36; $p < .001$) (Figures-1a&b)
- Trails-B score was predicted strongly by age (beta weight = .32 ; $p < .001$) but not by any other variable (Figure-1b).

Results: - MCI subjects:

- RAVLT-D scores were predicted by HPv (beta weight = .39; $p < .001$), APOE4 (beta weight = -.17; $p < .03$), and age (beta weight = .11; $p < .05$), but not by amyloid load (Figure-2a)
- HPv was predicted by age (beta weight = .31; $p < .001$) and APOE4 (beta weight = -.15; $p < .05$) but not amyloid load (Figure-2a)
- Amyloid Load was predicted very strongly by APOE4 (beta weight = .52; $p < .001$), but not age (Figure-2a)
- Trails-B scores were not predicted by HPv, age, amyloid load or APOE4 (Figure-2b).

Conclusions: APOE4 and age influence memory function, mediated mainly by neurodegeneration (i.e., HPv), although APOE4 also has a direct effect on memory in the MCI stage of AD. HPv is influenced most by age but also by APOE4 in MCI patients. Amyloid load is influenced most strongly by APOE4 in both CN and MCI groups. The effects of APOE4 on memory function in MCI appear to operate independently of amyloid load, and largely independently of HPv.

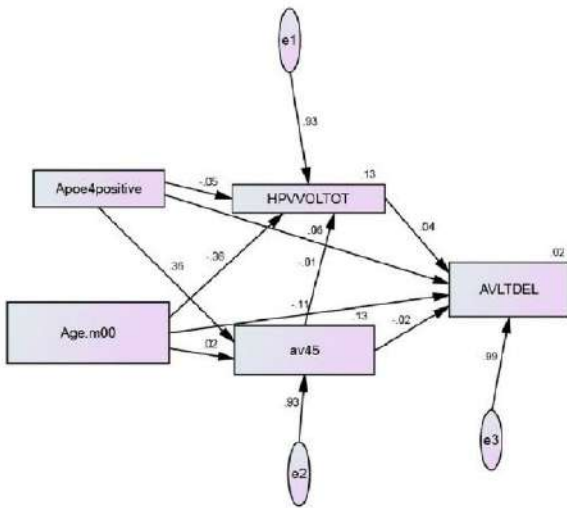


Figure 1a. Cognitively Normal
(Predictors of RAVLT Scores)

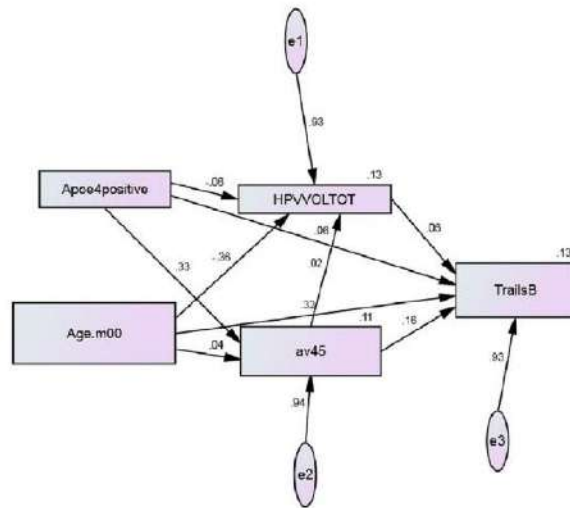


Figure 1b Cognitively Normal
(Predictors of Trails B scores)

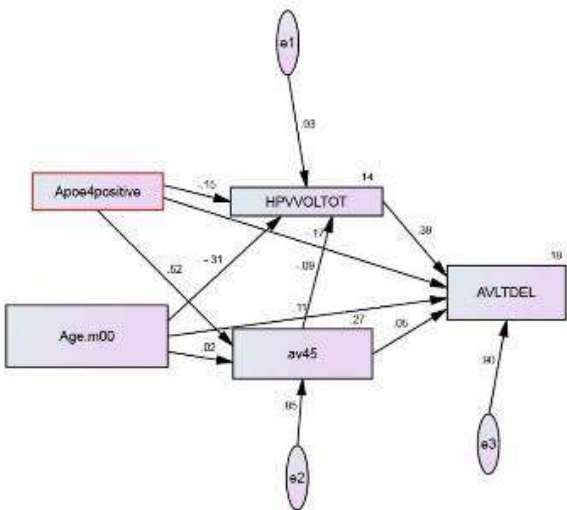


Figure 2a- MCI Patients
(Predictors of RAVLT scores)

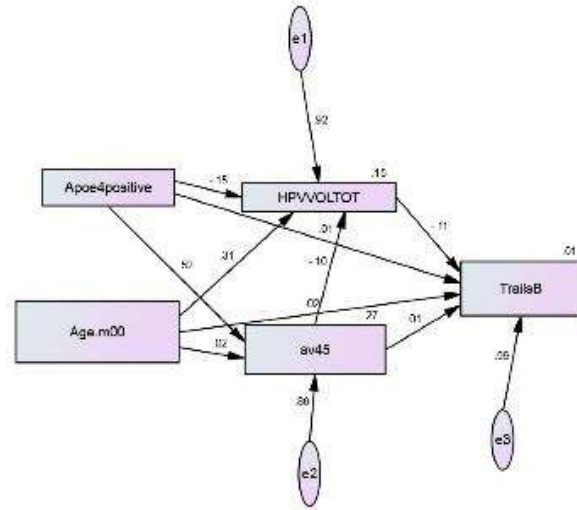


Figure 2b- MCI Patients
(Predictors of Trails B scores)

Keywords: APOE, MCI, hippocampus, amyloid, ADNI

P43 Presented by: Loewenstein, David

Submission ID: 37

Pittsburgh Compound-B (PiB): Radiologic-pathologic Correlations in a Series of 18 Autopsied Cases

Marta Marquie^{1,2}, Beatriz G. Perez-Nievas^{1,2}, Isabel Costantino^{1,2}, Rebecca Betensky³, Isabel Barroeta-Espar^{1,2}, Joseph Parisi⁴, Ronald Petersen⁴, Matthew Senjem⁴, Clifford Jack Jr.⁴, Matthew Frosch^{1,2}, Bradley Hyman^{1,2}, Keith Johnson², Val Lowe⁴, Teresa Gomez-Isla^{1,2}

¹ MassGeneral Institute for Neurodegenerative Disease, Charlestown, MA, United States

² Massachusetts General Hospital, Boston, MA, United States

³ Harvard School of Public Health, Boston, MA, United States

⁴ Mayo Clinic, Rochester, MN, United States

Introduction: The development of amyloid imaging has made it possible to identify amyloid deposition *in vivo* and recent studies have suggested that PiB binds to fibrillar A β in the form of amyloid plaques and cerebral amyloid angiopathy (CAA). **Objective:** To carefully study the correlations of *in vivo* [C-11]PiB PET uptake and postmortem pathological and biochemical measures of β -amyloid in a series of 18 brains from individuals who were imaged while alive and came to autopsy.

Methods: Pathological diagnoses were as follows: 6 Alzheimer's disease (AD), 6 dementia with Lewy bodies (DLB), 3 mixed AD/ DLB, 1 progressive supranuclear palsy and 2 controls. Relations between [C-11]PiB PET uptake measured as SUVR (standardized uptake value ratio in the region relative to cerebellar gray matter), multiple postmortem measures of amyloid deposition (PiB, ThioS and 10D5 plaque burdens, and NAB61 oligomeric A β burden) and ELISA detection of soluble A β species (A β 40, A β 42 and oligomeric A β) were studied in four regions of interest (ROI) (middle frontal, superior temporal sulcus, inferior parietal and occipital cortices).

Results: *In vivo* [C-11]PiB PET retention values very significantly correlated with all postmortem measures of amyloid deposition in the ROI. [C-11]PiB PET uptake also correlated with postmortem brain levels of A β 42 and oligomeric A β but not with measures of cognition. Most cases with SUVR values exceeding the cut-off of 1.50 for *in vivo* amyloid positivity had intermediate or frequent CERAD neuritic plaque scores at postmortem, except for three cases all of whom were DLB with sparse CERAD neuritic plaque scores. Of note, all three had substantial load of diffuse plaques and one also had CAA.

Conclusion: Our study supports an excellent correlation between antemortem PiB PET retention and postmortem brain β -amyloid accrual. In addition to neuritic plaques, diffuse plaques and CAA accounted for *in vivo* PiB binding in this autopsy series.

Keywords: PiB, PET, beta-amyloid, diffuse plaques, amyloid angiopathy

P45 Presented by: Marquie, Marta

Submission ID: 93

P47

Amyloid at the Threshold - Relationships between CSF Biomarkers, Amyloid PET, Glucose Metabolism, and Atrophy, with Implications for Diagnosis and Clinical Trials

Dawn Matthews¹, Randolph Andrews¹, Ana Lukic¹, Mark Schmidt², et al.

¹ ADM Diagnostics, LLC, Chicago, IL, United States

² Janssen Research and Development, Beerse, Antwerp, Belgium

Introduction: As clinical trials employ amyloid measurement, an inverse correlation between amyloid PET and CSF Abeta42 has supported either/or use of these markers, with fixed cutoffs. However, as trials focus on preclinical and early MCI populations, more patients may be near threshold, and understanding the relationships between these markers and other markers of degeneration may be important for optimal patient classification.

Methods: We evaluated 288 early MCI (EMCI) and 253 subjects with Normal (NL) diagnosis from ADNI having measures of amyloid (CSF and florbetapir), CSF tau, FDG PET, hippocampal volume, entorhinal cortical thickness, and cognitive endpoints including ADAScog and Logical Memory. Using a voxel-based multivariate classifier, we also determined FDG PET AD-signature scores reflecting expression of a pattern of disease decline. We examined concurrence across amyloid biomarkers in positive, negative, and threshold ranges, compared to other markers, and determined the percentage of amyloid PET cases within +/-5% of threshold.

Results: There was agreement between CSF and florbetapir in 85% of EMCI subjects with CSF Abeta<192 or >209, and in 84% of NLs. In the CSF range 193-209, 83% and 94% of subjects were amyloid negative in PET cortical average, though with cingulate values close to or at threshold. In those subjects with “emerging” CSF Abeta but negative amyloid PET, FDG Progression Score ($p<0.005$) and entorhinal cortical thickness (EMCI only) were significantly decreased from NL- values, intermediate to decrease in subjects with lower CSF and positive amyloid PET. 20% of EMCI and 23% of NLs had amyloid PET values within 5% of threshold.

Conclusion: Application of strict cutoffs may introduce variability in subjects near threshold. Technical measurement variation may impact positivity on 20% of subjects. Neurodegenerative markers including FDG PET may provide an early indicator to aid in classifying emerging subjects.

Keywords: *amyloid, FDG, EMCI, CSF, threshold*

P47 Presented by: Matthews, Dawn C

Submission ID: 121

P49

CogState Trajectories over 30 Months and the Effect of Amyloid Status and APOE E4 genotype in Cognitively Normal Individuals: The Mayo Clinic Study of Aging

Michelle Mielke, Teresa Christianson, Clint Hagen, Mary Machulda, Rosebud Roberts, Prashanthi Vemuri, Val Lowe, David Knopman, Kejal Kantarci, Clifford Jack, Ronald Petersen

Mayo Clinic, Rochester, MN, United States

Background: The CogState computerized battery has been incorporated as a secondary outcome measure in the A4 and DIAN-TU secondary prevention trials. We examined the practice effects of each CogState test compared to a standard neuropsychological battery, over a 30-month follow-up, and determined whether the presence of amyloid or of an APOE E4 allele was associated with performance.

Methods: We included 923 cognitively normal participants, aged 50-71, enrolled in the Mayo Clinic Study of Aging. All participants were test-naïve at baseline and completed multiple CogState visits and standard neuropsychological batteries over 30 months of follow-up; 413 underwent PiB PET. Amyloid positivity was defined as PiB PET SUVR>1.4. CogState tests included: Detection (DET) – simple reaction time; Identification (IDN) – choice reaction time; One Card Learning (OCL) – visual learning; One Back test (ONB) – working memory/attention; and the Groton Maze Learning Test (GMLT) – spatial working memory. Linear mixed models assessed the change in the CogState tests and individual- and domain-specific standard neuropsychological tests controlling for age, sex, and education. We included interactions with amyloid status and presence of an APOE E4 allele to determine whether these factors were associated with cognitive performance.

Results: Practice effects were greater for OCL accuracy and IDN speed compared to all individual- and domain-specific standard neuropsychological tests. Amyloid positive individuals performed worse, albeit non-significantly ($p>0.10$), at baseline on DET, IDN, OCL accuracy, and ONB. This worse performance was maintained over time but there were no differences in slopes by amyloid status. CogState performance did not differ by APOE E4 genotype at baseline or longitudinally.

Conclusion: Results suggest that CogState practice effects are similar to standard neuropsychological testing, with the exception of OCL accuracy and IDN speed. CogState test performance did not significantly differ by amyloid or APOE E4 status at baseline or longitudinally up to 30 months.

Keywords: *CogState; amyloid; APOE E4; longitudinal*

P49 Presented by: Mielke, Michelle M

Submission ID: 49

P51

Automated Voxel-based Quantitation of Amyloid PET in Prodromal AD: Validation Study with up to Eight Years of Follow-up

Arthur Mikhno^{1,2}, Janos Redei², John Mann^{1,3}, Ramin Parsey⁴

¹ Columbia University, New York, NY, United States

² i2Dx, Inc., San Francisco, CA, United States

³ New York State Psychiatric Institute, New York, NY, United States

⁴ Stony Brook University, Stony Brook, NY, United States

Background: Accurately identifying prodromal disease is a key challenge for early diagnosis and therapeutic intervention in AD. The objective of this study was to evaluate the utility of fully automated PET quantitation in prodromal AD. The approach was previously developed for differentiating healthy controls from AD using 90-minute [11C]PIB PET scans (Mikhno et al., JNM 2008). We adapted this approach to short 20-minute [18F]florbetapir PET scans and evaluated it in a MCI cohort.

Methods: Subjects with MCI at the time of their earliest [18F]florbetapir PET, and their corresponding T1 MRI scans, were selected from the ADNI database. Subjects were divided into converters (to AD) and non-converters; 31 converter (PET 1 to 3 years prior to conversion) and 29 non-converter subjects (5 to 8 years of MCI follow-up) were included. Voxel-wise SUVR maps (50-70 min, cerebellum reference) were partial volume corrected and transformed into MNI space. Optimal voxels that discriminate converter and non-converter groups were determined based on a voxel-wise t-score cluster analysis. SUVRs were obtained from the optimal voxels for each subject with a leave-one-out analysis.

Results: Receiver operating characteristic area (ROC) area under the curve was 0.912. For a SUVR cutoff value of 1.26 sensitivity was 87%, specificity 79%, and accuracy 83%; a higher cutoff of 1.29 yielded a 81% sensitivity, 83% specificity, and 82% accuracy.

Conclusions: To our knowledge, this approach outperforms other methods for identifying subjects in the prodromal phase of AD, and demonstrated here in a cohort with long follow-up. We have identified and quantified highly discriminative brain areas reflecting early amyloid deposition within the prodromal AD phenotype. The automated quantitation is robust across scanners and may be particularly useful in conjunction with short scans as acquired clinically, for applications in clinical trial enrichment, diagnosis of early AD, and pre-clinical disease.

Keywords: *prodromal AD, MCI, voxel-based, PET, Florbetapir*

P51 Presented by: Mikhno, Arthur

Submission ID: 19

Distinct [¹⁸F]AV1451 Retention Patterns in Clinical Variants of Alzheimer's Disease

Rik Ossenkoppele^{1,2}, Daniel Schonhaut^{1,2}, Suzan Baker³, Andreas Lazaris¹, Nagehan Ayakte^{1,2}, Averill Cantwell¹, Sam Lockhart², Jacob Vogel², Henry Schwimmer^{2,3}, Michael Schöll², James O'Neill³, Maria Gorno-Tempini¹, Bruce Miller¹, William Jagust^{2,3}, Gil Rabinovici^{1,2}

¹ Memory and Aging Center, University of California San Francisco, San Francisco, CA, United States

² Helen Will Neuroscience Institute, University of California Berkeley, Berkeley, CA, United States

³ Life Science Division, Lawrence Berkeley National Laboratory, Berkeley, CA, United States

Objective: To describe preliminary findings applying the putative tau PET ligand [¹⁸F]AV1451 (formerly named T807) in clinical variants of Alzheimer's disease (AD) and to compare the regional specificity of [¹⁸F]AV1451 to that of [¹¹C]PIB and [¹⁸F]FDG PET.

Methods: PET scans were performed in 4 posterior cortical atrophy (PCA), 1 logopenic variant primary progressive aphasia (lvPPA), 1 early-onset AD and 1 (memory-predominant) late-onset AD patients (all PIB+) and in 14 cognitively normal controls (Table 1). We created SUVR images for [¹⁸F]AV1451 (80-100 minutes, gray matter cerebellum as reference region) and [¹⁸F]FDG (30-60 minutes, pons-normalized), and DVR images for [¹¹C]PIB (0-90 minutes, gray matter cerebellum as reference region). We visually assessed [¹⁸F]AV1451, [¹¹C]PIB and [¹⁸F]FDG uptake patterns in 3 distinct AD variants, and performed voxel-wise contrasts (in SPM) between PCA patients and controls.

Results: Figure 1 shows asymmetric [¹⁸F]AV1451 uptake in parietal, temporal and frontal regions (left>right) in a patient with lvPPA, a classical temporoparietal pattern in a patient with memory-predominant AD, and mainly occipitotemporal and occipitoparietal involvement in a PCA patient. [¹⁸F]AV1451 and [¹⁸F]FDG appeared strikingly as mirror images, with regions of high [¹⁸F]AV1451 uptake corresponding to low [¹⁸F]FDG uptake and vice versa, while [¹¹C]PIB binding was observed throughout the association neocortex. Voxelwise contrasts with [¹⁸F]AV1451 and [¹⁸F]FDG showed that PCA patients significantly differed from controls in clinically affected posterior brain regions, while [¹¹C]PIB binding was greater in both posterior regions and in clinically less affected anterior regions (Figure 2).

Conclusions: [¹⁸F]AV1451 was specifically retained in brain regions closely related to the clinical presentation across distinct AD variants and overlapped substantially with hypometabolic regions in PCA, while [¹¹C]PIB binding was more diffuse and showed less overlap with [¹⁸F]FDG uptake. This provides preliminary in-vivo evidence that hypometabolism and symptomatology are more closely linked to tau than to Aβ pathology.

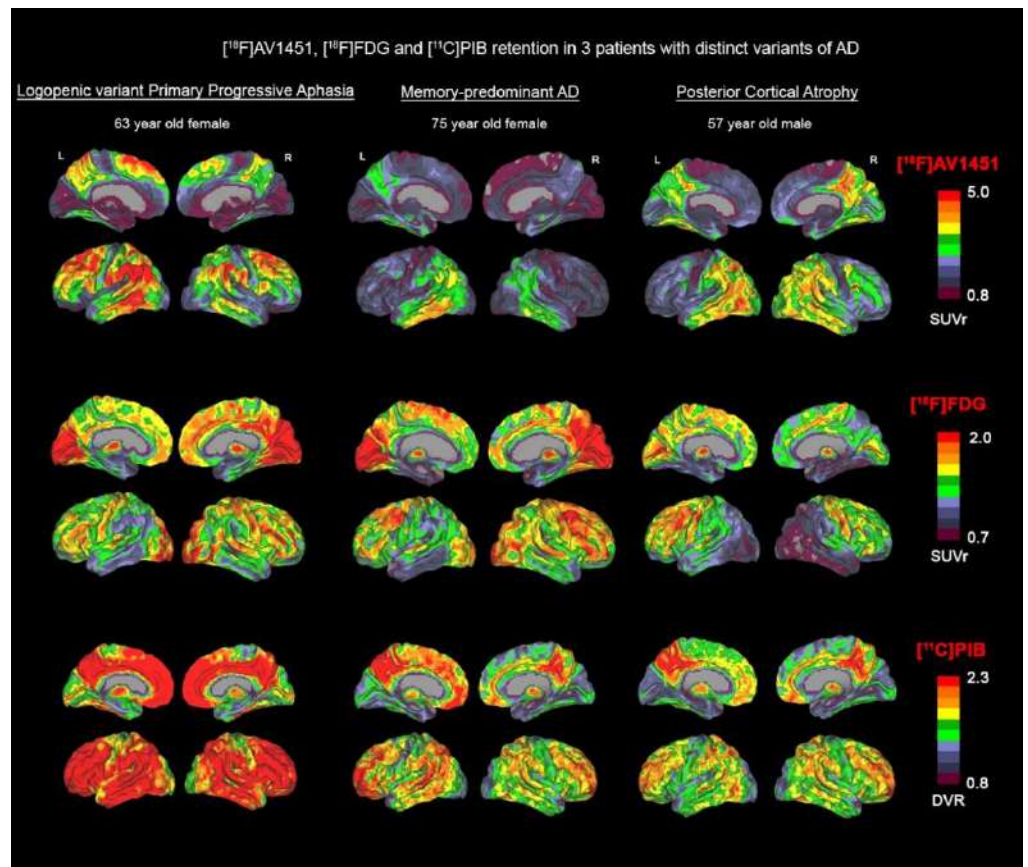
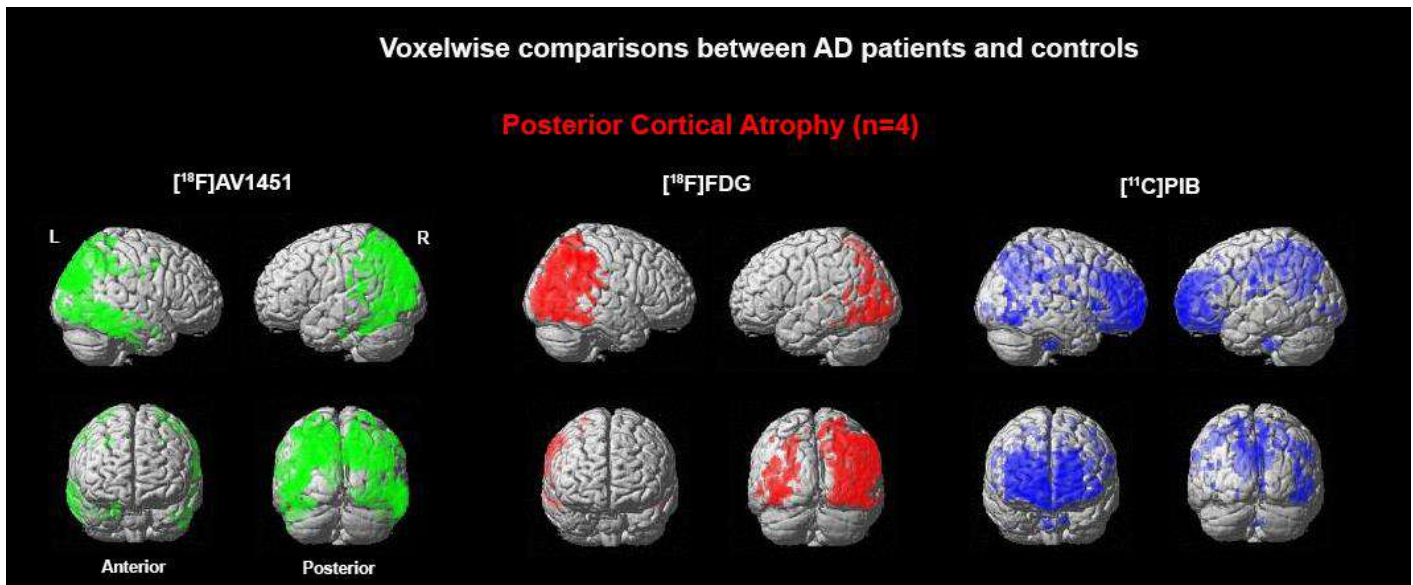


Figure 1. Demographics and regional PET uptake

	PCA	lvPPA	EOAD	LOAD	Controls
N	4	1	1	1	14
Age	61	63	59	73	79
Sex (m/f)	1/3	0/1	0/1	0/1	5/9
MMSE	23	-	27	20	29
[¹⁸F]AV1451 SUVR					
Occipital	2.22	1.67	1.71	1.62	1.07
Parietal	2.54	3.36	2.31	2.15	1.11
Temporal	2.13	3.13	1.81	2.28	1.15
Frontal	1.65	2.77	1.45	1.31	1.10
[¹¹C]PIB DVR					
Occipital	1.49	1.65	1.40	1.35	1.07
Parietal	1.80	2.17	1.81	1.88	1.17
Temporal	1.61	2.02	1.64	1.62	1.05
Frontal	1.79	2.28	1.79	1.85	1.11
[¹⁸F]FDG SUVR					
Occipital	1.31	1.89	1.77	1.78	1.59
Parietal	1.18	1.43	1.37	1.45	1.54
Temporal	1.13	1.25	1.27	1.21	1.35
Frontal	1.43	1.53	1.62	1.54	1.50



Keywords: AV1451, PIB, FDG, PET, Tau

P55 Presented by: Ossenkoppele, Rik

Submission ID: 113

P57

Task-fMRI Hyperactivity Predicts Cognitive Decline over Four Years in Cognitively-normal Older Adults with or without Amyloid Burden

Judy Pa¹, Jacob Vogel², William Jagust^{2, 3}

¹ Institute for Neuroimaging and Informatics, Department of Neurology, University of Southern California, Los Angeles, CA, United States

² Helen Wills Neuroscience Institute, University of California, Berkeley, CA, United States

³ Life Sciences Division, Lawrence Berkeley National Laboratory, Berkeley, CA, United States

Background: Elevated fMRI activity is often reported in older adults and may serve as a compensatory mechanism for age-related changes in neural processing. However, it is unclear if individuals with fMRI hyperactivity are at greater risk for future cognitive decline and how this risk is impacted by beta-amyloid (Ab) accumulation. The objective of this study was to evaluate the relationship between baseline fMRI hyperactivity and change in cognitive function.

Methods: 37 cognitively-normal older adults (mean age: 77 years, 23 women) were recruited to complete an fMRI scene encoding task and a PiB-PET scan and were tested annually on a comprehensive cognitive battery. Whole brain fMRI activation maps were created using a hits>misses contrast map. Using factor analysis of a comprehensive cognitive battery, composite scores were identified for global cognition and three sub-domains: working memory, processing speed, and episodic memory. Slopes of change over time were computed using annual cognitive scores in a mixed model analysis that was adjusted for baseline performance.

Results: All participants showed significant decline in global cognition and the three cognitive sub-domains over time relative to zero (all $p < .005$). Linear regression analysis of baseline fMRI hyperactivity in task-active memory encoding regions significantly predicted longitudinal cognitive decline in working memory ($p = .006$), which did not differ based on amyloid status. When stratified by amyloid status, higher baseline Ab load significantly predicted longitudinal cognitive decline in global cognition, processing speed, and episodic memory in amyloid-positive individuals (all $p < .05$).

Conclusions: Our findings suggest that while fMRI hyperactivity may serve as a compensatory mechanism at the time of testing, it is an indicator of subsequent cognitive decline in working memory function in cognitively older adults with or without amyloid burden. In older adults who already show amyloid positivity, relative Ab load is an indicator of subsequent decline in global cognition, processing speed, and episodic memory.

Keywords: *fMRI, PET, aging, amyloid, memory*

P57 Presented by: Pa, Judy

Submission ID: 65

P59**Patterns of Amyloid Plaque Deposition on AV-45 Positron Emission Tomography/Computed Tomography (PET/CT) Scans****Scans**

Amy McCann, David Creed, Jeff Burns, Eric Vidoni, Paul Welch, Mark Perry

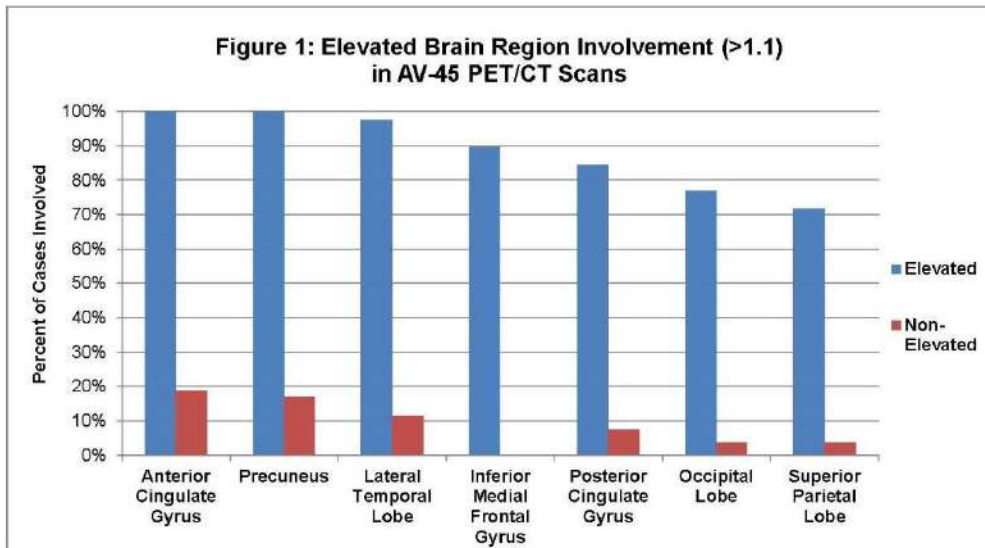
University of Kansas Medical Center, Kansas City, Kansas, United States

Background: Distribution of beta-amyloid plaque in the brain is an important clinical question in Alzheimer's disease (AD). Most previous plaque research is based on autopsy studies and FDG brain metabolism scans, with little known about plaque distribution using a newer imaging agent, AV-45. Therefore, this study's objective was to identify typical patterns of plaque deposition on AV-45 PET/CT scans to help improve diagnostic accuracy of AD.

Methods: A retrospective analysis was performed on 92 subjects who underwent AV-45 PET/CT scans from 2008-2014 as part of 1) clinical work-up for suspected AD, or 2) participation in our institution's AD Prevention Program. Scans were interpreted as "elevated" or "non-elevated" through visual and quantitative assessment of AV-45 activity in multiple brain regions by three independent readers using MIMneuro software. Brain regions with an SUVr greater than 1.1, compared to the cerebellum, were considered to be elevated.

Results: Thirty-nine scans (42%) were classified as elevated, with 98% agreement among readers. Activity was strongest in the anterior cingulate gyrus (100%), precuneus (100%), lateral temporal lobe (97.4%), inferomedial frontal gyrus (89.7%), posterior cingulate gyrus (84.6%), and occipital lobe (76.9%). The sensory motor cortex was spared in 97.4% cases. In non-elevated cases (n=53, 58%), elevated activity was quantitatively apparent in the anterior cingulate gyrus (18.9%), precuneus (17.0%), and lateral temporal lobe (11.3%), with sparing of the inferomedial frontal gyrus and sensory motor cortex (Figure 1).

Conclusions: The anterior cingulate gyrus, precuneus, lateral temporal lobe, inferomedial frontal gyrus, and posterior cingulate gyrus were involved in nearly all elevated cases. Although usually spared on FDG metabolism scans, the occipital lobe was involved in three-quarters of elevated cases, while the sensory motor cortex was spared in nearly all elevated cases, similar to FDG metabolism scans. Additional research is necessary to determine if these patterns remain constant over time.



P59 Presented by: Perry, Mark

Submission ID: 109

Comparison of CSF and [18F]Florbetapir Amyloid Measures for Predicting Memory Decline

Shannon Risacher¹, William Jagust³, Leslie Shaw⁴, John Trojanowski⁴, Paul Crane⁵, Paul Aisen⁶, Ronald Petersen⁷, Michael Weiner⁸, Andrew Saykin²

¹ Department of Radiology and Imaging Sciences, Indiana Alzheimer Disease Center, Indiana University School of Medicine, Indianapolis, Indiana, United States

² Department of Radiology and Imaging Sciences, Indiana Alzheimer Disease Center, Department of Medical and Molecular Genetics, Indiana University School of Medicine, Indianapolis, Indiana, United States

³ Department of Neurology, University of California-Berkeley, Berkeley, California, United States

⁴ Department of Pathology and Laboratory Medicine, University of Pennsylvania School of Medicine, Philadelphia, Pennsylvania, United States

⁵ Department of Medicine, University of Washington, Seattle, Washington, United States

⁶ Department of Neurology, University of California-San Diego, San Diego, California, United States

⁷ Department of Neurology, Mayo Clinic, Rochester, Minnesota, United States

⁸ Departments of Radiology, Medicine and Psychiatry, University of California-San Francisco; Department of Veterans Affairs Medical Center, San Francisco, California, United States

Introduction: This study evaluated the relative sensitivity of CSF and [18F]Florbetapir PET measures of amyloid for predicting one-year (1yr) and two-year (2yr) change in memory in healthy older adults (HC) and patients with early and late mild cognitive impairment (EMCI; LMCI) from ADNI.

Methods: 503 participants (106 HC, 254 EMCI, 143 LMCI) with CSF A β 1-42, [18F]Florbetapir PET, and longitudinal memory assessments were included. [18F]Florbetapir, CSF A β 1-42, clinical, demographic, and neuropsychological data were downloaded from the LONI database (adni.loni.usc.edu). [18F]Florbetapir PET scans were processed using standard techniques and intensity-normalized to the whole cerebellum to create standardized uptake value ratio (SUVR) images. Mean cortical [18F]Florbetapir SUVR was then extracted from a cortical ROI. Both the [18F]Florbetapir SUVR and CSF A β 1-42 measures were adjusted for age and gender and transformed into z-scores (higher z-score = more pathology). 1yr and 2yr memory decline was the slope of change in a composite memory score over the time period. The relationship between CSF and PET z-scores and 1yr and 2yr memory change was evaluated using linear regressions within each diagnostic group.

Results: 2yr decline in memory in HC was associated with baseline CSF A β 1-42 level ($p < 0.001$) but not cortical [18F]Florbetapir SUVR ($n = 106$; Figure 1). In EMCI, 1yr memory decline was significantly associated with both CSF ($p = 0.006$) and PET ($p = 0.036$) amyloid measures ($n = 254$; Figure 2A&B), while 2yr memory decline was only associated with cortical [18F]Florbetapir SUVR ($n = 172$; Figure 2C&D; $p = 0.048$). Finally, 1yr ($n = 143$) and 2yr ($n = 70$) memory decline were associated with both CSF (1yr: $p = 0.007$; 2yr: $p < 0.001$) and PET measures (1yr: $p = 0.003$; 2yr: $p < 0.001$) in LMCI (Figure 3).

Discussion: CSF and [18F]Florbetapir PET measures of amyloid may have different sensitivities for predicting future memory decline depending on clinical stage, suggesting that combining multiple types of amyloid measures may provide the best prediction of future decline.

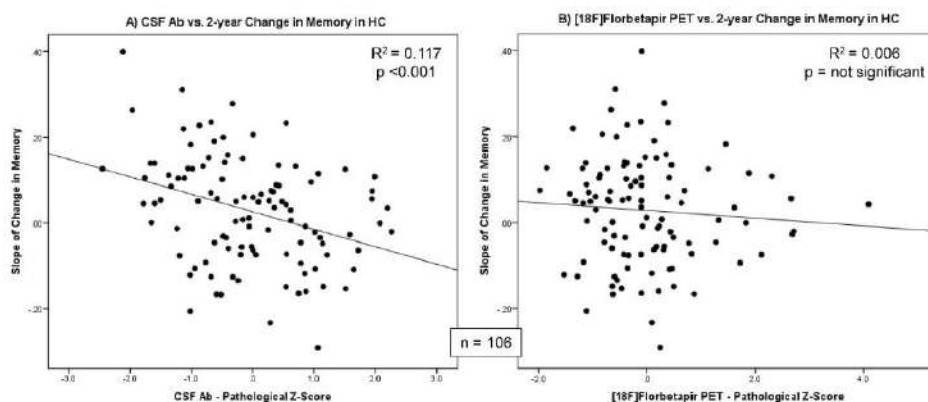


Fig 1

Fig 2

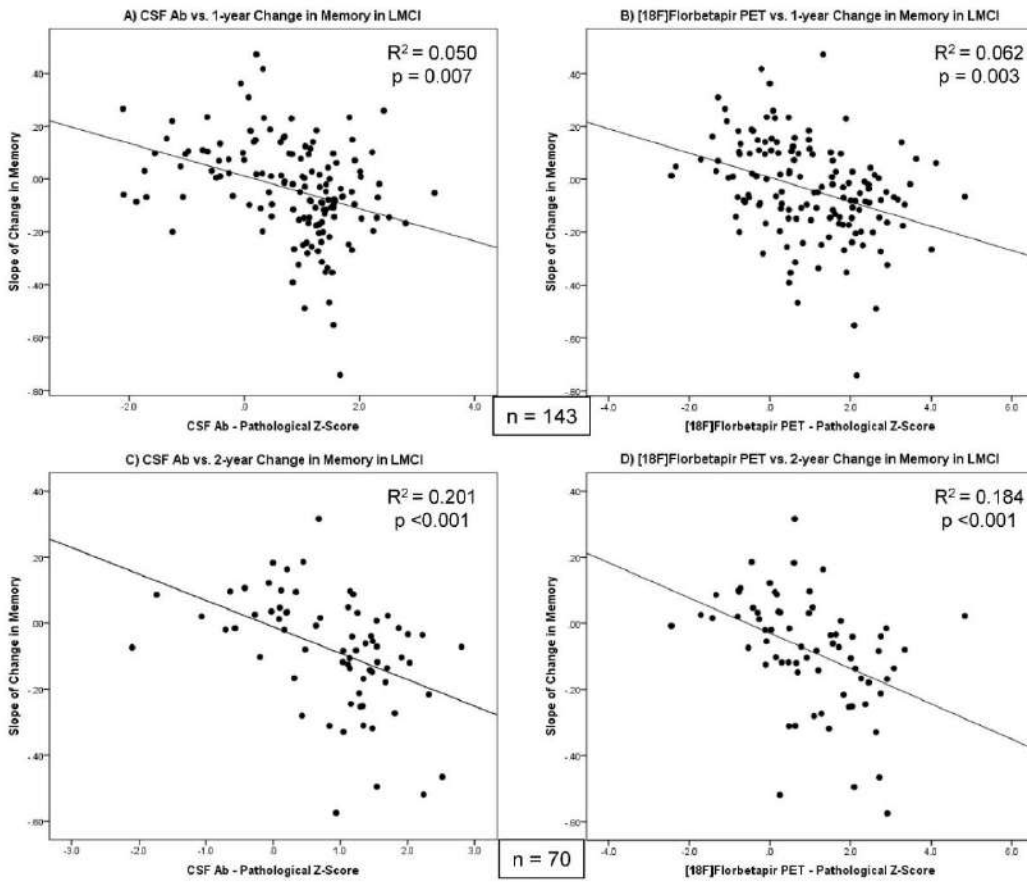
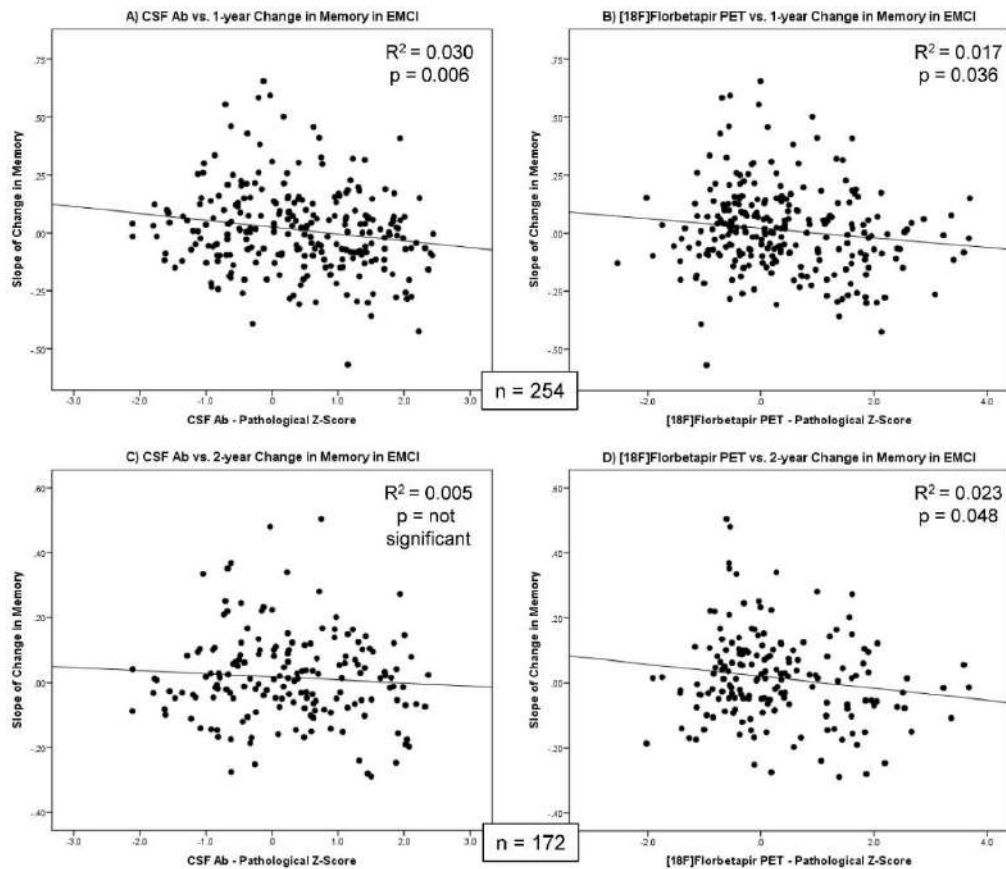


Fig 3

Keywords: [18F]Florbetapir, cerebrospinal fluid (CSF), Alzheimer's Disease Neuroimaging Initiative (ADNI), mild cognitive impairment (MCI), memory



**P61 Presented
by: Risacher, Shannon
L**

Submission ID: 83

P63

Improved Longitudinal [18F]-AV45 Amyloid PET by White Matter Reference and VOI-based Partial Volume Effect

Correction

Axel Rominger¹, Matthias Brendel¹, Marcus Hoegenauer¹, Andreas Delker¹, Julia Sauerbeck¹, Peter Bartenstein¹, John Seibyl²

¹ Dept. of Nuclear Medicine, University of Munich, Munich, N/A, Germany

² Institute for Neurodegenerative Disorders, New Haven, CT, United States

The majority of amyloid PET studies have used cerebellum as a reference region, and clinical studies have not accounted for atrophy-based partial volume effects (PVE). Longitudinal studies using cerebellum as reference tissue have revealed only small mean increases and high inter-subject variability in amyloid binding. We aimed to test the effects of different reference regions and PVE-correction (PVEC) on the discriminatory power and longitudinal performance of amyloid PET.

We analysed [18F]AV45 PET and MRI data of 962 subjects at baseline and 2y follow-up of 258 subjects. Cortical composite VOI values (COMP) for tracer uptake were generated using either full brain atlas VOIs, grey matter segmented VOIs or grey matter segmented VOIs after VOI-based PVEC. SUVR were calculated by scaling the COMP values to uptake in cerebellum, brainstem or white matter. Mean SUV, SUVR, and changes after PVEC were compared at baseline between diagnostic groups of healthy controls (HC; N=316), mild cognitive impairment (MCI; N=483) and AD (N=163). Receiver operating characteristics were calculated for the discriminations between HC, MCI and AD, and expressed as area under the curve (AUC). Finally, longitudinal [18F]AV45-PET data were used to analyze the impact of quantitation procedures on apparent changes in amyloid load over time.

Reference region SUV was most constant between diagnosis groups for the white matter. PVEC led to decreases of COMP-SUV in HC (-18%) and MCI (-10%), but increases in AD (+7%). Highest AUCs were found when using PVEC with white matter scaling for the contrast between HC/AD (0.907) or with brainstem scaling for the contrast between HC/MCI (0.658). Longitudinal increases were greatest in all diagnosis groups with application of PVEC, and inter-subject variability was lowest for the white matter reference.

Thus, discriminatory power of [18F]AV45-PET was improved by use of a VOI-based PVEC and white matter or brainstem rather than cerebellum reference region. Detection of longitudinal amyloid increases was optimized with PVEC and white matter reference tissue.

Keywords: [18F]-AV45-PET; Alzheimer's disease; reference region; partial volume effect correction

P63 Presented by: Rominger, Axel

Submission ID: 105

P65

Relationship between longitudinal amyloid accumulation and T807-TAU

Aaron Schultz^{1,4}, Jasmeer Chhatwal^{1,4}, Elizabeth Mormino^{1,4}, Molly LaPoint^{1,4}, Alex Dagley^{1,4}, Reisa Sperling^{3,4}, Keith Johnson^{2,4}

¹ MGH - Neurology, Boston, MA, United States

² MGH - Radiology, Boston, MA, United States

³ BWH - Center for Alzheimer Research and Treatment, Department of Neurology, Boston, MA, United States

⁴ Athinoula A. Martinos Center for Biomedical Imaging, Boston, MA, United States

Background: 18F-T807 is a new radioligand for in vivo imaging of tau pathology. We previously observed significant cross-sectional relationships between amyloid burden and T807 signal in inferior temporal regions; we now investigate the relationship between longitudinal rate of amyloid accumulation and inferior temporal T807 binding.

Methods: We examined 75 cognitively normal elderly with retrospective longitudinal PiB-PET imaging relative to cross-sectional T807-PET imaging from the Harvard Aging Brain Study (HABS – P01AG036694; Age=76.1±6.1; Baseline CDR=0; e4+/e4- 19/56). Longitudinal PiB measurements were made over a period of 3.2±1.2 years with 2.5±.7 PiB-PET visits per subject. Amyloid measurements were made as DVRs across a distributed cortical region using a cerebellar grey reference region. Tau measurements were made with T807-PET computed as SUVRs with a cerebellar grey reference. Both PiB and T807 utilized structural ROIs as defined by Freesurfer.

Results: The results show a significant relationship between baseline amyloid burden and inferior temporal T807 ($t(70) = 4.38$; $p < 0.001$), and a significant relationship with rate of accumulation ($t(70) = 2.36$; $p = 0.021$). When both baseline amyloid burden and rate of accumulation were included in the model, baseline amyloid burden remained significant ($p < 0.001$) whereas rate of accumulation did not ($p = 0.94$). All models included age at T807 scan, sex, and the time between the latest PiB scan and T807-PET imaging.

Conclusion: We observed a significant association between baseline amyloid burden and inferior temporal T807 binding, as well as an association between with T807-binding and the rate of amyloid accumulation, though the rate effect did not survive when controlling for baseline amyloid. As the inferior temporal cortex is among the earliest sites of neocortical tau pathology, these results are consistent with the hypothesis that amyloid pathology influences the spread of tau pathology into neocortex. Further follow-up and a larger sample size is needed to verify these preliminary results.

Keywords: Longitudinal, Amyloid, PIB, T807, TAU

P65 Presented by: Schultz, Aaron P

Submission ID: 101

P67

Comparison of White Matter and Cerebellar Reference Tissue in Estimating Change in Amyloid SUVR in SUMMIT and ACCTION

John Seibyl¹, Olivier Barret¹, Nzeera Ketter², Gerald Novak², H Brashear², Enchi Liu², Jianing Di², Kenneth Marek¹

¹ Molecular NeuroImaging, LLC, New Haven, CT, United States

² Janssen Research and Development, San Diego, CA, United States

Objectives: Multicenter clinical treatment trials in Alzheimer disease (AD) commonly employ PET amyloid imaging for determining participant eligibility as well as use as a biomarker assessing longitudinal changes of brain amyloid burden. There has been intense interest in optimizing quantitative methodology to improve the reliability of serial longitudinal assessments. We assessed the impact of different reference regions employed in calculating standard uptake value ratios (SUVR) measured serially in two Phase 2 AD immunotherapy studies - ACCTION and SUMMIT.

Methods: F18 Florbetapir PET scans were obtained at screening, weeks 50, 78, 104, or at the end of treatment/placebo or after early termination. A standardized volume of interest template was applied for calculation of the composite SUVR using four different reference regions; cerebellar grey, whole cerebellum, pons and subcortical white matter. Percent change from baseline was calculated for each subject (ACCTION n=115, SUMMIT n=130).

Results: For the ACCTION trial, combining treatment groups, baseline to one year follow-up demonstrated average % SUVR changes of -1.37 +/- 9.1%, -1.65 +/- 5.9%, -0.97 +/- 4.0%, and 0.40 +/- 3.9%, for SUVR reference regions of cerebellar grey, whole cerebellum, pons, and subcortical white matter, respectively. For the SUMMIT trial, also combining treatment cohorts, baseline to one year follow-up showed average percent SUVR change of 0.35 +/- 8.8%, -0.66 +/-5.9%, -0.43 +/- 5.8%. and 0.65 +/-4.6%, for cerebellar grey, whole cerebellum, pons, and subcortical white matter reference regions, respectively.

Conclusions: Subtle changes in brain amyloid burden require precision in quantitative methodologies. For both the Phase 2 studies presented, using the subcortical white matter as the reference region reduced the standard deviation by approximately 50% when compared to using the cerebellar grey matter as the reference region. This reduced variance may allow a better demonstration of small changes in brain amyloid in participants undergoing amyloid-reducing treatment.

Keywords: amyloid therapy, PET, SUVR

P67 Presented by: Seibyl, John

Submission ID: 111

Regional Correlations Between PiB-PET and Post-Mortem Burden of Amyloid Species

Sang Won Seo^{1,2,3,4}, Nagehan Ayakta^{1,2,3}, Manja Lehmann¹, Bruce Miller¹, Lea Grinberg¹, William Seeley¹, William Jagust^{1,2,3}, Gil Rabinovici^{1,2,3}

¹ Memory and Aging Center, Department of Neurology, University of California, San Francisco, CA, United States

² Helen Wills Neuroscience Institute, University of California, Berkeley, Berkeley, CA, United States

³ Lawrence Berkeley National Laboratory, Berkeley, CA, United States

⁴ Departments of Neurology, Samsung Medical Center, Sungkyunkwan University School of Medicine, Seoul, Seoul, Korea, Republic of (South)

Background: We investigated the region specific correlation between in vivo [11C]PiB retention and the postmortem burden of neuritic plaques (NP), diffuse plaques (DP) and cerebral amyloid angiopathy (CAA).

Methods: 30 subjects with PiB-PET during life and postmortem neuropathologic examination (28 with dementia and 2 with MCI, mean age at PET=66.6±8.5, interval from PET to autopsy 3.3±1.9 years) were assessed. PiB SUVR (gray cerebellum reference) and post-mortem A β burden were analyzed in five cortical ROIs: anterior cingulate, middle frontal, inferior temporal, angular and calcarine. PiB SUVRs were extracted in template space using customized ROIs matching regions sampled at autopsy. NP were quantified using CERAD, and DP/CAA and were classified by the pathologist as: none to sparse and moderate to frequent. PET to autopsy correlations were examined using multi-linear regression.

Results: The overall prevalence of pathology was 62.0% none-sparse/38.0% moderate-frequent for NP, 53.3%/46.7% for DP and 84.7%/15.3% for CAA. When examined separately (adjusting for PET-autopsy interval), moderate to severe NP ($\beta=0.426\sim0.856$, $p<0.05$) and DP ($\beta=0.278\sim0.931$, $p<0.05$) each correlated with PiB SUVR in all regions, while moderate to severe CAA predicted high PiB SUVR in the anterior cingulate and calcarine regions ($\beta=0.437/0.325$, $p=0.007/0.012$). When NP and DP or CAA were included in the same model, moderate to severe NP correlated with PiB SUVR in all regions ($\beta=0.409\sim0.853$, $p<0.05$), whereas DP in the anterior cingulate ($\beta=0.578$, $p=0.021$) independently correlated with PiB SUVR after controlling for NP. The significance of CAA disappeared after controlling for NP. Tests for trends across dose dependent amyloid burdens (none, sparse, moderate and frequent) showed that increased NP burdens in all regions and DP in the anterior cingulate and angular regions associated with high PiB SUVR.

Conclusion: In a dementia clinic population, regional PiB signal was dominated by NP, though DP contributed to signal in some regions.

Keywords: PiB, neuritic plaques, pathology

P69 Presented by: Seo, Sang Won

Submission ID: 45

P71**Weighted Two-point Correlation Functions for Longitudinal Amyloid-beta PET Analysis**Sepideh Shokouhi¹, Hakmook Kang², Baxter Rogers¹, Daniel Claassen³, William Riddle¹¹ Vanderbilt University, Department of Radiology, Nashville, TN, United States² Vanderbilt University, Department of Biostatistics, Nashville, TN, United States³ Vanderbilt University, Department of Neurology, Nashville, TN, United States

Statistical descriptors such as the two-point correlation function (S2) have found wide applications in astronomy and materials science. S2 measures the stochastic relationship between image voxel values as a function of distance between voxels, providing a detailed characterization of spatial patterns typically referred to as clustering or flocculence. The objective of this study was to translate this method into amyloid- β PET imaging in human brain using 11C-Pittsburgh compound B (11C-PiB) to detect and characterize longitudinal changes in the regional tracer distribution that may reflect changes in amyloid- β plaque accumulation. The conventional S2 metric produces correlation curves for each image voxel value, which are difficult to interpret if the image data contains a wide range of voxel values. In this study we formulate and evaluate a weighted two-point correlation function (wS2) as a new method to describe real-valued images with a single statistical function that is suited for PiB-PET implementation. We calculated the wS2 curves from PET images of different cortical regions of 20 subjects. The area under the wS2 curve and its slope were used to characterize the increase of clustered activity. We examined their association with regions size, injected dose and the more common quantitative metric, standardized uptake value ratio (SUVR). For all regions, the increase of the wS2 correlated with the SUVR increase but showed lower variance. We did not observe any confounding of wS2 measurements by region size or injected dose. The wS2 technique reduces the complexity of applying statistical descriptors to real-valued images, and it can detect subtle longitudinal changes in PiB-PET.

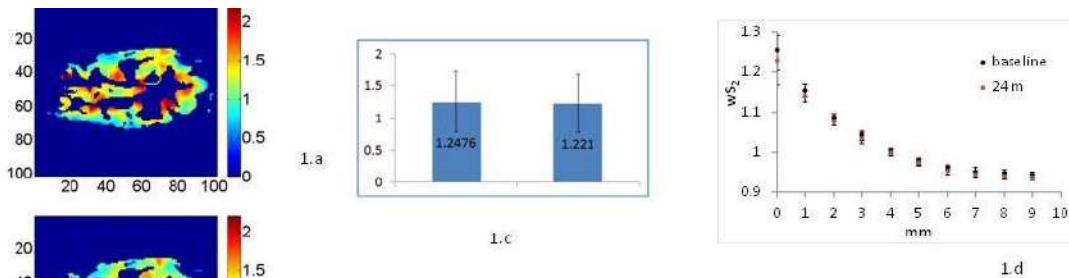


Figure 1: 11C-PIB image from the left temporal lobe at baseline (1.a) and follow-up (1.b) PET scan. Figure 1.c shows the calculated SUVR values of the images at baseline and follow-up and Figure 1.d shows their wS_2 curves

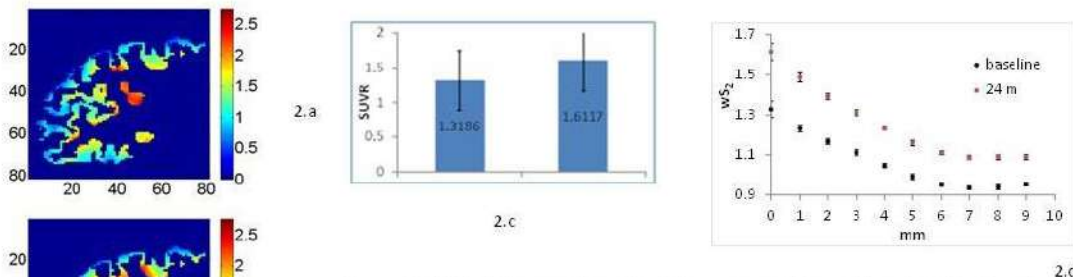


Figure 2: 11C-PIB image from the left temporal lobe at baseline (2.a) and follow-up (2.b) PET scan. Figure 2.c shows the calculated SUVR values of the images at baseline and follow-up and Figure 2.d shows their wS_2 curves.

Keywords: statistical descriptors, longitudinal amyloid beta-PET, two-point correlation functions

P71 Presented by: Shokouhi, Sepideh

Submission ID: 117

P73**Amyloid Deposition Is Not Associated with fMRI Activation during Digit Symbol Substitution Task in the Cognitively Normal Elderly**

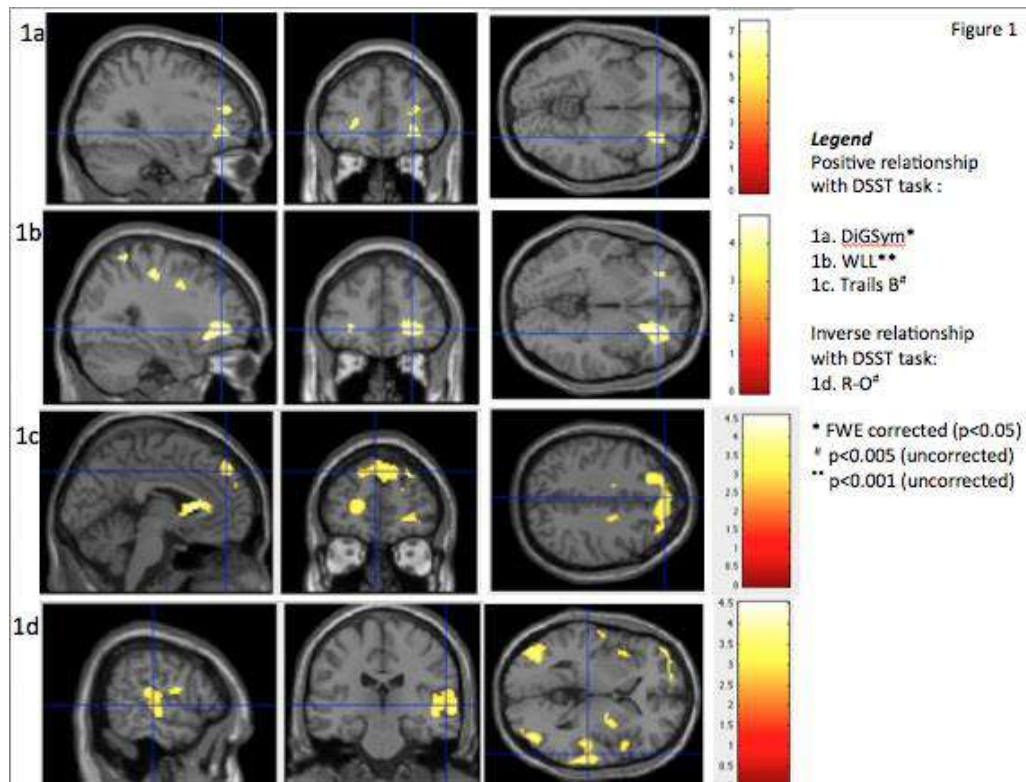
Dana Tudorascu, Beth Snitz, Helmet Karim, Robert Nebes, Ann Cohen, Julie Price, Chester Mathis, William Klunk, Howard Aizenstein

University of Pittsburgh, Pittsburgh, PA, United States

Introduction: Previous studies have shown that amyloid deposition is present in 20-30% of cognitively unimpaired older adults. However, questions remain about how amyloid burden relates to individual variation in cognition. We examined a sample of cognitively normal adults to investigate how cognition varies relative to task-related fMRI activity and amyloid burden. We address this question using an fMRI working memory task in our unimpaired elderly sample, who also underwent PiB PET imaging.

Methods: Data were from 31 subjects (mean age=75.61, sd=6.60), 19 PiB (-) (11f, 8m) and 12 PiB(+) (8f, 4m). Robust Regression using Weighted-Least-Squares SPM toolbox was used for first level analysis of fMRI Digit Symbol Substitution Task (DSST) data. Two sample t-tests were used to examine DSST activation between PiB(+) and PiB(-). Multiple regression models adjusted for PiB status were used to test associations between neuropsychological tests Trails B (mean=74.92 sec, sd=24.08), WAIS-R Digit Symbol (mean=54.38, sd=10.44), modified Rey-Osterrieth (R-O) figure delayed recall (mean=16.19, sd=3.33), CERAD Word List Learning (WLL) delayed recall (mean=9.13, sd=2.16) and DSST fMRI task activation.

Results: No significant differences were detected in task activation between PiB(+) and PiB (-) ($p < 0.005$ uncorrected). Positive associations were detected between task activation and i) Digit Symbol in middle frontal gyrus ($p < 0.05$, FWE corrected, Fig.1); ii) WLL in frontal lobe ($p < 0.001$, uncorrected, Fig.1); iii) Trails B in medial and lateral frontal regions ($p < 0.001$, uncorrected, Fig. 1). An inverse relationship was detected between DSST activation and R-O figure recall in medial temporal lobe ($p < 0.005$, uncorrected, Fig.1).



P73 Presented by: Tudorascu, Dana L

Submission ID: 33

P75

Using Neurostat and Statistical Stereotactic Surface Projection Maps to Compare Early Phase 18F-Florbetapir and FDG-PET Images

Angela Wang¹, Richard King², Satoshi Minoshima³, Norman Foster¹

¹ University of Utah, Center for Alzheimer's Care, Imaging and Research, Salt Lake City, UT, United States

² University of Utah, Alzheimer's Image Analysis Laboratory, Salt Lake City, UT, United States

³ University of Utah, Department of Clinical Radiology, Salt Lake City, UT, United States

Objective: To investigate whether cerebral blood flow rate obtained from early phase 18F-florbetapir (AV45) PET scans provide comparable information to metabolic measures of 18F-fluorodeoxyglucose (FDG) PET scans in Alzheimer's disease (AD) subjects.

Background: AV45 is typically used to image β -amyloid pathology in AD. The early phase florbetapir (eAV45) data reflect cerebral blood flow (CBF). It is also known that CBF is tightly coupled to the cerebral rate of glucose metabolism (CMRglu). Thus, eAV45 images might provide information similar to FDG images.

Methods: We processed FDG and concurrent eAV45 PET from 102 Alzheimer's Disease Neuroimaging Initiative (ADNI) subjects (22 normal, 36 significant memory concerns, 17 early mild cognitive impairment, 15 late mild cognitive impairment and 12 Alzheimer's disease). Images were spatially normalized to Talairach space with Neurostat. Uptake values, region of interest (ROI) values, and Z-scores were generated from stereotactic surface projections (SSP). We then calculated within-subject pixelwise and between-subject regional correlations for all subjects. Regional Z-scores and fractional spatial extent of abnormal pixels ($Z \geq 2$) in AD subjects were compared with Student's t-Tests. Logistic regression was performed to rank the optimal region predictors for distinguishing normals and ADs.

Results: There is high correlation in all subjects of within-subject pixel values and between-subject ROI values for eAV45 CBF and FDG CMRglu. Regional Z-scores and spatial extent of abnormalities for AD subjects are not statistically different for the two PET tracers. The top 2 predictors, in both PET modalities, for discriminating between AD and normal SSPs include the temporal and frontal lobes.

Conclusions: The high correlation and the similarity in the magnitude and spatial extent of abnormalities in the cortex indicate that eAV45 and FDG PET convey visually analogous information.

Keywords: *florbetapir, early, AV45, FDG, PET*

P75 Presented by: Wang, Angela Y

Submission ID: 85

P77

The Value of Amyloid Imaging in Differentiating Patients with Major Depressive Disorder vs Alzheimer's Disease with Depressive Symptoms

Guofan Xu, David Douglas, Murphy Greer, Andrew Quon

Stanford Hospital and Clinics, Stanford University, Palo Alto, CA, United States

Purpose: Many patients with depressive syndromes in late life present with cognitive impairment and often it is difficult to differentiate them from dementia patients who present with depression symptoms. The aim of this study was to evaluate brain amyloid burden in patients with major depression using Amyvid PET imaging in comparison with dementia subjects.

Methods: The study group comprised of 30 consecutive patients in our clinic who underwent clinical Amyvid PET scans, including 11 patients presenting with major depressive symptoms and 19 subjects with clinical diagnosis of AD or MCI. Clinical interpretations of the Amyloid imaging were provided by nuclear medicine physicians according to the Amyvid guideline. In addition, whole brain voxel-based comparisons were performed.

Results: Patients with confirmed diagnosis of major depression had significant less amyloid accumulation compared with those dementia patients. The percentage of positive amyloid scan is significantly lower among the depression group (3/11) compared with those dementia group (14/19). Those two positive Amyvid patients from the depression group eventually received diagnosis of AD in their follow-up clinical evaluations. The depression group has significantly less amyloid deposition in the posterior cingulate, bilateral parietal and frontal cortices ($p < 0.001$) than dementia subjects. Whole brain voxel-wise analysis revealed a significantly lower SUVR in depressed patients in the frontal, parietal, temporal and occipital areas ($p < 0.05$, FDRcorrected). There is no significant correlation between global amyloid burden and prior depression episodes, age at onset of depression, time since onset of first depression, or treatment of depression including ECT therapy.

Conclusion: Significant less amyloid burden is found in patients with late-life major depression relative to dementia subjects in specific brain regions, despite no differences in age, sex, education between the two groups. This finding suggests possible negative predictive value of Amyvid PET scan in differentiating patients with depressive syndrome and those dementia patients with presentation of depression symptoms.

Figure 1: Location of Amyloid deposition in the brain. Voxel-wise comparison showing positive Amyloid group (2 depression and 17 dementia patients) has significant more amyloid deposition in the posterior cingulate cortex, bilateral parietal, insula, and frontal cortices ($p < 0.05$, FDR corrected) than negative Amyloid group (9 depression and 2 MCI patients). Both of these two depression patients among positive Amyloid group were confirmed to have mixed Alzheimer's disease and depression on their follow-up clinical evaluation.

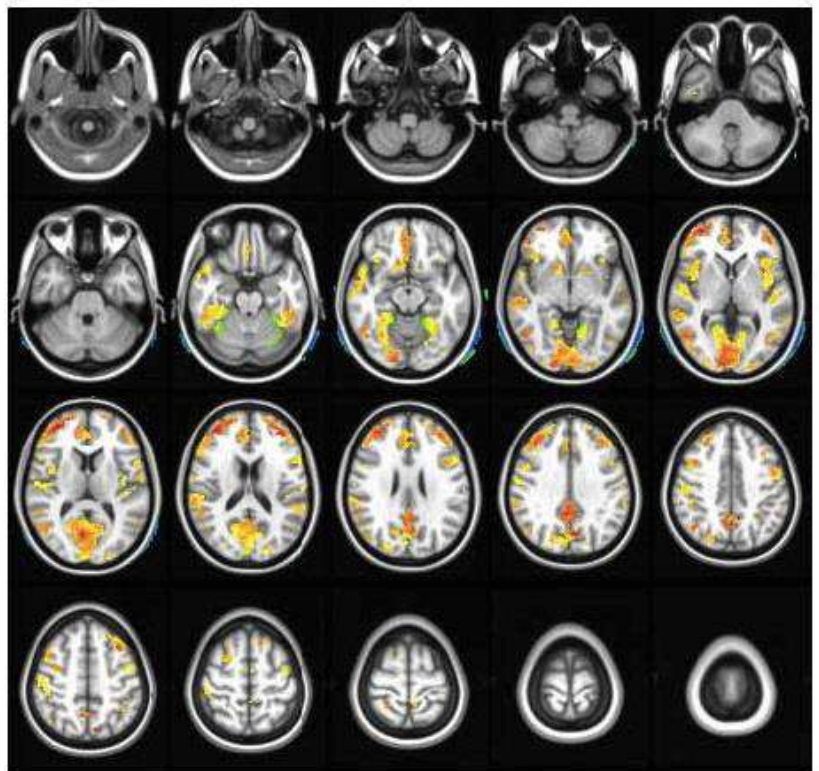
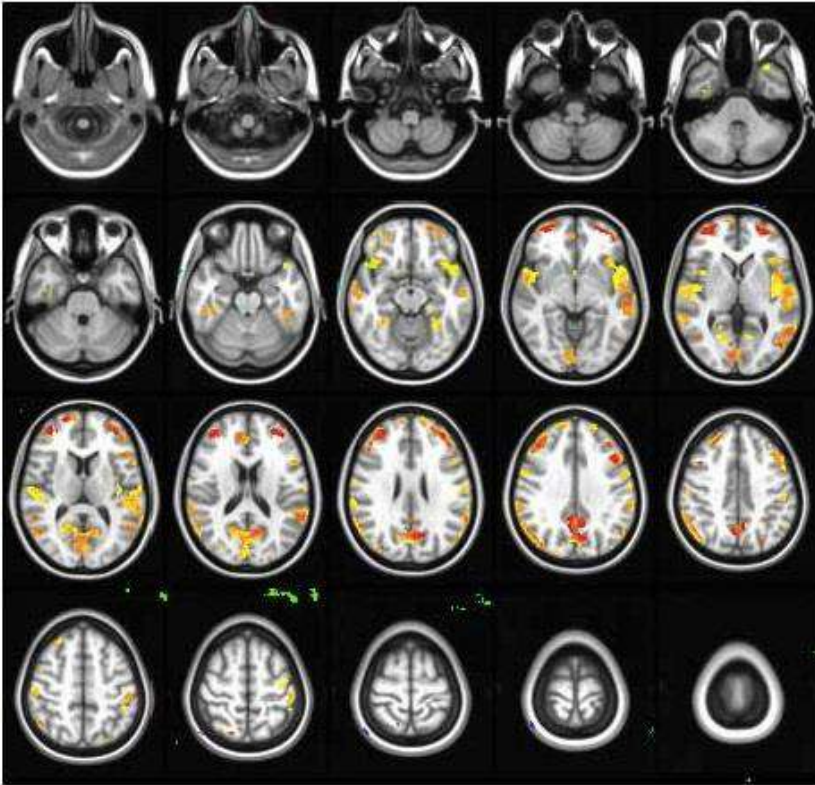


Figure 2: Depression group shows significant less brain amyloid burden compared to dementia patients. Voxel-wise comparison showing depression group (n=11) has significant less amyloid deposition in the posterior cingulate cortex, bilateral parietal, insula, and frontal cortices ($p < 0.05$, FDR corrected) than dementia subjects (n=19).



Keywords: *depression, AD, negative predict value*

P77 Presented by: Xu, Guofan

Submission ID: 23

P79

Longitudinal Change of Neuroimaging and Clinical Markers in Autosomal Dominant Alzheimer's Disease: Exploring Across-Group and Within-Individual Trajectories

Wai-Ying Wendy Yau¹, Eric McDade², Howard Aizenstein¹, Oscar Lopez², Chester Mathis³, Julie Price³, Beth Snitz², Lisa Weissfeld⁴, William Klunk^{1,2}

¹ Department of Psychiatry, University of Pittsburgh, Pittsburgh, PA, United States

² Department of Neurology, University of Pittsburgh, Pittsburgh, PA, United States

³ Department of Radiology, University of Pittsburgh, Pittsburgh, PA, United States

⁴ Statistics Collaborative, Inc., Washington, DC, United States

Background: The amyloid cascade hypothesis postulates that the aggregation and deposition of amyloid- β (A β) proteins in the brain is an initiating event in the pathogenesis of Alzheimer's disease (AD). Cross-sectional studies support the presence of a lengthy preclinical stage in AD pathogenesis, following a hypothesized sequence of brain amyloidosis, neurodegeneration, memory deficits and clinical impairment. However, this remains to be verified using longitudinal data.

Methods: Sixteen individuals carrying mutations for autosomal dominant AD (ADAD) were assessed longitudinally, with up to 8 assessments spanning up to 11 years. We measured brain amyloidosis (PiB PET), cerebral metabolism (FDG PET), hippocampal volume, delayed word recall and MMSE scores. Estimated years from onset (EYO) were calculated as the age of the individual at time of assessment minus parental age of onset. The overall trajectories for each biomarker were estimated and compared against cross-sectional data from 30 elderly controls (preclinical Stage-0). The within-individual progression of these markers was further examined in 7 individuals who had completed 7 or more assessments.

Results: We detected increase in cerebral A β deposition in ADAD from -5 EYO ($p < 0.05$), followed by decrease in cerebral metabolism (0 EYO), hippocampal volume and delayed word recall (+5 EYO), and MMSE scores (+7.5 EYO). Examination of within-individual trajectories revealed 3 typical phases of biomarker changes: 1) Early amyloidosis phase – increasing amyloidosis, no change in neurodegeneration markers or cognition; 2) Post-amyloid lag phase – plateaued amyloidosis, no change in neurodegeneration markers or cognition; 3) Late neurodegeneration phase – plateaued amyloidosis, progressive neurodegeneration and cognitive decline.

Conclusion: Our results support the amyloidosis – neurodegeneration – cognitive deficit sequence of AD pathogenesis, which appears to hold true even on the individual level. This knowledge is important for treatment trials targeting the preclinical stage, which require the use of biomarkers for participant selection and response monitoring in the absence of clinical symptoms.

P79 Presented by: Yau, Wai-Ying Wendy

Submission ID: 67

SESSION 4: Biomarkers (part 1)

Chairs: Clifford Jack, MD, *Mayo Clinic*
Victor Villemagne, PhD, *Austin Health*

In-vivo Staging of Preclinical Amyloid Deposition

Michel Grothe¹, Henryk Barthel², Osama Sabri², Stefan Teipel^{1,3}

¹ German Center for Neurodegenerative Diseases (DZNE) - Rostock, Rostock, N/A, Germany

² Department of Nuclear Medicine, University of Leipzig, Leipzig, N/A, Germany

³ Department of Psychosomatic Medicine, University of Rostock, Rostock, N/A, Germany

Neuropathological examinations suggest a distinct regional progression pattern of cortical amyloid deposition during Alzheimer's disease (AD) pathogenesis. Detection of early stages of cortical amyloid deposition by means of amyloid-sensitive PET has been hampered by the preclinical nature of these stages and the common practice of using thresholds based on global cortical signal for the detection of amyloid pathology.

We used multiregional analysis of partial volume-corrected AV45-PET data of 179 cognitively normal elderly individuals from the ADNI-2 cohort to determine nested stages of regional amyloid deposition from individual distribution profiles of amyloid pathology. Presence or absence of amyloid pathology was determined for each of 48 cortical regions based on supra-threshold region-to-whole cerebellum SUVR. In analogy to classical neuropathological studies, the frequency of regional amyloid-positivity across subjects was used to construct models of nested stages of amyloid deposition. Unbiased estimates of the consistency of this extrapolated staging scheme across individuals were assessed using a split-half training-test approach with 100 repetitions.

Frequency of amyloid-positivity was highest in temporobasal areas and the anterior cingulate cortex, intermediate in the remaining isocortical association areas and lowest in primary sensory-motor areas and the medial temporal allocortex. A model of nested stages was derived by grouping regions into four equally-spaced divisions from highest to lowest frequency (Figure 1). Only 3 subjects were found to deviate from this staging scheme (Figure 2). In unbiased training-test analyses, on average $51 \pm 8\%$ of the test subjects showed amyloid deposition in any of the 4 cortical divisions and in $92 \pm 5\%$ of these the deposition pattern was conform to the model of nested stages derived from the training data.

The nested stages of regional PET-evidenced amyloid pathology across cognitively normal subjects resemble previous neuropathological observations and suggest a largely consistent progression pattern of cortical amyloid deposition during the preclinical phase of AD.

Figure 1.

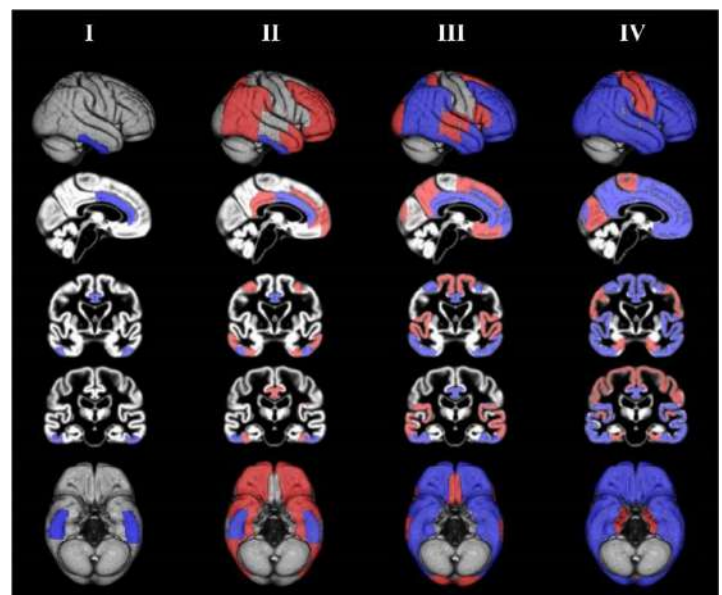
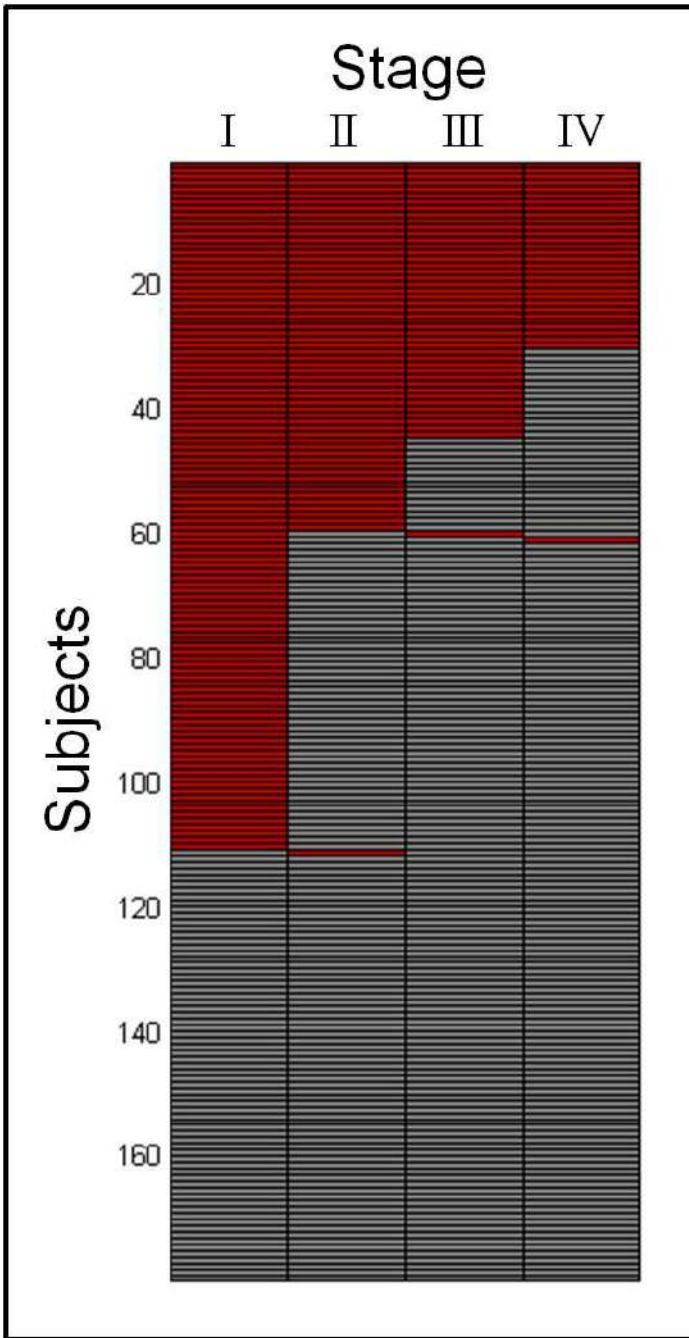


Figure 2.



Keywords: amyloid, regional progression pattern, florbetapir, AV45-PET, presymptomatic

Presented by: Grothe, Michel J.

Submission ID: 16

APOE ϵ 4 allele is Associated with an Earlier Onset of Amyloid Accumulation

Murat Bilgel^{1,2}, Yang An¹, Yun Zhou³, Dean Wong³, Jerry Prince^{2,3,4}, Susan Resnick¹

¹ *Laboratory of Behavioral Neuroscience, National Institute on Aging, NIH, Baltimore, MD, United States*

² *Department of Biomedical Engineering, Johns Hopkins University, Baltimore, MD, United States*

³ *Department of Radiology, Johns Hopkins Medical Institutions, Baltimore, MD, United States*

⁴ *Department of Electrical and Computer Engineering, Johns Hopkins University, Baltimore, MD, United States*

Background: Presence of the APOE ϵ 4 allele is associated with high amyloid levels, but how APOE ϵ 4 status affects the age of onset of amyloid accumulation has not been studied in longitudinal datasets.

Method: Using data for 104 participants with longitudinal Pittsburgh compound B (PiB) scans in the Baltimore Longitudinal Study of Aging (BLSA), we estimated the age at which each PiB+ individual began exhibiting increases in cortical PiB retention (as measured with DVR) using a nonlinear mixed effects model. We refer to this age as the PiB change point, which was modeled as a random effect.

We examined the effects of APOE ϵ 4 status on the PiB change point using Kaplan-Meier curves, the Cox model, and the accelerated failure time (AFT) model, adjusting for sex. The outcome in these analyses was the PiB change point for PiB+ individuals, and the age at last visit for PiB- individuals (censored).

Results: Kaplan-Meier curves were statistically different between the APOE ϵ 4 groups (log-rank test $p = 0.005$). The APOE ϵ 4+ group showed increased risk of reaching the PiB change point.

Cox model showed that ϵ 4+ individuals had a 3-fold risk of reaching the PiB change point compared to ϵ 4- individuals (hazard ratio = 2.88), and this effect was significant (chi-squared test $p = 0.002$).

The AFT model showed that ϵ 4+ individuals reach the PiB change point 15.6% (95% CI 6.1–25.1) earlier on average compared to ϵ 4- individuals (chi-squared test $p = 0.0013$). Using this in conjunction with the mixed effects model finding that the population-average PiB change point is 70.3, we approximated that the average APOE ϵ 4- PiB change point occurs at age 74.7 and the ϵ 4+ PiB change point at 63.1.

Conclusions: APOE ϵ 4 positivity is associated with a lower age of onset for amyloid accumulation in the BLSA.

This research was supported in part by the Intramural Research Program of NIH, National Institute on Aging.

Keywords: PiB change point, APOE

Presented by: Bilgel, Murat

Submission ID: 35

Longitudinal Assessment of A β Accumulation in Non-demented Individuals: a ¹⁸F-flutemetamol Study

Christopher Rowe¹, Vincent Doré², Pierrick Bourgeat³, Lennart Thurfjell⁴, Lance Macaulay⁵, Robert Williams⁷, Olivier Salvado³, David Ames⁶, Colin Masters⁷, Victor Villemagne^{1,7}

¹ Austin Health, Centre for PET, Melbourne, VIC, Australia

² Digital Productivity and Services Flagship, CSIRO, Melbourne, VIC, Australia

³ Digital Productivity and Services Flagship, CSIRO, Brisbane, VIC, Australia

⁴ MDx PET Biomarkers and Software, GE Healthcare, Uppsala, Uppsala, Sweden

⁵ Food and Nutrition Flagship, CSIRO, Melbourne, VIC, Australia

⁶ National Ageing Research Institute, Melbourne, VIC, Australia

⁷ The Florey Institute, The University of Melbourne, Melbourne, VIC, Australia

Objective: We investigated if longitudinal A β imaging with ¹⁸F-flutemetamol (Flute) PET can show change over time in A β burden as previously shown with ¹¹C-PiB in non-demented participants in the AIBL study .

Methods: Flute-PET was performed in 187 non-demented AIBL volunteers who had not previously had A β imaging, 50 with Mild Cognitive Impairment (MCI; 74.5 \pm 5.7 yo) and 137 healthy controls (HC; 74.5 \pm 5.6 yo). To date, a repeat scan at 18 months has been obtained in 76 participants. SUVR was calculated using the pons as reference region. Change was expressed as the yearly SUVR %change from baseline.

Results: At baseline, 54% of MCI and 23% of HC showed high Flute retention. At 18-month follow-up, increases in Flute SUVR were observed in 38/68 (56%) of HC and 6/7 (86%) of MCI. The increase for the whole cohort (accumulators & non-accumulators) was 1.8% (P=0.06). The prevalence of A β accumulators was similar in those HC who presented with either high or low A β burden at baseline (60% and 56%, respectively). The average change for A β accumulators was 2.6% per year, the same as we have reported for PiB accumulators. SUVR %change was the same for HC and MCI. Finally, despite presenting with an almost 40% greater prevalence of positive scans, the differences between HC accumulators with and without memory complaints were not significant.

Conclusions: With a relatively small sample size, there is a clear trend for an increase in Flute binding over time, similar to that observed with PiB in another AIBL cohort. Follow-up data collection continues.

Keywords: *Alzheimer's disease, A β , amyloid imaging, flutemetamol*

Presented by: Rowe, Christopher C

Submission ID: 11

SESSION 5: Technical

Chairs: Chester Mathis, PhD, *University of Pittsburgh*
Robert Koeppe, PhD, *University of Michigan*

Kinetics of AV-1451 Binding in Aging and Dementia

Suzanne Baker¹, Daniel Schonhaut³, Sameul Lockhart², Gil Rabinovici³, William Jagust^{1,2}

¹ Lawrence Berkeley National Lab, Berkeley, California, United States

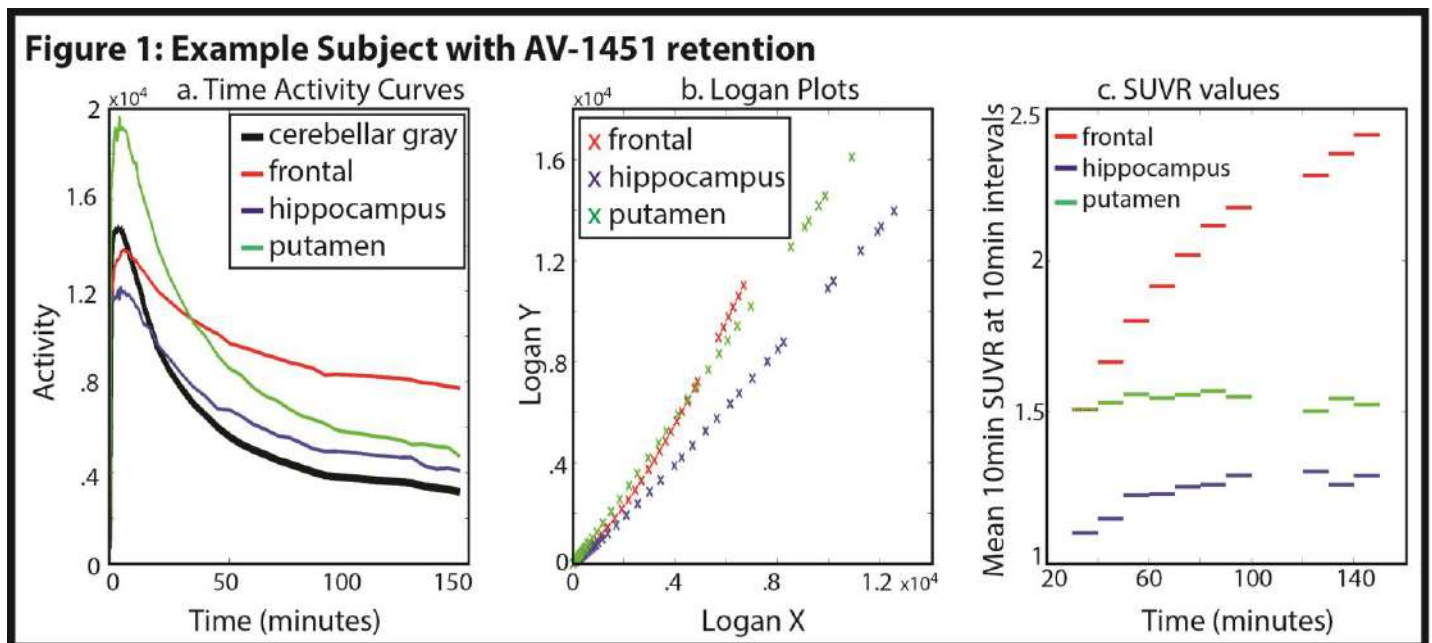
² Helen Wills Neuroscience Institute, UC Berkeley, Berkeley, California, United States

³ Memory and Aging Center, UCSF, San Francisco, California, United States

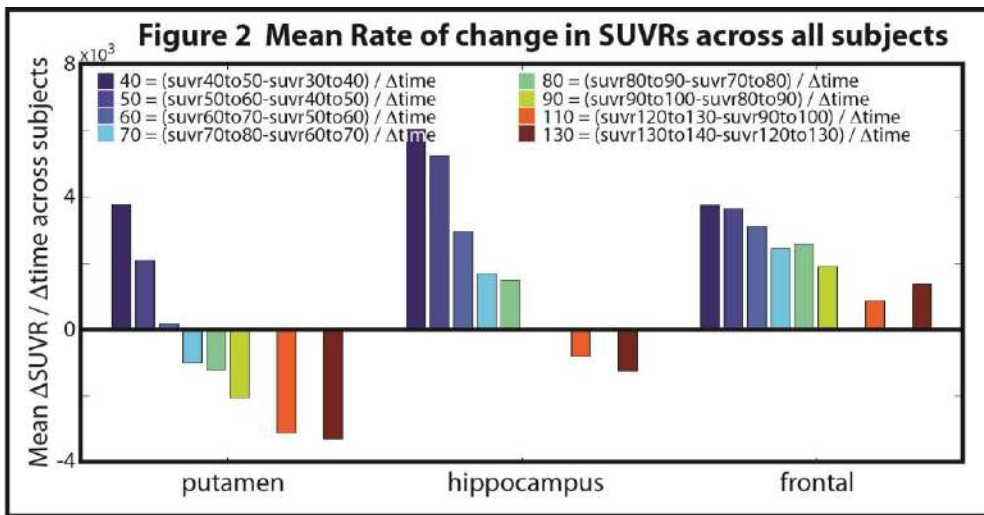
Aim: The objective of this study was to describe the dynamics of tau tracer [¹⁸F]AV-1451 (formerly [¹⁸F]T807) in different subjects.

Methods: AV-1451-PET was performed on 2 young controls, 15 older controls and 8 subjects with Alzheimer's Disease. Data were collected from 0-150 minutes post-injection, with a 20 minute break from 100-120 minutes. Time activity curves, Logan plots, and standardized uptake value ratios (SUVR, cerebellar gray reference) were analyzed to define the variability in tracer dynamics across regions and subjects.

Results: Figure 1 shows data from a subject with cortical tracer retention. Time activity curves (Figure 1a) and Logan plots (Figure 1b) are difficult to assess for steady state kinetics (rate of change in the target equals rate of change in the reference region). Figure 1c shows the change in SUVR at 10 minute intervals starting at 30 minutes, demonstrating that the frontal cortex continues to increase throughout the scan, whereas putamen and hippocampus appear to reach steady state (meaning the difference in SUVR values over time reaches zero within 150 minutes).



This change in SUVR value over time was calculated and averaged across all subjects and plotted in Figure 2. Steady state occurs when change in SUVR over time reaches zero (i.e., steady state is where the bar graphs cross 0). Three types of regions were found: 1. Early washout (ex. Putamen), where steady state occurs before 90 minutes; this pattern is found primarily in subcortical structures. 2. Late washout (ex. Hippocampus), where steady state occurs between 90-150 minutes, happens in medial temporal structures, 3. No steady state (ex. Frontal cortex), where steady state did not occur within 150 minutes post-injection, occurs primarily in cortical regions amongst individuals who retain tracer.



Conclusion: Different regions reach steady state at different times, which is partly driven by the amount of tau in that region.

Keywords: *Tau AV-1451 kinetics aging dementia*

Presented by: Baker, Suzanne L

Submission ID: 25

Are Low Levels of β -amyloid Deposition Clinically Significant?

Sylvia Villeneuve^{1,2}, Helaine St. Amant¹, Jacob Vogel¹, Shawn Marks¹, Miranka Wirth^{1,3}, William Jagust¹

¹ Helen Wills Neuroscience Institute, University of California, Berkeley, Berkeley, CA, United States

² Feinberg School of Medicine, Northwestern University, Chicago, IL, United States

³ Charité - Universitätsmedizin, Berlin, Berlin, Germany

Background: In a previous study¹ we suggested that the current SUVR thresholds of ~1.4-1.5 are too high to capture early amyloid accumulation. We showed evidence that by the time a person reaches these thresholds, amyloid is already widespread throughout the cortex and suggested an SUVR value of 1.21 as an optimal cutoff to detect early PIB-PET signal using whole-brain [11C]PIB retention. The goal of this study was to characterize individuals with intermediate levels of amyloid on a variety of demographic, cognitive and brain markers (Table 1).

Methods: This study included 242 subjects (183 normal older adults and 59 adults with mild cognitive impairment). Group comparisons between PIB- (SUVRs < 1.21), PIBi (SUVRs \leq 1.21 and >1.5) and PIB+ (SUVRs \geq 1.5) were first restricted to cognitively normal individuals and then repeated in the total sample.

Results: In normal older adults, group differences were found for age, ApoE4 status and memory complaint. PIBi and PIB- individuals were younger than PIB+ individuals, and PIBi and PIB+ individuals had a higher frequency of ApoE4 carrier status than PIB-. PIBi individuals also presented more memory complaints than PIB- individuals. When the analyses were performed in the total sample, the same results were found. Additionally, PIB+ individuals showed lower cortical thickness in AD-regions² as well as lower global cognition (MMSE score) than PIBi and PIB-.

Conclusions: While PIBi individuals showed similar memory complaint and ApoE4 status to PIB+, they were comparable to PIB- on the other markers. Given the strong relationship between ApoE4 and amyloid, these results support the idea that subjects with SUVR values between 1.21 and 1.5 are early accumulators. They also stress the importance of assessing memory complaint since it might be one of the earliest indicators of the disease expression.

¹Villeneuve et al., AAIC 2014; ²Wirth et al., JAMA Neurol. 2013

Table 1: Variables of interest

Demographic Markers	Cognitive Markers	Brain Markers
• Age	• Mini-Mental State Examination (MMSE)	• Hippocampal Volume
• Gender	• ¹ Memory complaint	• FDG AD-regions
• Education	• ¹ Factor Scores (baseline and change data)	• Cortical Thickness AD-regions
• ApoE ϵ 4 status	○ Episodic Memory	
	○ Executive Function	

¹Data only available in 137 cognitively normal older adults.

Presented by: Villeneuve, Sylvia

Submission ID: 14

Distinct Biomarker Topographies Predict Alzheimer's Disease Onset at Different Stages

Mathew Brier¹, Beau Ances^{1,2,3}, Karl Friedrichsen², Russ Hornbeck², Yi Su², Randall Bateman^{1,3}, John Morris^{1,3}, Tammie Benzinger^{2,3}

¹ Department of Neurology, Washington University in St. Louis, St. Louis, MO, United States

² Department of Radiology, Washington University in St. Louis, St. Louis, MO, United States

³ Knight Alzheimer Disease Research Center, Washington University in St. Louis, St. Louis, MO, United States

Progression of Alzheimer's disease (AD) is marked by the accumulation of amyloid β , decreased glucose metabolism, and brain atrophy. Each of these biomarkers defines individual topographies and accumulates in distinct spatiotemporal patterns. Current models of AD that summarize changes in each of these measures into a single composite variable discard information relevant to disease progression.

This study investigates the power of biomarker topographies to better predict disease progression. We used subjects enrolled in the Dominantly Inherited Alzheimer's Network (DIAN) study who carried causative genetic mutations for AD. We used a Random Forest (RF) classifier to predict estimated years until symptom onset (EYO) using regional PiB and FDG values and regional brain volumes. We split subjects into two groups based on EYO: an early group with $EYO \leq -10$ years and a late group with $EYO > -10$ years.

We found that each classifier for each datatype was well able to predict EYO in a hold out cross-validation set. However, the early classifier failed to predict EYO in the late group and vice versa. Further investigation of this failure to generalize revealed that, for each biomarker, the predictive topography early in the disease was significantly distinct from the predictive topography late in the disease. Additionally, the predictive topographies varied dramatically across biomarkers. This suggests that pathologic processes in specific brain regions are more or less relevant to disease progression depending on disease stage. This argues against the use of a single summary variable to describe disease progression and suggests that specific topographies are more useful.

Presented by: Brier, Mathew R

Submission ID: 41

Variable Isocortical vs. Limbic Distributions of [18F]-AV-1451 Binding in Braak Stage V-VI Alzheimer's Disease Subjects

Adam Schwarz¹, Sergey Shcherbinin¹, Bradley Miller¹, James Dickson², Abhinay Joshi², Michael Navitsky², Michael Devous, Sr², Mark Mintun²

¹ Eli Lilly and Company, Indianapolis, IN, United States

² Avid Radiopharmaceuticals, Philadelphia, PA, United States

Objectives: Recent neuropathological investigations have revealed both typical and atypical (hippocampal sparing, limbic predominant) patterns of neurofibrillary tangle pathology in Alzheimer's Disease [1]. To begin to assess whether in vivo [18F]-AV-1451 PET images exhibit similar neuroanatomical variants, we examined SUVR profiles in isocortical and limbic brain regions of AD subjects using a similar framework to that proposed for neuropathology.

Methods: We analyzed 80-100 minute [18F]-AV-1451 PET images, expressed as SUVR (cerebellar crus reference region) from N=45 control, MCI and AD subjects. N=16 of these subjects (all MCI or AD) were estimated to be Braak V-VI by examining SUVR values in superior temporal, extrastriate and striate visual cortices with respect to thresholds determined from 'tau negative' subjects [2]. SUVR values in isocortical (superior temporal gyrus, angular gyrus (parietal), middle frontal gyrus) and limbic (hippocampus, amygdala) ROIs were examined. A simple adaptation of the classification algorithm proposed in ref. [1] (without distinguishing hippocampal subfields) was applied.

Results: Hippocampal SUVR ranged from 1.12 to 1.67, mean cortical SUVR ranged from 1.16 to 3.74 and the hippocampal/cortical SUVR ratio ranged from 0.43 to 1.22 in the 16 Braak V-VI subjects. 9/16 subjects had greater SUVR in cortical regions than hippocampus. The classification procedure identified 2/16 as hippocampal sparing and 1/16 as limbic predominant. Rank order of average amygdala SUVR (not used for classification) across the three subtypes was consistent with ref. [1], but the separation between subtypes was substantially lower.

Conclusions: In this very preliminary investigation, it appeared that differential SUVR patterns, similar to neuropathological observations, were observed. However, the relationship between neurofibrillary tangle counts and in vivo [18F]-AV-1451 binding remains to be established and further methodological investigation in larger samples is warranted.

[1] Murray ME et al. (2011) Lancet Neurology 10: 785-96. [2] Schwarz AJ et al. (2014) Proc CTAD.

Keywords: AV1451, tau, PET, neuropathology, Alzheimer's

Presented by: Schwarz, Adam J

Submission ID: 60

SESSION 6: Tau PET

Chairs: Keith Johnson, MD, *Massachusetts General Hospital*
William Jagust, MD, *University of California Berkeley*

First-in-Human PET Study of a Novel Tau Tracer [¹⁸F]THK-5351

Ryuichi Harada¹, Nobuyuki Okamura^{1,2}, Shozo Furumoto³, Tetsuro Tago³, Katsutoshi Furukawa⁴, Aiko Ishiki⁴, Ren Iwata³, Manabu Tashiro³, Kazuhiko Yanai^{2,3}, Hiroyuki Arai⁴, Yukitsuka Kudo¹

¹ Division of Neuro-imaging, Institute of Development, Aging and Cancer, Tohoku University, Sendai, N/A, Japan

² Department of Pharmacology, Tohoku University School of Medicine, Sendai, N/A, Japan

³ Cyclotron and Radioisotope Center, Tohoku University, Sendai, N/A, Japan

⁴ Department of Geriatrics and Gerontology, Institute of Development, Aging and Cancer, Tohoku University, Sendai, Japan, Sendai, N/A, Japan

Objectives: In our previous PET studies, [¹⁸F]THK-5105 and [¹⁸F]THK-5117 successfully visualized PHF-tau in the brain of AD patients. However, these tracers show non-specific binding in the white matter and brainstem that may interfere with visual interpretation of PET images. To reduce these non-specific tracer retention, we developed a novel tau PET tracer [¹⁸F]THK-5351. In this study, we evaluated the binding and pharmacokinetic properties of [¹⁸F]THK-5351 and its clinical usefulness as tau PET tracer.

Methods: Binding affinity, kinetics and specificity of [¹⁸F]THK-5351 was evaluated by in vitro binding assay and autoradiography of human brain samples. Twenty participants including 10 normal subjects and 10 Alzheimer's disease (AD) patients underwent [¹⁸F]THK-5351 PET scans at Tohoku University. Two AD patients additionally underwent [¹⁸F]THK-5117 PET scans for direct comparison of THK-5351 and THK-5117. Standardized uptake value ratios at 50-60 min post injection were calculated for [¹⁸F]THK-5351 using the cerebellar cortex as the reference region.

Results: [¹⁸F]THK-5351 displayed high binding affinity (K_d = 2.9 nM) with AD brain homogenates. Dissociation of THK-5351 from the white matter was faster than that of THK-5117. Autoradiographic images of AD brain sections showed selective labeling ability of THK-5351 to PHF-tau. In clinical PET studies, significant [¹⁸F]THK-5351 retention was observed in the areas known to contain high concentrations of tau deposits in AD patients. As observed in previous [¹⁸F]THK-5117 PET studies, regional distribution of [¹⁸F]THK-5351 differed considerably from that of [¹¹C]PiB in AD patients. [¹⁸F]THK-5351 showed faster kinetics and lower retention in the subcortical white matter and brainstem than [¹⁸F]THK-5117.

Conclusions: [¹⁸F]THK-5351 showed selective binding ability to tau pathology in AD. Wide dynamic range and low white matter retention of [¹⁸F]THK-5351 allow sensitive detection of early tau pathology in AD.

Presented by: Harada, Ryuichi

Submission ID: 24

Potential for PET Imaging Tau Tracer 18F-AV-1451 (also known as 18F-T807) to Detect Neurodegenerative Progression in Alzheimer’s Disease

Mark Mintun¹, Michael Devous¹, Michael Pontecorvo¹, Abhinay Joshi¹, Andrew Siderow¹, Keith Johnson², Michael Navitsky¹, Ming Lu¹

¹ Avid Radiopharmaceuticals, Inc., Philadelphia, PA, United States

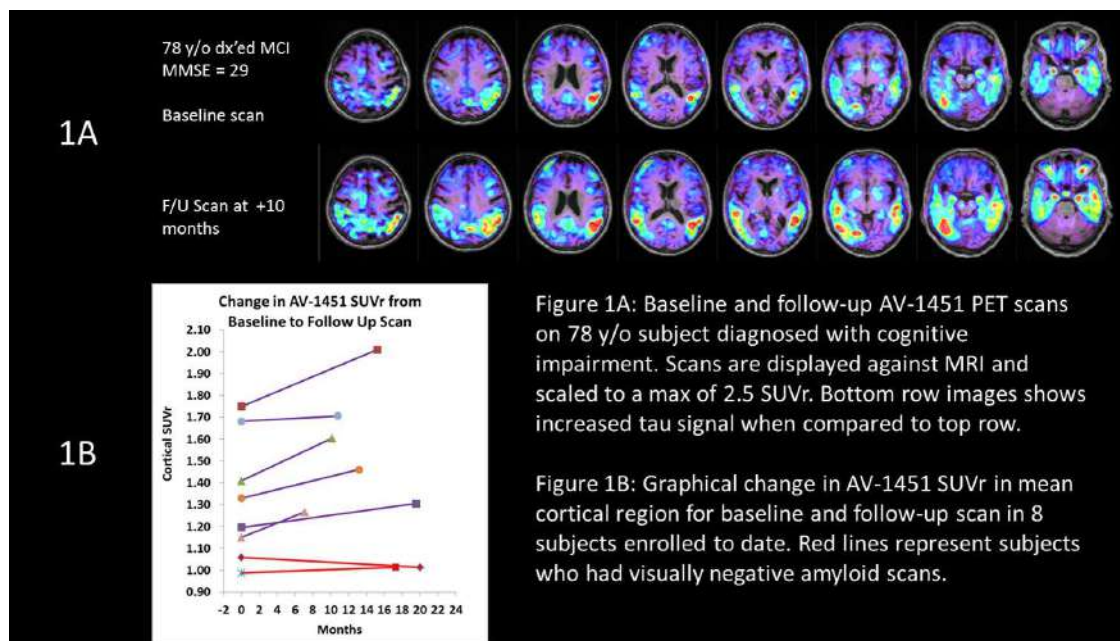
² Harvard Medical School, Boston, MA, United States

Background: Radioligands for PET imaging of aggregated tau might be used to follow progression in neurodegenerative tauopathies such as Alzheimer’s disease (AD). Given that these disorders advance slowly, it is critical to understand the magnitude of the change in tracer signal relative to reliability of the tracer measurement. Herein we report the first longitudinal data on the tau PET tracer, 18F-AV-1451 (aka 18F-T807).

Methods: We first conducted a test-retest study to quantitate the reliability of the PET tau signal. We then began an exploratory longitudinal study in a small number of subjects with suspected AD to estimate the magnitude of the tau signal change over time.

Results: Test-retest subjects (including healthy controls, MCI and AD subjects) imaged and reimaged (20 min scan starting 80 minutes after injection of 370 MBq of 18F-AV-1451) within 4 weeks (n=21; mean age 71) had cortical SUVR values (normalized to cerebellum gray) that were highly consistent (ICC > 0.93). The standard deviations of % changes of cortical regions were 4-5% over a range of baseline SUVRs (range = .8 to 2.5). Longitudinal PET tau imaging was done in eight subjects with MCI or AD. Two had visually negative amyloid scans, the lowest baseline cortical SUVR tau signals and minimal changes over time. Six subjects had positive amyloid scans and showed increase relative to baseline in cortical tau SUVR on follow up scans (mean interval = 12.7 months; range = 7.1 to 19.5 months). Mean ± S.D. annualized change in tau signal was 0.14 ± 0.08 SUVR units or 10.2% ± 6.0%.

Conclusion: While preliminary, these data suggest the PET tau signals change sufficiently over a relatively short period of time to provide meaningful measures of change, and that PET tau imaging with 18F-AV-1451 could be useful in furthering our understanding of disease progression.



Keywords: tau, PET, T807, AV-1451, neurofibrillary tangles

Presented by: Mintun, Mark

Submission ID: 95

Diagnostic Utility and Clinical Significance of Tau PET Imaging with [¹¹C]PBB3 in Diverse Tauopathies

Hitoshi Shimada¹, Hitoshi Shinotoh^{1,2}, Naruhiko Sahara¹, Shigeki Hirano^{1,3}, Shogo Furukawa^{1,3}, Keisuke Takahata¹, Yasuyuki Kimura¹, Makiko Yamada^{1,4}, Yasumasa Yoshiyama⁵, Ming-Rong Zhang⁶, Hiroshi Ito⁷, Makoto Higuchi¹, Satoshi Kuwabara³, Tetsuya Suhara¹

¹ Molecular Neuroimaging Program, Molecular Imaging Center (MONI), National Institute of Radiological Sciences (NIRS), Chiba-city, Chiba, Japan

² Neurology Chiba Clinic, Chiba-city, Chiba, Japan

³ Department of Neurology, Graduate School of Medicine, Chiba University, Chiba-city, Chiba, Japan

⁴ Precursory Research for Embryonic Science and Technology, Japan Science and Technology Agency, Chiyoda-ku, Tokyo, Japan

⁵ Department of Neurology, National Hospital Organization Chiba-East-Hospital, Chiba-city, Chiba, Japan

⁶ Molecular Probe Program, MONI, NIRS, Chiba-city, Chiba, Japan

⁷ Biophysics Program, MONI, NIRS, Chiba-city, Chiba, Japan

⁸ Advanced Clinical Research Center, Fukushima Medical University, Fukushima-city, Fukushima, Japan

Background and aims: Fibrillary tau pathology is considered to be a promising target for imaging and therapy in Alzheimer's disease (AD) and non-AD tauopathies such as progressive supranuclear palsy (PSP), corticobasal syndrome (CBS) and frontotemporal dementia (FTD). [¹¹C]PBB3 is a novel tau imaging PET ligand, which could visualize the tau deposition in AD and non-AD tauopathies. The aim of this study is to investigate the diagnostic utility and the clinical significance of tau PET imaging with [¹¹C]PBB3.

Methods: Participants were 16 mild cognitive impairments (MCI) patients, 21 AD patients, ten PSP patients, nine CBS patients, four FTD patients, and 34 healthy controls (HCs). We performed PET scans with [¹¹C]PBB3, [¹¹C]PIB and [¹⁸F]FDG PET and MRI scans. Standardized uptake value ratio was calculated for PET images using the cerebellar cortex as reference region. In a subset of patients, lumbar puncture was also performed to measure levels of cerebrospinal fluid (CSF) tau proteins. We assessed diagnostic utilities of each PET by area under the curve (AUC) of the receiver-operating characteristic.

Results: Ten of 16 MCI patients, 20 of 21 AD patients, one of nine CBS patient, one FTD patient, and three of 34 HCs were PIB-positive. Regional distribution of [¹¹C] PBB3 retention relative to HCs was different among patient groups, and was associated with neurological symptoms characteristic of each disease. [¹¹C]PBB3-PET discriminated between MCI and AD (AUC = 0.990; 95% CI, 0.964-1.000) and between HC and MCI (0.981; 0.941-1.000). [¹¹C]PBB3 binding correlated well with cognitive dysfunctions, but not with CSF tau.

Conclusions: [¹¹C]PBB3-PET enables differentiation of patients with MCI from those with AD and HCs, and provide objective indices reflecting the disease severity. Furthermore, [¹¹C]PBB3 PET is helpful to visualize specific distribution patterns of tau pathology associated with each neurological manifestation in a variety of non-AD tauopathies.

Keywords: *Tau imaging, [¹¹C]PBB3, Alzheimer's disease, mild cognitive impairment, non-AD tauopathies, CSF*

Presented by: Shimada, Hitoshi

Submission ID: 69

Entorhinal, Parahippocampal, and Inferior Temporal F18-T807 SUVR Correlates with CSF Total Tau and Tau T181P in Cognitively Normal Elderly

Jasmeer Chhatwal^{1, 3, 5}, Aaron Schultz^{1, 3, 5}, Gad Marshall^{1, 3, 4, 5}, Brendon Boot⁷, Teresa Gomez-Isla^{1, 5}, Julien Dumurgier^{1, 5}, Clemens Scherzer^{4, 5, 6}, Adrian Ivinson^{5, 6}, Allyson Roe¹, Bradley Hyman^{1, 3, 5, 6}, Reisa Sperling^{1, 3, 4, 5}, Keith Johnson^{1, 2, 3, 4, 5}

¹ Massachusetts General Hospital, Department of Neurology, Boston, MA, United States

² Massachusetts General Hospital, Department of Radiology, Boston, MA, United States

³ Martinos Center for Biomedical Imaging, Boston, MA, United States

⁴ Brigham and Women's Hospital, Department of Neurology, Boston, MA, United States

⁵ Harvard Medical School, Boston, MA, United States

⁶ Harvard NeuroDiscovery Center, Cambridge, MA, United States

⁷ Biogen Idec, Cambridge, MA, United States

Background: Cerebrospinal fluid (CSF) tau, phosphorylated tau (p-tau), and amyloid beta (A β 42) levels are among the most well validated AD biomarkers. F18-T807 is a newly developed radioligand that allows for *in vivo* imaging of tau pathology. Comparison of T807 binding to well-established CSF based biomarkers is a key step in the characterization of this new radioligand.

Methods: F18-T807 PET and CSF assays of total tau, p-tau, and A β 42 were obtained in 30 cognitively normal participants in the Harvard Aging Brain Study (mean age: 76.2y \pm 6.5y; PiB FLR: 1.24 \pm 0.25). Linear regression models were used to examine relationships between CSF measures and regional T807 SUVR.

Results: CSF tau and p-tau were significantly correlated with T807 SUVR in entorhinal (tau: r=0.48, p=0.007; p-tau r=0.40, p=0.03), parahippocampal (tau: r=0.48, p=0.008; p-tau: 0.44, p=0.015) and inferior temporal (tau: r=0.39, p=0.03; p-tau: r=0.42, p=0.02) regions. These correlations persisted after controlling for cortical thickness or volume measures, age, and CSF A β 42. The relationship of CSF tau and p-tau to T807 SUVR became progressively weaker when moving from inferior temporal to middle temporal (tau: r=0.24, p=0.19; p-tau: r=0.30, p=0.11) to superior temporal (tau: r = 0.15, p = 0.4; p-tau: r = 0.30, p=0.10) regions, areas with progressively less tau pathology in the clinically normal elderly. CSF A β 42 correlated with T807 SUVR in temporal neocortical regions, with the highest correlation seen in the inferior temporal cortex (r=-0.55, p=0.002). CSF A β 42 was not significantly correlated with entorhinal (r=-0.2905, p=0.12) or parahippocampal (r=-0.28, p=0.13) T807 SUVR.

Conclusions: T807 binding in entorhinal, parahippocampal, and inferior temporal ROIs regions was correlated with CSF tau and p-tau levels in cognitively normal elderly with tau largely restricted to these temporal lobe regions. These data support the link between T807-T807-PET and CSF-based measures of tau pathology.

Keywords: T807, tau, CSF

Presented by: Chhatwal, Jasmeer P

Submission ID: 115

KEYNOTE LECTURE 2

Chronic Traumatic Encephalopathy: the Last Seven Years

Ann McKee

Boston University School of Medicine, Boston, MA, USA

Repetitive brain trauma is associated with a progressive neurological deterioration, originally termed dementia pugilistica, and more recently, chronic traumatic encephalopathy (CTE). Most instances of CTE occur in association with the play of collision sports, such as American football and boxing, but CTE has also been reported blast injuries from improvised explosive devices, physical abuse, poorly controlled epilepsy, and head-banging behaviors. Symptoms of CTE include behavioral and mood changes, short-term memory loss, executive dysfunction, cognitive impairment and dementia. Like many other neurodegenerative diseases, CTE is diagnosed with certainty only by neuropathological examination of brain tissue.

Brains with advanced CTE show reduced brain weight; generalized or frontotemporal atrophy, enlargement of the lateral and third ventricles; cavum septum pellucidum; septal fenestrations; atrophy of the diencephalon and mammillary bodies and depigmentation of the locus coeruleus and substantia nigra. CTE is a tauopathy and is characterized by hyperphosphorylated tau (p-tau) pathology (neurofibrillary tangles, neurites and astrocytic tangles) in striking clusters around small blood vessels of the neocortex, typically at the sulcal depths. Severely affected cases show widespread p-tau pathology throughout the medial temporal lobes, diencephalon, and brainstem. Abnormalities in phosphorylated 43 kDa TAR DNA binding protein are found in most cases of CTE, often partially co-localized with phosphorylated tau protein. Beta amyloid (A β) deposition, as diffuse or neuritic plaques, is identified in 45% of subjects with CTE and is associated with age at death. A β plaques are not found in cases with early stages of CTE pathology or age at death less than 45 years. Compared to a normal aging population, A β deposition occurs at an earlier age and at an accelerated rate in CTE, and is associated with increased clinical and pathological severity.

To date, CTE has been identified neuropathologically in the brains of over 140 individuals; in 40%, CTE was associated with co-morbid neurodegenerative disease, including amyotrophic lateral sclerosis (10%), Alzheimer's disease (9%), Lewy body disease (8%) and Frontotemporal lobar degeneration (2%). Given the enormous importance of sports participation and physical exercise to physical and psychological health as well as disease resilience, it is critical to identify the genetic risk factors for CTE as well as the contribution of exposure variables, stress, alcohol, substance abuse and other factors to the development of CTE.

Future prospective, longitudinal, epidemiological, and animal modeling studies will be essential to establishing the incidence and prevalence of CTE as well as identifying the underlying pathogenic mechanisms to aid in the development of preventative and therapeutic strategies.

SESSION 7: Cognition

Chairs: Randy Buckner, PhD, *Harvard University/MGH*
Susan Resnick, PhD, *NIH/NIA*

Amyloid Negativity in Clinically Diagnosed ADNI Alzheimer's Disease Patients

Susan Landau^{1,2}, Allison Fero^{1,2}, William Jagust^{1,2}

¹ *University of California, Berkeley, Berkeley, CA, United States*

² *Lawrence Berkeley National Lab, Berkeley, CA, United States*

About one in seven ADNI patients with an AD phenotype are negative on florbetapir-PET, a rate that is in line with recent reports. Two possible explanations for this phenomenon are (1) false negative amyloid status due to image analysis problems and (2) AD misdiagnosis. We examined both possibilities, using florbetapir methodological tools, demographic and clinician report data, and other biomarkers (CSF-A β , t-tau, p-tau; APOE4; FDG-PET and structural MRI).

First we investigated potential PET problems by examining agreement with CSF-A β , the influence of different reference regions, and visual inspection. Florbetapir and CSF-A β +/- status agreed for 98% of patients; 3 patients were CSF-A β + and florbetapir-, but their florbetapir SUVRs were not close to the threshold, suggesting that image problems were not a major contributor to the florbetapir- group (Fig 1).

We also found that florbetapir- ADs (N=26/191; 14%) differed from their positive AD counterparts (165/191; 86%) in being more likely to be APOE4- (96% compared with 25% of florbetapir+ ADs) and male (85% compared with 55%). Florbetapir- ADs were also more likely to have a "possible" (rather than "probable") AD diagnosis, although clinician dementia severity ratings did not differ. In a voxelwise FDG-PET comparison, the florbetapir- ADs had higher metabolism in temporoparietal regions that are typically hypometabolic with AD, while the florbetapir+ group had higher metabolism in bilateral insula (Fig 2). The groups did not differ on hippocampal volume.

Fig 1. Florbetapir and CSF A β agree in 98% of ADs

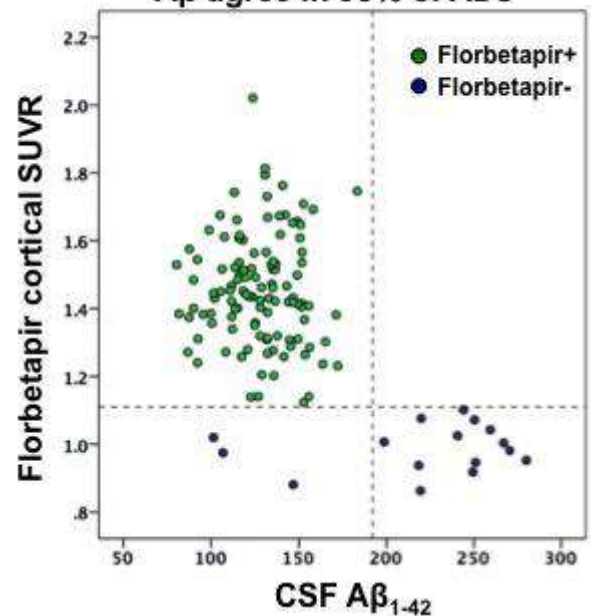
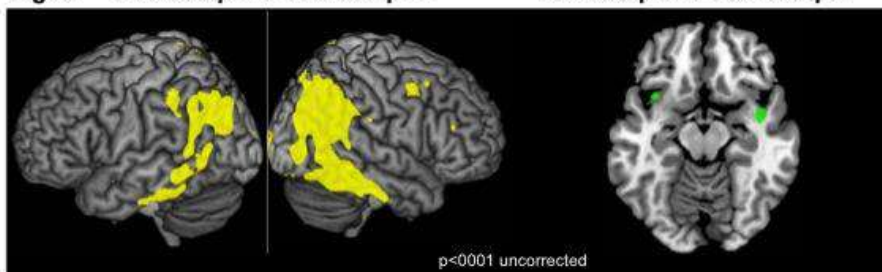
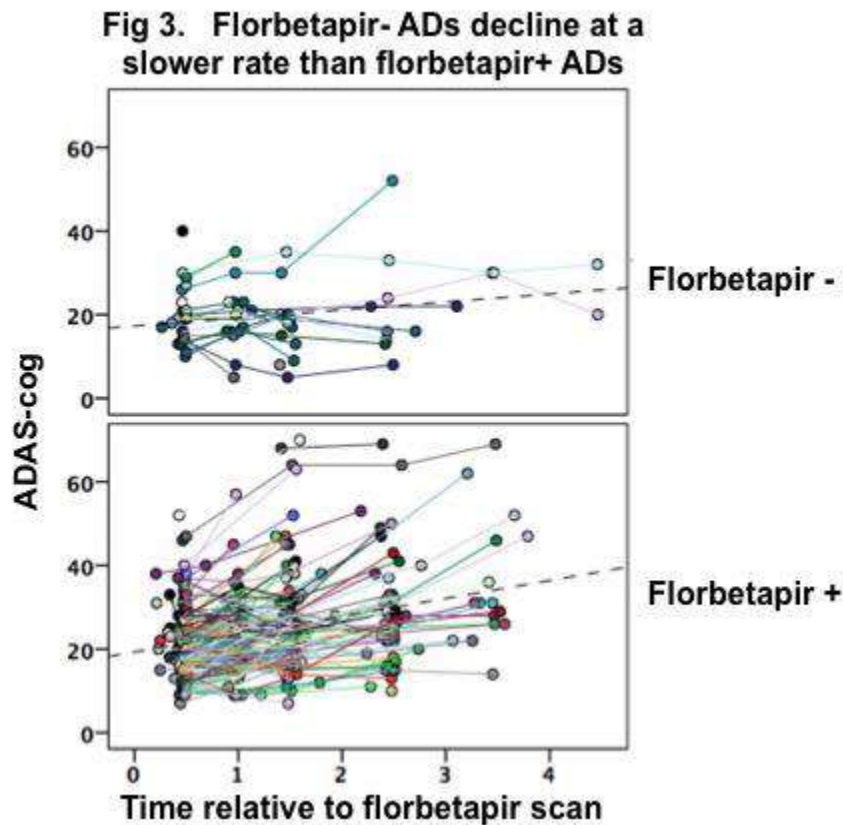


Fig 2. Florbetapir- > Florbetapir+

Florbetapir+ > Florbetapir-



Finally, florbetapir- ADs had lower CSF t-tau and p-tau, and slower decline on ADAS-cog over a mean 1.5 yr followup (Fig 3).



Florbetapir- ADNI patients with a clinical AD phenotype have a variety of clinical and biomarker features that differ from their florbetapir+ counterparts, suggesting that it is not PET abnormalities, but rather clinical diagnosis, that explains the findings.

Keywords: *florbetapir, CSF-A β , FDG, diagnosis*

Presented by: Landau, Susan M

Submission ID: 68

T807 PET Measures of Tau Pathology Associated with Episodic Memory Performance among Clinically Normal Older Individuals

Reisa Sperling, Elizabeth Mormino, Dorene Rentz, Aaron Schultz, J. Alex Becker, Julius Trey Hedden, Jorge Sepulcre, Jasmeer Chhatwal, Rebecca Amariglio, Katherine Papp, Gad Marshall, David Hsu, Neil Vasdev, Keith Johnson

Harvard Aging Brain Study, Massachusetts General Hospital, Harvard Medical School, Boston, MA, United States

Background: Accumulation of aggregated tau pathology is one of the hallmark neuropathologies of Alzheimer's disease, but is also observed in normal aging. Recent advances in molecular PET tracers now allow the detection of tau deposition *in vivo*. The association of tau and amyloid with cognitive performance among clinically normal (CN) older individuals remains to be elucidated.

Methods: We acquired neuropsychological testing, tau PET (18F-T807; inferior temporal region SUVR, cerebellar grey reference), and amyloid-beta (A β) PET (11C-PiB; cortical aggregate DVR) in 92 CN (mean age=75.7 \pm 6.3 years, CDR 0, MMSE=28.9 \pm 1.0) participating in the Harvard Aging Brain Study. PET imaging was acquired within 6 months of cognitive testing, and summarized as Memory and Executive Function Factor scores. We used multiple regression models to evaluate the associations between A β , tau, and cognitive factor scores, with age, gender, and education entered as covariates.

Results: Higher tau levels were associated with higher A β (partial $r = .27$; $p = 0.006$). When modeled separately, A β (partial $r = -.18$; $p = 0.04$) and tau (partial $r = -.28$; $p = 0.001$) each demonstrated a significant relationship with Memory, but not with Executive function. With both A β and tau in the model as simultaneous predictors, only tau demonstrated a significant relationship with memory (partial $r = -.27$; $p = 0.005$). There was no significant association between tau and Memory among A β - CN, (partial $r = -.13$; $p = 0.23$); whereas among A β + CN, tau burden was strongly associated with Memory performance (partial $r = -.45$; $p = 0.0008$).

Conclusions: An *in vivo* PET marker of tau pathology demonstrates a specific cross-sectional association with memory performance that appears stronger than the cross-sectional relationship between A β and memory. These findings are consistent with the hypothetical model that tau pathology is more proximal than A β to memory decline, and that the combination of A β and tau pathology may be particularly deleterious to memory function.

Keywords: *Tau, amyloid, memory*

Presented by: Sperling, Reisa A

Submission ID: 123

Preliminary Experience with [18F]AV1451 PET in Non-AD Neurodegenerative Syndromes

Gil Rabinovici^{1,2,3}, Daniel Schonhaut^{1,2}, Suzanne Baker³, Andreas Lazaris¹, Rik Ossenkoppele^{1,2}, Sam Lockhart², Henry Schwimmer², Jacob Vogel², Nagehan Ayakta², Howard Rosen¹, Bruce Miller¹, James O'Neil³, Adam Boxer¹, William Jagust^{1,2,3}

¹ Memory and Aging Center, University of California San Francisco, San Francisco, CA, United States

² Helen Wills Neuroscience Institute, University of California Berkeley, Berkeley, CA, United States

³ Life Sciences Division, Lawrence Berkeley National Laboratory, Berkeley, CA, United States

Background: [18F]AV1451 binds selectively to tau-positive inclusions in post-mortem specimens from non-AD tauopathies. Here we describe preliminary *in vivo* AV1451 PET findings in progressive supranuclear palsy (PSP), suspected chronic traumatic encephalopathy (CTE) and frontotemporal dementia associated with tau-negative, TDP43-positive inclusions (FTD-TDP).

Methods: [18F]AV1451 PET was performed in 5 patients with early-stage PSP (mean age 69.4, MMSE 24.6, PSP Rating Scale 24.4/100), 2 retired NFL players with neurobehavioral decline (at risk for CTE, ages 50 and 68), and 2 patients with presumed FTD-TDP: a 71 year-old with familial FTD due to *C9ORF72* mutation, and a 59 year-old with semantic-variant primary progressive aphasia. PIB-PET was negative in all patients except for 2 with PSP (one PIB+, another pending). 80-100 min SUVR images were created (gray matter cerebellum reference region). We compared AV1451 uptake in PSP patients to 16 cognitively normal controls (NC, mean age 78.4) using voxel-wise (SPM) and region of interest (ROI) approaches.

Results: On voxel-wise contrast, increased AV1451 was seen in PSP vs. NC in the midbrain, subthalamic nucleus and globus pallidus ($p < 0.001$ uncorrected, Figure 1), conforming to the expected distribution of tau pathology in early-stage PSP. ROI analysis confirmed elevated SUVR in globus pallidus (Mann-Whitney, $p < 0.01$). Increased binding in dentate nucleus of cerebellum was qualitatively discernable in 3/5 patients, but was not significant in group comparisons. One of 2 patients at risk for CTE showed focal AV1451 binding in left anterior temporal lobe (Figure 2). Both patients with presumed FTD-TDP showed increased AV1451 uptake in atrophic cortical regions (Figure 3).

Conclusions: We observed elevated AV1451 uptake in PSP and CTE in expected regions, though subcortical signal overlapped with binding in NC. Unexpected AV1451 binding was also found in patients with presumed tau-negative FTD-TDP pathology. Further work is needed to better characterize these findings.

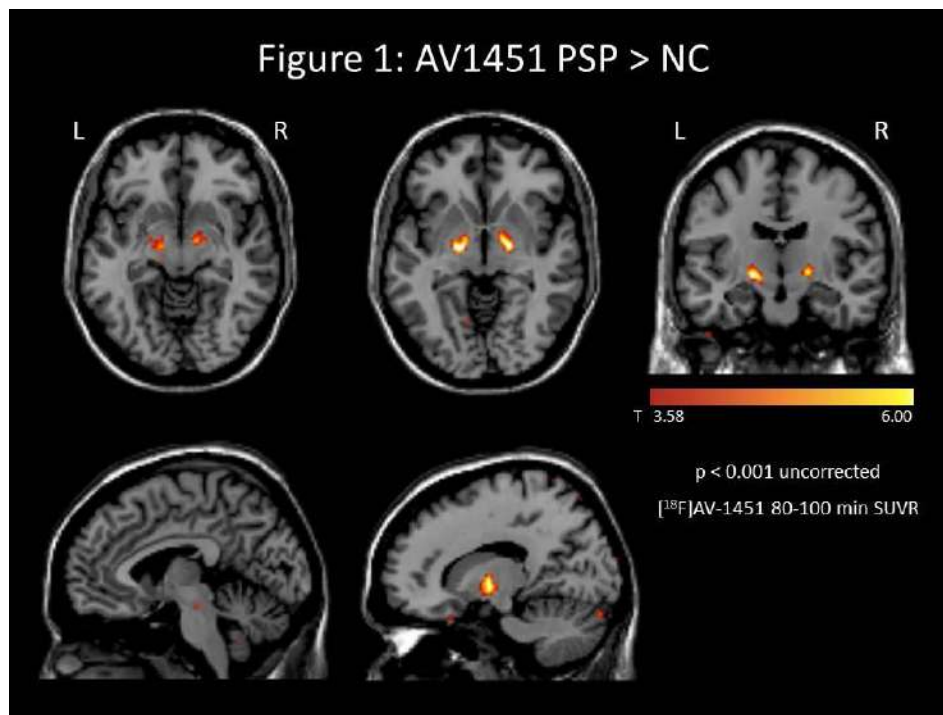


Figure 2: PIB and AV1451 in 68 yo retired NFL player with neurobehavioral decline

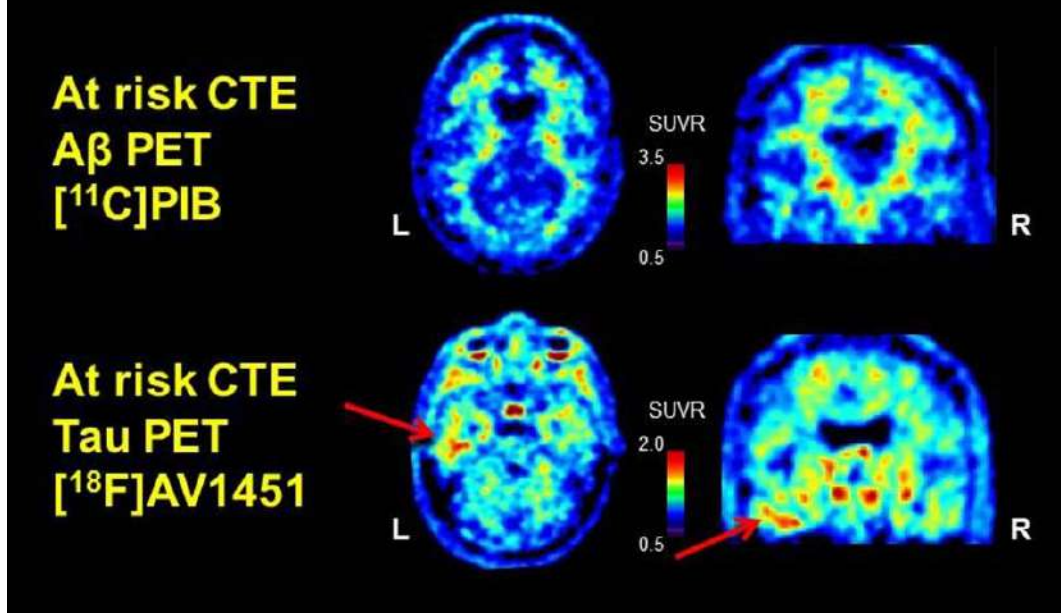
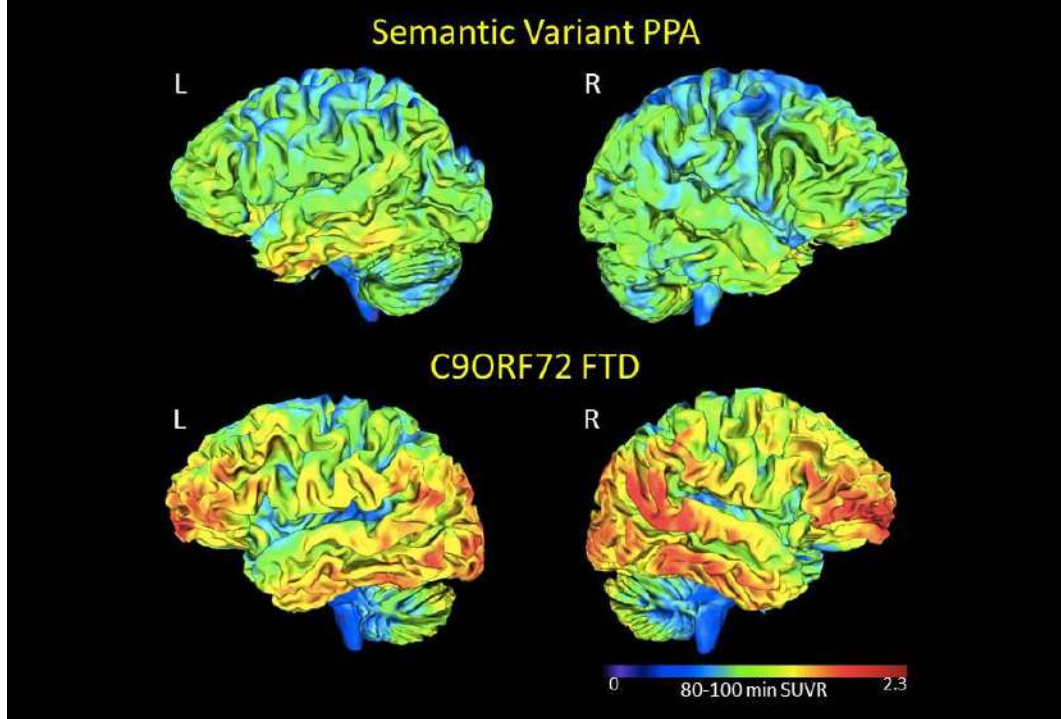


Figure 3: AV1451 in FTD-TDP



Keywords: Tau, frontotemporal dementia, progressive supranuclear palsy, chronic traumatic encephalopathy

Presented by: Rabinovici, Gil D

Submission ID: 39

Longitudinal Effects of Amyloid Accumulation on Cognition in a Healthy Adult Cohort Aged 30-89: Results from the Dallas Lifespan Brain Study

Denise Park¹, Michelle Farrell¹, Karen Rodrigue¹, Kristen Kennedy¹, Gérard Bischof¹, Michael Devous, Sr.²

¹ University of Texas at Dallas, Dallas, Texas, United States

² Avid Radiopharmaceutical, A Subsidiary of Eli Lilly, Philadelphia, PA, United States

Background: The Dallas Lifespan Brain Study focuses on the relationship of multiple brain biomarkers in healthy adults to changes in cognitive function in an effort to understand how the brain adapts to neural insult, allowing for the development of a model that predicts who will age well in the future. Here we report on the first longitudinal data from 76 healthy participants (age 30-89) who received a cognitive battery and amyloid imaging initially and 3.5 years later.

Methods: Amyloid was measured using 18F-Florbetapir using mean cortical standardized uptake ratio (SUVR) of 7 cortical ROIs normalized to a composite reference region consisting of whole cerebellum, pons and centrum semiovale. Cognitive constructs were created from multiple measures of episodic memory, processing speed, and reasoning.

Results: Predicting FUTURE Cognition from initial amyloid burden: Time 1 amyloid status predicted episodic memory and processing speed levels 3.5 years later. Moreover, amyloid burden interacted with age ($p = .01$) on processing speed such that amyloid was predictive only for older adults (55-89y), but not middle-aged adults (30-54y).

Predicting cognitive CHANGE from initial amyloid burden: Initial amyloid burden predicted decline in episodic memory and speed of processing also approached significance.

Predicting cognitive CHANGE from CHANGE in amyloid burden: Greater amyloid accumulation predicted cognitive decline in reasoning and was a marginally significant predictor of episodic memory and processing speed decline, even after controlling for initial amyloid burden. A significant age \times amyloid interaction was observed on episodic memory only in 50-69 year olds.

Conclusions: These results provide early evidence that small changes in amyloid burden predict cognitive change over 3.5 years in healthy adults. These may be the first results to demonstrate that the rate of amyloid accumulation is directly related to rate of cognitive decline in healthy adults, while taking into account initial levels of amyloid burden.

Effect of initial amyloid burden and change in burden on cognition over 3.5 years in healthy adults aged 30-89 (n=76)

Figure 1a. Effect of Time 1 amyloid on cognition 3.5 years later

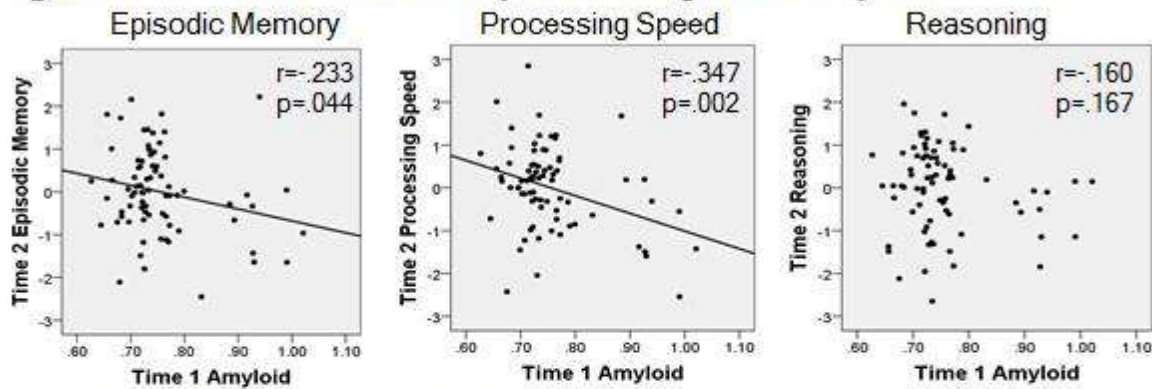


Figure 1b. Effect of amyloid change on cognitive change over 3.5 years

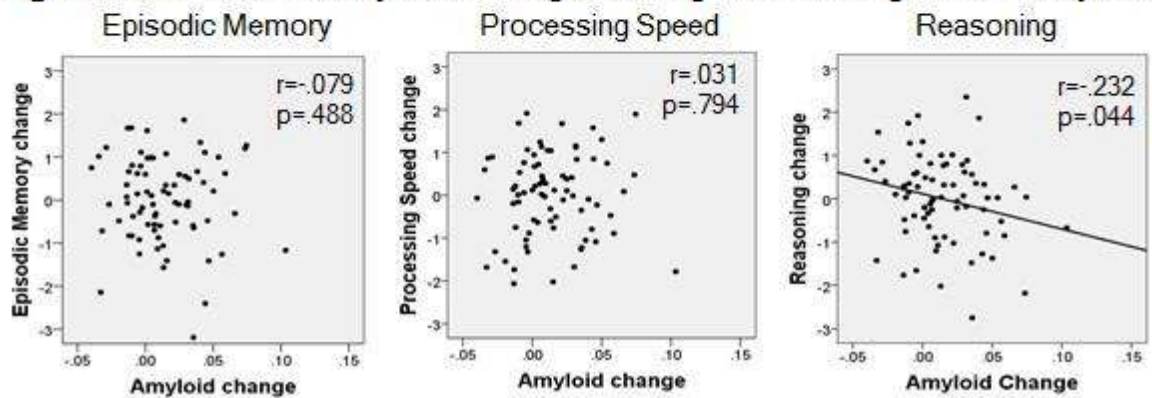


Table 1. Summary of amyloid effects on cognition

Cognitive Construct	Effect	Amyloid T1 on Cognition T2	Amyloid T1 on Cognitive Change	Amyloid Change on Cognitive Change
Episodic Memory	Amyloid	++	++	+
	Age x Amyloid	-	-	+
Processing Speed	Amyloid	++	+	+
	Age x Amyloid	++	-	+
Reasoning	Amyloid	+	-	++
	Age x Amyloid	+	-	-

++ = p<.05; + = p<.10; - p=ns

Keywords: amyloid imaging, lifespan, cognition, longitudinal

Presented by: Park, Denise C

Submission ID: 28

SPECIAL LECTURE

What Makes Association Networks Vulnerable to Neurodegeneration?

Randy Buckner

Harvard University, Boston, MA, United States

Association networks have long been known to be preferentially targeted by certain neurodegenerative processes prompting ideas about what makes them vulnerable. Ideas range from their late development to their connectivity properties to features of their basal metabolism.

In this talk I will step back and discuss how development and evolution of association cortex may set the stage for vulnerability. One possibility is that there is no one feature of association regions that makes them vulnerable to degeneration but rather that they possess a range of properties that distinguish association regions from sensory-motor regions.

POSTER SESSION (Even Numbers)

Even-numbered submissions organized by last name of author

P2

The Pattern of [11C]-Pittsburgh Compound-B Binding in the Brains of Adults with Down's Syndrome

Tiina Annus¹, Liam Wilson¹, Julio Acosta-Cabronero², Young Hong³, Tim Fryer³, Arturo Cardenas-Blanco², Shahid Zaman¹, Anthony Holland¹, Peter Nestor², et al.

¹ Cambridge Intellectual and Developmental Disabilities Research Group, Department of Psychiatry, University of Cambridge, Douglas House, 18b Trumpington Rd, CB2 8AH, Cambridge, Cambridgeshire, United Kingdom

² German Centre for Neurodegenerative Diseases (DZNE), Leipziger Str. 44, House 64, 39120, Magdeburg, Saxony-Anhalt, Germany

³ Wolfson Brain Imaging Centre, Department of Clinical Neurosciences, University of Cambridge, University of Cambridge School of Clinical Medicine Box 65 Cambridge Biomedical Campus, CB2 0QQ, Cambridge, Cambridgeshire, United Kingdom

Introduction: Adults with Down's syndrome (DS) invariably develop beta-amyloid (A β) pathology indistinguishable from sporadic Alzheimer's disease (AD). Due to the trisomy 21 and triplication of APP, DS presents as a natural model of A β over-production. Studies in DS are highly complementary to those in autosomal-dominant AD in understanding the role of A β . This study characterises the sequence of A β accumulation in DS brains, which has implications for disease staging in vivo and monitoring response to treatment.

Methods: Forty-nine adults with DS underwent [11C]PIB-PET with structural MRI. PIB images, a modified Brodmann atlas and FIRST subcortical maps were warped to a template, created from T1-images with ANTs, for quantification of regional non-displaceable binding potential. No participant without binding in the striatum had binding elsewhere and the distribution of striatal binding was bimodal with clear groups of negative and positive. The number of positive regions in PIB-positive group formed the basis for the accumulation model.

Results: Nine stages of PIB binding were identified: (1) striatum, (2) dorsal prefrontal and anterior cingulate cortex, (3) ventral prefrontal cortex and areas of the parietal lobe, (4) lateral temporal cortex and the rest of the parietal lobe, (5) sensory and motor areas, (6) associative visual and pre-motor cortex, and the rest of the temporal lobe, (7) occipital lobe, (8) thalamus and the medial temporal lobe, (9) amygdala. None of the participants were PIB positive in the hippocampus.

Conclusion: A β follows a pattern of accumulation measurable in vivo in DS. Evidence supports the initial involvement of the striatum as previously reported for DS and autosomal-dominant AD. In DS, the first cortical area affected by fibrillar A β is the prefrontal cortex, followed by parietal, then temporal areas and, at the very late stages, occipital cortex. This progression model has the potential to inform future anti-amyloid primary prevention trials.

Keywords: *Down's syndrome, Alzheimer's disease, PIB-PET, amyloid, MRI*

P2 Presented by: Annus, Tiina

Submission ID: 10

Clinical Utility of Amyloid Imaging in a Complex Case of Corticobasal Syndrome Presenting with Psychiatric

Symptoms

Mohamed Réda Bensaïdane^{1, 2, 3}, Marie-Pierre Fortin^{1, 2}, Geneviève Damasse^{1, 2}, Marise Chénard^{2, 4}, Christine Dionne^{2, 5}, Mélanie Duclos^{2, 6}, Rémi Bouchard^{1, 2, 7}, Robert Jr. Laforce^{1, 2, 3}

¹ *Clinique Interdisciplinaire de Mémoire, Quebec City, QC, Canada*

² *CHU de Québec, Quebec City, QC, Canada*

³ *Faculté de médecine, Université Laval, Quebec City, QC, Canada*

⁴ *Département de Gérontopsychiatrie, Quebec City, QC, Canada*

⁵ *Département de Gériatrie, Quebec City, QC, Canada*

⁶ *Département de Neuropsychologie, Quebec City, QC, Canada*

⁷ *McGill University, Montreal, QC, Canada*

Clinical indications of amyloid imaging in atypical dementia remain unclear. We report a 66-year-old female without past psychiatric history who was hospitalized for auditory hallucinations and persecutory delusions associated with cognitive and motor deficits. Although psychotic symptoms resolved with antipsychotic treatment, cognitive and motor impairments remained. She further showed severe visuoconstructive and executive deficits, ideomotor apraxia, elements of Gerstmann's syndrome, bilateral agraphesthesia and discrete asymmetric motor deficits. Blood tests were unremarkable. Structural brain imaging revealed diffuse fronto-temporo-parietal atrophy, which was most severe in the parietal regions. Meanwhile, FDG-PET suggested asymmetrical fronto-temporo-parietal hypometabolism, with sparing of the posterior cingulate gyrus (figure 1). A diagnosis of possible corticobasal syndrome (CBS) was made. Amyloid-PET using the novel tracer NAV4694 was ordered, and revealed significant deposition of fibrillar amyloid with a standardized uptake value ratio of 2.05 (figures 2 & 3). The primary diagnosis was CBS with underlying Alzheimer pathology and treatment with an acetylcholinesterase inhibitor was initiated. Determination of underlying pathological CBS subtype is not simple even when based on extensive investigation including clinical presentation, atrophy patterns on MRI, and regional hypometabolism on FDG-PET. By contrast, amyloid imaging quickly confirmed Alzheimer pathology, and allowed rapid initiation of treatment in this complex case with early psychiatric symptoms. This case study illustrates the clinical utility of amyloid imaging in the setting of atypical cases seen in a tertiary memory clinic.

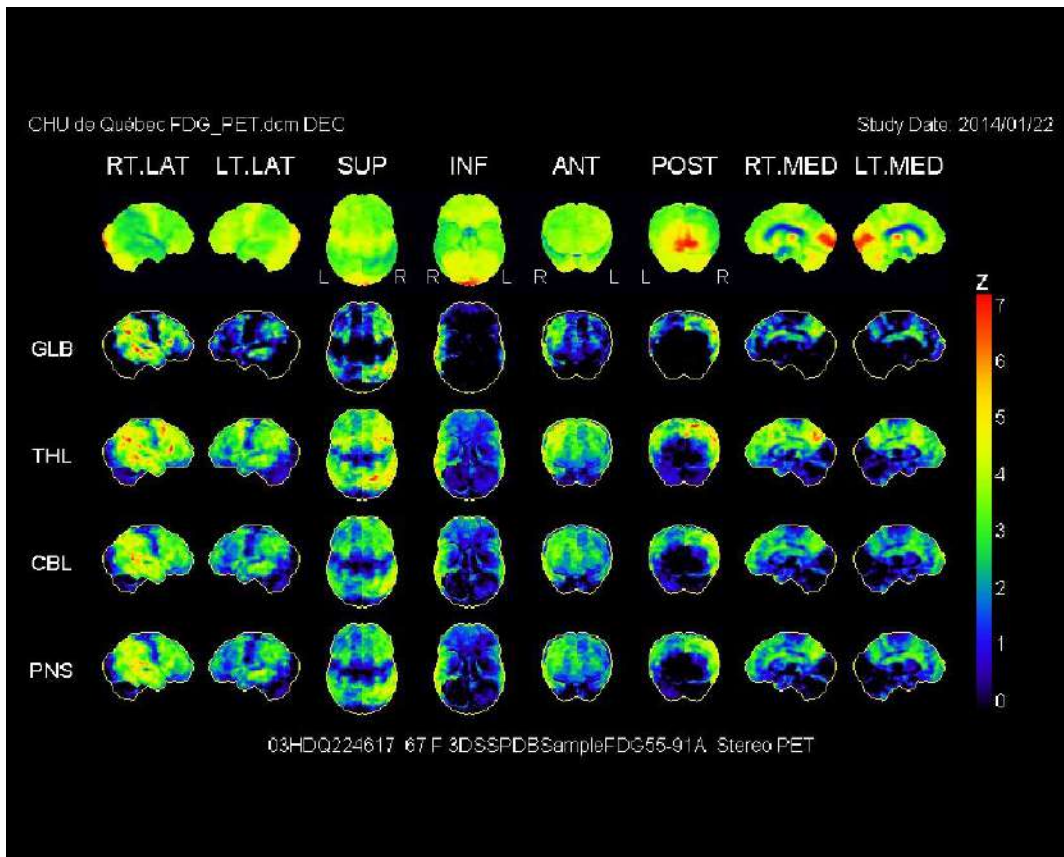


Figure 1. FDG-PET of the brain.

Figure 2. Amyloid-PET in axial plane.

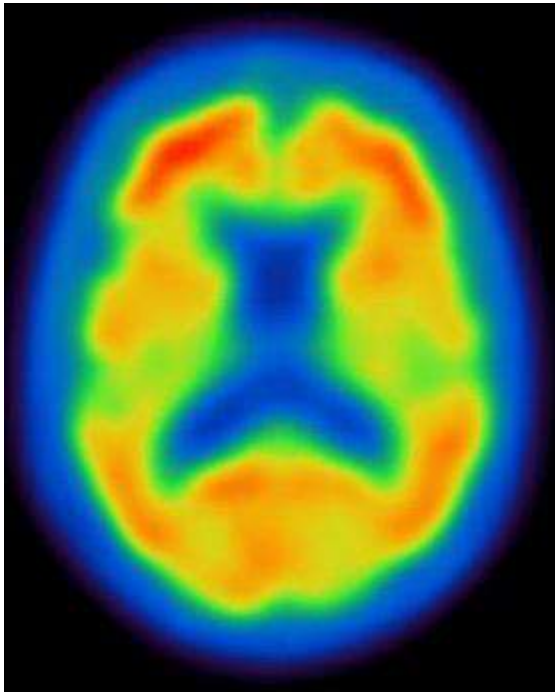
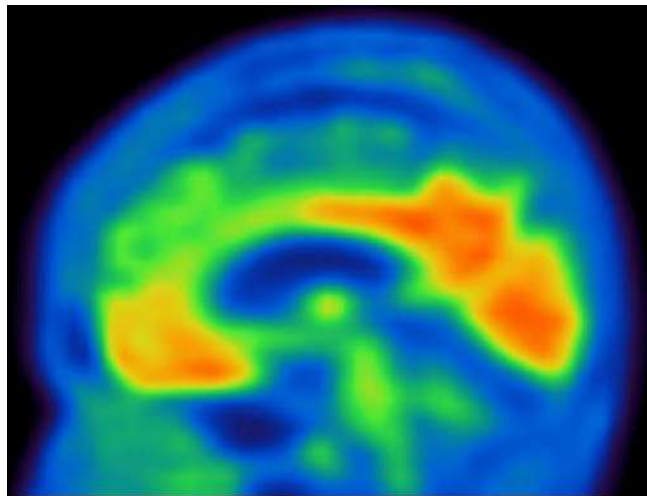


Figure 3. Amyloid image in sagittal plane.



Keywords: corticobasal syndrome, Alzheimer, NAV4694, amyloid-PET

P4 Presented by: Bensaïdane, Mohamed Réda

Submission ID: 8

Temporal Progression of Cerebral Amyloid Deposition as Measured by ^{11}C -PiB PET Imaging

Murat Bilgel^{1,2}, Susan Resnick¹, Dean Wong³, Bruno Jedynak⁴, Jerry Prince^{2,3,5}

¹ Laboratory of Behavioral Neuroscience, National Institute on Aging, NIH, Baltimore, MD, United States

² Department of Biomedical Engineering, Johns Hopkins University, Baltimore, MD, United States

³ Department of Radiology, Johns Hopkins Medical Institutions, Baltimore, MD, United States

⁴ Department of Applied Mathematics and Statistics, Johns Hopkins University, Baltimore, MD, United States

⁵ Department of Electrical and Computer Engineering, Johns Hopkins University, Baltimore, MD, United States

Background: The temporal ordering of changes in amyloid deposition has not been thoroughly investigated on the whole-brain scale.

Method: We estimated the temporal trajectories of cerebral amyloid deposition using 75 participants with 2 to 7 PiB-PET scans (mean 3.6, SD 1.5) from the Baltimore Longitudinal Study of Aging (BLSA). Distribution volume ratio (DVR) images were extracted from 70-minute PiB PET scans and spatially normalized using co-registered MRIs to a study-specific template in MNI space. We modeled each participant's cerebral amyloid status with a latent variable that we call the PiB progression score (PiB-PS). PiB-PS was assumed to be a linear transformation of age described by two parameters. This allowed us to account for differences in the age of onset of amyloid deposition as well as in the rate of accumulation. The trajectory of amyloid deposition at each voxel was assumed to be a linear function of PiB-PS. The model parameters were estimated using an expectation-maximization algorithm. We calculated the predicted DVR images using the estimated trajectory parameters for different values of PiB-PS to show the longitudinal changes in PiB. To examine the temporal ordering of PiB changes, we calculated for each voxel the value of PiB-PS at which a given DVR (1.00 to 2.80 with 0.02 increments) will be attained.

Results:

Figure 1. Predicted DVR images at three stages of amyloid deposition, as characterized by the PiB-PS.

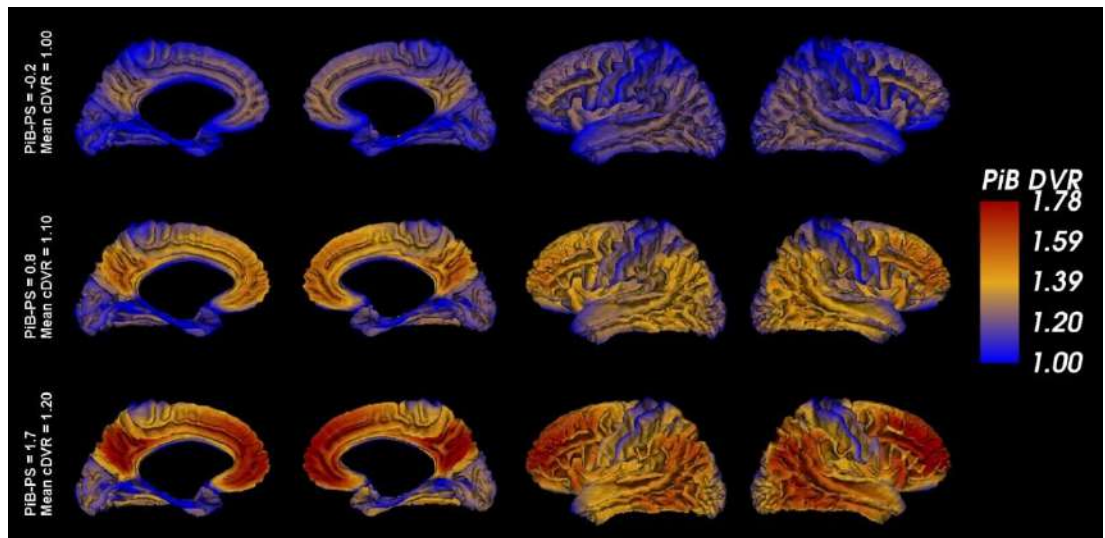
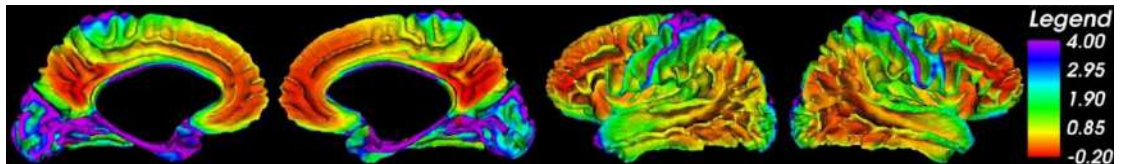


Figure 2. Images showing the value of PiB-PS at which a DVR of 1.32 will be attained. A lower value (red) means that the voxel will reach a DVR of 1.32 earlier.



Conclusions: Our findings suggest that amyloid deposition as evident in PiB imaging begins in the precuneus, closely followed by the lateral and medial frontal lobe, and then the parietotemporal regions. These findings must be confirmed using specifically designed statistical tests.

Keywords: PiB, DVR, longitudinal progression

P6 Presented by: Bilgel, Murat

Effects of Asymptomatic B-amyloid Positivity on Regional Cerebral Metabolism and CSF-pTau Levels

Andrea Bozoki, Monica Gentchev, David Zhu

Michigan State University, East Lansing, Michigan, United States

Objective: We hypothesized that clinically healthy individuals with a high burden of cerebral amyloid would demonstrate subtle regional hypometabolism in medial temporal regions, consistent with early phospho-tau (pTau) mediated neuronal damage.

Methods: Using the normal control group from ADNI as our subject population, we used the brain volume analysis program Freesurfer to identify regions of interest including entorhinal cortex, hippocampus, amygdala, basal forebrain, middle temporal gyrus and posterior cingulate on a high-resolution volumetric MR image, and coregistered it to each individual's FDG-PET. We selected these regions a priori based on the pathologic stages of tangle deposition delineated by Braak and Braak. Each subject's global amyloid burden (SUVR) was quantified using AV-45 data made available from U. of Utah.

Results: While ApoE4 – individuals had the predicted findings of increasing hypometabolism with increasing amyloid SUVR in all examined regions, the ApoE4+ group demonstrated a relative *hypermetabolism* that grew more pronounced with increasing amyloid SUVR. This hypermetabolism was restricted to entorhinal cortex, hippocampus and amygdala, and was not present in temporal neocortex or posterior cingulate, suggesting sites of pathologic neuronal overactivity in specifically those brain regions known to be affected earliest by ptau-mediated neurodegeneration. The substantial difference in regional metabolism between APOE4- and + individuals was recapitulated by a similar series of positive correlations between regional brain metabolism and CSF pTau values, again seen most prominently in the earliest-affected medial temporal regions, and only in ApoE4+ individuals.

Conclusion: Surprisingly, we found that ApoE status substantially modulates both regional metabolism and the relationship between regional metabolism and CSF pTau levels, suggesting one mechanism by which the ApoE4 allele may cause earlier emergence of clinical symptoms in AD.

Keywords: *FDG-PET; pre-symptomatic Alzheimer's disease*

P8 Presented by: Bozoki, Andrea C

Submission ID: 86

Amyloid Exerts Distributed Effect on Glucose Metabolism in Preclinical Alzheimer's Disease

Matthew Brier¹, John McCarthy², Karl Friedrichsen³, Tammie Benzinger^{3,4}, Russ Hornbeck³, Yi Su³, Randall Bateman^{1,4}, John Morris^{1,4}, Beau Ances^{1,3,4}

¹ Department of Neurology, Washington University in St. Louis, St. Louis, MO, United States

² Department of Mathematics, Washington University in St. Louis, St. Louis, MO, United States

³ Department of Radiology, Washington University in St. Louis, St. Louis, MO, United States

⁴ Knight Alzheimer Disease Research Center, Washington University in St. Louis, St. Louis, MO, United States

The progression of preclinical Alzheimer's disease (AD) is characterized by the accumulation of amyloid β and decreased cerebral metabolism. Amyloid deposition likely precedes metabolic changes by several years and is thought to be one of the causative mechanisms of neural dysfunction. Previous work has demonstrated a robust negative relationship between PIB (measuring amyloid) and FDG (measuring glucose metabolism). Those analyses were largely univariate, considering only single brain regions, and were blind to potential interactions occurring across the rest of the brain. One hypothesis regarding AD pathophysiology proposes that AD is a disease of networks; dysfunction in one part of the brain can exert influence in other related brain regions. In this study, we first analyzed PIB and FDG topographies from subjects enrolled in the Dominantly Inherited Alzheimer's Network (DIAN) study who have AD causing genetic mutations. We leverage canonical correlation, a multivariate statistical technique, which identifies linear combinations of variables (PIB topographies) that are maximally correlated with other linear combinations of variables (FDG topographies). This allows for the testing of two hypotheses: 1) amyloid reduces glucose metabolism only in the areas directly affected by amyloid and 2) amyloid is capable of disrupting brain function in remote areas not directly affected by amyloid. We observed a significant negative canonical correlation between PIB and FDG in mutation carriers. The correlated PIB and FDG topographies overlap but substantial divergences are also present. Both hypothesized processes may occur in AD. Further, the identified topographies are biologically meaningful because the data projected onto the calculated topographies were highly related to the estimated years until disease onset, a quantity predicted based on family history. Notably, these relationships were absent in siblings not carrying the genetic mutations. These results suggest that amyloid disrupts brain function locally but also exerts a distributed pathologic influence.

P10 Presented by: Brier, Matthew R

Submission ID: 42

Striatal Amyloid Burden Measured by Quantitative [¹⁸F]flutemetamol PET Imaging on End of Life Subjects

Tom Beach¹, Dietmar Thal², Johan Lilja³, Chris Buckley⁴, Adrian Smith⁴, Gill Farrar⁴, Michelle Zanette⁵, Paul Sherwin⁵

¹ *Civin Laboratory for Neuropathology, Banner Sun Health Research Institute, Sun City, AZ, United States*

² *Institute of Pathology – Laboratory of Neuropathology, Center for biomedical Research, University of Ulm, ULM, ULM, Germany*

³ *GE Healthcare, Uppsala, Stockholm, Sweden*

⁴ *GE Healthcare, Amersham, Buckinghamshire, United Kingdom*

⁵ *GE Healthcare, Princeton, NJ, United States*

Objectives: To determine how quantitative [¹⁸F]flutemetamol PET imaging of striatal amyloid load relates to the phases of A β pathology as determined post mortem. Plaques in the striatum are pathognomonic for phase 3 of A β pathology and represent progression to pre AD as indicated by the revised 2012 neuropathology criteria. Detection of striatal amyloid may provide a means to help stage amyloid progression.

Methods: Image analysis: [¹⁸F]Flutemetamol PET images from end of life subjects were spatially normalized to MNI standard space and a standardised pons volume of interest (VOI) was applied automatically to provide the SUV reference. The application of striatal VOIs (post-hoc) was made in person using a pre-defined procedure using an oblique sagittal plane through the thalamus and striatum with striatal VOIs applied to the caudate nucleus encompassing the anterior putamen. SUVR_{PONS} was calculated to assess uptake in the striatum. Figure 1 shows the placement of striatal VOIs and their overlay on an A β phase 2 and an A β phase 4 case.

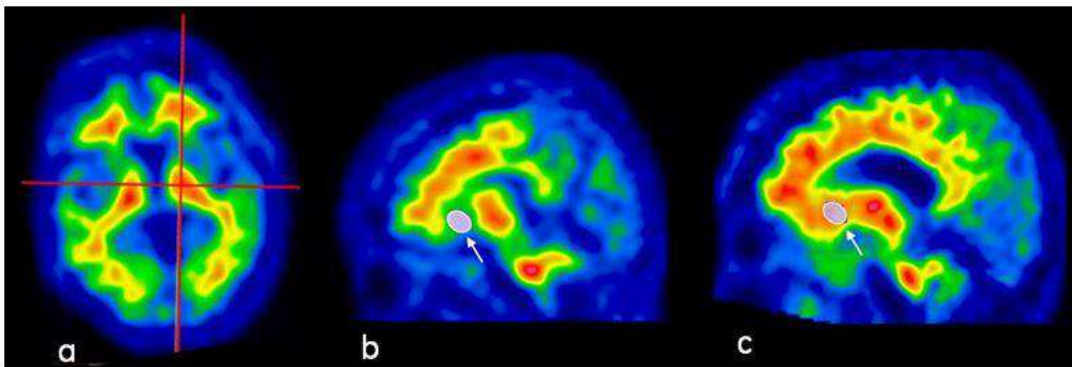


Figure 1. a) Oblique sagittal plane position for striatal VOI overlay b) overlay on A β phase 2 case, c) overlay on a A β phase 4 case. Arrow indicates a VOI element in the oblique sagittal plane.

Results: Figure 2. Shows the level of striatal uptake with A β phase from the end of life study GEO67-026 (106 autopsy cases). A small number of cases were removed from the analysis where striatal assessment was compromised by gross lesions.

Conclusion: [¹⁸F]flutemetamol PET imaging and quantification is well suited to detection of striatal amyloid pathology in vivo. We found a high concordance between amyloid phases and where amyloid appears in the striatum (phases 3 to 5) and striatal SUVR. In conjunction with cortical assessments of amyloid burden, this may be useful identifying amyloid burden associated with pre-AD.

Keywords: *Striatum, Pons, [¹⁸F]Flutemetamol, amyloid-phase, plaques*

P12 Presented by: Buckley, Chris J

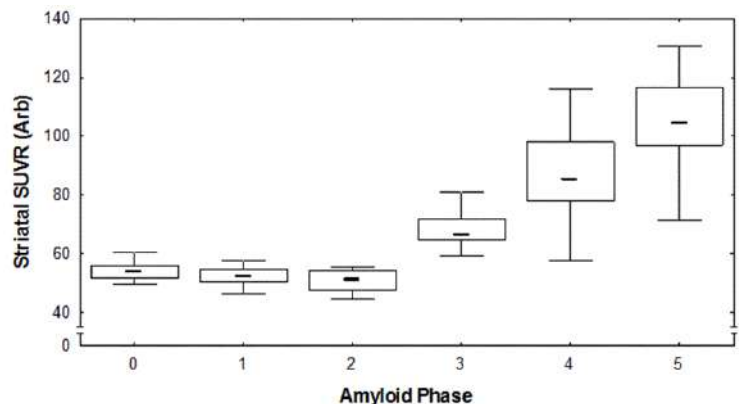


Figure 2. Striatal SUVR_{PONS} and A β phases. Quartile box plot, line indicates median

Submission ID: 82

Detecting Treatment Effects in Clinical Trials with Florbetapir-PET: An Alternative Statistical Approach to SUVr

Funan Shi^{1,2}, Thomas Bengtsson¹, David Clayton¹, Peter Bickel²

¹ Genentech, Inc, South San Francisco, CA, United States

² University of California, Berkeley, Berkeley, CA, United States

Background: Recent trials for amyloid-targeted therapies have used SUVr from florbetapir-PET to assess amyloid burden. There are inherent statistical problems when calculating ratios of signals that make SUVr problematic for detecting small changes only in the numerator.

Methods: We observed two dominant features in data from ADNI and a phase2 trial, NCT01723826. First, plots of $\Delta T = T_2 - T_1$ vs. $\Delta R = R_2 - R_1$ show strong linear relationships (Fig1), where T and R denote target- and reference-region SUV's, respectively. Second, residuals from regressions of T on R are highly correlated (Fig2), implying strong longitudinal within-patient effect. Therefore, we propose a linear-regression-based alternative to $\delta SUVr = T_2/R_2 - T_1/R_1$ for analyzing longitudinal changes. The data suggest a linear model: $\Delta T = \alpha + \beta \Delta R + \varepsilon$, where α represents the average change in the *target* signal when the *reference* signal remains constant, $\Delta R = 0$. Simulations were performed to ascertain the power to detect 50% reduction in amyloid accumulation based on empirically motivated ranges of parameters derived from the two datasets.

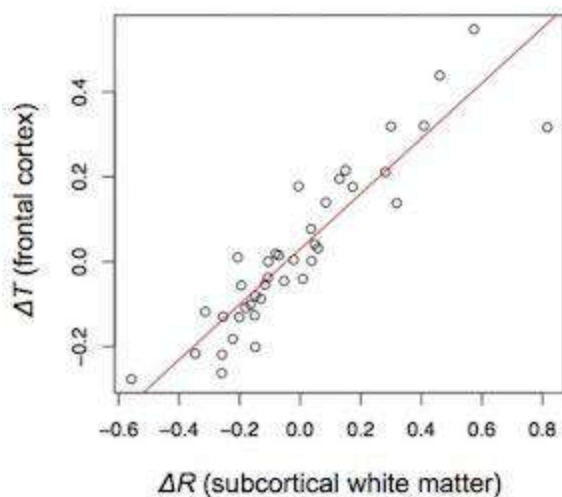


Fig 1. Correlations between changes in SUV in target (ΔT) and reference (ΔR) regions. (ADNI AD group, UC Berkeley data set)

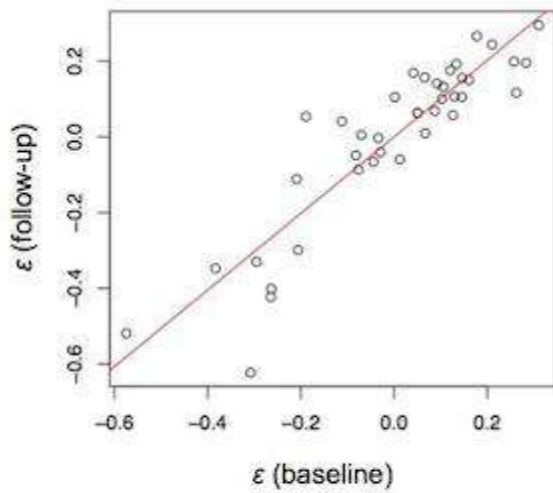


Fig 2. Residuals (ϵ) from linear regressions of T vs. R at baseline and follow-up (ADNI AD group, UC Berkeley data set).

Results: Fig3 shows power as a function of within-patient effect (σ_z) and residual variability (σ_ϵ). Simulations are based on generating target SUV's conditioned on bootstrapped reference SUV's. σ_z does not affect the regression method's power to detect changes in target SUV, but significantly degrades that of $\delta SUVr$. These simulations and analytical derivations confirmed that power is improved by an increase in the coefficient of variation of the reference SUV's, and an increase in the magnitude of the within-patient effect.

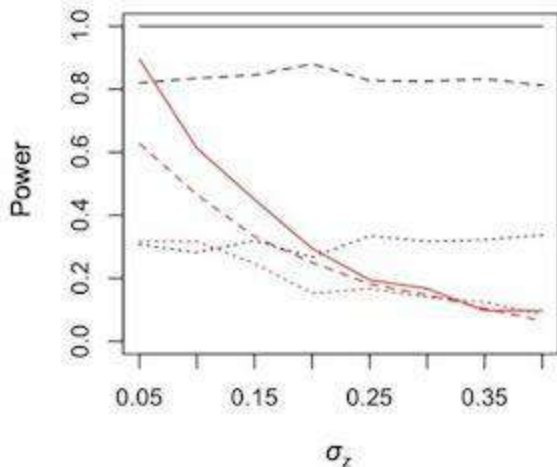


Fig 3. Simulations showing the power to detect a 50% treatment effect using linear regression methods (black) and $\delta SUVr$ (red) for three values of σ_z (.01, .02, .04). Setup: $n=60$ (treatment), $n=30$ (placebo), $\beta=.8$, $\alpha=.03$ (placebo), $\alpha=.015$ (treatment), 2-sided .05 level test.

Conclusion: Describing changes in target SUV's through a linear regression framework allows for statistical inference with power equal to or greater than that detectable through δSUV .

Keywords: florbetapir-PET, linear regression, SUVr, methodology

P14 Presented by: Clayton, David

Submission ID: 48

Effect of Cognitively Stimulating Activities on PiB-PET in Cognitively Normal Elderly

Ann Cohen¹, Beth Snitz², Eric McDade², Howard Aizenstein¹, Robert Nebes¹, Lisa Weissfeld³, Julie Price⁴, Chester Mathis⁴, Oscar Lopez², William Klunk^{1,2}

¹ University of Pittsburgh School of Medicine, Department of Psychiatry, Pittsburgh, Pa, United States

² University of Pittsburgh School of Medicine, Department of Neurology, Pittsburgh, Pa, United States

³ Statistics Collaborative, Washington, D.C., United States

⁴ University of Pittsburgh School of Medicine, Department of Radiology, Pittsburgh, Pa, United States

Postmortem studies have shown that brain amyloid-beta (Ab) is present in 25-50% of cognitively normal elderly control subjects and Pittsburgh Compound-B (PiB) PET studies have shown similar findings in vivo. PiB retention in some controls can be as high as that observed in Alzheimer's disease (AD). An overarching question from these findings is why, in the face of substantial amyloid burden, some people develop AD and others remain normal. To that end, enriched lifestyle has been reported to confer resistance to development of dementia but the effect on Ab remains unclear. The present study explored the effects of participation in cognitively stimulating activities on PiB retention in a group of cognitively normal adults

Cognitively normal elderly controls (n=110; age: 82.7±6.6y; education: 14.8±2.7y) underwent PiB-PET and the Florida Cognitive Activity Scale. PiB SUVR (50-70 min) was then analyzed on both an ROI and voxel-wise basis using SPM8.

A significant negative correlation was observed between global cortical PiB retention and participation in cognitively stimulating activities ($r=-0.304$, $p<0.001$), this correlation remained significant after correction for age ($r=-0.228$, $p=0.01$). Further, when subjects were split into quartiles based on participation in cognitively stimulating activities, PiB retention was significantly higher ($p<0.01$) in subjects with lower participation in cognitively stimulating activities, however, when corrected for age this relationship only reached a trend level ($p=0.071$). Additionally, a voxel-wise analysis in a subset of subjects revealed that participation in highly stimulating cognitive activities was associated with significantly lower PiB retention in several cortical regions ($p<0.01$), including frontal, parietal and precuneus.

These data suggest that participation in cognitively stimulating activities is associated with reduced Ab in the cortical brain regions. It remains unclear, however, if participation in stimulating activities decreases as a result of increasing Ab or if cognitively stimulating activities may confer a resistance to Ab deposition.

P16 Presented by: Cohen, Ann D

Submission ID: 84

P18

Methods for the Quantitation of AV-1451 Uptake

Mintun

Michael Devous, Sr, Abhinay Joshi, Ian Kennedy, Michael Navitsky, Michael Pontecorvo, Mark

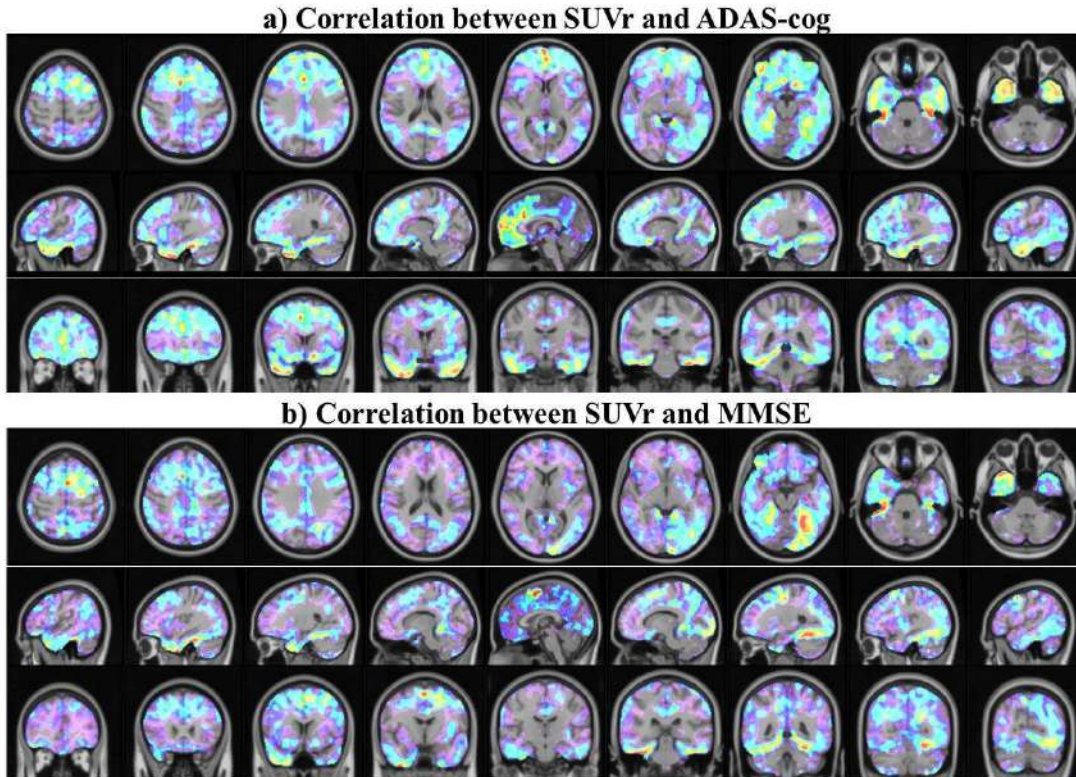
Avid Radiopharmaceuticals, Inc., Philadelphia, PA, United States

Background: 18F-AV-1451 is a PET tracer for assessment of neurofibrillary tau pathology. Understanding the impact of tau pathology on cognition or exploring longitudinal changes in AV-1451 uptake may require quantitation methods that reflect both the amplitude and extent of regional tracer distribution.

Methods: 18F-AV-1451 data were acquired 80-100 min post injection in 156 subjects [14 young clinically normal controls (YCN), 39 older controls (OCN), 70 Mild Cognitive Impairment (MCI) and 33 Alzheimer's Disease (AD)]. SUVR was calculated on a voxel-wise basis and for AAL VOIs across neocortical and mesial temporal lobe regions. Quantitative measures were evaluated for diagnostic group separation and for correlation to cognitive scores (ADAS cog and MMSE). Evaluations were conducted for VOIs, voxel-wise SUVR-thresholded images, and z-score images (relative to YCN). Voxel-wise correlation images were obtained between SUVR and ADAS-cog or MMSE. Both intensity-based and an extent-based metrics were employed. Finally, SUVR images were entered into a multi-block discriminant analysis (MUBADA) to identify regions providing maximal diagnostic group separation (YCN, OCN, MCI AD and A β ⁺ vs. A β ⁻ subgroups, florbetapir SUVR > 1.10 considered A β ⁺).

Results: Both intensity and extent metrics showed differences between diagnostic groups only for certain regions. MMSE was more strongly correlated to posterior regions, while ADAS-cog was more strongly correlated to a combination of temporal and frontal regions (figure 1).

Figure 1: Correlation between SUVR and cognitive scores
(images are overlaid on MRI and scaled $0.1 \leq r \leq 0.5$)



MUBADA identified 2 dimensions that explained 97% of the variance in regional image pattern between groups (figure 2).

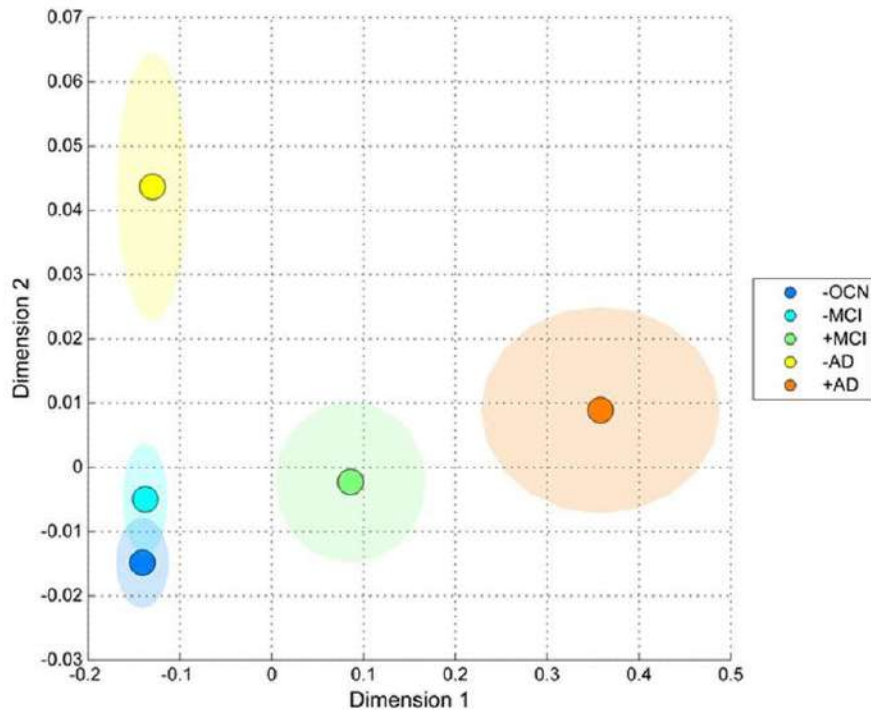


Figure 2. MUBADA of subjects (excluding YCN and A β + OCN). Input data were SUVR images, no quintile normalization was applied.

Dimension 1 separated A β + MCI and AD from all other groups, and Dimension 2 separated A β - AD from A β - MCI and OCN.

Conclusions: Intensity and extent metrics differ between groups for some regions, and voxel values correlated with cognition. Discriminant analyses provided additional power to understand group differences related to both amyloid and tau pathology.

Keywords: *tau, PET, T807, AV-1451, neurofibrillary tangles*

P18 Presented by: Devous, Sr, Michael D

Submission ID: 100

P20

[F18] T807 PET Imaging of Hyperphosphorylated Tau to Differentiate PSP from PD

Stephen Gomperts, Sara Makaretz, Aaron Shultz, Christina Caso, Scott McGinnis, John Growdon, Brad Dickerson, Keith Johnson

Massachusetts General Hospital, Boston, MA, United States

Background: Distinguishing progressive supranuclear palsy (PSP) from idiopathic Parkinson disease (PD) is often difficult, especially early in their course. Early stage clinical phenotypes often fail to fulfill classical diagnostic criteria, which continue to evolve as our understanding of clinicopathologic relationships deepens. The defining neuropathological lesions of PSP are region-specific neurofibrillary tangles, composed of paired helical filaments (PHF) and glial inclusions of 4-repeat tau isoforms. In contrast, PD is characterized by alpha-synuclein aggregates, although NFT accumulation has been observed in PD dementia. We are evaluating the potential of [F18]T807 PET imaging of PHF-tau as a biomarker for the 4-repeat tauopathies.

Methods: To date, 4 PSP subjects and 4 PD subjects have undergone standardized neurologic examinations, [F18]T807 and [C11]PiB PET, and MRI. [F18]T807 retention was expressed as the SUVR using the cerebellar grey matter, although comparisons with other reference regions are underway. [C11]PiB retention was expressed as the distribution volume ratio with cerebellar reference. PET data were spatially transformed to MNI space. PSP and PD group [F18]T807 SUVR data were compared statistically using Freesurfer to that of a group of 19 similarly aged healthy control subjects (HCS) with negligible cortical PiB retention.

Results: [F18]T807 binding was elevated in globus pallidus, anterior putamen, internal capsule, midbrain/subthalamic region, deep cerebellar nuclei, and frontal cortex in PSP compared to HCS ($p < 0.05$, uncorrected). Regional [F18]T807 was anatomically variable across PD cases, and the map comparing the PD group to HCS did not reveal consistent differences. Cortical [C11]PiB binding was negligible in the PSP cases and variable in PD cases.

Conclusions: Our preliminary data in a small number of subjects suggest that the anatomy of [F18]T807 binding in PSP appears to be compatible with the known anatomic distribution of PHF-tau in PSP. The significance of elevated [F18]T807 retention in some PD subjects is the subject of ongoing investigation.

Keywords: *T807,tau,PSP,PD,amyloid*

P20 Presented by: Gomperts, Stephen N.

Submission ID: 118

Comparison of NIA-AA Staging with CSF and Neuroimaging Biomarkers

Brian Gordon^{1,2}, Stephanie Vos³, John Morris^{2,4}, David Holtzman^{2,4,5}, Anne Fagan^{2,4,5}, Tammie Benzinger^{1,2}

¹ Washington University in St. Louis Department of Radiology, St. Louis, Missouri, United States

² Washington University in St. Louis Knight Alzheimer's Disease Research Center, St. Louis, Missouri, United States

³ Maastricht University Department of Psychiatry and Neuropsychology, Maastricht, Limburg, Netherlands

⁴ Washington University in St. Louis Department of Neurology, St. Louis, Missouri, United States

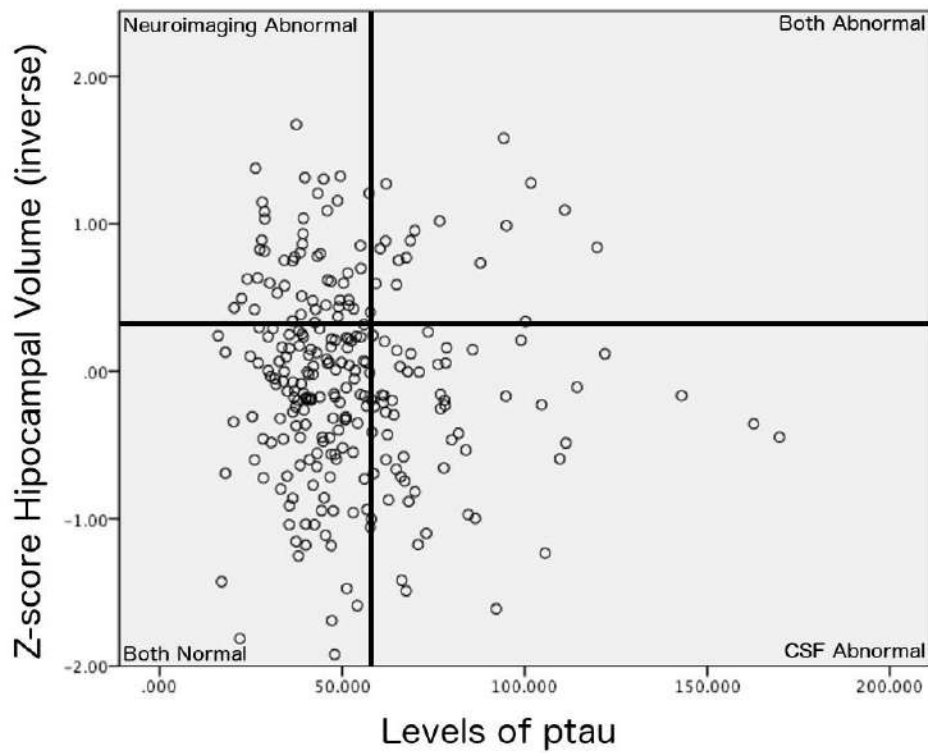
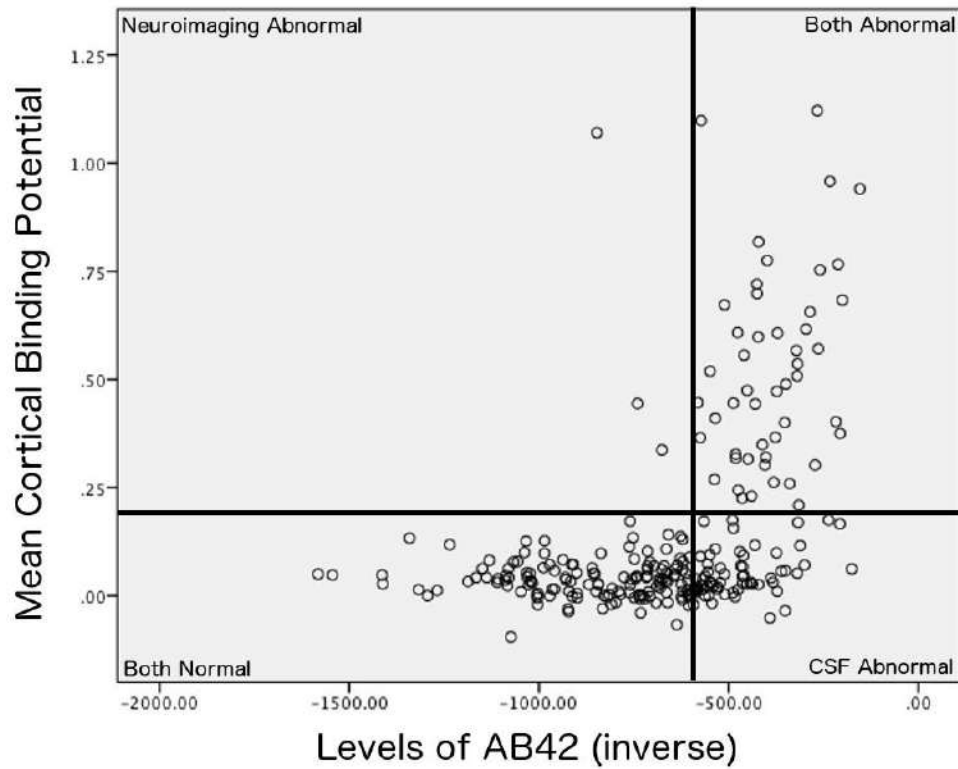
⁵ Washington University in St. Louis Hope Center for Neurological Disorders, St. Louis, Missouri, United States

Background: Using the National Institute of Aging and Alzheimer's Association (NIA-AA) criterion, cognitively normal individuals can be classified into preclinical stages using cerebrospinal fluid (CSF) assays and neuroimaging techniques. Prior work has utilized either CSF or a limited set of neuroimaging biomarkers, but no analyses have taken an integrated approach. In a population of cognitively normal adults we examined amyloid PET, hippocampal volume, and CSF measures of A β 42, tau, and ptau. We contrasted the congruency between neuroimaging and CSF biomarkers, and looked at the longitudinal predictive value of each set of biomarkers on cognition.

Methods: Participants consisted of 258 cognitively normal individuals with a Clinical Dementia Rating (CDR) of 0 at baseline (mean age=66.8, range 45.6-88.8, females=154). Subjects had CSF assays, PET amyloid imaging, and a structural MRI within 24 months of one another (mean lag 6.4 months, range 0-24), and a minimum of one longitudinal clinical assessment (mean 3.9 years of follow up, range .7-9.3). For each biomarker subjects were classified as normal or abnormal using cutoffs derived from an ROC analysis comparing the current cohort against very mildly demented individuals (CDR=0.5). Subtle cognitive decline was determined as the lowest 10% of individuals on a z-score composite of three neuropsychological tests. Subjects were then classified according to NIA-AA staging.

Results: There was a high concordance of abnormal classification between amyloid measured with CSF and PET (82%) but only a modest agreement between hippocampal volume and measures of tau (51%) and ptau (54%). When following individuals longitudinally, there was a greater rate conversion to dementia in more advanced NIA-AA stages defined using either CSF and neuroimaging biomarkers.

Conclusions: NIA-AA staging serves as a useful framework to divide preclinical phases leading to Alzheimer's disease. While both have predictive value, classifications by CSF and neuroimaging markers are not always concordant.



Keywords: *Alzheimer's, biomarkers, NIA-AA, PET, CSF*

P22 Presented by: **Gordon, Brian A**

Submission ID: 112

P24

In vitro and In vivo Evaluation of RO6931643, RO6924963 and RO6958948 Candidate PET Tracers for Aggregated Tau

Michael Honer¹, Henner Knust¹, Luca Gobbi¹, Hiroto Kuwabara², Dieter Muri¹, Heather Valentine², Robert Comley¹, Susanne Ostrowitzki¹, Robert Dannals², Dean Wong², Edilio Borroni¹

¹ Roche Pharmaceutical Research and Early Development, Roche Innovation Center Basel, Basel, N/A, Switzerland

² The Johns Hopkins University School of Medicine, Department of Radiology, Nuclear Medicine – PET Center, Baltimore, MD, United States

Objectives: Tau aggregates and A β plaques are key histopathological features in AD and are considered as targets for therapeutic intervention as well as biomarkers for diagnostic in vivo imaging agents. This study describes the in vitro and in vivo characterization of three novel compounds that bind specifically to tau aggregates and have potential to become PET tracers.

Methods: RO6931643, RO6924963 and RO6958948 were identified as high affinity competitors at the [3H]T808 binding site on tau aggregates in late stage AD brain tissue. Binding of tritiated compounds to tissue sections of AD patients was analyzed by autoradiography and co-staining of tau aggregates and Ab plaques using specific antibodies. Following identification and in vitro characterization all three tracer candidates were radiolabeled with a PET nuclide and tested in baboons. Since the baboons used for this experiment are considered devoid of any significant tau load, this experiment aimed solely to assess brain uptake, clearance and metabolism.

Results: [3H]RO6931643, [3H]RO6924963 and [3H]RO6958948 bound with high affinity and specificity to tau aggregates, clearly lacking affinity for concomitant A β plaques in human AD Braak V tissue sections. Radioligand specificity for tau aggregates was supported by binding patterns in AD brain sections comparable to the established radioligand [3H]T808, low nonspecific binding in healthy brain tissue as well as macroscopic and microscopic co-localization of radioligand binding and tau-antibody staining. RO6931643, RO6924963 and RO6958948 were successfully radiolabeled with a PET nuclide to high specific activity, radiochemical purity and yield. Following intravenous administration in baboons, [11C]RO6931643, [11C]RO6924963 and [18F]RO6958948 PET scans indicated good brain entry, rapid washout and a favorable metabolic pattern.

Conclusions: [11C]RO6931643, [11C]RO6924963 and [18F]RO6958948 are promising PET tracers for visualization of tau aggregates in AD and other tauopathies. Validation of these tracer candidates in healthy controls and patients with AD is currently ongoing (ClinicalTrials.gov Identifier: NCT02187627).

P24 Presented by: Honer, Michael

Submission ID: 34

P26

Development of a CAA Selective Radioligand for PET Imaging: a Preclinical Study in PSAPP Mice

Milos Ikonomic, Eric Abrahamson, Manik Debnath, Lan Shao, Li Shao, Guo-Feng Huang, William Paljug, James Ruszkiewicz, William Klunk, Chester Mathis

University of Pittsburgh, Pittsburgh, PA, United States

Background: Cerebral amyloid angiopathy (CAA) is a major neuropathological feature of Alzheimer's disease (AD) and is linked to increased incidence of intracerebral hemorrhage. Therefore, developing a PET radiotracer selective for CAA would be beneficial for specifically detecting and following this pathology *in vivo*.

Methods: Eleven hydrophilic fluorescent compounds with methoxy groups to allow future C-11-radiolabeling were synthesized, tested for high-affinity binding to A β fibrils, and individually injected into 10-12 month old transgenic PSAPP mice. Fifteen minutes after injection, mice were exsanguinated and euthanized, and brains were removed, immersion-fixed in 4% paraformaldehyde, cryoprotected in sucrose, and sectioned on a freezing sliding microtome in coronal plane into 40-microns thick sections. Sections were immediately mounted on histological slides and coverslipped without processing. Unprocessed sections were examined using fluorescent microscopy for detection of the injected compound. Images of entire sections (3 equally spaced coronal sections per animal) were captured and archived. The same sections were then processed using thioflavine-S histofluorescence and re-imaged using the same strategy as for the unprocessed sections.

Results: Comparison of images of unprocessed and thioflavin-S processed sections were evaluated to determine compound localization in 1) large leptomeningeal (i.e., pial) arteries, 2) penetrating cortical (i.e., parenchymal) arterioles and capillaries, and 3) parenchymal plaque deposits in brains of PSAPP mice. Tested compounds showed variable retention in the three locations of interest. Three lead compounds localized preferentially to amyloid deposits in pial vessels along the surface of the brain and the cerebral sulci and to a lesser extent to amyloid deposits in parenchymal vessels, and demonstrated minimal binding to parenchymal plaques.

Conclusion: Three lead compounds identified in this study selectively detected CAA over parenchymal A β plaques in PSAPP mice and might be promising candidates for CAA-specific radiotracers, which could be further tested in human clinical trials.

P26 Presented by: Ikonomic, Milos

Submission ID: 124

P28

Amyloid Negativity in Progressive Cognitive Decline: Is it a Safety or a Risk for Alzheimer's Disease?

Kenji Ishii, Kenji Ishibashi, Muneyuki Sakata, Kei Wagatsuma, Jun Toyohara, Kiichi Ishiwata, Shigeo Murayama

Tokyo Metropolitan Geriatric Hospital and Institute of Gerontology, Tokyo, Japan

A negative amyloid PET scan is inconsistent with a neuropathological diagnosis of Alzheimer's disease at the time of image acquisition, however it does not guarantee to escape Alzheimer's disease in the future. We often observe multiple-pathology in the neuropathological examination in the autopsy series of dementias in elderly-elders. Our hypothesis is that an existence of certain non-Alzheimer type neurodegenerative disorder can induce and/or accelerates amyloid pathology to develop a "secondary" Alzheimer's disease. To test this hypothesis, we examine the longitudinal amyloid deposition in amyloid negative subjects with progressive cognitive declines.

We studied 15 PiB negative patients with progressive cognitive decline, including 10 MCI subjects and five dementia patients. Annual follow up of PiB-PET scan was performed for three years. The PiB-PET images acquired 50-70 min post injection were co-registered to individual MRI data of same visit, and automated VOI analysis were performed using DARTEL template, standard set of volumes of interest, and cerebrospinal fluid volume correction. The mean cortical uptake (mcSUVR) was calculated as the average of composite VOIs. We set the cut off level of mcSUVR for PiB positivity at 1.5.

In the follow up observation, 3 MCI subjects and 2 dementia patients turned out to be PiB positive. The averaged annual rate of mcSUVR increase in those subjects was 4.9%. It was significantly higher than the averaged annual increase rate of 2.3% in PiB positive MCI and AD in our previous study. The FDG-PET images of those incidental PiB positive subjects initially showed non-AD type hypometabolism, but overlapped by AD type hypometabolism after PiB positive conversion. Our results suggest that non-Alzheimer neurodegeneration may induce "secondary" Alzheimer's disease with more rapid progression than sporadic cases. Further studies are required in larger sample size longer observation to clarify the details of overlapping pathology.

P28 Presented by: Ishii, Kenji

Submission ID: 102

P30

In vivo Competition between [11C]PiB and NAV4694 in a Transgenic Rat Model of Amyloidosis

Min Su Kang^{1,2}, Maxime Parent^{1,2}, Eduardo Zimmer^{1,2}, Monica Shin^{1,2}, Sonia Carmo⁵, Antonio Aliaga⁴, Cornelia Reininger⁶, Jean-Paul Soucy⁴, Serge Gauthier², A. Claudio Cuello⁵, Pedro Rosa-Neto^{1,2,3,4,5}

¹ Translational Neuroimaging Laboratory, Verdun, Quebec, Canada

² McGill Center for Studying in Aging, Verdun, Quebec, Canada

³ Brain Imaging Centre - Douglas Research Centre, Verdun, Quebec, Canada

⁴ McConnell Brain Imaging Centre - McGill University, Montreal, Quebec, Canada

⁵ Department of Pharmacology - McGill University, Montreal, Quebec, Canada

⁶ Navidea Biopharmaceuticals Inc., Dublin, OH, United States

Background: Pittsburgh compound B ([11C]PiB) is used to track and detect brain amyloidosis for Alzheimer's Disease (AD). Considering its importance, there have been many new agents developed that are generally comparable with those of [11C]PiB such as [18F]NAV4694. However, the comparison in the binding sites of the two agents is still elusive. We aimed to measure the competitive binding of [11C]PiB by cold NAV4694 in the McGill-R-Thy1-APP rat expressing human amyloids. We hypothesized a dose-dependent blocking effect of NAV4694 on [11C]PiB specific binding.

Methods: A total of four male Tg rats (19 months) were scanned: first using [11C]PiB only and second time with either 12nmol/kg (n = 2) or 200nmol/kg (n = 2) of NAV4694 (precursor provided by Navidea Biopharmaceuticals Inc.) injection 15 minutes prior to the scan. Binding potential (BPND) maps were generated using Simplified Reference Tissue Method with the cerebellum as a reference region. The effect of NAV4694 blockage was measured as the percentage difference of BPND at the voxel level.

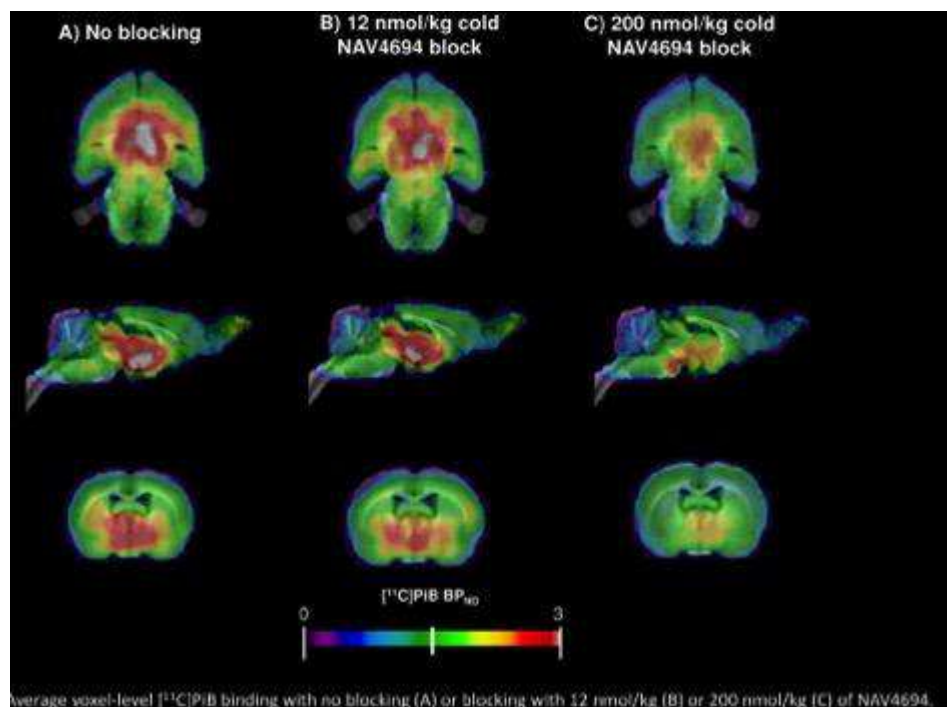
Results: 12nmol/kg dose significantly reduced 5-13% of [11C]PiB BPND across the cortical mantle compared to no blocking. 200nmol/kg dose induced widespread blocking of [11C]PiB binding, with an average of [11C]PiB BPND reduction of 23.2% in the frontal cortex, 9.7% in the parietal and temporal cortices, 14.7% in the hippocampus, 24.2% in the striatum and 20% in the thalamus.

Discussion: The results reveal at least a partial overlap between the binding sites of [11C]PiB and NAV4694. However, the high doses of cold competitor injection did not meet the expected degree of reduction (5 and 83.3 times the dissociation constant Kd of NAV4694, respectively). This may suggest that there is high levels of non-specific binding of the amyloid radioligands in this animal model, or that [11C]PiB and [18F]NAV4694 bind to different sites or conformations of amyloid.

Keywords: *In vivo* PET, amyloid, [11C]PiB, [18F]NAV4694, competitive binding

P30 Presented by: Kang, Min Su

Submission ID: 116



P32**Investigating the Utility of FDG and AV45 PET in both Two-classification and Multi-classification of Alzheimer's Disease and Its Prodromal Stages**

Chunfei Li¹, Qi Zhou¹, Mohammed Goryawala², Mercedes Cabrerizo¹, David Loewenstein³, Warren Barker⁴, Ranjan Duara⁴, Malek Adjouadi¹

¹ Center for Advanced Technology and Education, Florida International University, Miami, FL, United States

² University of Miami, Miller School of Medicine, Department of Radiology, Miami, FL, United States

³ Psychological Services and Neuropsychology Laboratory, Mount Sinai Medical Center, Miami, FL, United States

⁴ Wien Center for Alzheimer's Disease & Memory Disorders, Mount Sinai Medical Center, Miami, FL, United States

Objective: This study aim to explore the independent and interactive effects of the two commonly used ¹⁸F amyloid radiotracers on the diagnosis of Alzheimer Disease (AD) and its prodromal stages (EMCI and LMCI) from cognitive normal (CN). It is also aimed to examine diagnostic power of the two PET radiotracers using multi-group classification.

Methods: Two-way ANOVA was performed to determine the contribution of each radiotracer and identify if there is a significant interaction effect between them. The features used in this method are the average FDG-PET for 5 ROIs (FDG_bl), and the average AV45 SUVR for 4 ROIs (AV45_bl). Then, support vector machine (SVM) using the Gaussian radial basis function was applied to FDG data (five ROIs and whole brain), AV45 data (4 ROIs and 3 reference regions) and the combination of both, for two-group as well as multi-group classification with a 10-fold cross-validation.

Results: The results indicate that the effect of the AV45 is significant when using both additive and non-additive multiple linear regression models, where the additive model considers the effect of the AV45 and FDG independently, and the non-additive model considers the AV45, FDG and their interactive effect (Table 1). On the other hand, the effect of the FDG is shown to be significant only when using the additive model. Results also show that there exists a significant interaction effect between the AV45 and FDG. The classification experiments shows that the main accuracy based on FDG is larger than AV45, except for CN vs. LMCI and CN vs. EMCI (Table 2).

Conclusions: The two ¹⁸F amyloid radiotracers are highly correlated with respect to the diagnosis while FDG is preferred in both two-group classification and multi-group classification over AV45. When using both two-group and multi-group classifications, results indicate that combining FDG and PET improves slightly the classification accuracy.

Table 1. P-values of Two-way ANOVA

PET radiotracers	Non- additive model	Additive model
	$lm(DX \sim AV45_bl + FDG_bl + AV45_bl * FDG_bl)$	$lm(DX \sim AV45_bl + FDG_bl)$
AV45	< 0.001	< 0.001
FDG	0.105	< 0.001
Interaction	< 0.001	N/A

Table 2. Accuracy of SVM using 10-fold cross validation (%)

	AV45	FDG	AV45 and FDG
Two-group Classification			
CN vs. AD	83.59	90.11	92.6712
CN vs. LMCI	74.42	71.47	75.438
CN vs. EMCI	65.09	61.17	62.99
EMCI vs. AD	81.16	88.23	87.08
EMCI vs. LMCI	68.06	70.32	70.65
LMCI vs. AD	62.39	73.93	74.45
Multi-group Classification			
CN vs. EMCI vs. LMCI vs. AD	45.64	48.06	50.4

Keywords: Alzheimer's Disease, AV45 PET, FDG PET, Classification

P32 Presented by: Li, Chunfei

Submission ID: 122

P34

Differential Cortical Ribbon Binding of Amyloid and Tau Tracers in Alzheimer's disease

Yi Li¹, Wai Tsui¹, Henry Rusinek¹, Nobuyuki Okamura², Mony de Leon¹, et al.

¹ NYU MEDICAL CENTER, new york, NY, United States

² Tohoku University School of Medicine, Sendai, Miyagi Prefectur, Japan

Neurofibrillary tangles (NFT) and amyloid beta (A β) plaques, the two characteristic lesions of Alzheimer's disease (AD) show different spatial distributions within neocortical lamina. Amyloid plaques are dispersed throughout the width of the cortical ribbon whereas NFT pathology tends to be located in inferior lamina, closer to the white matter boundary. Using PET radiotracers for A β and tau lesions, we developed an image analysis tool to measure the distance of tracer-positive voxels to the gray-white matter junction. In a study of 5 AD and 5 normal subjects who received both 11C-PiB and 18F-THK5117 PET, we observed that the distribution of A β positive voxels was more widely distributed relative to the THK (tau) positive voxels. The average A β distance was further from the white matter than for tau positive voxels. This effect was found for all subjects and for all regions, even after adjusting for regional non-specific white matter binding of the tracers. The differential tracer binding measurements were validated at post mortem. This distance metric may be of value in testing tau and other tracers for their anatomical selectivity. There may also be potential value in examining other neurodegenerative disorders, such as chronic traumatic encephalopathy where the post mortem distributions of tau pathology are more superficial than those of AD.

Keywords: *amyloid plaques, neurofibrillary tangles*

P34 Presented by: Li, Yi

Submission ID: 52

P36**Increased PiB Accumulation Occurs in the White Matter of PiB Positive Subjects**

Val Lowe, Matthew Senjem, Scott Przybelski, Stephen Weigand, David Knopman, Bradley Boeve, Kejal Kantarci, Clifford Jack, Ronald Petersen

Mayo Clinic Foundation, Rochester, MN, United States

Background: C-11 PiB binds to brain white matter (WM) by unclear mechanisms. It is a prominent finding in all subjects. It is important to understand any potential variability in PiB WM binding to assess the suitability of WM as a normalization region. We hypothesized that PiB binding to WM may vary in subjects and therefore we evaluated PiB negative and PiB positive subjects for differences in WM PiB uptake.

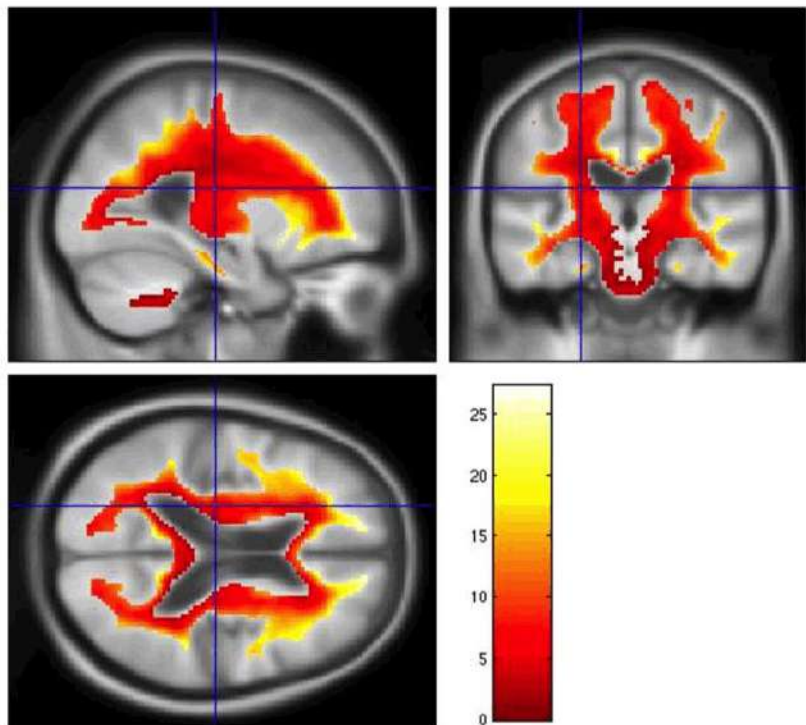
Methods: WM PiB uptake in subjects that were AD PiB-positives (n=61) and MCI PiB-positives (n=188) was compared to the WM PiB uptake in aged-matched PiB-negative CN subjects (n=249). WM PiB uptake in PiB-positive CN subjects (n=402) was also compared to PiB-negative CN subjects (n=804). SPM analysis was performed to assess differences in white matter uptake in PiB positive groups as compared to PiB negative groups. Within each analysis, an explicit mask created by averaging the WM segmentations from MRI across all subjects and thresholding at a value of 0.6 was used to restrict the analysis to WM regions. An FDR correction for multiple comparisons and a $p < 0.05$ threshold was used.

Results: Significantly elevated PiB uptake was seen in the WM of all PiB positive groups as compared to their matched PiB negative reference groups. The elevated uptake of PiB was diffuse throughout the WM without any particular regional variations. (Figure 1)

Conclusions: Elevated PiB uptake in WM structures is a characteristic of all PiB positive AD, MCI and CN groups relative to PiB negative subjects. This finding may be an important consideration in selection of normalization regions for quantitation of amyloid PET. The mechanism of elevated PiB uptake in the WM in PiB positive cases is under investigation. While other PET amyloid imaging drugs may follow this same pattern of increased uptake, this will need to be confirmed in further studies.

Figure 1. White matter PiB uptake in PiB positive CN subjects that is greater than PiB negative CN subjects seen as heat-scale increasing intensity and shown in three orthogonal views of a standard MRI template and shown within an explicit WM mask. (FDR corrected, $p < 0.05$)

P36 Presented by: Lowe, Val J



Regional Dynamics of Local Amyloid Burden on Hypometabolism in 24-month Follow-up

Sulantha Mathotaarachchi^{1,5}, Sara Mohades¹, Thomas Beaudry¹, Monica Shin^{1,5}, Seqian Wang^{1,5}, Andrea Benedet^{1,5}, Tharick Pascoal^{1,5}, Maxime Parent^{1,5}, Min Kang^{1,5}, Vladimir Fonov^{1,5}, Sarinporn Manitsirikul¹, Serge Gauthier⁶, Aurélie Labbe^{3,4}, Pedro Rosa Neto^{1,2}

¹ Translational Neuroimaging Laboratory, McGill Centre for Studies in Aging, Douglas Mental Health University Institute., Montreal, Quebec, Canada

² Department of Neurology & Neurosurgery and Psychiatry, McGill University., Montreal, Quebec, Canada

³ Department of Epidemiology, Biostatistics & Occupational Health, McGill University., Montreal, Quebec, Canada

⁴ Douglas Mental Health University Institute., Montreal, Quebec, Canada

⁵ Department of Neurology & Neurosurgery, McGill University., Montreal, Quebec, Canada

⁶ Alzheimer's Disease Research Unit, McGill Centre for Studies in Aging, Douglas Mental Health University Institute., Montreal, Quebec, Canada

Rationale: The longitudinal analysis of co-localized biomarkers might provide further insights regarding direct effects of amyloidosis on tissue glucose metabolism. We developed a surface based analysis to assess such interactions across the spectrum of clinical manifestations of Alzheimer's disease.

Aims and Hypothesis: Here we investigated the regional effects of amyloid burden on neurodegeneration in 24-month follow-up by using vertex-based linear regression models. We hypothesized stage-dependent regional effect of amyloid retention on the rate of glucose metabolism.

Methods: [18F]FDG and [18F]Florbetapir PET images were acquired 24 months apart from 214 subjects (65 Cognitively Normal [CN], 111 Early Cognitive Impairment [EMCI], 19 Late Cognitive Impairment [LMCI], 19 Alzheimer's Disease [AD]) from the Alzheimer's Disease Neuroimaging Initiative (ADNI) database. The respective standardized uptake value ratio (SUVR) maps were subsequently generated using cerebellar grey-matter and pons as reference regions for [18F]Florbetapir and [18F]FDG PET images, respectively. [18F]Florbetapir SUVR maps were normalized for the average white-matter SUVR uptake and the [18F]FDG SUVR maps were normalized for the average full brain uptake. The effects of [18F]Florbetapir on rate of metabolism were computed using a vertex-based multivariate linear regression models correcting for baseline glucose metabolism, age, gender and APOE genotype.

Results: In 24 month observation period, the rate of metabolism is not affected by the baseline [18F]Florbetapir load in CN and EMCI. However, at LMCI and AD stage [18F]Florbetapir load shows a linear relationship with the rate of metabolic decline in temporo-parietal areas and precuneus (Figure 1).

Rate of Hypo-metabolism ~ Age + APOE4 + Baseline Amyloid Load + Baseline Glucose Metabolism + Gender

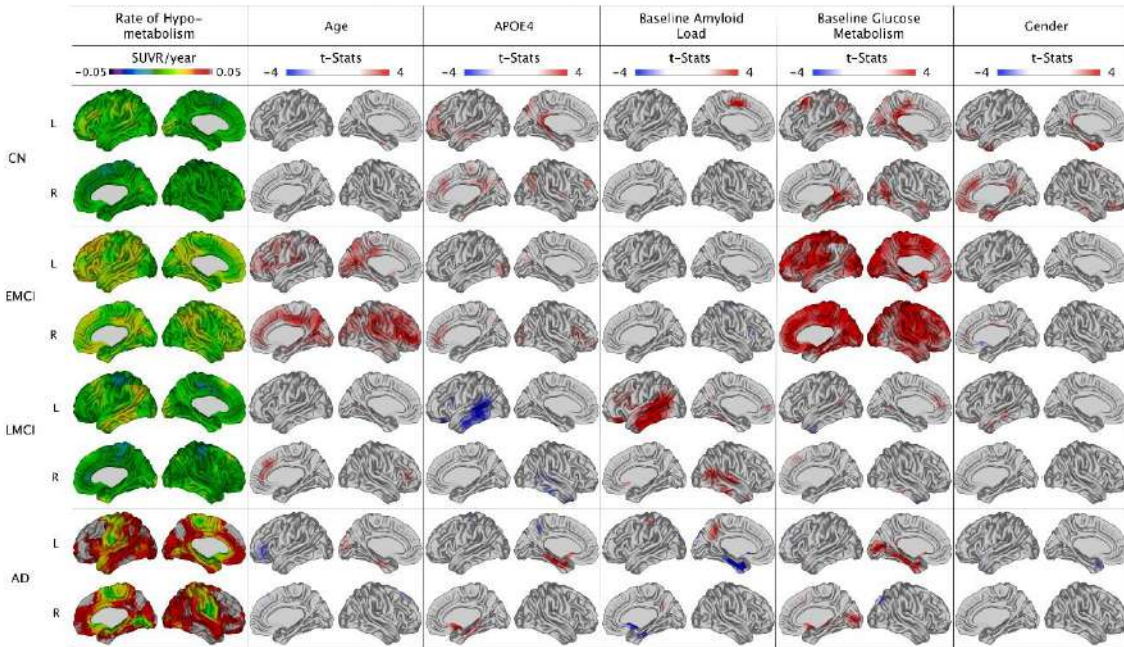


Figure 1: Vertex-based multivariate linear regression model explaining the effect of amyloid load on the rate of hypo-metabolism in each disease stage, corrected for baseline glucose metabolism, age, gender and apoe genotype. Only LMCI and AD stages show positive effect from amyloid load on hypo-metabolism in temporo-parietal and precuneus regions.

Discussion

Lack of effect in CN and EMCI indicates that regional brain glucose metabolism is independent to the local amyloid concentrations. In contrast, in LMCI and AD stages, the rate of hypo-metabolism at temporo-parietal areas as well as in precuneus depend on the local tissue amyloid burden.

Keywords: *amyloid, glucose metabolism, alzheimer's disease, pet*

P38 Presented by: Mathotaarachchi, Sulantha

Submission ID: 120

P40

Early Striatal Binding of PiB-PET Amyloid Distinguishes Down's Syndrome and Autosomal Dominant Alzheimer Dementia Mutation Carriers From Late Onset Deposition

Eric McDade¹, Annie Cohen¹, Brad Christian², Julie Price¹, Chet Mathis¹, William Klunk¹, Ben Handen¹

¹ University of Pittsburgh, Pittsburgh, PA, United States

² University of Wisconsin, Madison, Wisconsin, United States

Background: The definitive mechanisms of fibrillar A β deposition remain to be identified. However, in AD there appears to be two major ages of onset, middle age and late-onset. The former is typically associated with genetic alterations (i.e. ADAD and DS) that results in an overproduction or altered processing of APP. Late-onset there is associated with an aberrant clearance of extracellular A β species. It is possible that these different groups might have differences patterns of A β deposition, as we previously demonstrated in ADAD with early striatal binding.

Methods: All subjects were non-demented. 23 DS subjects, age 44.8 years, global SUVR 1.70 \pm 0.33; 16 elderly subjects, age 75.6 years, global SUVR 1.79 \pm 0.33; and 13 ADAD mutation carriers, age 33 years, global SUVR 1.81 \pm 0.59 underwent PiB PET scans. All subjects were determined to be amyloid PiB positive based on cutoffs in any of 6 regions most commonly associated with AD using the cerebellum as a reference.

Results: Compared to the elderly non-demented group, both the DS and ADAD groups had significantly more amyloid deposition in the bilateral striatum. Between the DS and ADAD groups there was no increased amyloid deposition in the medial occipital cortex. There were no areas of increased amyloid deposition in the elderly non-demented group compared to the other groups.

Conclusion: Using amyloid PET we have identified a unique pattern of early fibrillar A β deposition in the bilateral striatum associated with both DS and ADAD – both associated with increased production of A β 1-42. This pattern of early striatal deposition could provide important information about the dynamics of cerebral amyloidosis.

Keywords: *Down's syndrome, Autosomal Dominant Alzheimer Dementia, striatum.*

P40 Presented by: McDade, Eric

Submission ID: 62

P44

Tau Imaging with 18F-(S)-THK-5117 in MCI and AD Patients Using a PET Multi-tracer Concept

Agneta Nordberg^{1, 5}, Konstantinos Chiotis¹, Laure Aubert¹, Anders Wall², My Jonasson², Mark Lubberink², Jonas Eriksson³, Ove Almkvist¹, Nobuyuki Okamura⁴, Gunnar Antoni²

¹ Karolinska Institutet, Center of Alzheimer Research, Translational Alzheimer Neurobiology, Stockholm, not applicable, Sweden

² PET center, Section of Nuclear Medicine & PET, Dept of Radiology, Oncology and Radiation Sciences, Uppsala University, Uppsala, not applicable, Sweden

³ Dept of Medicinal Chemistry, Preclinical PET platform, Uppsala University, Uppsala, not applicable, Sweden

⁴ Dept of Pharmacology, Tohoku University School of Medicine, Sendai, not applicable, Japan

⁵ Dept Geriatric Medicine, Karolinska University Hospital Huddinge, Stockholm, not applicable, Sweden

Objectives: Combination of different biomarkers will not only improve the understanding of AD disease mechanisms but will also probably be necessary for reliable clinical diagnosis. We therefore explore the possibility to visualize the pathological deposition of tau in different stages of AD as well as in other forms of dementia using the PET Tau tracer 18F-(S)THK5117, in order to better understand the temporal evolution of AD pathophysiology and the possible role of tau imaging as a new and early biomarker for AD progression and for evaluation of new drug targets.

Methods: Our multi-tracer PET concept includes 18F-(S) THK-5117 for imaging of tau as well as 11C-PIB for measurement of fibrillar amyloid plaques deposition and 18F-FDG for cerebral glucose metabolism. Patients with clinical diagnosis of AD, mild cognitive impairment (MCI), different non-AD dementia were included as well as healthy young and old controls. All patients were undergoing neuropsychology testing and CSF biomarker assays.

Results: A significant different regional pattern of retention of 18F-(S) THK-5117 was observed in brain of both MCI and AD patients in comparison to 11C-PIB retention and 18F-FDG uptake respectively. A variation in intensity of brain 18F-(S) THK-5117 retention was observed among MCI and AD patients and the pattern differed significantly from healthy controls. A correlation was also observed between 18F-(S)-THK-5117 retention and cognitive performance.

Conclusions: The introduction of novel tau PET imaging will provide a crucial new non-invasive tool for the investigation of neurofibrillary tangle pathology in vivo and moreover, most probably, shed light onto the underlying interrelationship of tau pathology with other aspects of the AD disease, such as cognitive decline and amyloid burden.

Keywords: *Tau, PET imaging, 18F-(S)-THK5117, 11C-PIB, 18F-FDG*

P44 Presented by: Nordberg, Agneta

Submission ID: 106

P46**Beta-amyloid Deposition is Associated with Increased Brain Activity during Working Memory and Executive Control Tasks among Cognitively Normal Elderly**

Hwamee Oh^{1,2}, Jason Steffener^{1,2}, Ray Razlighi^{1,2}, Christian Habeck^{1,2}, Dan Liu², Sarah Janicki^{1,2}, Yaakov Stern^{1,2}

¹ Department of Neurology, Columbia University, New York, NY, United States

² Taub Institute for Research on Alzheimer's disease and the Aging Brain, Columbia University, New York, NY, United States

The accumulation of beta amyloid ($A\beta$) peptides, a pathological hallmark of Alzheimer's disease, has been associated with functional alterations in cognitively normal older adults, most often in the context of episodic memory tasks. Using functional magnetic resonance imaging (fMRI), we examined whether functional alterations as a form of hyperactivation would be present when cognitively normal older adults are engaged in working memory (WM) and executive control (EXE) tasks, which recruit frontal and parietal cortices. Forty-two young and 57 cognitively normal older adults underwent fMRI sessions with 2 types of tasks: (1) Letter Sternberg task in which 1, 3, or 6 letters were presented as study stimuli, followed by a 7-sec retention phase until a probe letter appeared for subjects to respond; (2) executive contextual task in which subjects were given a single (either letter case or vowel/consonant judgment task) or a dual (switching between letter case and vowel/consonant decisions) task. Older subjects additionally completed 18F-Florbetaben positron emission tomography (PET). Based on an averaged cortical standardized uptake value ratio (SUVR) using a gray matter cerebellum reference region, older subjects were grouped into either amyloid-positive ($A\beta+$) or amyloid-negative ($A\beta-$), resulting in 43 as $A\beta-$ and 14 as $A\beta+$. Consistent with previous reports, age-related increases in brain activity was found in WM and EXE brain networks. In addition, $A\beta$ -related activity increases were observed in brain regions that are commonly recruited by all subjects during these tasks (Fig. 1). Furthermore, $A\beta$ -related increased activity was found in brain regions that were not part of commonly recruited brain networks, perhaps suggesting some compensatory activation (Fig. 2). The present results of $A\beta$ -related brain activity increases in the fronto-parietal control networks suggest that $A\beta$ -related functional alterations are not specific to the long term memory system but influence the neural systems supporting working memory and executive function as well.

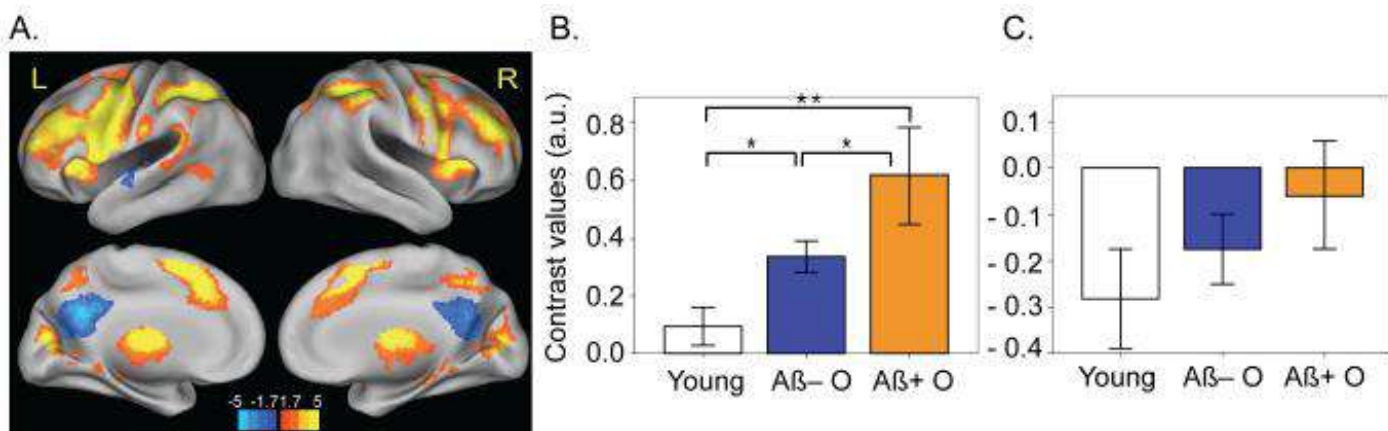


Figure 1. Age and $A\beta$ deposition are associated with increased brain activity in a verbal working memory brain network common across all subjects. (A) Brain regions demonstrating activation and deactivation in relation to working memory load (1, 3, or 6 letters) during a retention phase of the letter Sternberg task. Warm colors indicate activation and cool colors indicate deactivation. Results are thresholded at $p<0.05$, cluster corrected for multiple comparisons. (B) Plots display mean contrast values of significant clusters showing load-related increases in activation (i.e., warm colored regions in panel A) for each group. (C) Plots display mean contrast values of significant clusters showing load-related increases in deactivation (i.e., cool colored regions in panel A) for each group. Error bars represent s.e.m. * $p<0.05$; ** $p<0.01$

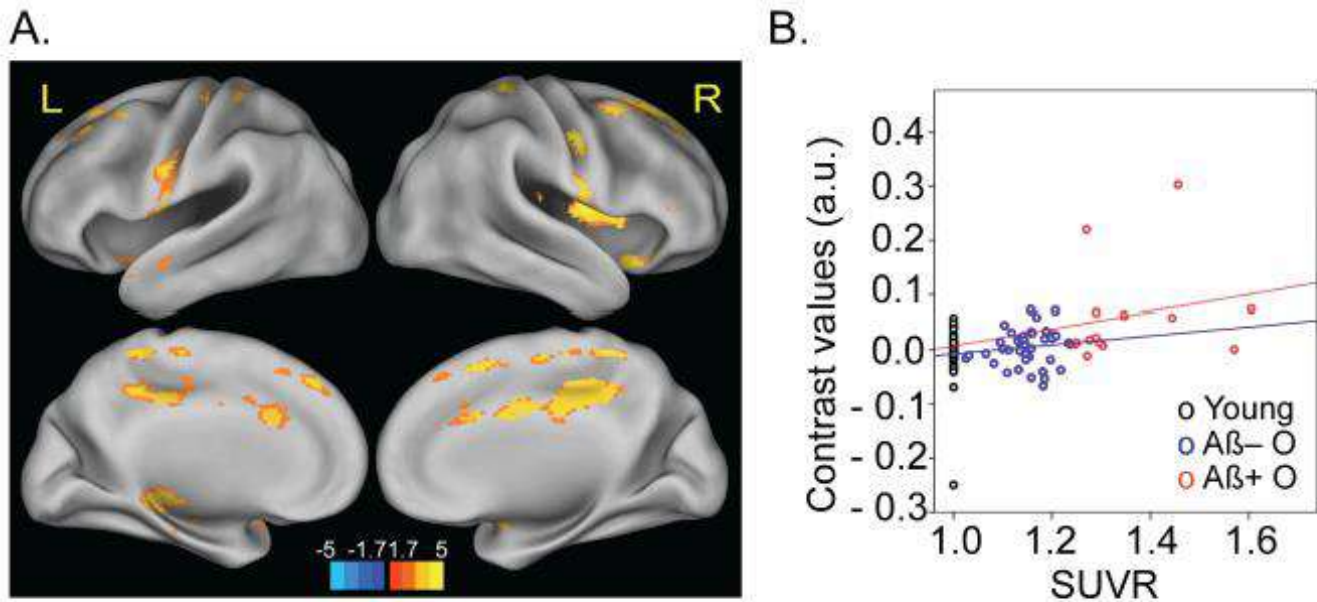


Figure 2. Parametric increases for working memory load relates to A β deposition as a continuous measure. (A) Warm colors indicate regions showing a positive relationship between linear increases of activity across working memory load level and global SUVR. These regions mostly do not overlap with regions common across all subjects. Results are thresholded at $p < 0.05$, cluster corrected for multiple comparisons. (B) Scatterplots indicate that greater parametric increases were positively related to the amount of amyloid deposition as measure by global SUVR index. Contrast values of young subjects are displayed on the left for comparison purposes.

Keywords: Beta-amyloid, fronto-parietal network, normal aging

P46 Presented by: Oh, Hwamee

Submission ID: 78

Validation of Automated Analysis of Tracer Binding on THK Tau PET Images

Nobuyuki Okamura^{1, 2}, Ryuichi Harada², Shozo Furumoto³, Katsutoshi Furukawa⁴, Aiko Ishiki⁴, Ren Iwata³, Manabu Tashiro³, Kazuhiko Yanai^{1, 3}, Hiroyuki Arai⁴, Yukitsuka Kudo²

¹ Department of Pharmacology, Tohoku University School of Medicine, Sendai, Miyagi, Japan

² Division of Neuro-imaging, Institute of Development, Aging and Cancer, Sendai, Miyagi, Japan

³ Cyclotron and Radioisotope Center, Tohoku University, Sendai, Miyagi, Japan

⁴ Department of Geriatrics and Gerontology, Institute of Development, Aging and Cancer, Tohoku University, Sendai, Miyagi, Japan

Background: Novel tau PET tracer, [¹⁸F]THK-5117 and [¹⁸F]THK-5351, have been developed and tested in humans. These pilot studies have demonstrated a difference of tracer distribution between Alzheimer's disease (AD) patients and a healthy elderly population. The purpose of this study is to evaluate the clinical utility of automated volumes of interest (VOI) analysis on THK PET images. We further investigated whether the brainstem could be used as an alternative reference region for the analysis of THK PET images.

Methods: Fourteen participants including 6 elderly healthy control (HC) subjects and 10 AD patients underwent dynamic PET scans for 90 min after injection of [¹⁸F]THK-5351. Automatic delineation of volumes of interest was performed using PNEURO tool of PMOD (ver.3.4) software. Hammers atlas was used for this analysis. Regional SUVR values were calculated using cerebellum (SUVR-C) or brainstem (SUVR-B) as reference regions. Group difference of regional SUVR values was evaluated by calculating effect size coefficients.

Results: Neocortical SUVR values in AD patients reached a plateau at 50 min post-injection. Regional SUVR value at 50-60 min post injection was elevated in the areas known to contain high concentrations of tau deposits in AD. Effect size value was especially high in the parahippocampal gyrus, amygdala, middle and inferior temporal gyrus and superior parietal gyrus. SUVR-B showed slightly better capability in discriminating between AD and HC than SUVR-C. SUVR values from automated VOI analysis correlated well with those from manual VOI analysis.

Conclusion: The results show that automated VOI analysis is useful for the evaluation of [¹⁸F]THK-5351 PET images. Brainstem would be a suitable alternative reference region for computation of regional tracer retention.

Keywords: *Alzheimer's disease, tau, PET, imaging*

P48 Presented by: Okamura, Nobuyuki

Submission ID: 30

Determining Total Amyloid Plaque Burden in AV-45 Positron Emission Tomography/Computed Tomography (PET/CT) Scans

David Creed, Amy McCann, Jeff Burns, Eric Vidoni, Paul Welch, Mark Perry

University of Kansas Medical Center, Kansas City, Kansas, United States

Background: Development of Alzheimer's Disease (AD) prevention programs and treatments to slow beta-amyloid plaque deposition necessitates reliable methods of quantifying severity of plaque burden in the brain. This study's objective was to evaluate the degree of plaque deposition in the cerebral cortex with 18F (AV-45) PET/CT scans in 1) patients with clinical diagnoses of AD, or 2) participants in our institution's AD Prevention Program.

Methods: A retrospective analysis was performed on 92 patients who underwent AV-45 PET/CT scans from 2008-2014 at our institution. Scans were interpreted as "elevated" or "non-elevated" through visual and quantitative assessment of AV-45 activity in multiple brain regions by three independent readers using MIMneuro software. Additional quantitative analyses determined total amount of plaque deposition using: 1) total cerebral grey matter (GM) z-score, 2) SUVR (compared to cerebellum) of total cerebrum, or 3) SUVR of total cerebral GM.

Results: Thirty-nine patients (42%) were classified as elevated, with 98% agreement among readers. GM z-scores in elevated cases ranged from 2.13-18.95 compared to -3.23-2.87 in non-elevated cases, and were categorized by severity: 2.0-6.9 (mild), 7.0-11.99 (moderate), and 12+ (severe). SUVR measurements of cerebral hemispheres, cerebral GM, and average SUVR of anterior cingulate gyrus, precuneus, lateral temporal lobe, inferior medial frontal gyrus, posterior cingulate gyrus, and superior parietal lobe also progressively increased in all groups (Figure 1). Z-score stereotactic surface projections demonstrated progressive cortical involvement (Figure 2). Incidence of occipital lobe plaque increased with severity of overall plaque deposition, with 4%, 53%, 92%, and 100% in normal, mild, moderate, and severe cases, respectively. The sensory motor cortex was spared in all but one case.

Conclusions: Total cerebral GM z-score may be a reliable indicator to quantify plaque burden in AV-45 PET/CT scans. However, longitudinal research is necessary to determine its clinical utility in determining therapy response or disease progression.

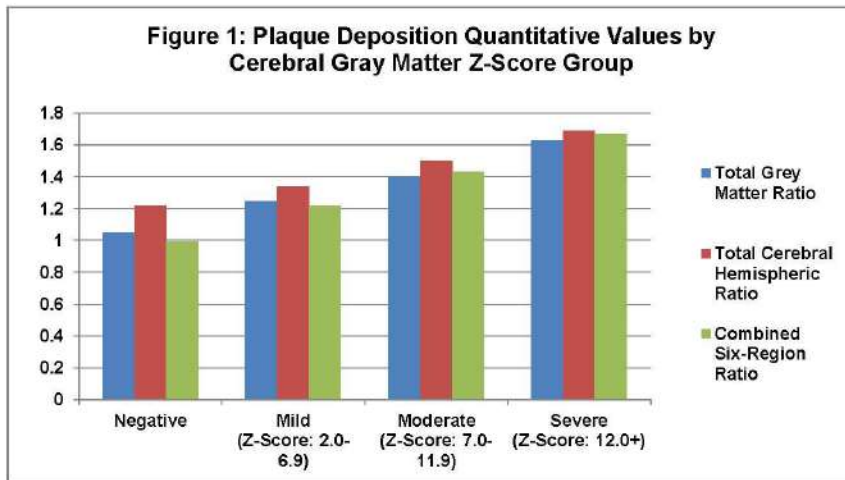
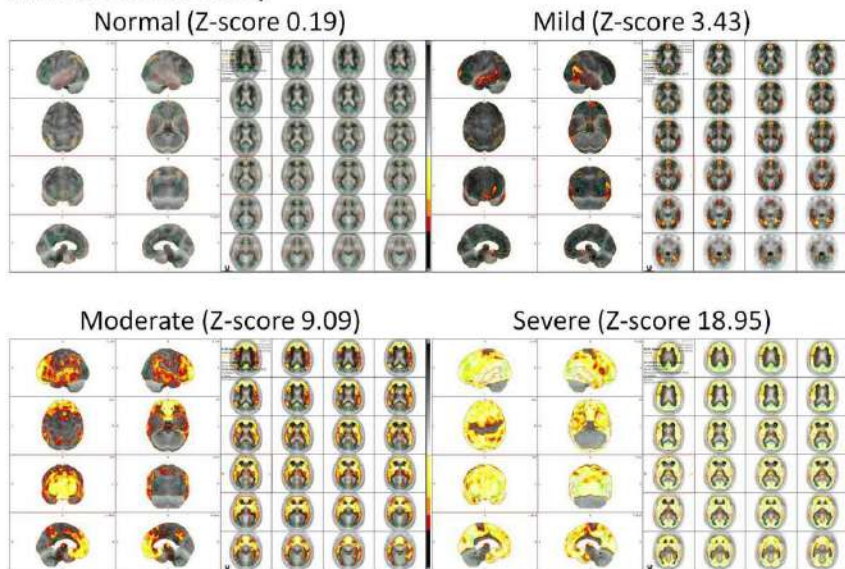


Figure 2: Plaque Deposition Surface Projection by Cerebral Gray Matter Z-Score Group



P50 Presented by: Perry, Mark

Submission ID: 110

P54**Relationships between Florbetapir PET Amyloid and 18F-AV-1451 (aka 18F-T807) PET Tau Binding in Cognitively Normal Subjects and Patients with Cognitive Impairments Suspected of Alzheimer's Disease**

Michael Pontecorvo, Michael Devous, Abhinay Joshi, Ming Lu, Andrew Siderowf, Anupa Arora, Mark Mintun

Avid Radiopharmaceuticals, Inc., Philadelphia, PA, United States

Background: 18F-AV-1451 is a PET tracer for imaging tau pathology in which additional characterization across clinical populations would be useful.

Methods: We conducted 18F-AV-1451 PET in 156 subjects [14 young clinically normal controls (YCN), 39 older controls (OCN), 70 Mild Cognitive Impairment (MCI) and 33 cases with Alzheimer's Disease (AD)]. PET scans were acquired 80-100 min post-injection of 370 MBq 18F-AV-1451. SUV_r was calculated using AAL VOIs for mean cortical (average of occipital, parietal and temporal cortices) and hippocampal regions with a cerebellum gray reference region. Subjects were categorized as amyloid positive (A β +) or negative (A β -) based on florbetapir PET SUV_r (threshold 1.10).

Results: Cortical tau SUV_r in AD was greater than MCI (t-test; $p < 0.05$). No significant difference was seen in cortical tau SUV_r between OCN and YCN. Cortical tau SUV_r in the A β + AD subjects (SUV_r = 1.55 ± 0.33 ; $n=21$) and MCI subjects (1.26 ± 0.28 ; $n=32$) was greater ($p < 0.05$) than that seen their A β - counterparts (SUV_r = 1.03 ± 0.09 and SUV_r = 1.04 ± 0.12 , respectively). The A β - subjects from both the AD and MCI groups had cortical tau SUV_r values that were indistinguishable from controls. Across all A β - subjects, there was a significant correlation of age with hippocampal tau SUV_r ($r=0.28$, $p=0.005$), consistent with an age-related accumulation of tau in the mesial temporal structures independent of amyloid. There was a significant negative correlation between cortical tau SUV_r and MMSE ($r=-0.48$; $n=156$) which was higher when A β - subjects diagnosed with AD and MCI were excluded ($r=-0.60$; $n=106$).

Conclusions: Consistent with post-mortem studies, we observed the greatest tau deposition as detected by 18F-AV-1451 PET in AD cases, followed by MCI. This relationship appeared dependent on the presence of amyloid pathology. There was also correlation between tau binding and cognitive impairment as measured by MMSE.

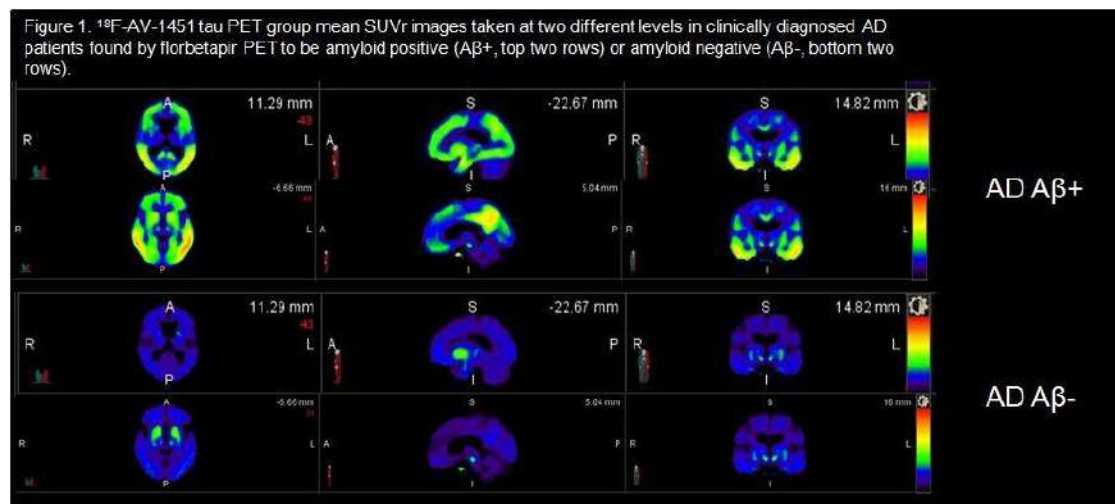


Figure 2. ^{18}F -AV-1451 tau PET group mean SUVr images taken at two different levels in clinically diagnosed MCI patients found by florbetapir PET to be amyloid positive ($\text{A}\beta^+$, top two rows) or amyloid negative ($\text{A}\beta^-$, bottom two rows).

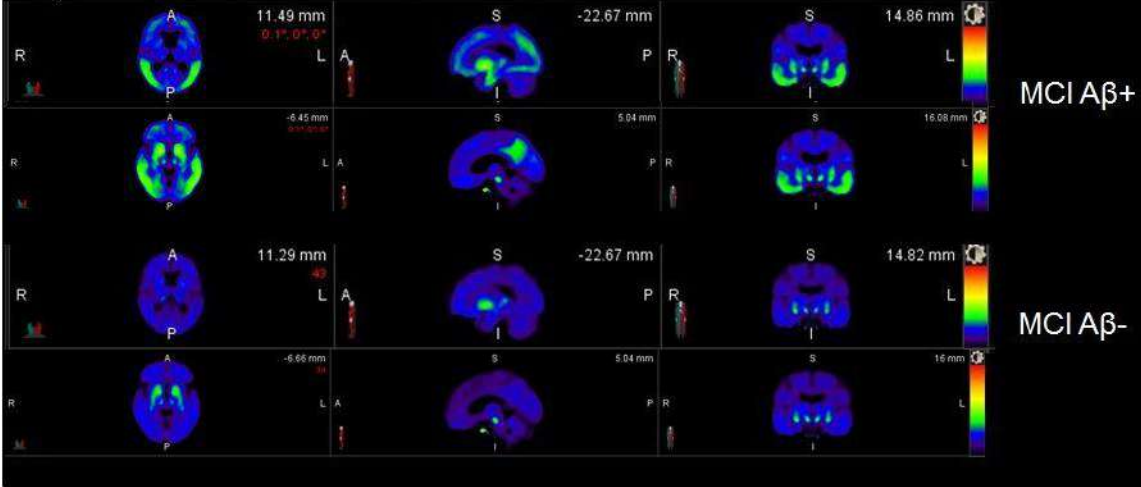
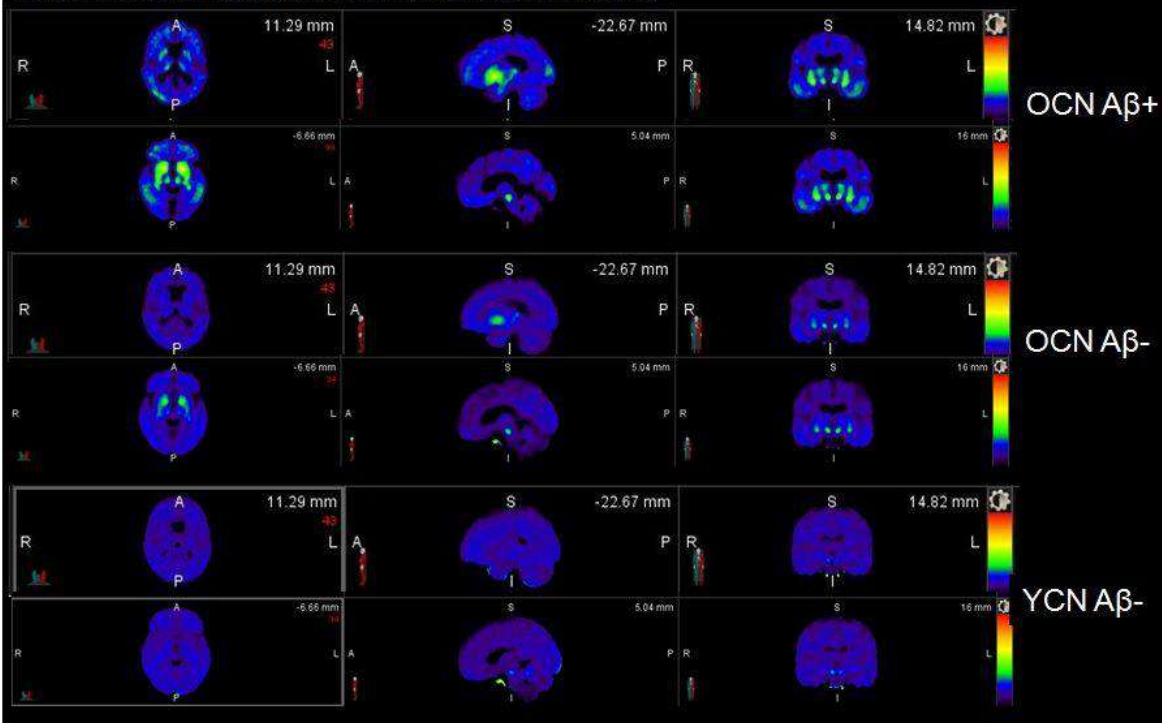


Figure 3. ^{18}F -AV-1451 tau PET group mean SUVr images taken at two different levels in clinically normal older controls (OCN) found by florbetapir PET to be amyloid positive ($\text{A}\beta^+$, top two rows) or amyloid negative ($\text{A}\beta^-$, middle two rows), and in young clinically normal subjects (YCN) (bottom two rows).



Keywords: *Tau, T807, AV-1451, amyloid, cognition*

P54 Presented by: Pontecorvo, Michael J

Submission ID: 98

P56

Brain Amyloid Load Is Associated with Impaired Executive Functioning in Elderly Individuals at-risk to Develop

Dementia

Juha Rinne^{1,2}, Nina Kemppainen^{1,2}, Tiia Ngandu^{3,4}, Alina Solomon^{4,5,6}, Riitta Parkkola⁷, Jarkko Johansson¹, Jenni Lehtisalo³, Tuomo Hänninen⁸, Teemu Paajanen⁹, Tiina Laatikainen^{3,10}, Hilikka Soininen⁵, Miia Kivipelto^{3,4,5,6}

¹ Turku PET Centre, University of Turku, Turku, Finland, Turku, Turku, Finland

² Division of Clinical Neurosciences, Turku University Hospital, Turku, Turku, Finland

³ Department of Chronic Disease Prevention, National Institute for Health and Welfare, Helsinki, Helsinki, Finland

⁴ Alzheimer's Disease Research Center, Karolinska Institutet, Novum 5th floor, Stockholm, Stockholm, Sweden

⁵ Department of Neurology, Institute of Clinical Medicine, University of Eastern Finland, Kuopio, Kuopio, Finland

⁶ Aging Research Center, Karolinska Institutet, Novum 5th floor, Stockholm, Stockholm, Sweden

⁷ Department of Clinical Radiology, Turku University and Turku University Central Hospital, Turku, Turku, Finland

⁸ Department of Neurology, Kuopio University Hospital, Kuopio, Kuopio, Finland

⁹ Finnish Institute of Occupational Health, Helsinki, Helsinki, Finland

¹⁰ Institute of Public Health and Clinical Nutrition, University of Eastern Finland, Kuopio, Kuopio, Finland

Background: FINGER study is a randomized 2-year multi-domain lifestyle intervention in subjects at increased risk of cognitive decline based on a risk score.^{1,2} A sub-group of the study population participated in a PET study to investigate amyloid deposition at baseline and at the end of intervention. At present, association of PIB data to baseline characteristics and cognition are reported. Preliminary analyses of the multi-domain intervention suggest better preservation of cognition in the intervention as compared to the non-intervention group.

Methods: Altogether 48 elderly subjects (mean age 71.4; SD 5.2) underwent a [11C]PIB PET scan, brain MRI and neuropsychological examination. Subjects were divided into two groups (PIB+ and PIB-) based on a visual PET scan analysis. Hippocampal atrophy and brain vascular changes were visually graded according to Scheltens and Fazekas scores. Between-groups differences in the cognitive function were analyzed.

Results: Twenty subjects (42%) were PIB positive. PIB- group performed better in executive functions than PIB+ group (Z-score difference $p = 0.02$). PIB+ group had higher amount of white matter lesions and hippocampal atrophy (Fazekas score 2-3: 50% in PIB+ vs. 29% in PIB-; Scheltens score 1-3: 40% right, 45% left in PIB+ vs. 29% and 21% in PIB-).

Conclusions: The high percentage of PIB positive subjects (42% as compared to estimated 20% prevalence of amyloid positives among healthy controls in this age group³) provides evidence of a successful recruitment process of the at-risk population for AD in the FINGER trial. The results suggest an association between early brain amyloid accumulation and decline in executive functions, as well as increased vascular changes and hippocampal atrophy in amyloid positive subjects. Follow-up evaluation will show whether multi-domain intervention will result in less amyloid accumulation with time than the control group.

References:

1. Kivipelto et al. *Alzheimers Dement* 2013;9(6):657-665., 2. Ngandu et al. *Int J Environ Res Public Health* 2014;10;11(9):9345-9360, 3. Rowe et al. *Nbiol Aging* 2010;31:1275-1283

Keywords: *Amyloid, dementia, intervention, PIB, risk factor*

P56 Presented by: Rinne, Juha O

Submission ID: 20

Association of Vitamin E Use and Two-Year Amyloid Accumulation in Healthy Older Adults and Early Mild Cognitive Impairment

Shannon Risacher¹, Karmen Yoder¹, William Jagust³, Paul A⁴, Ronald Petersen⁵, Michael Weiner⁶, Andrew S²

¹ Department of Radiology and Imaging Sciences, Indiana Alzheimer Disease Center, Indiana University School of Medicine, Indianapolis, Indiana, United States

² Department of Radiology and Imaging Sciences, Indiana Alzheimer Disease Center, Department of Molecular and Medical Genetics, Indiana University School of Medicine, Indianapolis, Indiana, United States

³ Department of Neurology, University of California-Berkeley, Berkeley, California, United States

⁴ Department of Neurology, University of California-San Diego, San Diego, California, United States

⁵ Department of Neurology, Mayo Clinic, Rochester, Minnesota, United States

⁶ Departments of Radiology, Medicine and Psychiatry, University of California-San Francisco; Department of Veterans Affairs Medical Center, San Francisco, California, United States

Introduction: Amyloid plaque accumulation is considered a precursor to the development of Alzheimer's disease (AD). However, factors modulating rate of accumulation are understudied. Vitamin E (VitE) is a lipid-soluble antioxidant that has been previously investigated as a treatment for mild cognitive impairment (MCI) and AD. The present study sought to evaluate the impact of VitE supplement use on rate of amyloid accumulation over two years in cognitively healthy older adults (HC) and patients diagnosed with early MCI (EMCI) from the Alzheimer's Disease Neuroimaging Initiative (ADNI).

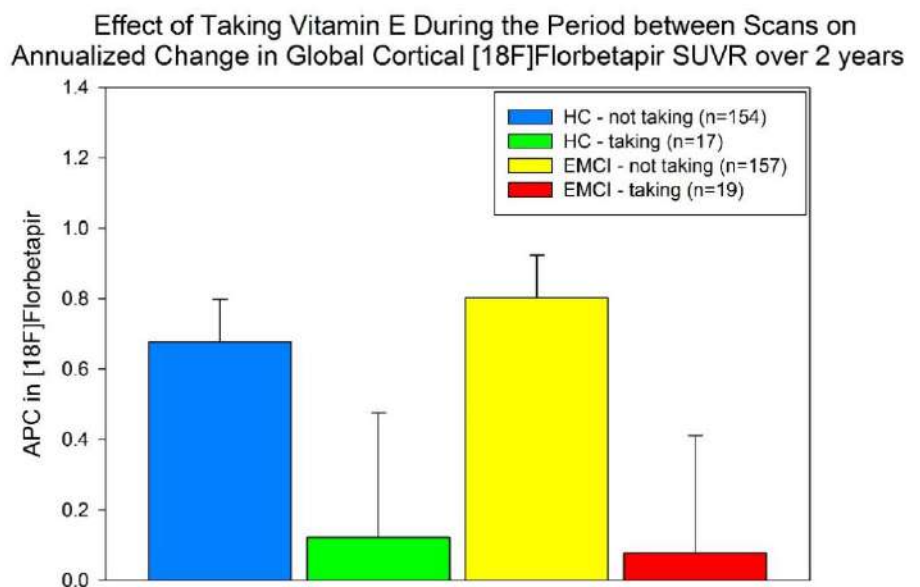
Methods: 348 participants (171 HC, 177 EMCI) from ADNI with two [¹⁸F]Florbetapir PET scans (approximately two years apart) were included. Diagnostic, APOE genotype, medication, and demographic information, as well as [¹⁸F]Florbetapir and MPRAGE scans from baseline and follow-up were downloaded from the LONI ADNI database (adni.loni.usc.edu). 36 participants (17 HC, 19 EMCI) were taking VitE supplements during the two-year period according to the medication record. [¹⁸F]Florbetapir scans were processed using standard techniques with intensity normalization to a composite region of interest (ROI) that included the cerebellum, pons, and cerebral white matter to create SUVR images. Mean SUVR was extracted from a cortical ROI for both baseline and follow-up and the annualized percent change (APC) was calculated. A two-way ANCOVA evaluating diagnosis by VitE supplement status was used to assess the impact of VitE use on rate of amyloid accumulation, covaried for age, gender, APOEε4 carrier status, and baseline amyloid positivity status.

Results: Both HC and EMCI participants who were taking VitE showed reduced rates of amyloid accumulation over two years (VitE: p=0.013). No interaction between VitE and diagnosis was observed.

Discussion: VitE may reduce the rate of amyloid plaque accumulation in preclinical or mildly symptomatic older adults possibly due to its antioxidant effects. Replication and mechanistic follow-up studies in expanded samples are warranted.

Keywords: Vitamin E, Longitudinal Amyloid Imaging, [¹⁸F]Florbetapir PET, Alzheimer's Disease

Neuroimaging Initiative (ADNI), early mild cognitive impairment (EMCI)



P58 Presented by: Risacher, Shannon L

Submission ID: 81

Longitudinal Multitracer PET Imaging Studies in Familial and Sporadic Alzheimer's Disease

Elena Rodriguez-Vieitez¹, Stephen F. Carter^{1, 2}, Laure Saint-Aubert¹, Ove Almkvist^{1, 3, 4}, Karim Farid¹, Michael Schöll^{1, 5}, Konstantinos Chiotis¹, Steinunn Thordardottir^{4, 6}, Anders Wall⁷, Caroline Graff^{4, 6}, Bengt Långström⁸, Agneta Nordberg^{1, 4}

¹ Department NVS, Center for Alzheimer Research, Division of Translational Alzheimer Neurobiology, Karolinska Institutet, Huddinge, Stockholm, Sweden

² Wolfson Molecular Imaging Center, University of Manchester, Manchester, Manchester, United Kingdom

³ Department of Psychology, Stockholm University, Stockholm, Stockholm, Sweden

⁴ Department of Geriatric Medicine, Karolinska University Hospital Huddinge, Huddinge, Stockholm, Sweden

⁵ MedTech West and the Department of Clinical Neuroscience and Rehabilitation, University of Gothenburg, Gothenburg, Gothenburg, Sweden

⁶ Department NVS, Center for Alzheimer Research, Division of Neurogeriatrics, Karolinska Institutet, Huddinge, Stockholm, Sweden

⁷ Department of Radiology, Oncology and Radiation, Section of Nuclear Medicine & PET, Uppsala University, Uppsala, Uppsala, Sweden

⁸ Department of Chemistry, Uppsala University, Uppsala, Uppsala, Sweden

Objectives: Early astrocytosis was reported from cross-sectional multitracer PET imaging in autosomal-dominant Alzheimer's disease (ADAD) and sporadic AD (sAD)¹. Here we sought to validate the cross-sectional findings by a longitudinal follow-up investigation in a larger cohort, and investigate regional and temporal distributions of brain astrocytosis, amyloid deposition and glucose metabolism.

Methods: 52 baseline participants (26 followed-up at 2.8 ± 0.6 years) included ADAD-carriers (n=11), non-carriers (n=16), sporadic MCI (sMCI) (n=17) and sAD (n=8). Participants underwent baseline and follow-up PET scans with ¹¹C-Deuterium-L-Deprenyl (¹¹C-DED), ¹¹C-PIB, and ¹⁸F-FDG; apolipoprotein E (APOE) genotyping, and neuropsychological testing. Linear mixed-effects models (LMMs) were applied to longitudinal PET data versus estimated years to symptoms onset (EYO).

Results: Increased ¹¹C-DED binding and ¹¹C-PIB retention were first observed in ADAD-carriers from EYO ≈ -20 years, and subsequently followed opposite time courses. ¹¹C-DED binding in ADAD-carriers declined steadily, while ¹¹C-PIB retention displayed increase rates. Individual symptomatic ADAD-carriers demonstrated both higher ¹¹C-PIB and lower ¹¹C-DED than sMCI/sAD. Presymptomatic ADAD-carriers (EYO ≈ -12 years) showed incipient hypometabolism. ¹⁸F-FDG uptake showed decline rates in ADAD-carriers, as well as in PIB-positive MCI until 5-years after diagnosis. Hypometabolism was more pronounced in individual symptomatic ADAD-carriers compared to sMCI/sAD. The longitudinal progression in the three tracers was accompanied by measures of cognitive decline.

Conclusions: The longitudinal investigation demonstrated that PET data was reproducible after a mean follow-up time of 2.8 years, statistically strengthening the cross-sectional findings. Early and declining astrocytosis, increasing amyloid-plaque deposition and decreasing glucose metabolism characterized AD evolution. The observed type of early astrocytosis might have downstream pathological consequences, potentially identifying a new therapeutic target.

¹A. Nordberg (2014), Neurodegener. Dis. 13, 160-162.

Keywords: *autosomal-dominant Alzheimer's disease, Amyloid, Astrocytosis, PET imaging, 11C-deuterium-L-deprenyl*

P60 Presented by: Rodriguez-Vieitez, Elena

Submission ID: 74

Semiquantitative Analyses and Visual Assessment of the Novel β -Amyloid Tracer [18F]NAV4694

Axel Rominger¹, Matthias Brendel¹, Franziska Scheiwein¹, Julia Sauerbeck¹, Andreas Delker¹, Peter Bartenstein¹, John Seibyl², Cornelia Reininger³

¹ Dept. of Nuclear Medicine, University of Munich, Munich, N/A, Germany

² Institute for Neurodegenerative Disorders, New Haven, CT, United States

³ Navidea Biopharmaceuticals, Andover, MA, United States

[18F]-labelled A β tracers recently developed for clinical use for imaging amyloid pathology in Alzheimer disease (AD) show higher non-specific white matter binding compared to [11C]-Pittsburgh compound-B, complicating the visual assessment. The aim of the current study was to analyze semiquantitative estimates of [18F]NAV4694, using different reference regions in order to support the visual interpretation. Furthermore cut-off values were calculated for optimal discriminatory power.

152 PET scans with [18F]-NAV4694 of subjects with probable AD (N=36), MCI (N=57) and HC (N=59) were available for these analyses. Amyloid scans read by three independent expert readers were scored as either amyloid-positive or -negative. Furthermore images were coregistered to the individual T1w MRI and cortical composite (COMP) volume of interest values (VOIs) as well as striatal VOIs were applied. Standard uptake value ratios (SUVR) were calculated by scaling to either uptake in cerebellar grey matter (CBL-GM), whole CBL (wCBL), brainstem (BST), or white matter (WM).

69/152 subjects were read amyloid-positive. Mean COMP-SUVR of A β positive cases was 2.08 \pm 0.39, and 1.19 \pm 0.10 when CBL-GM was used as reference region (Cohen's d=3.13, effect size correlation r=0.84). Mean COMP-SUVR of A β positive cases was 0.95 \pm 0.09 and 0.69 \pm 0.04 in negative subjects when referencing against WM (Cohen's d=3.72, effect size correlation r=0.88). Putaminal SUVR correlated highly significantly with COMP-SUVR (R=0.94; p<0.001). Optimal discrimination thresholds of COMP-SUVR were determined with 1.44 for CBL-GM (AUC: 0.984), and with 0.79 (AUC: 0.998) for WM as reference region. All analyses with wCBL or BST as reference region were inferior.

The novel amyloid tracer [18F]NAV4694 allows excellent differentiation between visually rated amyloid-positive and -negative subjects by means of semiquantitative analyses both in AD and MCI subjects. Highest discriminatory power resulted from referencing against white matter. Striatal uptake highly correlates with cortical uptake, therefore enabling further facilitation in the visual interpretation of these scans.

Keywords: amyloid; PET; NAV4694; visual assessment; quantitation

P62 Presented by: Rominger, Axel

Submission ID: 104

Relationship between Post-mortem THK-5117 Binding and In-vivo PET Biomarkers Uptake in Alzheimer's Disease

Laure Saint-Aubert¹, Laetitia Lemoine¹, Amelia Marutle¹, Gunnar Antoni^{2,3}, Jonas Eriksson³, Nobuyuki Okamura⁴, Inger Nennesmo⁵, Per-Göran Gillberg¹, Agneta Nordberg^{1,6}

¹ Translational Alzheimer Neurobiology, Karolinska institutet, Stockholm, Sweden, Sweden

² Preclinical PET Platform, Department of Medicinal Chemistry, Faculty of Pharmacy, Uppsala University, Uppsala, Sweden, Sweden

³ PET Centre, Centre for Medical Imaging, Uppsala University Hospital, Uppsala, Sweden, Sweden

⁴ Department of Pharmacology, Tohoku University School of Medicine, Sendai, Japan, Japan

⁵ Department of Pathology, Karolinska University Hospital, Stockholm, Sweden, Sweden

⁶ Department of Geriatric Medicine, Karolinska University Hospital Huddinge, Stockholm, Sweden, Sweden

Introduction: New PET tracers specific for tau protein are now being developed, in order to visualize and understand the time course of neurofibrillary tangles deposition in Alzheimer's disease (AD). We investigate in vitro the regional binding distribution of the tau tracer 18F-THK5117, and its relationship to the regional uptake of in vivo PET biomarkers in patients with AD.

Method: Three patients with confirmed AD, that underwent 18F-FDG and 11C-PIB PET scans during clinical care, donated their brain after death.

Ante-mortem analyses: For each patient, manual segmentation of regions of interest (ROIs) was performed on a selected coronal section of T1 MR, and mean uptake values were calculated for each ROI on the registered PIB and FDG PET images.

Post-mortem analyses: Autoradiography was performed on frozen sections of the three patients' left hemisphere. Manual segmentation of ROIs on the autoradiograms was performed, and mean uptake values were calculated for each ROI.

Results: In all three cases, 3H-THK5117 specific binding was highest in temporal regions.

In case 1, a significant negative correlation was found between 3H-THK5117 binding on autoradiography and both 18F-FDG ($r=-0.807$, $p<0.001$) and 11C-PiB ($r=-0.565$, $p=0.035$) in vivo uptake. In case 2, significant negative correlations were found between 3H-THK5117 binding and FDG PET scan ($r=-0.850$, $p<0.001$). No significant correlation was found with 11C-PiB uptake. No correlation was found in case 3 between 3H-THK5117 binding and 18F-FDG/11C-PiB.

Conclusion: 3H-THK5117 shows a highest binding in temporal regions, consistently with tau pathology in AD. The binding pattern in case 1 is similar to regional in vivo hypometabolism, illustrating the relationship between tau deposition and neuronal dysfunction. On the contrary the relationship with in vivo 11C-PiB illustrates the different patterns of lesions' progression. Discrepancies between the 3 different patients need to be related to their individual pathology.

Keywords: *Tau, in vitro, PET, Alzheimer's disease*

P64 Presented by: Saint-Aubert, Laure

Submission ID: 94

P66

Partial Volume Effect Simulations to Assess Regional Gray and White Matter Content in Brain PET and its Impact on Measuring Longitudinal Changes in Amyloid Burden

Sandra Sanabria Bohorquez, Farshid Faraji, David Clayton, Alex de Crespigny

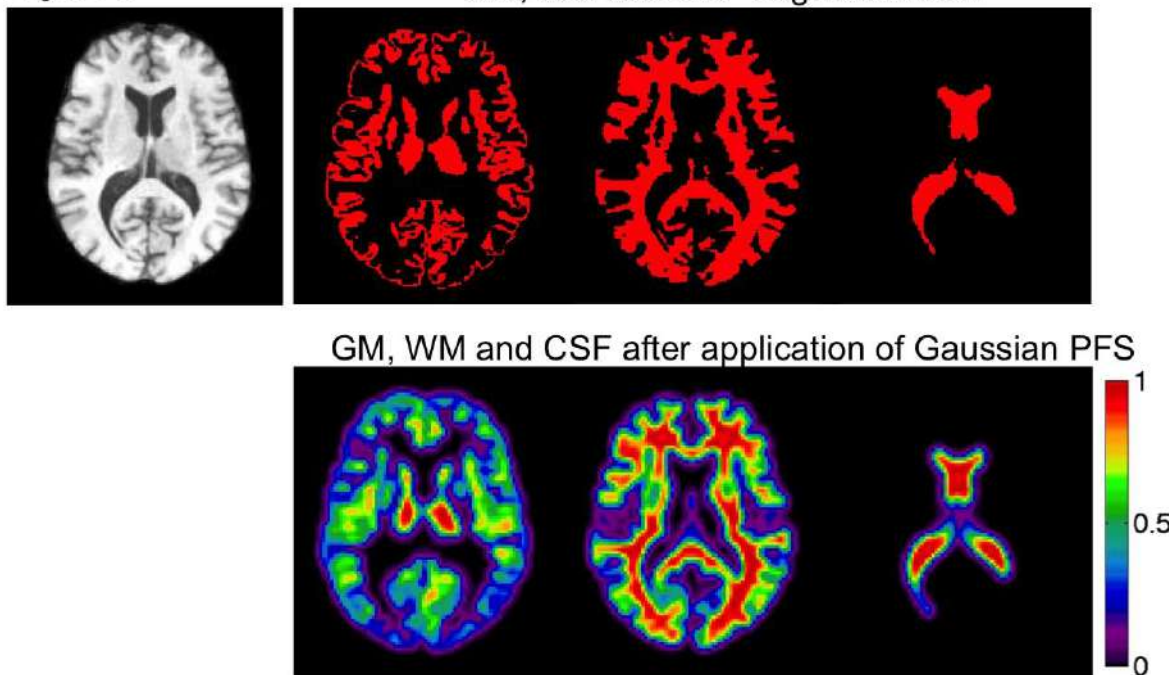
Genentech Inc., South San Francisco, CA, United States

Objective: Most current F-18 amyloid tracers display higher uptake in white matter (WM) than gray matter (GM). Recent work suggested the use of MRI derived GM masks to reduce WM signal contamination in AAL template VOIs (1). The purpose of this work was to estimate the contributions from GM, WM and CSF to the GM-masked AAL template VOIs due to the *limited spatial resolution* of PET and to assess the impact of brain atrophy on SUV_r.

Methods: 7 mild-to-moderate AD patients underwent volumetric MRI. For each scan, GM, WM and CSF segmentations in the MNI space were obtained using FreeSurfer. PET spatial blurring was simulated by convolving the segmented images with a 3D Gaussian PSF with constant FWHM (Figure 1). A subject specific VOI template was created by applying the GM segmentation mask to the standard AAL template. The subject VOIs were applied over the PET-like GM, WM images, and the average contribution of each tissue component was calculated.

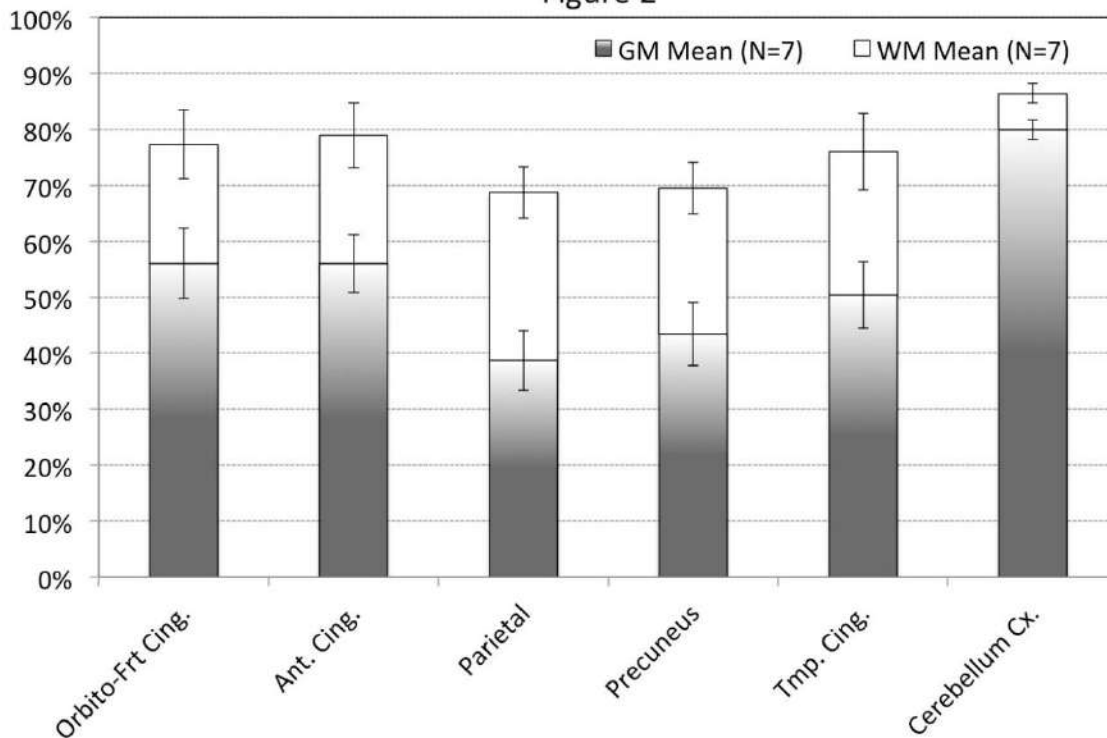
Figure 1

GM, WM and CSF segmentations



Results: There was marked WM contribution to all VOIs (Figure 2). In the parietal VOI the GM:WM volume ratio was only 1.3:1 resulting in ~40% of counts coming from GM using a tracer with an actual 2:1 WM:GM signal ratio. With such a tracer, and assuming WM and GM atrophy rates ~3% and ~5% (2) respectively, simulations suggest that SUV_r changes of up to 0.05 in an average AAL VOI are possible solely due to the effects of atrophy and partial volume.

Figure 2



Conclusions: Quantification of amyloid burden can be considerably affected by the VOI GM and WM content as well as variable atrophy rates. These factors should be considered during analysis of longitudinal amyloid PET and support the use of voxel-wise analysis methods.

References

1) Seibyl et al., SNMMI Annual Meeting, #138, 2014. 2) Thompson et al., J Neurosci 2003; 23(3):994.

Keywords: *Longitudinal, Partial Volume Effect, Amyloid Imaging*

P66 Presented by: Sanabria Bohorquez, Sandra

Submission ID: 22

Michael Schöll^{1,2}, Daniel Schonhaut³, Jacob Vogel¹, Samuel Lockhart¹, Suzanne Baker⁴, Henry Schwimmer¹, Rik Ossenkoppele³, Gil Rabinovici³, William Jagust¹

¹ UC Berkeley, Berkeley, CA, United States

² University of Gothenburg, Sweden, Gothenburg, Västra Götaland, Sweden

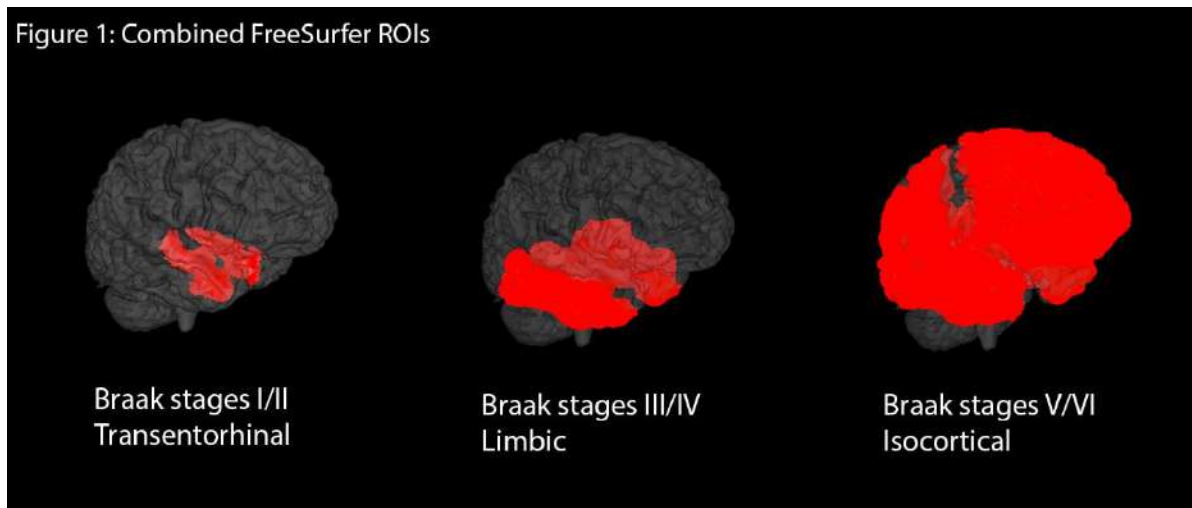
³ UC San Francisco, San Francisco, CA, United States

⁴ UC Berkeley, Lawrence Berkeley National Lab, Berkeley, CA, United States

Background: Tau pathology related to Alzheimer's disease (AD) has previously been classified into six consecutive Braak stages describing the gradual regional deposition of hyperphosphorylated tau protein over the course of the disease. The PET ligand [18F]-AV1451 binds to paired helical filament tau assemblies with high affinity and selectivity, rendering possible the *in vivo* assessment of tau pathology.

Objective: To explore the practicality of tau PET imaging as a diagnostic tool for AD progression by emulating Braak staging based on patterns of [18F]-AV1451 uptake.

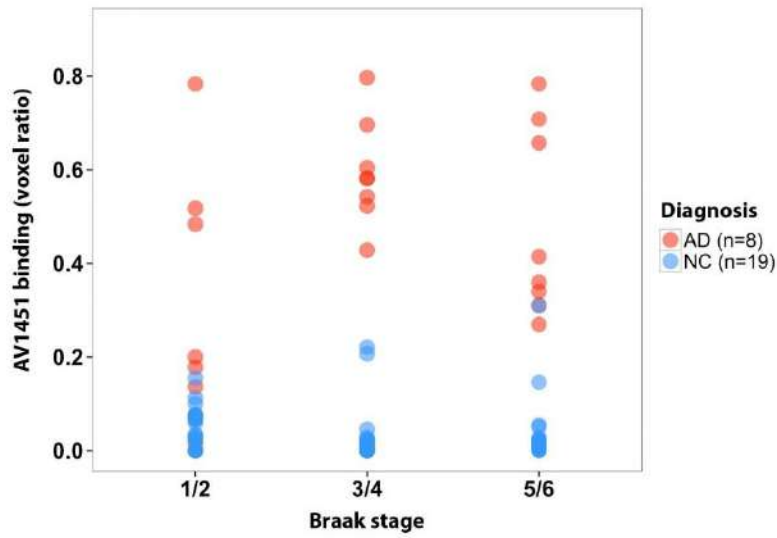
Methods: Seventeen elderly (age 78.6 ± 5.1 y) and two young (21, 22 y) normal controls (NCs), as well as eight AD patients (63.9 ± 8.0 y) underwent PET scanning with [18F]-AV1451 (80-100 min SUVR, cerebellar grey matter reference). Based on the original Braak staging (Braak et al., 1991 and 2006), we created regions of interest (ROIs) corresponding anatomically to the transentorhinal (I/II), limbic (III/IV), and isocortical (V/VI) Braak stages of tau deposition using combinations of FreeSurfer labels (Figure 1). High AV1451 binding was identified by calculating a ratio of voxels > 2 SD above NC mean over total voxel count within each ROI.



Results: We found clear separation of NCs from AD patients throughout Braak stages (Figure 2). Linear regression identified higher AV1451 uptake in later Braak stages as being highly predictive of higher uptake in previous stages, independent of ApoE status or age (Figure 3). The two young NCs showed minimal binding in all stages. Most elderly NCs resembled the younger NCs, while the two elderly NC with highest binding in the first stage showed greater binding in subsequent stages, suggesting presymptomatic disease.

Conclusion: Our findings demonstrate the potential of tau PET imaging as a progression marker of AD pathology in the context of traditional Braak staging.

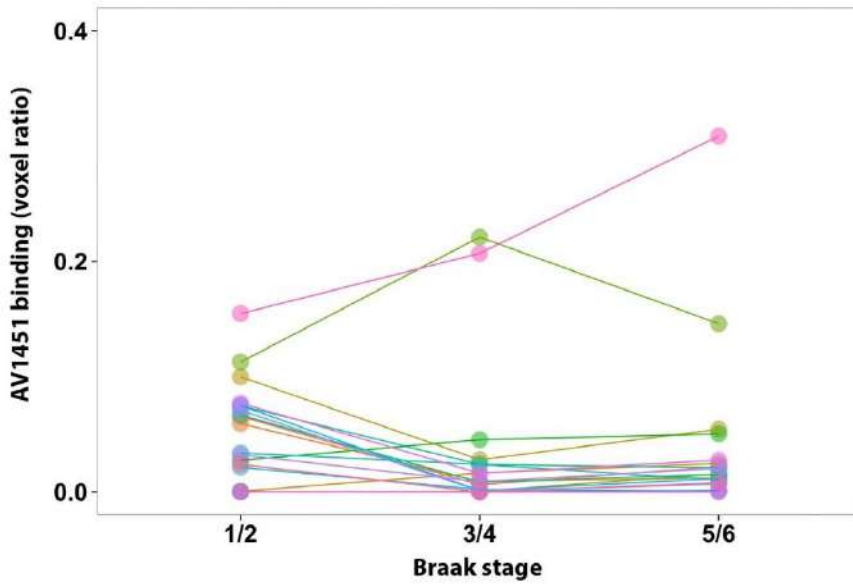
Figure 2



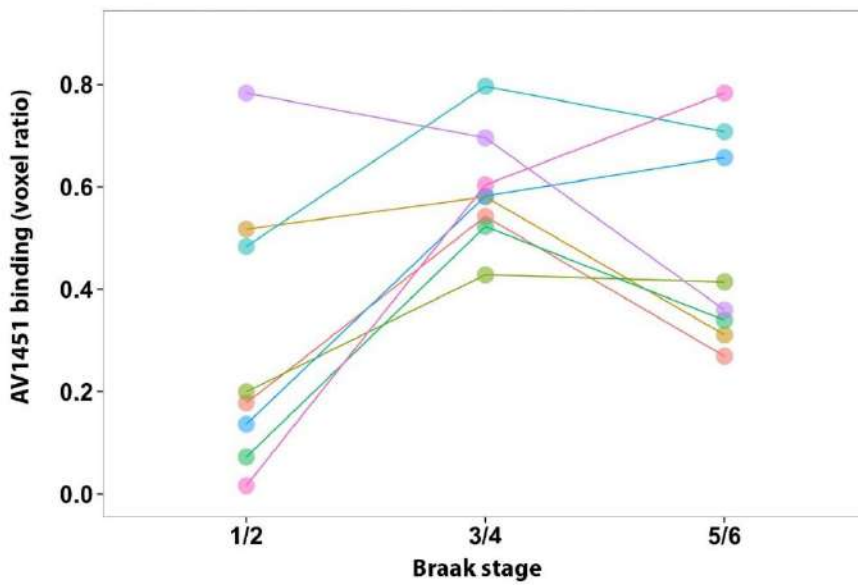
Keywords: Tau, PET, AV1451, Braak

P68 Presented by: Schöll, Michael

Normal controls (n=19)



AD patients (n=8)



P70

Early Experience with the High Contrast Novel B-Amyloid Tracer 18F NAV4694: Correlation of Visual Interpretation with Clinical and Quantitative Parameters

John Seibyl¹, Phillip Kuo², Cornelia Reininger³

¹ *Institute for Neurodegenerative Disorders, New Haven, CT, United States*

² *University of Arizona, Tucson, AZ, United States*

³ *Navidea Biopharmaceuticals, Columbus, OH, United States*

Objectives: NAV 4694 PET imaging in Alzheimer patients demonstrates a more heterogeneous pattern of cortical uptake than the current generation of F-18 amyloid radiotracers available for clinical use. Scintigraphic patterns include more intense focal uptake in posterior cingulate/precuneus, frontal cortex, and caudate and hyperintense gray matter. The clinical relevance of these findings is unknown. The purposes of the present investigation are: 1) to correlate PET scan phenomenology with clinical information and quantitative PET assessments, 2) to compare quantitative analyses with and without gray/white matter segmentation.

Methods: 107 NAV4694 PET images from two multicenter trials recruiting healthy volunteers, MCI, and AD participants were visually read by a consensus panel of three experienced experts who recorded comments specific to the cortical uptake. These features were compared with clinical and demographic data and regional SUV_r measurements obtained both with and without MRI-derived correction maps.

Results: Fifty scans were consensus negative and 57 positive. Readers had very high agreement rates. Mean age and MMSE scores were 62.6 +/- 19.2 y and 27.5 +/- 3.0, respectively, for the negative scans, and 73.6 +/- 6.3 and 24.7 +/- 4.7, respectively, for the positive studies. SUV_rs were correlated with MMSE (-0.4629, p< 0.0001) in positive scan subjects. Mean SUV_rs were 2.2 +/- 0.4 and 1.3 +/- 0.1, respectively, for the positive and negative scan cases. There were no differences in either composite or individual regional SUV_rs when MRI-derived segmentation was performed. Features associated with higher composite SUV_rs were caudate and/or precuneus uptake, and super scans (higher gray matter uptake than adjacent white matter).

Conclusions: NAV4694 is a promising next generation amyloid PET tracer with high contrast, reflected in more heterogeneous cortical uptake, excellent quantitative stability, and possibly simpler, more robust image processing algorithms which are not reliant on concomitant MRI.

Keywords: NAV4694, amyloid, PET

P70 Presented by: Seibyl, John

Submission ID: 70

Tau and Amyloid Deposits Relate to Distinctive Cortical Atrophy Patterns in Cognitively Normal Elderly

Jorge Sepulcre^{1,2}, Aaron Schultz², Alex Becker¹, Reisa Sperling^{2,3,4}, Keith Johnson^{1,3,4}

¹ Division of Nuclear Medicine and Molecular Imaging, Department of Radiology, Massachusetts General Hospital and Harvard Medical School, Boston, MA, United States

² Athinoula A. Martinos Center for Biomedical Imaging, Charlestown, MA, United States

³ Centre for Alzheimer Research and Treatment, Department of Neurology, Brigham and Women's Hospital and Harvard Medical School, Boston, MA, United States

⁴ Department of Neurology, Massachusetts General Hospital and Harvard Medical School, Boston, MA, United States

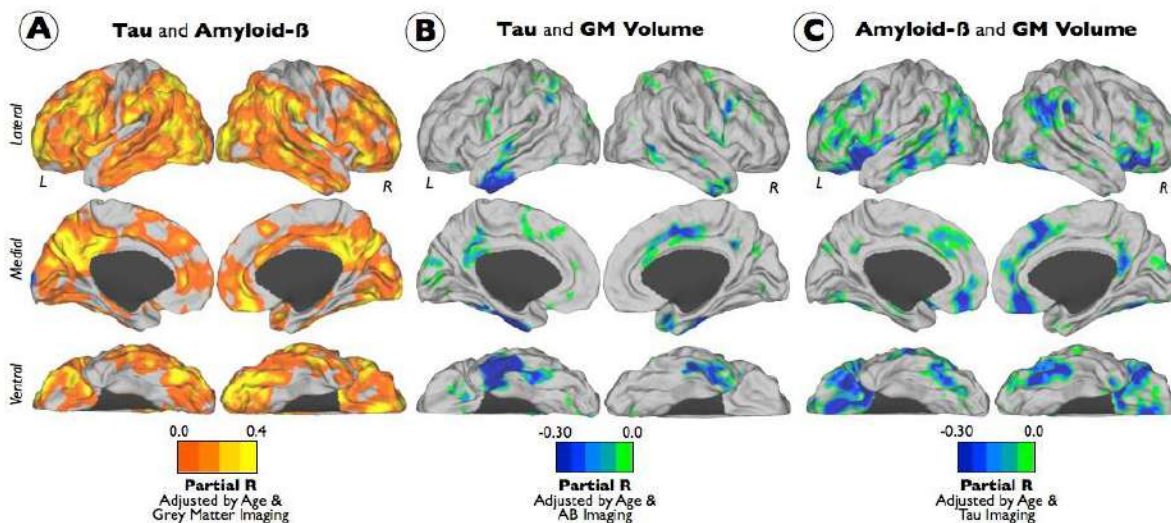
Background: Alzheimer's disease neurodegeneration is a complex phenomenon where misfolded amyloid- β (Ab) and Tau proteins accumulate in the human brain even decades before any cognitive manifestation. It has not been possible until recently to investigate in-vivo relationships of Tau, Ab, and atrophy. In this study, we aim to evaluate the brain spatial distribution of a novel PET Tau tracer –known as 18F-T807- and identify its association with Ab deposition and grey matter (GM) volume loss in a sample of cognitively normal participants in the Harvard Aging Brain Study.

Methods: Sixty-six subjects (mean age (SD): 75.4 (6.3), M/F: 32/34) underwent two PET imaging acquisitions and MRI. Using cerebellar grey reference, PiB PET data was expressed as DVR and T807 as SUVR. We used a voxel-based morphometry strategy to obtain the segmented GM volume maps of each individual. Finally, we used voxel-by-voxel and regions of interest regressions to investigate focal spatial correspondences between maps of 18F-T807, 11C-PiB and GM volume.

Results: We found that deposits of T807 and PiB correlated positively in distributed heteromodal areas of frontal, parietal and temporal lobes, most highly in precuneus and posterior cingulate regions (Figure 1-A; controlling by GM volume). Second, Tau deposits and GM volume had spatial negative correlations in regions of the lateral inferior temporal lobe, and in lesser extend several cingulate areas (Figure 1-B; controlling by PiB). Third, we found spatial negative correlations between A β deposits and GM volume in lateral temporal, parietal and frontal cortex, as well as, areas in orbito-frontal, fronto-insular and cingulate areas of the brain (Figure 1-C; controlling by T807).

Conclusions: Our results suggest a related spatial distribution of Tau and Ab in key heteromodal areas of the human brain as well as distinctive cortical association with GM atrophy in preclinical stages of Alzheimer's disease.

Spatial Associations of Tau, Amyloid- β and Grey Matter Volume in Cognitively Normal Elderly (N=66)



Keywords: Tau, Amyloid beta, Grey matter volume, Aging, Alzheimer's disease

P72 Presented by: Sepulcre, Jorge

P74

Parametric Binding Potential Maps of the Tau Imaging Tracer [¹⁸F]-AV-1451 (T807)

Sergey Shcherbinin¹, Adam Schwarz¹, Michael Devous², Abhinay Joshi², Michael Navitsky², James Dickson², Mark Mintun²

¹ Eli Lilly & Company, Indianapolis, IN, United States

² Avid Radiopharmaceuticals, Inc., Philadelphia, PA, United States

Objectives: We examined the neuroanatomical dependence of binding properties of the PET tracer [¹⁸F]-AV-1451 (also known as [¹⁸F]-T807) by voxel-wise maps of the non-displaceable binding potential for subjects with various degrees of cognitive impairment.

Methods: We analyzed dynamic PET scans for 4 young cognitively normal (YCN) subjects, 5 old cognitively normal (OCN) subjects, 5 subjects with amyloid-positive mild cognitive impairment (MCI) and 5 subjects with amyloid-positive Alzheimer's Disease (AD). These dynamic PET scans were acquired from 0 to 60 and from 80 to 100 minutes post-injection of approximately 10mCi [¹⁸F]-AV-1451. The dynamic PET datasets were spatially normalized to the MNI stereotaxic space using PMOD v3.5 software (PNEURO toolbox). The parametric binding potential (BP_{cer}) maps were then calculated (PXMOT toolbox) using the Logan graphical analysis with the cerebellum crus as the input reference region. For all subjects and voxel-wise time-activity curves, identical reference tissue clearance rate (0.2/min) and starting point of linearization (40min) were utilized. The resulting BP_{cer} maps were compared to the corresponding SUVR_{cer} maps generated using the same reference region and the average of the 80-100 minute frames.

Results: We observed an increased [¹⁸F]-AV-1451 binding potential BP_{cer} and a non-uniform distribution across cortical regions for MCI and AD subjects. Specifically, the range of ROI-mean values calculated in AAL atlas-based temporal, occipital, parietal and frontal lobes was 0.299-0.458 for AD subjects, 0.095-0.205 for MCI subjects, 0.046-0.080 for OCNs and 0.021-0.050 for YCNs. The binding potential BP_{cer} patterns were highly concordant with the corresponding SUVR_{cer}-1 maps, with Pearson correlation coefficients ranging between 0.98 and 0.99 in the aforementioned four cortical regions.

Conclusions: This preliminary voxel-wise kinetic modeling for 19 subjects is supportive of [¹⁸F]-AV-1451 80-100 minutes time frames as a reasonable setup for imaging of tau pathologies. Further dynamic studies are planned and exploration of other kinetic modeling methodology is warranted.

Keywords: *tau, binding, tracer, kinetics, modeling*

P74 Presented by: Shcherbinin, Sergey

Submission ID: 32

P76**Understanding the Diagnostic Accuracy of [18F]Flutemetamol**

Adrian Smith¹, Chris Buckley¹, Paul Jones¹, Michelle Zanette², Sherwin Paul², Milos Ikonovic³, Gill Farrar¹

¹ GE Healthcare, Amersham, Buckinghamshire, United Kingdom

² GE Healthcare, Princeton, New Jersey, United States

³ Department of Neurology, University of Pittsburgh, Pittsburgh, Pennsylvania, United States

Objective: To examine cases where there was discordance in [18F]flutemetamol image reads compared to underlying neuritic plaque density in end-of-life subjects who underwent brain autopsy.

Methods: Five readers assessed [18F]flutemetamol PET images from a cohort of 106 end-of-life subjects during a Phase 3 clinical trial. Images were dichotomised as either negative or positive. The standard of truth was post-mortem assessment of amyloid plaque burden, using Bielschowsky silver stain (neuritic only) and amyloid- β immunohistochemistry (fibrillar forms).

Results: The cohort contained a broad range of underlying amyloid plaque burden. Of the 106 subjects, only 10 were assessed incorrectly by majority PET read; 3 false positives and 7 false negatives. Eight of these subjects had borderline pathology. False positive cases were mostly interpreted as positive by all readers (two by 5/5 and one by 4/5 readers). In all these cases fibrillar amyloid was present. However, false negatives were associated with lower inter-rater agreement (two by 3/5, four by 4/5 and one by 5/5 readers) with atrophy also confounding the read result. Examining regional assessments of PET positivity also showed a marked drop in inter-rater agreement at the threshold corresponding to the division between CERAD “moderate” and “sparse” neuritic plaque categories.

Conclusion: These data suggest in the majority of cases readers will dichotomise [18F]flutemetamol images correctly but may disagree in a minority of cases particularly when borderline pathology is present. Clinical implications of such PET interpretation warrants further discussion.

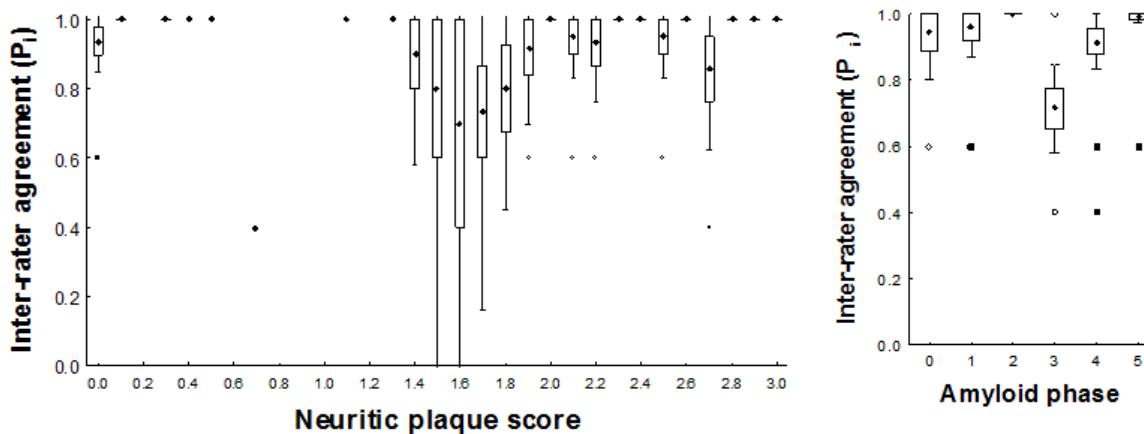


Figure 1. Inter-rater agreement drops sharply at the threshold between Sparse and Moderate (None=0, Sparse = 1, Moderate = 2 and Frequent =3)

Keywords: [18F]Flutemetamol, diagnostic accuracy, image reading, borderline pathology

P76 Presented by: Smith, Adrian PL

Submission ID: 76

P78**Longitudinal Processing Speed, Working Memory and Inhibitory Control in Relation to Baseline Preclinical Amyloid Staging**

Beth Snitz¹, Dana Tudorascu¹, Robert Nebes¹, Ann Cohen¹, Howard Aizenstein¹, Julie Price¹, Chester Mathis¹, Lisa Weissfeld², William Klunk¹

¹ University of Pittsburgh School of Medicine, Pittsburgh, PA, United States

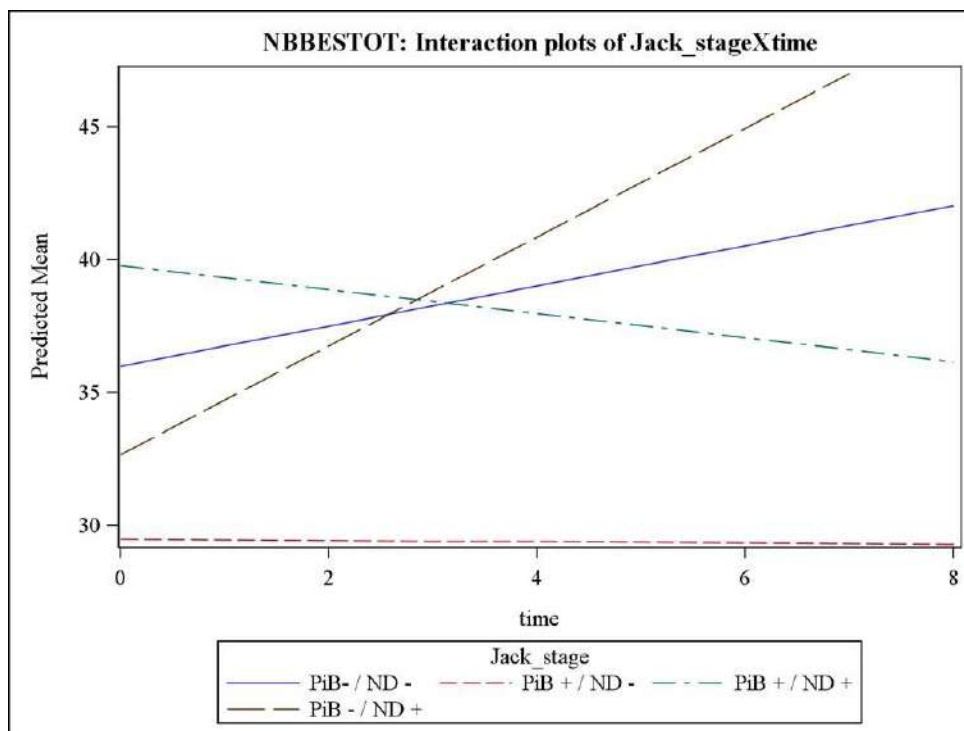
² Statistics Collaborative, Washington DC, District of Columbia, United States

Background: Preclinical staging according to biomarkers of amyloid and neurodegeneration (ND) have been proposed to represent meaningfully different risk profiles for clinical dementia in aging. Little is known about whether preclinical staging accounts for some variability in cognitive decline in specific domains central to theories of normal cognitive aging—namely, information processing resources, working memory, and inhibitory efficiency.

Methods: Participants were n=80 older adults (mean age 73.9 years) screened at study entry via comprehensive neuropsychological assessment for normal cognition. Baseline PiB(+) was defined by regional PiB positivity in any one of six specified regions. Baseline ND positivity was defined as either FDG-PET posterior cortical atrophy index cutoff < 1.0245 or hippocampal W-score < -0.90 (both cutoffs based on 85% sensitivity to AD). Measures of processing speed included conceptual and perceptual comparison choice (same/different) reaction time (RT); working memory tasks included auditory N-back and letter-number sequencing; inhibition measures included Hayling and Stroop paradigms. Participants completed cognitive tasks at baseline, 24-months, and thereafter annually. Linear mixed models with random intercepts and trend were used to analyze baseline preclinical neuroimaging stage as predictors of longitudinal cognition.

Results: At baseline, n=30 participants were PiB(-) / ND(-); n=16 were PiB(+) / ND(-); n=8 were PiB(+) / ND(+); and n=26 were PiB(-) / ND (+). Mean follow-up time was 41.6 months. A significant group x time interaction was observed for N-back [$F(3,194)=3.21$, $p=.024$] (Figure 1). No other group x time interactions were observed for other cognitive outcomes. In main effects models, there were significant group effects for Stroop measures.

Conclusions: Preclinical amyloid/ND staging does not predict different rates of cognitive decline in processing speed or inhibitory control. Findings are suggestive that working memory trajectories may be related to preclinical biomarker stages, with steepest decline associated with both amyloid and neurodegeneration marker positivity.



P78 Presented by: Snitz, Beth E.

Submission ID: 88

P80

Age-dependent Effect of Cortical Amyloid-Beta Deposition on Hippocampal Activity in Cognitively Normal Adults

Zhuang Song, Denise Park

Center for Vital Longevity, University of Texas at Dallas, Dallas, TX, United States

Age and cortical amyloid-beta ($A\beta$) deposition are two major risk factors for Alzheimer's disease (AD). The interaction between age and $A\beta$ deposition is not well understood in the context of cognitive and neural changes in the course of AD development. The medial temporal lobe is a critical brain region for understanding the pathogenesis of AD because it is not only vulnerable to early AD pathology but also primarily responsible for memory decline. In the present study we test the hypothesis that cortical $A\beta$ deposition is related to aberrant functional activity in the medial temporal lobe and this relationship is age-dependent. Cognitively normal adults (aged from 45 to 90, $N=120$) from the Dallas Lifespan Brain Study had cortical $A\beta$ deposition assessed by florbetapir F 18 positron emission tomography (PET). All of these participants also underwent fMRI scanning while viewing natural scene pictures, and made a "yes/no" judgment as to whether there was water in the scene. The analysis focused on the medial temporal activation resulting from a contrast of task versus baseline (a fixation cross), controlling for gender and education. We found an Age x Amyloid Burden interaction on activity in the left anterior hippocampus ($p=0.004$) as well as in the right anterior hippocampus ($p=0.03$). Both the middle aged (45-60) and very old (80-89) showed no relationship between cortical $A\beta$ burden and evoked fMRI activity in the MTL. However, in the age groups of 60s and 70s, high cortical $A\beta$ burden was associated with reduced fMRI activity evoked by the task in bilateral anterior hippocampi. These findings suggest that disrupted medial temporal lobe activity associated with amyloid deposition is not universal, but linked to age. The disruption begins in old age and is curtailed in both middle and very old age.

Keywords: age, amyloid-beta, hippocampus, fMRI

P80 Presented by: Song, Zhuang

Submission ID: 90

Chirality of [¹⁸F]THK-5105 Affects its Preclinical Characteristics as a PET Tau Imaging Probe

Tetsuro Tago^{1,2}, Shozo Furumoto^{1,3}, Nobuyuki Okamura⁴, Ryuichi Harada⁵, Hajime Adachi^{1,2}, Yoichi Ishikawa¹, Kazuhiko Yanai⁴, Ren Iwata¹, Yukitsuka Kudo⁵

¹ Cyclotron and Radioisotope Center, Tohoku University, Sendai, Miyagi, Japan

² Graduate School of Pharmaceutical Sciences, Tohoku University, Sendai, Miyagi, Japan

³ Frontier Research Institute for Interdisciplinary Sciences, Tohoku University, Sendai, Miyagi, Japan

⁴ Tohoku University School of Medicine, Sendai, Miyagi, Japan

⁵ Institute of Development, Aging and Cancer, Tohoku University, Sendai, Miyagi, Japan

Objectives: Noninvasive imaging of tau pathology in the Alzheimer's disease (AD) brain would facilitate diagnosis and staging of AD. Recently, we have developed [¹⁸F]THK-5105 as a tau imaging probe for PET. THK-5105 has a chiral center within a side chain, and its racemate was used in the previous studies. In this study, we performed preclinical characterization and comparison of optically pure [¹⁸F]THK-5105 enantiomers as a PET tau probe.

Methods: Binding selectivity of radioligands for tau lesions was evaluated by autoradiography (ARG) using AD brain sections. In vitro binding kinetics for AD brain homogenates was assessed, and association and dissociation constants (kon and koff values, respectively) were determined. Pharmacokinetics of radioligands in normal mice was evaluated by ex vivo biodistribution study.

Results: ARG images demonstrated high binding selectivity of both enantiomers for tau over amyloid-β. (*S*)-form showed slow dissociation from AD brain homogenates compared with (*R*)-form, resulting in the higher binding affinity of (*S*)-form (koff/kon=Kd<10 nM). Clearance of radioactivity from the mouse brain of (*S*)-form was faster than that of (*R*)-form (2 min/60 min %ID/g ratio: (*R*)-form=7.2±0.81; (*S*)-form=11±1.7, p=0.005), which was suggested to reflect the difference in clearance from blood. (*R*)-form showed high accumulation in the bone compared with (*S*)-form (%ID/g at 120 min: (*R*)-form=1.9±0.058; (*S*)-form=0.47±0.13, p<0.0001), suggesting (*R*)-form was more susceptible than (*S*)-form to defluorination in mice.

Conclusions: Preclinical evaluation of optically pure [¹⁸F]THK-5105 revealed the differences in binding affinity for AD tau aggregates and pharmacokinetics in normal mice between enantiomers. [¹⁸F](*S*)-THK-5105 tended to have favorable properties as a PET tau imaging probe compared with [¹⁸F](*R*)-THK-5105. Further evaluation is under way to clarify whether these trends are applicable to other THK tau probes.

Keywords: *Alzheimer's disease, Positron Emission Tomography, tau imaging*

P82 Presented by: Tago, Tetsuro

Submission ID: 66

P84

Amyloid-Beta Burden is Inversely Associated with Gray Matter Volume but not Semantic Memory Performance in Cognitively Normal First-Degree Relatives at Risk for Alzheimer's Disease

Christopher van Dyck, Shuo Wang, Nicole Barcelos, Beata Planeta-Wilson, Adam Mecca, Joel Gelernter, Peter Van Ness, Richard Carson

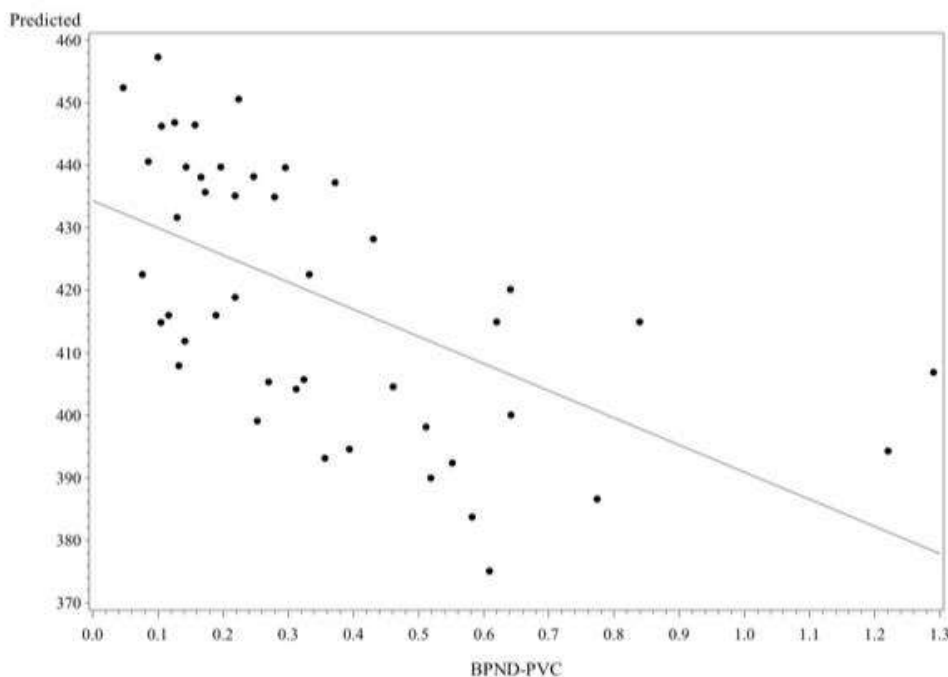
Yale University School of Medicine, New Haven, CT, United States

Theoretical models of preclinical Alzheimer's disease (AD) have proposed that cerebral amyloidosis leads to neurodegeneration and subsequent cognitive decline. This study investigated the relationship between amyloid deposition, gray matter volume, and neuropsychological test performance in pre-symptomatic individuals at varying genetic risk for AD.

Methods: Cognitively normal subjects aged 50-66 with a first-degree family history for AD were genetically screened to select three groups: APOE genotype $\epsilon 4\epsilon 4$ ($n=15$), $\epsilon 3\epsilon 4$ ($n=15$), and $\epsilon 3\epsilon 3$ ($n=15$), matched for age and sex. Subjects were then studied with $[^{11}\text{C}]\text{PiB}$ PET, MRI, and neuropsychological testing. PET and MR images were co-registered for application of a ROI template (AAL for SPM2) to generate regional time-activity curves with cerebellum as reference region. BPND was then computed using SRTM2 for a mean cortical ROI consisting of frontal, posterior cingulate-precuneus, lateral parietal, and lateral temporal ROIs. MRI images were segmented into gray matter, white matter, and CSF. Mask images of these segments were smoothed to the system resolution ($\sim 6\text{mm}$), and gray matter values of BPND were partial volume corrected (PVC).

Results: APOE- $\epsilon 4\epsilon 4$ subjects demonstrated significantly higher PVC mean cortical BPND than APOE- $\epsilon 3\epsilon 3$ ($p<0.001$), and APOE- $\epsilon 3\epsilon 4$ were marginally higher than APOE- $\epsilon 3\epsilon 3$ ($p=0.063$, generalized linear model, adjusted for age and sex). In the overall sample, PVC BPND was inversely related to gray matter volume within the mean cortical ROI ($P=0.029$, linear mixed effects model, adjusted for age, sex, and APOE genotype). There was no significant association between mean cortical BPND and semantic memory performance. PVC improved the overall separation of APOE groups, although this effect was not statistically significant.

Gray matter volume (mL) as a function of partial volume corrected $[^{11}\text{C}]\text{PiB}$ BP_{ND} in mean cortical ROI



Conclusions: In cognitively normal middle-aged individuals at varying genetic risk for AD, amyloid burden is significantly related to gray matter volume but not to semantic memory performance. These findings are consistent with models of preclinical AD in which neurodegeneration occurs before manifest cognitive decline.

Keywords: Amyloid-Beta, Gray Matter, Semantic Memory, Preclinical Alzheimer's Disease, Partial Volume Correction

P84 Presented by: van Dyck, Christopher H

Submission ID: 126

A 52-week Pilot Study Targeting A β with PBT2: Neuroimaging Results

Victor Villemagne^{1,2}, Christopher Rowe¹, Kevin Barnham², Robert Cherny², Michael Woodward³, Svetlana Pejoska¹, Gareth Jones¹, Rudy Tanzi⁴, Colin Masters²

¹ Austin Health, Centre for PET, Melbourne, VIC, Australia

² The Florey Institute, The University of Melbourne, Melbourne, V, Australia

³ Austin Health, Aged Care & Residential Services, Melbourne, VIC, Australia

⁴ Massachusetts General Hospital, Aging and Genetics Research Unit, Boston, MA, United States

Objectives: The trial aimed to explore putative imaging markers to help inform future clinical trial design of PBT2 in Alzheimer's disease (AD).

Methods: We conducted a 52-week, double-blind, randomized, placebo-controlled trial involving 42 patients with mild AD (71.1 \pm 9.2 years, MMSE 24.2 \pm 2.5) with a baseline ¹¹C-PiB-SUVR \geq 1.7. Participants received either PBT2 (250mg/day) or placebo for 52 weeks. Primary outcome measure was A β burden as measured by ¹¹C-PiB-PET at baseline and 12 months. Participants also underwent periodic neuropsychological evaluation, FDG-PET and MRI scans.

Results: PBT2 was well tolerated. At baseline, there were no significant between-group differences in age, gender, ApoE, hippocampal volume, PiB or FDG SUVR. Baseline ¹¹C-PiB-SUVR ranged between 1.73 and 3.31 (median 2.5). Despite PBT2-treated patients showing a significant decrease in A β burden at 12 months (-2.5%, p=0.048) post-hoc, this was accompanied by a similar decrease in the placebo group (-3.1%, p=0.06), yielding no significant between-group differences. Similarly, no significant between-group differences were found on cognition, FDG or MRI volumetrics, though a trend towards a slower rate of hippocampal atrophy on PBT2-treated patients (p=0.09) was observed. When analysed separately, PBT2-treated participants with baseline >SUVR 2.5 (n=11) showed significant reductions in PiB-SUVR (p=0.002) while those with <SUVR 2.5 (n=14) did not (p=0.6), and while the between-groups differences became more pronounced, they did not reach statistical significance.

Conclusions There were no between-group differences in A β burden in PBT2 treated and untreated mild AD patients, despite a significant reduction in A β in the PBT2-treated patients, especially in those with a baseline PiB-SUVR \geq 2.5.

Keywords: *Alzheimer's disease, A β , PBT2, therapeutics*

P86 Presented by: Villemagne, Victor L

Submission ID: 12

Case Report: Longitudinal Measures of Beta-amyloid Burden and Grey Matter Atrophy in an Adult with Down's Syndrome without Dementia

Liam Wilson¹, Tiina Annus¹, Young Hong², Julio Acost-Cabronero³, Tim Fryer³, Peter Nestor², Anthony Holland¹, Shahid Zaman¹, et al.

¹ Cambridge Intellectual and Developmental Disabilities Research Group, Department of Psychiatry, University of Cambridge, Douglas House, 18b Trumpington Rd, CB2 8AH, Cambridge, Cambridgeshire, United Kingdom

² Wolfson Brain Imaging Centre, Department of Clinical Neurosciences, University of Cambridge, University of Cambridge School of Clinical Medicine Box 65 Cambridge Biomedical Campus, CB2 0QQ, Cambridge, Cambridgeshire, United Kingdom

³ German Centre for Neurodegenerative Diseases (DZNE), Leipziger Str. 44, House 64, 39120, Magdeburg, Saxony-Anhalt, Germany

Introduction: People with Down's syndrome (DS) typically develop Alzheimer's disease (AD) neuropathology in middle age. However, the regional dynamics of A β accumulation in vivo in this population are not well understood. We investigated the regional A β accumulation, and grey matter atrophy, in one adult with DS without dementia.

Methods: A 45 year old male with DS underwent [11C]-PiB PET, T1 MRI, clinical assessment for dementia and neuropsychological testing (using CAMDEX-DS), repeated after ~42 months. Cortical and subcortical regions of interest were defined using a manually improved Brodmann atlas and FSL-FIRST, respectively. Binding potentials (BPND) at each region were calculated for baseline (time 0) and repeat (time 1) scans. Additionally, serial grey matter change was estimated using a tensor based morphometry approach.

Results: No significant clinical changes were reported at time 1. Twelve regions of interest showed significantly increased BPND at time 1, with the largest increases occurring in subcortical structures (left putamen, caudate, globus pallidus and thalamus). There was a significant positive correlation between BPND at time 0 and the magnitude of BPND change at time 1 ($r=0.579$, $p<0.001$). Changes in BPND, however, were largely independent of grey matter atrophy rates, which were more prominent in retrosplenial and hippocampal areas.

Conclusions: Regions with a high baseline BPND appeared to be at greater risk of developing further A β pathology. However, this bore no relationship to grey matter atrophy in the participant, which appeared to evolve independently of A β pathology. The methodology and findings of this case report may be useful in informing future longitudinal studies of A β accumulation in larger cohorts of people with DS.

Keywords: *Down Syndrome, PiB-PET, MRI, atrophy*

P88 Presented by: Wilson, Liam R

Submission ID: 108

P90**Between Cohort Transferability of Clinical Trial Enrichment with Amyloid Imaging and Hippocampal Volume**Robin Wolz^{1,2}, Katherine Gray^{1,2}, Derek Hill¹¹ Ixico Plc, London, London, United Kingdom² Imperial College London, London, London, United Kingdom

Background: Biomarkers are more and more used to enrich populations in MCI / mild AD clinical trials. Amyloid burden and structural neurodegeneration from MRI have both been qualified by the EMA as enrichment markers. The transferability of these biomarkers between trial cohorts has not yet been well characterized. Here, the performance of these biomarkers are assessed individually and in combination on both the ADNI-1 MCI and ADNI-II L-MCI cohorts.

Methods: Included are the 153 MCI and 107 L-MCI subjects from the ADNI I/II cohorts for which an Amyloid marker is available from Amyloid PET (ADNI II) and CSF A-beta (ADNI I). Clinical follow-up with MMSE/CDR-SB was required for 24 months. Following [1], we calculated required sample sizes per arm and trial cost for a hypothetical 2-year randomized trial based on the 24 month change in MMSE and CDR-SB. Compared was enrichment based on Amyloid positivity (Am+) to one where the Am+ group was further enriched through automatically extracted hippocampal volume [1,2]. We consider trials that use amyloid PET and/or structural MRI as an inclusion criteria and use market-benchmarked trial costs [1].

Results:

		Sample Size		Trial Cost	
		MMSE	CDR-SB	MMSE	CDR-SB
Unenriched	ADNI I	1199	418	109	38
	ADNI II	459	841	42	77
Amyloid	ADNI I	704	284	81	33
	ADNI II	281	303	34	37
Amyloid & HCV	ADNI I	288	171	55	26
	ADNI II	206	179	26	27

Table 1 summarizes results for sample sizes and trial cost (\$m) for the different enrichment strategies and different clinical endpoints in the two cohorts. While screen failure rates go up with more strict inclusion criteria, the number of subjects that need to undergo screening goes down due to significantly reduced sample sizes (data not shown).

Conclusions: The presented results show that trial characteristics like sample size and cost can be significantly different across cohorts and clinical endpoints. Individual and combined enrichment cannot just help to reduce required sample sizes and trial cost, but can also help to significantly reduce this variability across cohorts and clinical endpoints.

References:

[1] Yu. Neurobiology of aging 35(4), 808-818, 2014

[2] Wolz.NeuroImage, 49(2):1316-25, 2010

Keywords: Alzheimer's disease, MCI, clinical trials, enrichment, hippocampal volume**P90 Presented by: Wolz, Robin***Submission ID: 80*

SESSION 8: Biomarkers (part 2)

CHAIRS: Andrew Saykin, PhD, *Indiana University School of Medicine*
Julie Price, PhD, *University of Pittsburgh*

Optimizing PiB-PET SUVR Calculations by a Large-Scale Analysis of Longitudinal Reliability

Christopher Schwarz¹, Matthew Senjem², Jeffrey Gunter², Nirubol Tosakulwong³, Scott Przybelski³, Stephen Weigand³, Anthony Spychalla¹, Ronald Petersen⁴, Val Lowe¹, Clifford Jack¹

¹ Department of Radiology, Mayo Clinic and Foundation, Rochester, MN, United States

² Department of Information Technology, Mayo Clinic and Foundation, Rochester, MN, United States

³ Department of Health Sciences Research, Division of Biostatistics, Mayo Clinic and Foundation, Rochester, MN, United States

⁴ Department of Neurology, Mayo Clinic and Foundation, Rochester, MN, United States

Background: Many methods exist for automatic quantitative evaluation of Amyloid- β pathology in PiB-PET images by Standardized Uptake Value Ratio (SUVR), varying in choice of target gray-matter region, reference region, and use of partial volume correction (PVC). Because there is no gold-standard, methods are typically validated by agreement with binary visual assessment or by case-control separability. Cross-site data comparability is challenged by significant effects from implementation differences. Longitudinal reliability of intra-subject serial SUVR values is critical for clinical trials, but has not been widely used to compare methods.

Methods: We studied 79 participants (age 52-91, mean=73) from the Mayo Clinic Study of Aging and Alzheimer's Disease Research Center studies with 3 serial scans of 3T MP-RAGE T1-w MRI and PiB-PET. PiB scans were registered to corresponding T1-w images and an in-house standard template/atlas was warped to each T1-w image using ANTs software. SPM12b Unified Segmentation and Longitudinal-Freesurfer 5.3 were each used to segment cortical gray matter. PVC was optionally applied using a single-compartment (Meltzer) model. All combinations of target region, reference region, and PVC were calculated for each scan and values were analyzed in a linear mixed-effects model. Methods were compared on two separate criteria: maximizing intra-class correlation (ICC) of within-subject values (longitudinal stability), and minimizing frequency of apparently-decreasing (i.e. implausible) intra-subject trajectories.

Conclusions: Methods using PVC generally outperformed paired counterparts without. Reference regions in the pons and cerebellum (GM, WM, GM+WM, crus, and eroded variants) were generally equivalent with each other. The highest-ICC variants used eroded supratentorial WM reference ROIs, but these variants had more frequent implausible trajectories. Target regions based on narrow cortical GM-ribbon segmentations generally outperformed wider, atlas-based cortical ROIs, presumably by identifying GM with the least partial-volume contamination from nearby WM. Freesurfer and SPM cortical segmentations were generally equivalent, although Freesurfer failed to segment 6/237 scans.

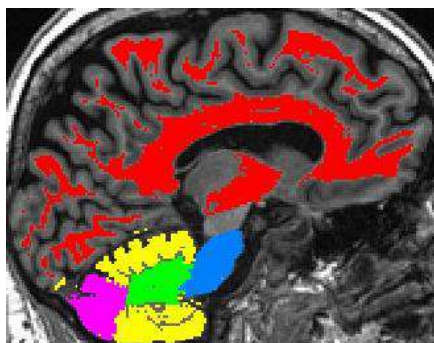


Figure 1: Reference ROIs Tested:

Supratentorial WM

Pons

Cerebellar WM

Cerebellar GM

Crus (overlaps Cerebellar GM)

Not illustrated: variants from morphological erosions and combinations of above ROIs

Keywords: SUVR, Reference-Region, Longitudinal, PVC

Presented by: Schwarz, Christopher G

Submission ID: 27

Beta-amyloid Deposition in Non-amnestic Clinical Presentations

Keith Josephs, Jennifer Whitwell, Joseph Duffy, Edythe Strand, Mary Machulda, Daniel Drubach, Matthew Senjem, Clifford Jack Jr, Ronald Petersen, Val Lowe

Mayo Clinic, Rochester, MN, United States

Background: β -amyloid deposition is one of two cardinal features required for pathological diagnosis of Alzheimer's disease (AD). Most subjects with AD have an amnestic presentation although a fairly large number have a non-amnestic presentation and instead present with behavioral change, speech problems, dyspraxia, agnosia, aphasia or visual spatial/perceptual deficits. Such patients are considered to have had an atypical presentation of AD (ATAD). Furthermore, such symptoms are typically associated with another class of neurodegenerative diseases, the frontotemporal lobar degenerations. There is no data on the frequency of β -amyloid deposition in subjects having a non-amnestic presentation.

Methods: Two hundred and two subjects presenting with non-amnestic clinical features underwent β -amyloid assessment with [11C] Pittsburgh compound B (PiB) PET and volumetric MRI to determine β -amyloid status. Subjects were considered positive for β -amyloid deposition if their global PiB SUVR was >1.5 .

Results: The average age of the cohort was 68 years (range 42-86); 50% were female. β -amyloid deposition was most frequently positive in subjects presenting with visual spatial/perceptual deficits (100%), followed by aphasia (55%), dyspraxia (50%), agnosia (27%), behavioral dyscontrol (12%) and speech impairment (7%). Differences in the frequencies of β -amyloid deposition across symptoms were not driven by age at evaluation or at onset. Within the positive subjects, global PiB SUVR was significantly higher in those with visual spatial/perceptual deficits compared to all other groups ($p<0.05$).

Conclusions: Beta-amyloid deposition is strongly associated with specific symptom types in ATAD, particularly visual spatial/perceptual deficits. In fact, visual spatial/perceptual deficits may be an excellent biomarker for β -amyloid deposition.

Keywords: *Aphasia; agnosia; non-amnestic; frontotemporal lobar degeneration*

Presented by: Josephs, Keith A

Submission ID: 107

Between SNAP and a Hard A β Rock: Characterizing the Fate of Preclinical Alzheimer's Disease

Samantha Burnham¹, Pierrick Bourgeat², Vincent Doré³, Belinda Brown⁴, Olivier Salvado², Ralph Martins⁴, Lance Macaulay⁵, Colin Masters⁶, Christopher Rowe⁷, Victor Villemagne^{6,7}

¹ CSIRO, Digital Productivity & Services Flagship, Perth, WA, Australia

² CSIRO, Digital Productivity & Services Flagship, Brisbane, QLD, Australia

³ CSIRO, Digital Productivity & Services Flagship, Melbourne, VIC, Australia

⁴ Edith Cowan University, Centre of Excellence for Alzheimer's Disease Research and Care, Perth, WA, Australia

⁵ CSIRO, Food and Nutrition Flagship, Melbourne, VIC, Australia

⁶ The University of Melbourne, The Florey Institute, Melbourne, VIC, Australia

⁷ Austin Health, Centre for PET, Melbourne, VIC, Australia

Objective: The objective of the study was to characterize a two-imaging marker construct in the preclinical stages of Alzheimer disease.

Methods: 493 cognitively unimpaired individuals (HC, 73.0 \pm 6.2years; 56%female) were included in the study. A β status (A) was determined with either PiB, flutemetamol or florbetapir, while neurodegeneration (N) was established using hippocampal volume. Following Jack et al, individuals were categorized as either A-N-, A+N-, A+N+, or suspected non-Alzheimer disease pathophysiology (SNAP, A-N+). Clinical progression, cognitive domain-specific trajectories and global composite scores for 461 HC were assessed.

Results: 65% of HC were classified as A-N-, 18% as A+N-, 5% as A+N+, and 12% as A-N+. Participants in the A-N- group were significantly younger, and while males were more prevalent among A+N+ and A-N+, females were more prevalent among A+N- and A-N-. ApoE4 carriage was more frequent in A+N-(48%) and A+N+(58%) than in A-N-(19%) and A-N+(23%). While no significant differences were observed in baseline scores significantly faster cognitive decline was observed in A+N+(-0.30SD/yr) and A+N-(-0.08SD/yr) when compared to A-N-(+0.02SD/yr). The A-N- and A-N+ groups did not show significant decline over time, although A-N+ was associated with a lower baseline performance. While A+N+ and A+N- were more impaired in memory domains, A-N+ were more impaired in language and executive domains. Within 4.5 years, 22.2% of A+N+ progressed to amnesic MCI/AD, compared to only 7.3% of A-N+(2MCI, 1AD, 1VaD)

Conclusions: Increasing marker abnormality was reflected in faster cognitive decline. Distinct cognitive domains were affected in those with AD and non-AD pathology, likely suggesting different underlying pathophysiological mechanisms.

Keywords: *Abeta, Alzheimer's disease, SNAP, neurodegeneration, cognitive decline*

Presented by: Villemagne, Victor L

Submission ID: 7

Funding for this conference was made possible in part by grant R13 AG042201 from the National Institute on Aging and the National Institute of Biomedical Imaging and Bioengineering.

The views expressed in written conference materials or publications and by speakers and moderators do not necessarily reflect the official policies of the Department of Health and Human Services; nor does mention by trade names, commercial practices, or organizations imply endorsement by the U.S. Government.

The 9^h Human Amyloid Imaging Conference is supported through educational grants from:

PLATINUM



For further information
concerning Lilly grant funding
visit www.lillygrantoffice.com

GOLD

The Biogen Idec logo features the text "biogen idec" in a blue, lowercase sans-serif font, enclosed within a white rectangular frame with a thin black border.

biogen idec

Transforming Discovery into Care

Silver



Bronze



Associate

